July 20, 2020

Sent via email (references attached as exhibits)

County of Lake
Board of Supervisors
Attn: Carol Huchingson, County Administrative Officer
255 N. Forbes Street
Lakeport, CA 95453
Carol.huchingson@lakecountyca.gov

Re: Supplemental Comments on the Guenoc Valley Mixed-Use Planned Development Project and Related Approvals and Environmental Review Documents (SCH No. 2019049134)

Dear Supervisors:

These comments are submitted on behalf of the Center for Biological Diversity (the "Center") regarding the Guenoc Valley Mixed-Use Planned Development Project ("Project") and associated approvals and environmental review. These comments follow our April 21, 2020 and July 6, 2020 comments on the same.

The Center is a non-profit, public interest environmental organization dedicated to the protection of native species and their habitats through science, policy, and environmental law. The Center has over 1.7 million members and online activists throughout California and the United States. The Center has worked for many years to protect imperiled plants and wildlife, open space, air and water quality, and overall quality of life for people in California, including Lake County.

The Center writes to object to the last-minute addition of new materials and substantive changes to the EIR and the Project. These materials were made public on the County's website only on Friday afternoon, July 17, less than two business days before the Board's hearing to approve the Project.[1] These include significant substantive changes made to the EIR (such as the last-minute addition of a GHG carbon-offset purchase program) and constitute significant new information requiring recirculation and the opportunity for public comment and review. These

[1] These materials include a Response to Comments on the FEIR, an "Errata to Final EIR," a revised Mitigation Monitoring and Reporting Program, Findings and Facts, and Supplemental Staff Report. The County added additional materials—including a lengthy letter from the developer's attorney, Katherine Phillipakis, to the County that included numerous exhibits, some describing last-minute changes to the Project—to the County's website for the Project agenda item on or about 5 pm on July 20, 2020. We have not had the opportunity to review these eleventh-hour materials and do not address them here.

changes were made in a mis-named and misleadingly named "Errata to Final EIR."[2] At a bare minimum, the Board should continue the hearing in order to give the public adequate time to review and comment on these new materials and changes.

Please note that due to the last-minute nature of the responses to our comments on the FEIR and the changes to the FEIR and the Project, we did not have the time necessary for us to fully review and respond to the new materials. These comments provide responses to some points raised in the Applicant's responses to our comments on the FEIR, but are not exhaustive.

A. The Center's Limited Review of the New Materials Indicates That the EIR's Analysis of and Mitigation for the Project's GHG-related Impacts Is Inadequate.

Our limited review of the new materials indicates that the Applicant's Responses and the late changes to the EIR and project documents do not correct the deficiencies we identified in our comments on the FEIR regarding impacts from the Project's greenhouse gas emissions.

The Response states that the TDM now provides a "goal" of 15% reduction in VMT. (New MM 3.13-4 added the following statement: "The goal of the TDM Program shall be a 15 percent in reduction in the VMT generated by the Proposed Project.") But this is not an enforceable standard, and nothing in the TDM or EIR appears to *require* the TDM measures to achieve a 15% reduction in VMT. Accordingly, this is not the type of specific, enforceable performance standard that CEQA requires. The Applicant also revised the TDM to add quantified "expected reductions," for proposed VMT reduction strategies, but these numbers are not supported by substantial evidence and appear to have been pulled from thin air.

The Applicant has not shown that its new dial-a-ride service will reduce VMT or GHG emissions. In fact, the availability of free non-shared on-demand automobile transportation for users of the Project appears likely to *increase* VMT by inducing additional vehicle travel. The Applicant has also failed to show why additional *transit* options are infeasible. Nor does the Response explain why contributions to a regional transit fund, or funding of other options for reducing regional or County VMT, were not evaluated or considered or determined to be infeasible on the basis of substantial evidence.

The Applicant's late addition of a carbon offset purchase program is significant new information requiring recirculation. Furthermore, the new program does not comply with CEQA's requirements for mitigation. The Fourth District Court of Appeal invalidated a similar greenhouse gas mitigation measure last month. (*Sierra Club, et al. v. County of San Diego*, No. D075478 and consolidated cases, Cal. App. 4th Dist. June 12, 2020 ["*Sierra Club*"].) In that

[2] Webster defines "Errata" as: "a list of errors in a printed work discovered after printing and shown with corrections." (https://www.merriam-webster.com/dictionary/errata) The County's improper use of this term to describe the considerable changes to the EIR and Project (such as the last-minute addition of a carbon-offset purchase program) misleads the public about the nature of the document and downplays the significance of these last-minute changes. Additionally the "Errata" document's inconsistent use of redline to indicate changes to the FEIR makes it difficult if not impossible for the public to determine what has been added, altered, or remains the same from the EIR. This makes it nearly impossible to adequately review the document and provide comments.

case, the court concluded that a San Diego County mitigation measure relying on offsets purchased from "CARB-approved" registries violated CEQA by failing to ensure adequate standards for offsets listed by carbon registries (including offsets from international sources) and improperly deferring and delegating the formulation of mitigation. Here, the mitigation measure assumes without evidence that third-party registries will ensure that the mitigation will be real, permanent, additional, quantifiable, verifiable and enforceable, as required by CEQA. (*Id*. at 49.) Unless an offset credit truly represents a GHG reduction commensurate with Project emissions, the mitigation will be illusory and ineffective. Voluntary, private offset markets, particularly those that include international sources for offsets, are extremely difficult to verify and enforce. (*Id*. at 51-52.) For these reasons, the Project's proposed purchase of GHG offsets credits for mitigation fails to meet CEQA's requirements. The implementation of a carbon offset purchase program may itself have potentially significant environmental impacts that must be considered in the EIR.

Additionally, the EIR cannot justify its introduction and use of a new threshold of significance ("BAAQMD Service Pop Threshold Converted to total MT CO2e3 per year") less than two business days before the project is set to be approved. This is significant new information requiring recirculation.

B. The Center's Limited Review of the New Materials Indicates That the EIR's Analysis of and Mitigation for the Project's Wildfire and Wildfire Evacuation-related Impacts Is Inadequate.

Our limited review of the new materials indicates that the Applicant's Responses and the late changes to the EIR and project documents do not correct the deficiencies we identified in our comments on the FEIR related to wildfire and wildfire evacuation.

The EIR cannot justify its decision to ignore the insurmountable scientific evidence that development in the Wildland Urban Interface ("WUI"), like that proposed by the Project, increases the likelihood of wildfire ignition and wildfire risk. The Response argues that the Project is somehow categorically different than other low-density development in the WUI described in the numerous studies cited and provided by the Center. But the County provides no evidence that this is the case. Syphard et al. (2020) states:

> Large fire probability increases with the co-occurrence of human-caused ignitions and severe wind conditions (Abatzoglou et al. 2018). This means that, as population increases and development further encroaches into wildland vegetation, there is an increased risk that a human-caused ignition will coincide in place and time with hot, dry weather; flammable vegetation; and severe wind conditions. Data show that fires tend to be most frequent at low to intermediate housing and population densities (Syphard et al. 2009, Bistinas et al. 2013). Thus, the rapid increase in the spread of exurban development like that occurring now in California (Radeloff et al. 2018), has the potential to both increase the number of ignitions and decrease the overall distance between wildlands and housing.

Additionally, air-borne embers can travel and ignite structures over 1 km away from a fire front. (Syphard et al. 2020, stating “most homes do not burn from direct flame contact or from the radiant heat of the fire front, but rather from embers blown from the fire front, even from a kilometer or more away.”) Given the great distances that wind-driven embers can travel, the EIR fails to provide substantial evidence that its fire-break features will prevent wildfire spread on the Project site.

As we previously pointed out, the vast majority of the measures in the Wildfire Prevention Plan remain, as the Applicant acknowledges, “recommended measures” (Response to FEIR comments at p. 1, p. 6), not *required* measures. The fact that the general condition of approval contains catchall language stating that the use “shall substantially conform” to “all requirements in the Final Environmental Impact Report” does not remedy this deficiency.

The new “Project Design Feature” 2.4 described in the Mitigation Monitoring and Reporting Program of preparing an emergency evacuation plan and/or fire evacuation plan in the future and providing it to residents, guests, and employees, is improperly deferred mitigation. As we explained in our comments on the DEIR and FEIR, and as fire expert Dr. Thomas Cova confirmed, the County should prepare a wildfire evacuation study that evaluates the Project’s impacts on new and existing residents’ and visitors’ ability to evacuate in the event of a wildfire. The Applicant and the County have offered no reason to defer this crucial analysis.

C. The Center’s Limited Review of the New Materials Indicates That the EIR’s Analysis of Biological Impacts Is Inadequate.

To mitigate impacts to wildfire and increased human ignitions, the FEIR states “The Proposed Project will include the installation of approximately 32 miles of new joint trench and underground electrical infrastructure in the proposed resort community areas to the extent feasible.” (FEIR at 2-59). In addition the FEIR states, “Gas propane tanks would be underground throughout the Guenoc Valley Site to reduce the risk of gas related wildfires and control for temperature fluctuations. Each residential estate would be serviced by individual underground propane tanks. Each resort community would utilize shared propane tank systems with localized underground distribution systems to serve the hotel and resort residential structures.” (FEIR at 2-60). There appears to be no analysis of impacts to biological resources from such underground pipelines and storage areas. Thirty two miles of tunneling and trenching could have significant impacts to groundwater hydrology, surface water features, and the biological and aquatic resources in and adjacent to the tunneled/trenched areas (*e.g.*, Loew et al. 2007; Butscher et al. 2011). There is also potential for leakage as storage tanks or pipelines corrode, which could have adverse impacts on water quality and biological resources (as well as human safety). Although the provided references are not specific to the Project area, these studies highlight the potential impacts to biological resources in and adjacent to the Project area. The EIR should adequately assess and mitigate impacts due to undergrounded and trenched utilities to sensitive species and habitats in and adjacent to the Project area.

The proposed Project would lead to increased paved roads and road capacity, which would likely lead to increased traffic, vehicle speed, noise, light, etc. Such changes would, in effect, create greater barriers for wildlife movement and habitat connectivity. Yet the Project Proponent states that "Because roadways are largely existing, would be improved through paving, and are currently subject to use by vehicles louder than passenger vehicles, roadway noise resulting from the Proposed Project would not be a new or significant impact." (Memorandum at 24). However, much of the current road network consists of 72 miles of farm roads (mostly dirt and gravel roads), that, when paved, could become greater movement barriers for many species because of increased noise and/or other reasons listed above. For example, Brehme et al. (2013) found that dirt and secondary roads were more permeable to some small mammals and lizards, while all of the species included in the study avoided the rural 2-lane highway.

The authors state, "All the study species exhibited increased road avoidance and thus experienced decreased connectivity as road improvement and traffic increased." (Brehme, Tracey, Clenaghan, & Fisher, 2013). Similarly, Shilling (2020) and Vickers, (2020) reported preliminary results indicating that species richness along roadways decreased as traffic noise increased. The UC Davis researchers found a significant difference between species richness and species type (mammals), with lower richness and fewer species at crossing structures compared to background areas 1 km away from the roads (Shilling, 2020). They also found that as traffic noises surpassed 60 dBC, the number of visits by small to large mammals decreased and most of the species in their study avoided traffic noise (Shilling, 2020). It is clear that different species have variable sensitivities to noise and light associated with roads and development; this can lead to changes in species distributions near areas with human activity, which can have ecosystem-level impacts (*e.g.*, Suraci et al. 2019). Thus, although these studies were not conducted in the Project area, they are just a few examples that demonstrate that different species have different avoidance behaviors and thresholds with varying levels of disturbance due to roads and development, whether it is from increased noise, traffic, or otherwise. Such impacts to wildlife movement and habitat connectivity should not be dismissed in the EIR.

D. The Board Should Deny the Approval.

We request that the Board deny the requested approvals at the July 21, 2020 hearing, or, at a minimum, continue the hearing and direct the EIR to be revised and recirculated for public review and comment prior to approval of the Project.

Given the possibility that the Center will be required to pursue legal remedies in order to ensure that the County complies with its legal obligations including those arising under CEQA, we would like to remind the County of its duty to maintain and preserve all documents and communications that may constitute part of the "administrative record" of this proceeding. The administrative record encompasses any and all documents and communications that relate to any and all actions taken by the County with respect to the Project, and includes "pretty much everything that ever came near a proposed [project] or [] the agency's compliance with CEQA. . . ." (*County of Orange v. Superior Court* (2003) 113 Cal.App.4th 1, 8.) The administrative record further includes all correspondence, emails, and text messages sent to or received by the County's representatives or employees, that relate to the Project, including any correspondence, emails, and text messages sent between the County's representatives or employees and the Applicant's representatives or employees. Maintenance and preservation of the administrative record requires that, *inter alia*, the County (1) suspend all data destruction policies; and (2) preserve all relevant hardware unless an exact replica of each file is made.

Please do not hesitate to contact the Center with any questions at the number or email listed below.

Sincerely,

Peter J. Broderick
Staff Attorney
Center for Biological Diversity
1212 Broadway, Suite #800
Oakland, CA 94612
Tel: (510) 844-7100
pbroderick@biologicaldiversity.org

cc:
Supervisor Moke Simon – moke.simon@lakecountyca.gov
Supervisor Bruno Sabatier – Bruno.sabatier@lakecountyca.gov
Supervisor Eddie Crandell – eddie.crandell@lakecountyca.gov
Supervisor Tina Scott – tina.scott@lakecountyca.gov
Supervisor Rob Brown – rob.brown@lakecountyca.gov
Principal Planner Mark Roberts – mark.robers@lakecountyca.gov

References

Brehme, C. S., Tracey, J. A., Clenaghan, L. R. M. C., & Fisher, R. N. (2013). Permeability of roads to movement of scrubland lizards and small mammals. *Conservation Biology*, *27*(4), 710–720.

Butscher, C., Huggenberger, P., & Zechner, E. (2011). Impact of tunneling on regional groundwater flow and implications for swelling of clay-sulfate rocks. *Engineering Geology*, *117*(3–4), 198–206.

Loew, S., Luetzenkirchen, V., Ofterdinger, U., Zangerl, C., Eberhardt, E., & Evans, K. (2007). Environmental impacts of tunnels in fractured crystalline rocks of the Central Alps. In *Groundwater in Fractured Rocks* (pp. 507–526). IAH.

Shilling, F. (2020). Wildlife Behavior in Response to Traffic Disturbance Wildlife Behavior in Response to Traffic Disturbance.

Suraci, J. P., Clinchy, M., Zanette, L. Y., & Wilmers, C. C. (2019). Fear of humans as apex predators has landscape-scale impacts from mountain lions to mice. *Ecology Letters*. *22*(10), 1578-1586

Syphard, A. K, Keely, J. E. (2020). Why Are So Many Structures Burning In California? Fremontia, 47(2), 28.

Vickers, T. W. (2020). Project Title: Santa Ana Mountains to eastern Peninsular Range Conservation Connectivity Infrastructure Planning Project for Interstate 15 and Closely Associated Roadways.

Exhibit 1

Conservation Biology

Contributed Paper

Permeability of Roads to Movement of Scrubland Lizards and Small Mammals

CHERYL S. BREHME,* ‡ JEFF A. TRACEY,* LEROY R. McCLENAGHAN,† AND ROBERT N. FISHER*

*Western Ecological Research Center, U.S. Geological Survey, 4165 Spruance Road, Suite 200, San Diego, CA 92101-0812, U.S.A.
†Biology Department, San Diego State University, 5500 Campanile Drive, San Diego, CA 92182-4614, U.S.A.

Abstract: *A primary objective of road ecology is to understand and predict how roads affect connectivity of wildlife populations. Road avoidance behavior can fragment populations, whereas lack of road avoidance can result in high mortality due to wildlife-vehicle collisions. Many small animal species focus their activities to particular microhabitats within their larger habitat. We sought to assess how different types of roads affect the movement of small vertebrates and to explore whether responses to roads may be predictable on the basis of animal life history or microhabitat preferences preferences. We tracked the movements of fluorescently marked animals at 24 sites distributed among 3 road types: low-use dirt, low-use secondary paved, and rural 2-lane highway. Most data we collected were on the San Diego pocket mouse (*Chaetodipus fallax*), cactus mouse (*Peromyscus eremicus*), western fence lizard (*Sceloporus occidentalis*), orange-throated whiptail (*Aspidoscelis hyperythra*), Dulzura kangaroo rat (*Dipodomys simulans*) (dirt, secondary paved), and deer mouse (*Peromyscus maniculatus*) (highway only). San Diego pocket mice and cactus mice moved onto dirt roads but not onto a low-use paved road of similar width or onto the highway, indicating they avoid paved road substrate. Both lizard species moved onto the dirt and secondary paved roads but avoided the rural 2-lane rural highway, indicating they may avoid noise, vibration, or visual disturbance from a steady flow of traffic. Kangaroo rats did not avoid the dirt or secondary paved roads. Overall, dirt and secondary roads were more permeable to species that prefer to forage or bask in open areas of their habitat, rather than under the cover of rocks or shrubs. However, all study species avoided the rural 2-lane highway. Our results suggest that microhabitat use preferences and road substrate help predict species responses to low-use roads, but roads with heavy traffic may deter movement of a much wider range of small animal species.*

Keywords: avoidance, connectivity, conservation planning, habitat fragmentation, heteromyid, reptiles, road ecology, urban ecology

Resumen: *Un objetivo principal de la ecología de caminos es entender y predecir como afectan los caminos la conectividad de las poblaciones silvestres. El comportamiento de evitación de caminos puede fragmentar poblaciones, mientras que la falta de evitación puede resultar en alta mortandad debido a colisiones. Muchas especies animales pequeñas enfocan sus actividades a microhábitats particulares dentro de su hábitat mayor. Buscamos estudiar como los diferentes tipos de caminos afectan el movimiento de pequeños vertebrados y conocer si ciertas respuestas hacia los caminos pueden ser predecibles basándose en la historia de vida del animal o el microhábitat. Rastreamos los movimientos de animales marcados con fluorescencia en 24 sitios distribuidos entre 3 tipos de caminos: tierra de bajo uso, camino secundario pavimentado de bajo uso, y carretera rural de 2 carriles. La mayoría de los datos que colectamos fueron sobre* Chaetodipus fallax, Peromyscus eremicus, Sceloporus occidentalis, Aspidoscelis hyperythra, Dipodomys simulans *(tierra, pavimentación secundaria), y* P. maniculatus *(solamente en carretera).* C. fallax *y* P. eremicus *se movían hacia los caminos de tierra pero no hacia una carretera de baja pavimentación de anchura similar o hacia la carretera, indicando que evitan los caminos con sustrato pavimentado.* S. occidentalis *y* A. hyperythra *se movían hacia la tierra y los caminos secundarios pavimentados pero evitaban la carretera rural de 2 carriles, indicando que pueden evitar el ruido, las vibraciones o el disturbio visual de un constante flujo de tráfico.* D. simulans *no evitaba el camino de tierra ni los caminos secundarios con pavimento. En general, el camino de tierra y los caminos*

‡*email cbrehme@usgs.gov*
Paper submitted August 14, 2012; revised manuscript accepted November 25, 2012.

DOI: 10.1111/cobi.12081

secundarios fueron más permeables para las especies que prefieren forrajear o tomar el sol en áreas abiertas de su hábitat en lugar de bajo rocas o arbustos. D. simulans *no evitó el camino de tierra ni los caminos secundarios pavimentados. Sin embargo todas las especies estudiadas evitaron la carretera de 2 carriles. Nuestros resultados sugieren que las preferencias de uso de microhábitat y sustrato de caminos ayudan a predecir las respuestas de las especies hacia caminos de bajo uso, pero los caminos con tráfico pesado pueden disuadir el movimiento de un rango mucho mayor de especies animales pequeñas.*

Palabras Clave: conectividad, ecología de caminos, ecología urbana, evitación, fragmentación de hábitat, heterómido, planificación de la conservación, reptiles

Introduction

Terrestrial and aquatic areas have become increasingly permeated by roads. Roads affect movement patterns, demographics, and spatial distribution of local species. They can adversely affect wildlife by fragmenting habitats, creating population sinks, and acting as conduits for the spread of invasive species (e.g., Forman et al. 2003; Fahrig & Rytwinski 2009; Taylor & Goldingay 2010). They can positively affect wildlife by increasing connectivity between suitable habitat patches and food resources (e.g., Huey 1941; Getz et al. 1978; Forman et al. 2003).

A current need in the field of road ecology is to understand and predict how roads affect the probability wildlife populations will persist (Roedenbeck et al. 2007; Fahrig & Rytwinski 2009; Rytwinski & Fahrig 2012). This will likely require the development of demographic and spatial-movement models that incorporate behavioral responses to roads (e.g., Jaeger et al. 2005; Tracey 2006; Frair et al. 2008). Roads are highly variable, ranging from rarely traveled dirt roads to multilane highways with heavy traffic. Correspondingly, the responses of animals to different road types are expected to be highly variable.

To address variation in animal responses to different road attributes and traffic patterns, Jaeger et al. (2005) incorporated 3 types of road-specific avoidance behavior (road-surface avoidance related to road substrate and width, and, noise and car avoidance related to traffic) in their model for predicting when animal populations are at risk from roads. However, data to test these models are lacking because much of the current literature on road-related movement behavior typically focuses on either a single species or road type (e.g., Fahrig & Rytwinski 2009; Taylor & Goldingay 2010). There are also relatively few data available on reptiles, although this taxon is thought to be substantially and negatively affected by roads (Andrews et al. 2008). Finally, few researchers have incorporated both multiple road types and taxonomic classes in their studies to ascertain how animal communities respond to these linear features of the landscape.

Scrublands are distributed throughout mid-latitude deserts and areas with Mediterranean-type climates. Scrublands are characterized by low-growing shrubs adapted to arid conditions and range from open habitats with sparse vegetation cover to areas with dense vegetation (Kellman 1980). Our study area was in coastal sage scrubland of southern California (U.S.A.). Much of this area is fragmented by urbanization, disturbed, or permeated with highways, secondary roads, dirt roads, and trails (O'Leary 1995; Noss et al. 2000).

We sought to understand how roads affect habitat connectivity for small vertebrate populations within these scrublands. We assessed the movement patterns of 4 small-mammal species and 2 lizard species relative to 3 types of roads: low-use dirt roads, a secondary paved road, and a primary paved highway. We also examined whether animal responses to roads differed among species with different life-history strategies and whether species' microhabitat-use preferences could be used to predict their responses to roads.

Methods

Study Site

Our study area was in San Diego County, California, within the San Diego National Wildlife Refuge (Otay-Sweetwater Unit) and in Rancho Jamul, a 1915-ha ecological preserve managed by the California Department of Fish and Game. The coastal sage scrub (CSS) vegetation was dominated by California sagebrush (*Artemisia californica*), buckwheat (*Eriogonum fasciculatum*), and a variety of herbs and grasses. The region has a Mediterranean-type climate characterized by hot, dry summers and cool, wet winters. Average annual precipitation is 350 mm, and approximately 95% of the annual mean rainfall occurs from November through April. The CSS vegetation averaged 63% shrub cover, 30% grass and herb cover, and 28% open ground (total greater than 100% due to measures at multiple height categories [Brehme 2003]). There were 3 road types in the study area: 1.8 km of low-use unimproved dirt roads with an average width of 4.7 m (SD 1.3) and traffic volume of 0–20 vehicles/day; a 1.6-km low-use, secondary, 2-lane paved road (Millar Ranch Road) with an average width of 6.6 m (SD 0.2) and traffic volume of 200–500 vehicles/day (Traffic Section of San Diego County Public Works); and over 24 km of high-use, primary, 2-lane paved highway (State Highway 94) with an average width of 11.2 m (SD 0.9) and traffic volume of 7,400–18,000 vehicles/day

(California Department of Transportation). Road widths were measured as the width of grading for dirt roads and width of pavement for paved roads. Native soil or vegetation extended to the road edge for all unimproved and improved road types. During the study, there was no evidence of mowing or other vegetation-management activities.

Data Collection

Eight linear trapping arrays were installed along the length of each of the 3 road types. We chose sites where CSS vegetation extended at least 50 m from both sides of the road to avoid confounding the presence of a road with any other edge. Linear trapping arrays consisted of 3, 9-L pitfall traps connected by a 15-m drift fence (7.5 m between each bucket), 4 Sherman live traps (along both sides of fence halfway between each bucket), and one funnel trap. We baited all traps with birdseed and rolled oats. Arrays were diagonal to the road to increase effectiveness of intercepting animals moving both parallel and perpendicular to the road. At one end of the array, the pitfall trap was 1 m from the road edge, and at the other end, the pitfall trap was 11 m from the road edge. The middle pitfall trap was 5 m from the road edge. Pitfall-array materials and installation procedures are described in Fisher et al. (2008). Trap arrays remained open during each trapping period and were checked every morning at sunrise. We conducted ten 3-night trapping sessions at each array from April to December of 2001.

We used fluorescent-powder tracking (Lemen & Freeman 1985; Fellers & Drost 1989) to track the movements of small mammals and reptiles captured in the trap arrays. The fluorescent powder (Radiant Color, Richmond, California, U.S.A.) is nontoxic and is a safe and effective means of tracking small-scale animal movements (Stapp et al. 1994). The powder-tracking technique allowed us to study species' direct responses to roads. Tracking movements over longer distances and periods of time (e.g., with radiotelemetry) would better document infrequent crossings, but the use of fluorescent dye allows for documentation of fine-scale movement activity that telemetry does not (Lemen & Freeman 1985).

To differentiate among individuals, we dusted each animal released from an array with 1 of 20 base colors or unique mixtures of base colors. We were careful to dust only the body and to avoid the head area to prevent the animal from breathing in the powder (Stapp et al. 1994). Prior to their natural activity period, we placed it on the lid of the center bucket 5 m from the road edge. This allowed for a standard release distance from the road for all animals without the drift fence acting as a barrier to movement in any direction. When releasing an animal, the handler crouched down parallel to the animal and the road, released the animal, slowly backed away staying parallel to the road, and then left the area. This release strategy was to prevent the handler from scaring the animal toward or away from the road. We traced the fluorescent powder tracks at night with a portable 12-watt long-wave ultraviolet lamp. We laid a 50-m measuring tape over the trail until the powder could no longer be traced. For each animal, we recorded the total distance of the fluorescent track and made a diagram of the animal's movements in relation to the road. We recorded locations of burrows where tracks ended at burrow entrances. We tracked the movement of most individuals only one time to avoid problems with pseudoreplication (Hurlbert 1984). We traced a small number of animals on several occasions to examine the variability of results for individuals. For these animals, only the result of their first tracking occasion was used in statistical analyses.

We categorized all movements as either road use or habitat use. Road use was when an animal moved over the road for any distance of the track length. Habitat use was when an animal stayed in the scrubland during the entire tracking period. We included in our analyses only animals tracked for a minimum of 10 m. For the Dulzura kangaroo rat (*Dipodomys simulans*), we included 2 movements of approximately 9.5 m because there were a low number of total tracks. Because all animals were released within 5 m of the road, this minimum track distance allowed us to document movements relative to the road or well away from the array in any direction. We calculated permeability as the number of animals that exhibited road use divided by the total numbers of animals tracked for each species and road type.

Analyses

To test whether animals avoided or used the roads more than expected by chance, we compared observed species movement paths with paths simulated from species-specific correlated random walk (CRW) models. The CRW models represent predicted movement without any behavioral response to the roads. We parameterized CRW models with tracking data from at least 3 individuals of each species. We used only paths within the interior scrubland and well away from the road to represent typical movements within an animal's habitat. We used recorded spatial coordinates at 1.0-m intervals along the path to calculate move and turn angles. The move angle was the direction of movement, and the turn angle was the angle of the current move step minus the angle of the previous move step.

We parameterized the simulations in 2 stages. First, for each individual animal's movement path, we estimated the mean turn angle and concentration parameter that determined the dispersion of a von Mises distribution (Fisher 1993). Second, we fitted a von Mises distribution to the mean turn angles for all paths and a gamma distribution to the concentration parameter of the turn angles for all paths. When simulating a path, we randomly drew a mean turn angle from the von Mises distribution and a concentration parameter from the gamma distribution. We added the turn angle to the move angle of the previous move step to obtain the move angle for the current move step. The move-step length was 1.0 m, and the total length was constrained to the average length of the observed paths for each species. We simulated 1000 paths for each species. To determine the expected number of animal movements onto roads if there was no barrier effect, we determined the number of CRW paths that transected a line 5 m from the start point. We parameterized and simulated all CRW models with a program written in R (R Development Core Team 2010). We compared the number of observed versus expected road movements with Fishers' exact tests. A significant result suggested the animals moved onto roads more or less than expected under the null hypothesis.

Individual animal movement behavior may be affected by population density (Swihart & Slade 1984; Hanski 1999). Therefore, we determined whether relative abundance differed among the roadside habitats with one-way analysis of variation for each species. For our index of species abundance, we used the minimum number of animals known alive. We calculated this index by removing all recaptures within each 3-day trapping session at each array. Although minimum number known alive can be biased as an abundance estimator, it is proportional to population sizes and is thus a reasonable index of abundance (Slade & Blair 2012).

Results

We dusted 306 animals with fluorescent powder and released them 5 m from the road edge. One-third of the animals were not included in our analyses because their track lengths were <10 m. Most of the small mammals that were not used in the analyses were tracked to a nearby burrow on the side of the road on which they were released, and there were no obvious tracks coming out of the burrow. Small reptiles and those with smooth scales (many snakes, skinks, side-blotched lizards [*Uta stansburiana*], and whiptails [*Aspidoscelis* spp.]) did not retain the powder dye well; thus, many of their tracks were lost within several meters. Some species were excluded due to too few captures. The 181 individuals we used in the analyses (125 small mammals, 56 lizards) were followed an average of 20.7 m (SE 0.8).

We also tracked 19 animals on a second occasion to test the repeatability of individual results. All these animals repeated their initial movement types. Seventeen (12 mammals and 5 lizards) stayed within the scrubland on both tracking occasions, whereas 2 (1 mammal and 1 lizard) repeatedly crossed the road. We present the results for 4 small mammal species and 2 lizard species. These species represent movements of 54 San Diego pocket mice (*Chaetodipus fallax*), 57 cactus mice (*Peromyscus eremicus*), 6 Dulzura kangaroo rats (dirt and secondary paved road only), 8 deer mice (*Peromyscus maniculatus*) (highway only), 26 western fence lizards (*Sceloporus occidentalis*), and 30 orange-throated whiptail lizards (*Aspidoscelis hyperythra*) (secondary paved road and highway only).

Small Mammals

San Diego pocket mice were tracked an average distance of 25.1 m (SE 1.6) from the point of release. Species-specific movement simulations predicted a permeability of 42% (percentage of animals moving onto road) if the roads had no effect on movement. Twenty-seven percent of San Diego pocket mice movements were tracked onto the dirt roads (Fisher's exact test, $n = 22$, $p = 0.194$). The majority of these movements (4 out of 5) were crossing events to the habitat on the other side of the road. The percentage of movements onto the secondary road was significantly lower than expected at 9.5% ($n = 21$, $p = 0.003$). The 2 movements onto the secondary road were not crossings, but along the edge of the road returning to the habitat on the same side of the road. There were no movements of San Diego pocket mice onto the primary highway ($n = 11$, $p = 0.004$) (Fig. 1). The relative abundance of pocket mice did not differ significantly among the 3 road types ($F_{2,21} = 1.493, p = 0.248$).

Cactus mice were tracked an average distance of 19.0 m (SE 1.2). Species-specific movement simulations predicted an expected road permeability of 30%. All the movements onto the dirt road were direct crossing events to the other side of the road (Fig. 2). Although 25% of the individuals went onto the dirt road (meaning there was no significant barrier effect [$n = 20$, $p = 0.626$]), no individuals were tracked onto the secondary paved road or primary highway ($n = 18$, $p = 0.003$ and $n = 19$, $p = 0.002$, respectively). Relative abundance of cactus mice did not differ significantly among the 3 road types ($F_{2,21} = 0.676, p = 0.522$).

Dulzura kangaroo rats were tracked an average of 14.6 m (SE 2.4). Movement simulations for this species predicted a road permeability of 41%. Although there were few animals tracked, most of them went onto the roadways. Of the 3 individuals tracked near the dirt road, all went onto the road ($n = 3, p = 0.070$), which indicates the road was more permeable to this species than the surrounding habitat. One individual's burrow entrance was in the middle of the roadway. Two out of 3 individuals tracked went onto the secondary paved road ($n = 3, p = 0.572$), which indicates this road was not a barrier to movement. One individual ran along the length of the road and the other crossed the road (Fig. 3).

Deer mice were tracked adjacent to the highway for an average length of 19.9 m (SE 2.3). Species-specific

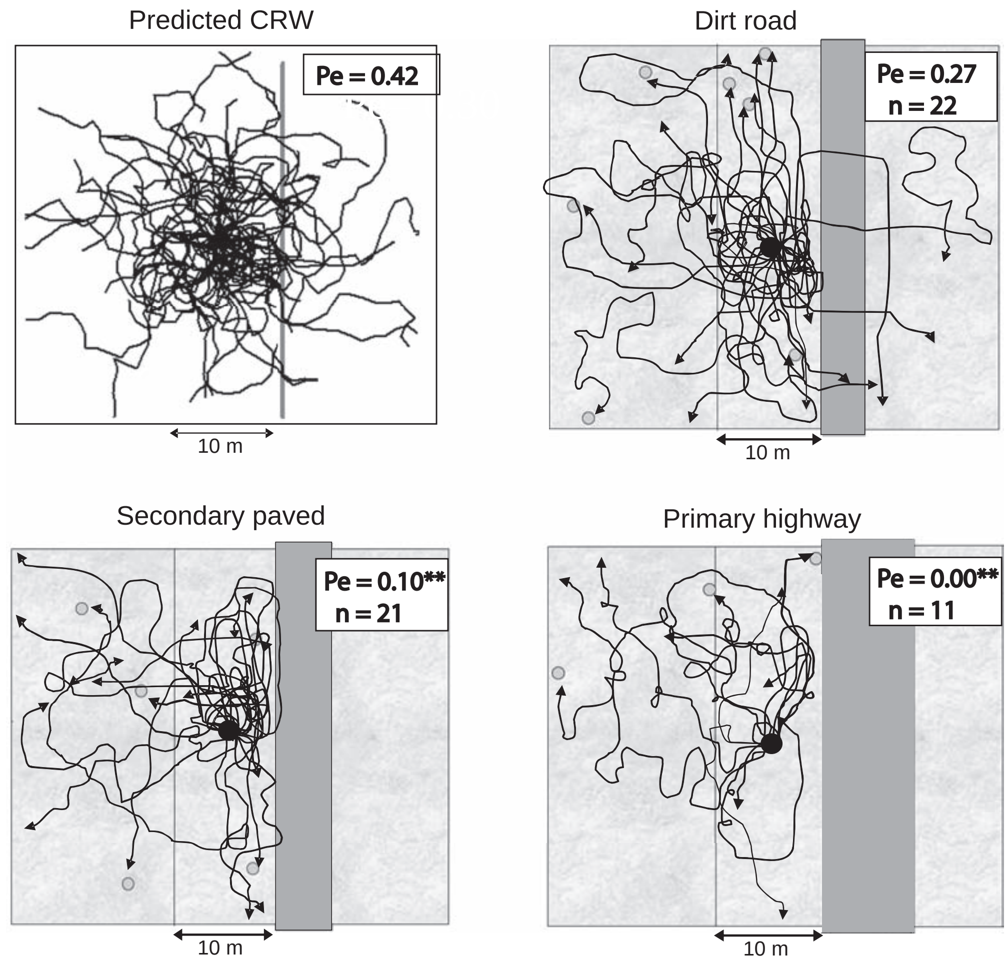

Figure 1. Predicted (correlated random walk, CRW) and observed permeability (Pe) of road types to movement of the San Diego pocket mouse (Chaetodipus fallax). Each drawing shows movements tracked at multiple independent release sites superimposed onto a single frame (gray circles, burrows; $^{**}p < 0.01$).

movement simulations predicted a road permeability of 37%. No deer mice went out onto the road, which indicates the rural highway was a significant barrier for this species ($n = 8, p = 0.030$). Many individuals were tracked to burrow entrances that were within a few meters of the road.

Lizards

Western fence lizards were tracked an average distance of 17.4 m (SE 2.2) from point of release. Species-specific movement simulations predicted an expected road permeability of 31%. The permeability of the dirt roads to movement of western fence lizards was higher than expected; 66% of lizards went onto the dirt road ($n = 9$, $p = 0.030$). These were a mixture of crossing events and movement along the road. A high percentage (56%) of individuals also went onto the secondary paved road ($n = 9$, $p = 0.146$). These movements were all along the road and no crossing events were recorded. However, most of these tracks were lost on the pavement, so we could not determine which side of the road the animal went to. In comparison, not a single western fence lizard went onto the highway (Fig. 4). Although permeability between the expected and observed values for the highway was not significant ($n = 6, p = 0.186$), the permeability of the highway to fence lizard movements was significantly lower than permeability of the dirt ($p = 0.028$) and secondary paved roads ($p = 0.044$) to movements of fence lizards. Their relative abundance did not differ among road types ($F_{2,21} = 0.006, p = 0.994$).

Movement simulations predicted road permeability of 31% for orange-throated whiptail if the roads had no effect on movement behavior. The average track length was 17.0 m (SE 1.3) by the secondary and primary paved roads. Although 33.3% of orange-throated whiptails crossed the secondary paved road ($n = 6$, $p = 1.00$), none were tracked out onto the highway ($n = 24$, $p \leq 0.001$) (Fig. 5). Only one whiptail was captured by the dirt road, and its track length was <10 m. Whiptail abundance next to the paved road and highway did not differ significantly ($t_{14} = 1.612, p = 0.129$). However, the

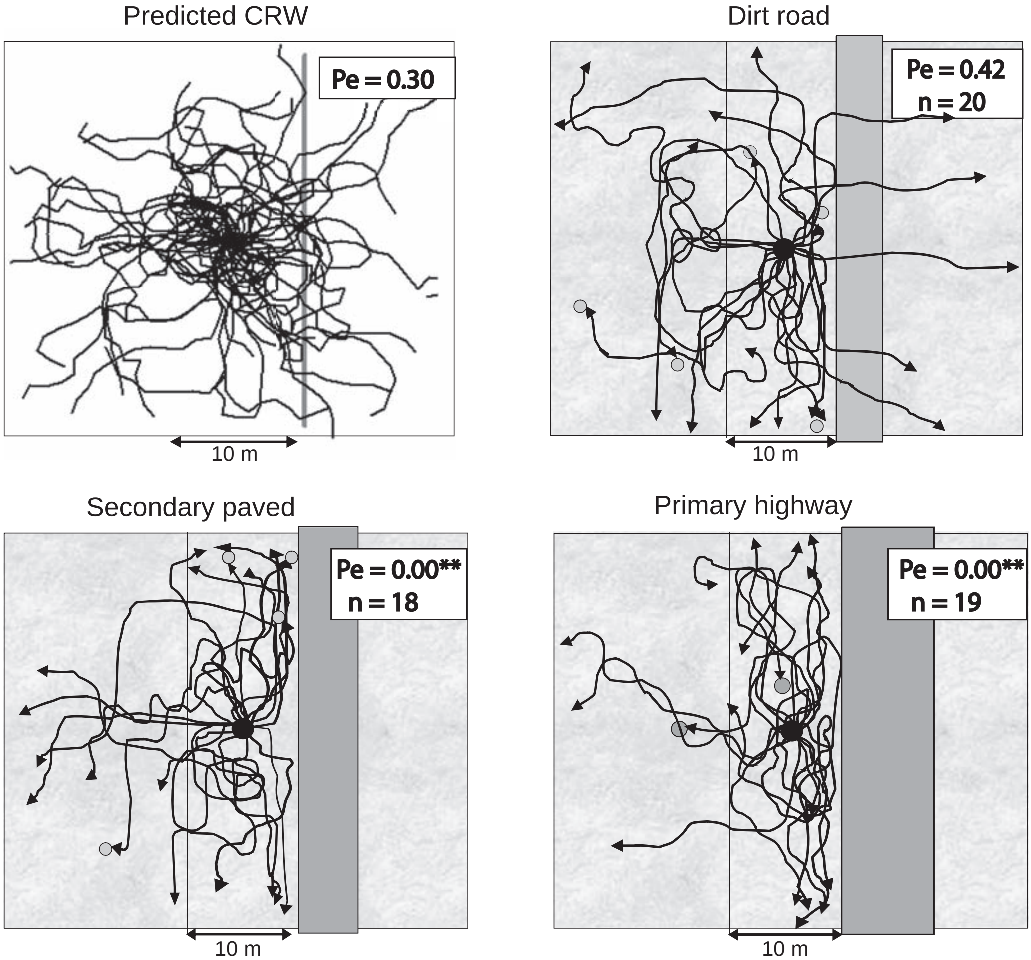

Figure 2. Predicted (correlated random walk, CRW) and observed permeability (Pe) of road types to movement of the cactus mouse (Peromyscus eremicus). Each drawing shows movements tracked at multiple independent release sites superimposed onto a single frame (gray circles, burrows; $^{**}p < 0.01$).

success rate in tracking the whiptail for distances >10 m was significantly greater by the highway (24/32) than by the paved road (6/20, $p = 0.002$).

Discussion

Although they live in open scrub habitats, San Diego pocket mice and cactus mice prefer to move and forage under microhabitats of shrub and rock cover rather than open areas (Meserve 1976; Price & Kramer 1984). Thus, they may quickly pass through or avoid areas of open ground. This is consistent with their movements relative to the dirt road, which were primarily direct crossings to shrub and rock cover on the other side of the road. One cactus mouse crossed the dirt road on 2 occasions. This result indicates the dirt road was within its home range. In contrast to the dirt road, there were no documented movements of either species across the secondary paved road or highway even though the distances required to cross either road were well under the average tracked distances of the species. The secondary road differed from the dirt roads by an average added width of 1.9 m, the addition of pavement, and an increased traffic volume averaging one vehicle every 5 minutes. It is unknown which of these factors or combination thereof resulted in their avoidance of this road. However, because of the low traffic volume and little difference in width, it is likely that these species were avoiding the road substrate. White-footed mice (*Peromyscus leucopus*) and eastern chipmunks (*Tamias striatus*) avoid crossing paved roads regardless of traffic volume (McGregor et al. 2008). By comparing roads with different substrates and traffic volumes, our results support the hypothesis that many small mammal species avoid paved road substrates. The reasons for this are not understood and deserve further study. However, mammals are particularly sensitive to odors in their environment. Road pavement surfaces, such as asphalt and coal tar, contain complex mixtures of volatile and non-volatile compounds. Even very minute concentrations of smells and chemicals that mimic pheromones may elicit instinctive behavioral

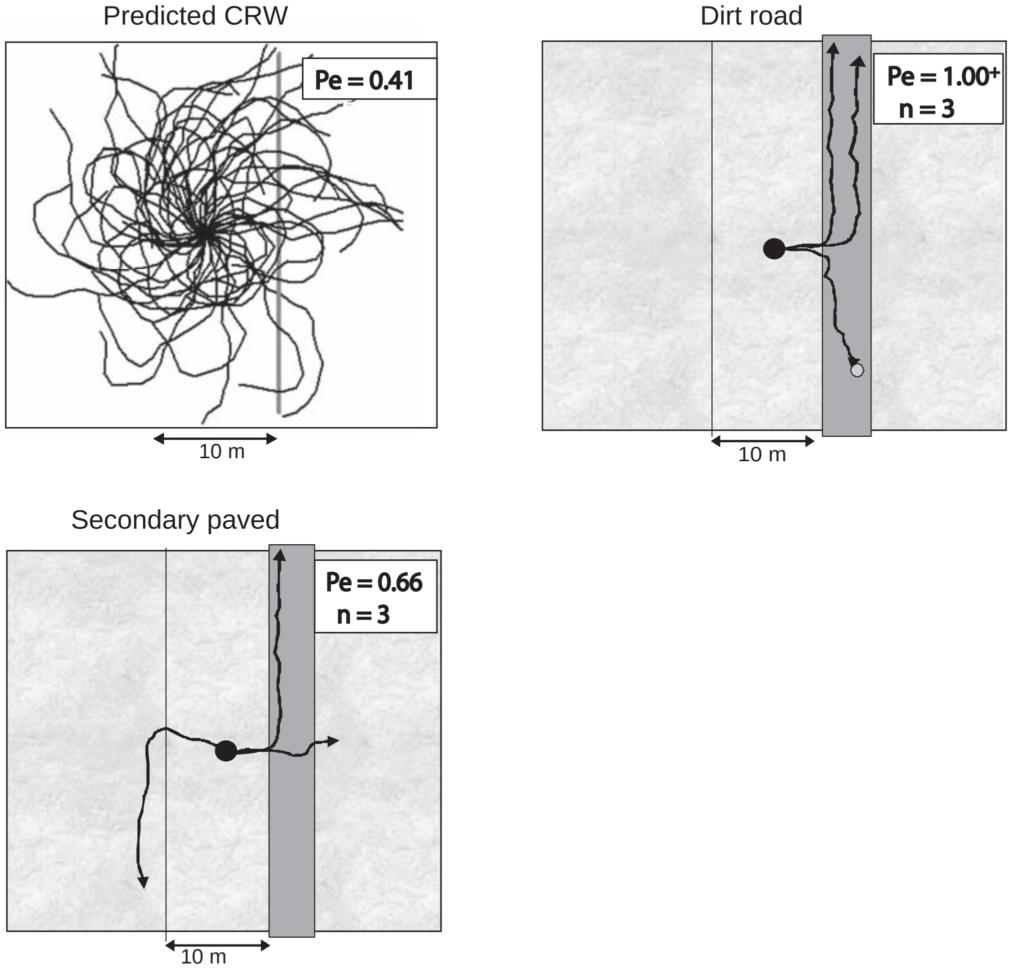

Figure 3. Predicted (correlated random walk, CRW) and observed permeability (Pe) of road types to movement of Dulzura kangaroo rat (Dipodomys simulans). Each drawing shows movements tracked at multiple independent release sites superimposed onto a single frame (gray circle, burrows; +p < 0.10).

responses in some species (e.g., Leinders-Zufall et al. 2000).

However, the avoidance of pavement is not generalizable to all species of small mammals. The yellow-necked mouse (*Apodemus flavicollis*) regularly crossed both dirt and paved roads of similar width (Rico et al. 2007). In our study, 2 out of 3 Dulzura kangaroo rats went out onto the secondary paved road. Although we did not capture any Dulzura kangaroo rats by the highway, this species accounted for the majority of dead animals we observed on the highway (3 out of 7) (Brehme 2003), which indicates the highway was also somewhat permeable to movement for this species. The higher than expected permeability of dirt roads to movements of the Dulzura kangaroo rat is consistent with results of a previous study on the Stephens' kangaroo rat (*D. stephensi*) (Brock & Kelt 2004). Kangaroo rats may preferentially use dirt roads for movement within their habitat. These bipedal heteromyids prefer to move and forage within open-ground areas of scrub habitats and respond positively to disturbances such as fire (e.g., Meserve 1976; Price & Kramer 1984; Brehme et al. 2011). In areas with denser vegetation, low-use dirt roads and trails may provide an increased opportunity for kangaroo rats to disperse to open scrub habitats. Alternately, we would expect negative effects from high-traffic roads on kangaroo rats. Traffic noise can disrupt communication in kangaroo rats (Shier et al. 2012) and nonavoidance of these roads would very likely result in increased mortality rates from vehicular traffic.

Because many reptiles may be attracted to open spaces and paved surfaces for thermoregulatory purposes, it is often hypothesized that these animals do not avoid roads (e.g., Klauber 1939; Jochimsen et al. 2004; Andrews et al. 2008). The dirt and secondary paved roads in our study were highly permeable to movement of western fence lizards (67% and 56%, respectively). Their movements on the dirt roads consisted of crossings and movements along the road; thus, the road was in part used as a conduit for movement. In contrast, their

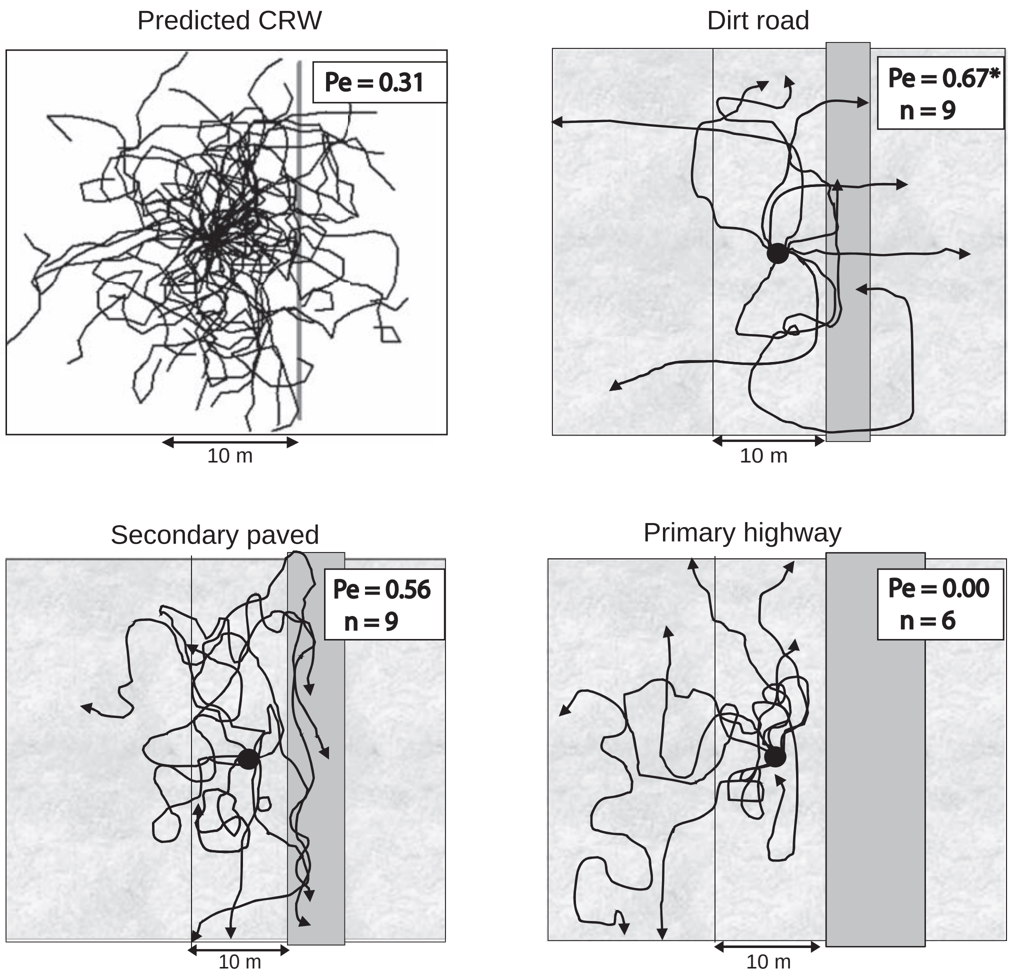

Figure 4. Predicted (correlated random walk, CRW) and observed permeability (Pe) of road types to movement of the western fence lizard (Sceloporus occidentalis). Each drawing represents movements tracked at multiple independent release sites that are superimposed onto a single frame ($^{*}p < 0.05$).

movements on the secondary road were often erratic and irregular along the road edge. This suggests the paved road was used for basking which was regularly observed during the study. The complete absence of movements onto the highway was in stark contrast to their response to the dirt and secondary paved roads. Similarly, although the secondary road was permeable to movement of the orange-throated whiptail, this species also completely avoided the highway.

Delaney et al (2010) found that genetic diversity is lower in populations of western fence lizards that are separated by a highway than in populations in continuous habitat. Because of the high permeability of the secondary paved road to these 2 species, we think it is unlikely that the additional width of the highway (4.6 m) alone adequately explains their marked avoidance of the highway. However, the level of traffic (average 1 vehicle/7 seconds) was 40-fold higher on the highway than on the secondary paved road; thus, the constant stream of vehicular traffic and corresponding noise and vibration may have been sufficient to deter use of the highway. On the basis of our own literature search and recent reviews on responses of reptiles to roads (Andrews et al. 2008; Rytwinski & Fahrig 2012), we believe ours is the first study to document behavioral road avoidance in lizards.

All the study species exhibited increased road avoidance and thus experienced decreased connectivity as road improvement and traffic increased. By studying both small mammals and reptiles we were able to make direct comparisons of behavior between taxa with different microhabitat preferences and life-history strategies. Species microhabitat-use preferences within their habitat may be an important predictive factor for road permeability (Fig. 6). Animals that are more likely to focus their activities in open areas within their habitat were more likely to venture out onto low-use roads. In our study, the 3 species (Dulzura kangaroo rat, western fence lizard, orange-throated whiptail) that use open areas for foraging

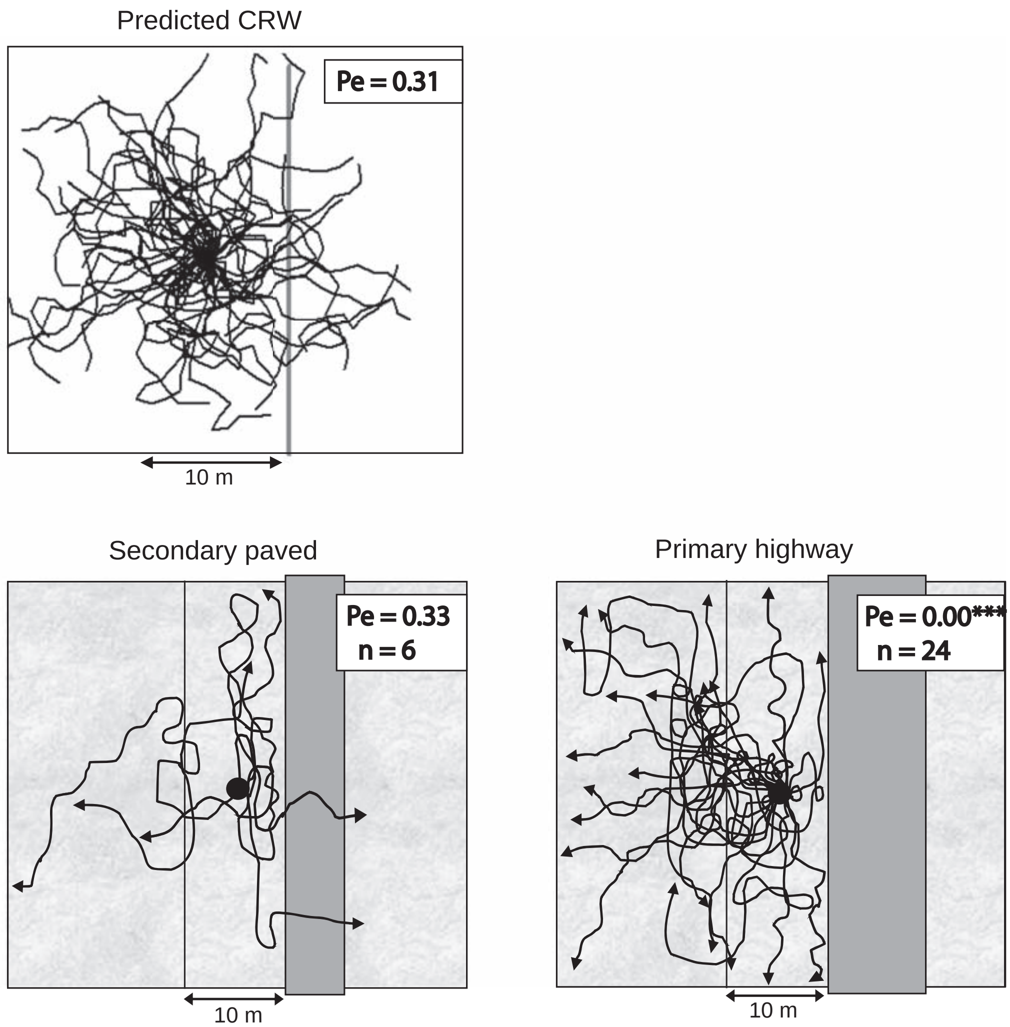

Figure 5. Predicted (correlated random walk, CRW) and observed permeability (Pe) of road types to movement of orange-throated whiptail lizard (Aspedoscelis hyperythra). Each drawing shows movements tracked at multiple independent release sites superimposed onto a single frame ($^{***}p < 0.001$).

or thermoregulation ventured onto dirt and secondary paved roads more than the species (San Diego pocket mouse, cactus mouse) that prefer to forage within or under the cover of rocks and shrubs.

Thus, one would predict that the populations of small animals with closed microhabitat preferences would be in most danger of becoming fragmented by any type of road. For instance, small mammal and reptile species that avoid open ground, such as the cotton rat (*Sigmodon hispidus*), prairie vole (*Microtus ochrogaster*), Eastern massasauga rattlesnake (*Sistrurus c. catenus*), rosy boa (*Lichanura trivirgata*), and many rainforest species, avoid crossing even narrow dirt roads (Swihart & Slade 1984; Weatherhead & Prior 1992; Goosem 2001; Rochester et al. 2005). Whereas generalist species and those with open microhabitat preferences would be more likely to cross roads, use roads for activity, and as conduits for movement. However, even these species may avoid roads with heavy traffic due to the constant disturbance from noise, vibrations, and lights. Therefore, roads with moderate traffic would be expected to pose the greatest risk of vehicular mortality for generalists and open microhabitat specialists due to the use of roads by both animals and vehicles (Seiler 2003). Our results pertain to small mammals and lizards with home ranges that are small relative to the road matrices within the study area. It is expected that movements onto roads would be more common for animals that make long migratory movements or that have large home ranges relative to the road matrices within their habitat.

Our results show that a 2-lane rural highway through open scrubland can create a significant movement barrier for species of small mammals and reptiles. Behavioral mechanisms appear to be road surface avoidance for some small mammal species and traffic avoidance for lizard species. Avoidance of improved roads may be a beneficial response in that mortality from vehicular traffic is avoided or minimized. However, networks of

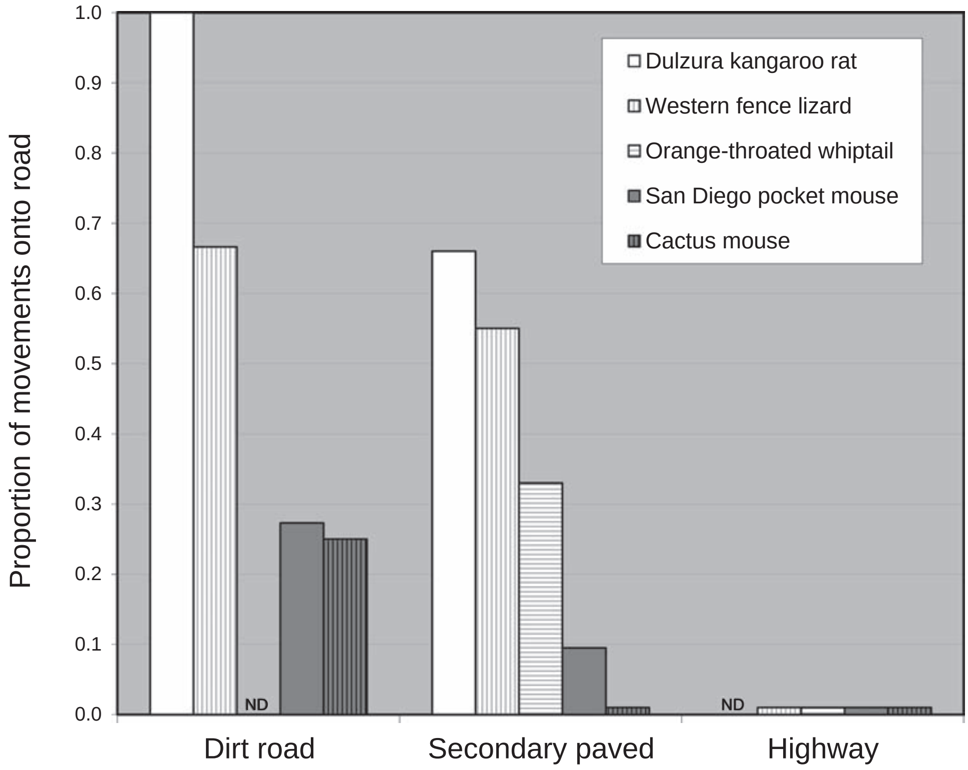

Figure 6. Road permeability relative to species microhabitat-use preferences (white bars, species that typically forage in and use open areas of their habitat; gray bars, species that primarily forage under vegetation cover; ND, no data for species at specific road type). Expected permeability range 0.30–0.41 with no road response.

roads throughout a landscape may divide habitat into fragments that are too small to sustain some populations over the long term. Barrier fencing and safe-crossing structures may reduce the effects of habitat fragmentation for species that avoid roads and reduce road mortality for species that do not avoid roads (e.g., Boarman & Sazaki 1996; Dodd et al. 2004).

More research is needed to determine whether road response patterns are consistent across other habitats and small animal species, whether microhabitat-use preferences can also help predict the use of road-crossing structures, and to further understand the population-level effects of movement-behavior decisions (Fahrig 2007; Rytwinski & Fahrig 2012). If generalizations are found, they will help us to identify vulnerable species and potentially detrimental roads within their habitat, inform population and spatial-movement models, and inform management decisions and mitigation measures for both studied and unstudied species.

Acknowledgments

We thank J. Diffendorfer and J. O'Leary for guidance throughout the project. This manuscript was improved by the helpful comments of S. Riley, E. Boydston, D. Ouren, K. Miles, and an anonymous reviewer. We thank D. Palmer, K. Sullivan, S. Millus, A. Holman, S. Black, J. Ordonio, D. Stokes, C. Rochester, S. Hathaway, A. Atkinson, W. Boarman, C. Haas, M. Mendelsohn, R. Lovich, A. Hebbert, A. Herring, and D. Clark for field and other project assistance. We are grateful to A. Pigniolo for conducting the archaeological survey. Finally, we thank Caltrans, California Department of Fish and Game, and the U.S. Fish and Wildlife Service for allowing us to conduct this study on their lands. The use of trade, product, or firm names in this publication does not imply endorsement by the U.S. Government.

Literature Cited

Andrews, K. M., J. W. Gibbons, and D. M. Jochimsen. 2008. Ecological effects of roads on amphibians and reptiles: a literature review. Pages 121–143 in J. C. Mitchell, R. E. Jung Brown, and B. Bartholomew, editors. Urban herpetology. Society for the Study of Amphibians and Reptiles, Salt Lake City, Utah.

Boarman, W. I., and M. Sazaki. 1996. Highway mortality in desert tortoises and small vertebrates: success of barrier fences and culverts. Pages 169–173 in G. Evink, D. Ziegler, P. Garret, and J. Berry, editors. Highways and movement of wildlife. Report FHWA-PD-96–041. Florida Department of Transportation, Orlando.

Brehme, C. S. 2003. Responses of terrestrial vertebrates to roads in a coastal sage scrub ecosystem. MS thesis. San Diego State University, San Diego, California.

Brehme, C. S., D. R. Clark, C. J. Rochester, and R. N. Fisher. 2011. Wildfires alter rodent community structure across four vegetation types in southern California, USA. Fire Ecology **7:**81–98.

Brock, R. E., and D. A. Kelt. 2004. Influence of roads on the endangered Stephens' kangaroo rat (*Dipodomys stephensi*): Are dirt and gravel roads different? Biological Conservation **118:**633–640.

Delaney, K. S., S. P. D. Riley, and R. N. Fisher. 2010. A rapid, strong, and convergent genetic response to urban habitat fragmentation in four divergent and widespread vertebrates. PLoS ONE 5(9): e12767. DOI: 10.1371/journal.pone.0012767.

Dodd, N., W. J. Barichivich, and L. L. Smith. 2004. Effectiveness of a barrier wall and culverts in reducing wildlife mortality on a heavily traveled highway in Florida. Biological Conservation **118:**619–631.

Fahrig, L. 2007. Non-optimal animal movement in human-altered landscapes. Functional Ecology **21:**1003–1015.

Fahrig, L., and T. Rytwinski. 2009. Effects of roads on animal abundance: an empirical review and synthesis. Ecology and Society **14**. Available from http://www.ecologyandsociety.org/vol14/iss1/art21/ (accessed May 2013).

Fellers, G. M., and C. A. Drost. 1989. Fluorescent powder- a method for tracking reptiles. Herpetological Review **20:**91–92.

Fisher, N. I. 1993. Statistical analysis of circular data. Cambridge University Press, Cambridge, United Kingdom.

Fisher, R., D. Stokes, C. Rochester, C. Brehme, S. Hathaway, and T. Case. 2008. Herpetological monitoring using a pitfall trapping design in southern California. Techniques and methods 2-A5. U.S. Geological Survey, Reston, Virginia. Available from http://pubs.usgs.gov/tm/tm2a5/ (accessed January 2013).

Forman, R. T., et al. 2003. Road ecology: science and solutions. Island Press, Washington, D.C.

Frair, J. L., E. H. Merrill, H. L. Beyer, and J. M. Morales. 2008. Thresholds in landscape connectivity and mortality risks in response to growing road networks. Journal of Applied Ecology **45:**1504–1513.

Getz, L. L., F. R. Cole, and D. L. Gates. 1978. Interstate roadsides as dispersal routes for *Microtus pennsylvanicus*. Journal of Mammology **59:**208–212.

Goosem, M. 2001. Effects of tropical rainforest roads on small mammals: inhibition of crossing movements. Wildlife Research **28:**351–364.

Hanski, I. 1999. Metapopulation ecology. Oxford University Press, Oxford, United Kingdom.

Huey, L. M. 1941. Mammalian invasion via the highway. Journal of Mammology **22:**383–385.

Hurlbert, S. H. 1984. Pseudoreplication and the design of ecological field experiments. Ecological Monographs **54:**187–211.

Jaeger, J. A. G., J. Bowman, J. Brennan, L. Fahrig, D. Bert, J. Bouchard, N. Charbonneau, K. Frank, B. Gruber, and K. Tluk von Toschanowitz. 2005. Predicting when animal populations are at risk from roads: an interactive model of road avoidance behaviour. Ecological Modeling **185:**329–348.

Jochimsen, P. M., C. R Peterson, K. M. Andrews, and J. W. Gibbons. 2004. A literature review of the effects of roads on amphibians and reptiles and the measures used to minimize those effects. Idaho Fish and Game Department, Boise; U.S. Department of Agriculture Forest Service, Washington, D.C.

Kellman, M. C. 1980. Plant geography. 2nd edition. Palgrave Macmillan, New York.

Klauber, L. M. 1939. Studies of reptile life in the arid southwest. Bulletin of the Zoological Society of San Diego **14:**2–64.

Leinders-Zufall, T., A. P. Lane, A. C. Puche, W. Ma, M. Novotny, M. T. Shipley, and F. Zufall. 2000. Ultrasensitive pheromone detection by mammalian vomeronasal neurons. Nature **405:**792–796.

Lemen, C. A., and P. W. Freeman. 1985. Tracking mammals with fluorescent pigments: a new technique. Journal of Mammology **66:**134–136.

McGregor, R. L., D. J. Bender, and L. Fahrig. 2008. Do small mammals avoid roads because of traffic? Journal of Applied Ecology **45:** 117–123.

Meserve, P. L. 1976. Habitat and resource utilization by California rodents. Journal of Animal Ecology **45:**647–666.

Noss, R. F., E. T. LaRoe III, and M. J. Scott. 2000. Endangered ecosystems of the United States: a preliminary assessment of loss and degradation. 28. National Biological Service, Washington, D.C.

O'Leary, J. F. 1995. Coastal sage scrub: threats and current status. Fremontia **23:**27–31.

Price, M. V., and K. A. Kramer. 1984. On measuring microhabitat affinities with special reference to small mammals. Oikos **42:**349–354.

R Development Core Team. 2010. R: a language and environment for statistical computing. R Foundation for Statistical Computing, Vienna.

Rico, A., P. Kindlmann, and F. Sedlacek. 2007. Barrier effects of roads on movements of small mammals. Folia Zoologica **56:**1–12.

Rochester, C. J., R. N. Fisher, and J. E. Diffendorfer. 2001. Natural history of the rosy boa (Charina trivergata). U.S. Geological Survey Technical Report. San Diego, California.

Roedenbeck, I. A., L. Fahrig, C. S. Findlay, J. E. Houlahan, J. A. G. Jaeger, N. Klar, S. Kramer-Schadt, and E. A. Van der Grift. 2007. The Rauischholzhausen agenda for road ecology. Ecology and Society **12**. Available from http://www.ecologyandsociety.org/vol12/iss1/art11/. (accessed May 2013)

Rytwinski, T., and L. Fahrig. 2012. Do species life history traits explain population responses to roads? A meta-analysis. Biological Conservation **147:**87–98.

Seiler, A. 2003. The toll of the automobile: wildlife and roads in Sweden. PhD dissertation. Swedish University of Agricultural Sciences, Uppsala.

Shier, D. M., A. J. Lea, and M. A. Owen. 2012. Beyond masking: endangered Stephens' kangaroo rats respond to traffic noise with footdrumming. Biological Conservation **160:**63–68.

Slade, N. A., and S. M. Blair. 2012. An empirical test of using counts of individuals captured as indices of population size. Journal of Mammalogy **81:**1035–1045.

Stapp, P., J. K. Young, S. Vandewoude, and B. Van Horne. 1994. An evaluation of the pathological effects of fluorescent powder on deer mice (*Peromyscus maniculatus*). Journal of Mammalogy **75:**704–709.

Swihart, R. K., and N. A. Slade. 1984. Road crossing in *Sigmodon hispidus* and *Microtus ochrogaster*. Journal of Mammalogy **65:**357–360.

Taylor, B. D., and R. L. Goldingay. 2010. Roads and wildlife: impacts, mitigation and implications for wildlife management in Australia. Wildlife Research **37:**320–331.

Tracey, J. A. 2006. Individual-based modeling as a tool for conserving connectivity. Pages 343–368 in K. R. Crooks and M. Sanjayan, editors. Connectivity conservation. Cambridge University Press, Cambridge, United Kingdom.

Weatherhead, P. J., and K. A. Prior. 1992. Preliminary observations of habitat use and movements of the eastern massasauga rattlesnake (*Sistrurus c. catenatus*). Journal of Herpetology **26:** 447–452.

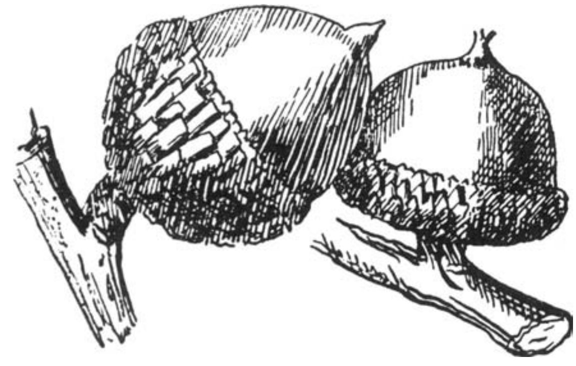

Exhibit 2

Engineering Geology 117 (2011) 198–206

Contents lists available at ScienceDirect

Engineering Geology

journal homepage: www.elsevier.com/locate/enggeo

Impact of tunneling on regional groundwater flow and implications for swelling of clay–sulfate rocks

Christoph Butscher *, Peter Huggenberger, Eric Zechner

University of Basel, Institute of Geology and Paleontology, Applied and Environmental Geology, Bernoullistrasse 32, 4056 Basel, Switzerland

A R T I C L E I N F O

Article history:
Received 22 July 2010
Received in revised form 18 October 2010
Accepted 23 October 2010
Available online 31 October 2010

Keywords:
Regional groundwater flow
Groundwater modeling
Tunnel engineering
Swelling
Clay–sulfate rocks

A B S T R A C T

Tunnels play a key role in many transportation concepts. The swelling of clay–sulfate rocks leads to serious damage to many tunnels crossing such rock, producing great difficulties and high extra costs in tunnel engineering. The swelling is caused by the transformation of the sulfate mineral anhydrite into gypsum, entailing a 60% volume increase. The transformation involves anhydrite dissolution in water, transport of the solution with groundwater flow, and gypsum precipitation at a different location. Therefore, the knowledge of groundwater flow systems at the tunnel and adjacent areas is essential to better understand the swelling processes. The present study investigates the groundwater flow systems at the Chienberg tunnel in Switzerland before and after the tunnel excavation, based on numerical flow modeling. The models include faults and the hydrostratigraphic layering in the subsurface to assess the role of the hydrogeological setting. The results of this study indicate effects on groundwater flow caused by the tunneling, which may trigger rock swelling by favoring anhydrite dissolution and gypsum precipitation, including (1) increase of flow rates around the tunnel, (2) broadened, shifted and more distributed capture zones leading to a change in origin and age of groundwater, (3) access of groundwater from preferential flow paths (e.g. faults) due to the drainage effect of the tunnel, and (4) change in geochemical equilibrium conditions because of decreased pore water pressures in the tunnel area.

1. Introduction

Efficient transport strongly relies on road and railway tunnels, both in long-distance traffic (e.g., European alpine transit) and in metropolitan areas. The swelling of clay–sulfate rocks poses a severe threat to this important infrastructure. The problems associated with swelling clay–sulfate rocks are well known in tunnel engineering (Einstein, 1996): The swelling may result in a heave of the tunnel floor, destruction of the lining or uplift of the entire tunnel section, producing major difficulties and high additional costs during tunnel construction and maintenance. Worldwide, extensive repair work in tunnels due to the swelling of clay–sulfate rocks was, and still is, necessary. European examples include several tunnels in the Jura Mountains in Switzerland (e.g., Belchen, Chienberg, Adler tunnel), and tunnels around the Stuttgart metropolitan area in southern Germany (e.g., Wagenburg, Engelberg, Freudenstein tunnel). In these examples, the difficulties are associated mainly with the Triassic Gipskeuper ("Gypsum Keuper") Formation.

The threats imposed by swelling clay–sulfate rocks in tunneling are mostly counteracted on an engineering level by constructive measures. Measures include either the application of a strong, rigid supporting formwork to limit deformation, or allowing floor heave in an excavated zone under the tunnel floor to limit swelling pressures (Pierau and Kiehl, 1996). Other authors suggest combining both strategies by implementing a deformable zone (Kovári and Chiaverio, 2007). However, there is no consensus among experts as to which measure is most appropriate. The reason for this lack of consensus is the limited understanding of the involved processes during swelling in such rock (Anagnostou, 2007). To date, there is no accepted relation describing the swelling heave as a function of swelling pressure in clay–sulfate rocks. Field and laboratory measurements often give contradictory indications of the magnitude of swelling heaves and pressures (Madsen and Nüesch, 1991; Nüesch et al., 1995; Pimentel, 2007), and the results from one site cannot directly be transferred to other sites. For these reasons, reliable predictions of expected swelling heaves and pressures at an actual construction project are not yet possible.

Generally, the swelling is caused by the transformation of anhydrite into gypsum under water uptake (hydration of anhydrite). Gypsum is subject to a 60% increase in volume, compared to anhydrite. An important reason for the uncertainties described above is the fact that the transformation of anhydrite into gypsum does not take place directly, but indirectly via anhydrite solution, followed by gypsum precipitation (Jeschke et al., 2001). Between dissolution and re-precipitation, the solutes are transported with groundwater flow, i.e., dissolution and precipitation occurs at different locations.

Rock swelling does not occur every time a tunnel is constructed in clay–sulfate rocks. An explanation for this is provided by the

* Corresponding author. Tel.: +41 61 267 34 47; fax: +41 61 267 29 98.
E-mail address: christoph.butscher@unibas.ch (C. Butscher).

0013-7952/$ – see front matter © 2010 Elsevier B.V. All rights reserved.
doi:10.1016/j.enggeo.2010.10.018

fundamental work of Tóth (1999). He demonstrated that geochemical conditions in the subsurface, such as redox potential, pH and ion concentrations, depend on groundwater residence times and flow patterns or, generally, on the hydrogeological setting. The regional groundwater flow system is therefore a key factor controlling dissolution and precipitation of the sulfate minerals in clay–sulfate rocks, and the knowledge of hydraulic head field at a regional scale is a major requirement for understanding the swelling phenomena. In spite of the important role of the groundwater system in understanding the swelling processes in clay–sulfate rocks, the relation between hydrogeological setting and swelling has not been investigated so far.

Because swelling often starts immediately after tunnel excavation, fast changes in the groundwater flow system are likely to be responsible for the observed swelling phenomena. The generation of fractures in the excavation damaged zone (Tsang et al., 2005) around the tunnel, which is induced by the tunnel excavation and resulting stress redistribution, involves a sudden increase of rock permeability. In addition, atmospheric pressures exist at the tunnel walls after tunnel excavation, leading to a decrease in pore water pressure around the tunnel. The effect of these changes induced by the tunnel excavation on the regional flow field is an important issue to be evaluated in detail, because changes in regional groundwater flow may significantly change the geochemistry of the pore water. For example, these changes my produce rapid access of meteoric surface water or formation water with relatively low ion concentrations to the clay–sulfate rocks.

This study investigates the effects of a tunnel excavation on regional groundwater flow systems depending on the hydrogeological setting. The aim is to provide a conceptual framework to define the relations between morphological, hydrological and geological structures and rock swelling. These relations are a first step towards understanding the complex coupled hydraulic-mechanical and geochemical processes that occur during rock swelling. The overall aim is to contribute to an improved scientific basis for decisions made during project planning, cost planning and realization of tunnel projects in clay–sulfate rocks.

2. Methodology

2.1. Test site

The test site of the present study is the Chienberg road tunnel, which was built between 2000 and 2006 to bypass the town of Sissach in Switzerland (Figure 1). Already during construction of the tunnel, major problems occurred with the swelling of clay–sulfate rocks of the Gipskeuper ("Gypsum Keuper") Formation. During a lengthy interruption of the excavation, the open floor of the tunnel experienced a heave of about 1.5 m within three months at the top heading. The swelling continued after the installation of the supporting formwork and lead also to heaves of the ground surface above the tunnel, hence, causing damage to houses. Observable swelling phenomena are restricted to two separate sections of the tunnel. Other sections that also cut the Gipskeuper Formation are, until date, not subject to swelling. Expensive countermeasures, including the construction of a deformable zone under the road surface, have been successfully implemented to prevent further heave of the road surface in the tunnel and the ground surface above (Kovári and Chiaverio, 2007). The swelling process in the deformable zone, however, continues to date.

The study area is part of the Swiss Jura Mountains. The Jura Mountains are subdivided into the Tabular Jura in the North, and the Folded Jura in the South (c.f. Figure 1). The Folded Jura is thrusted northward over the Tabular Jura. The Chienberg tunnel is located in the Tabular Jura near to the main thrust of the Folded Jura. The geological units of the Jura Mountains comprise Triassic and Jurassic sediments of varying hydraulic permeability overlying a pre-Mesozoic

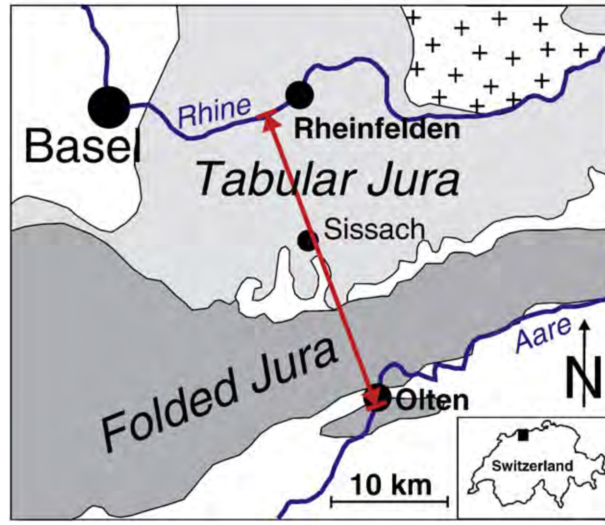

Fig. 1. Study area and location of the cross-section of Fig. 2 (arrow).

basement (Figures 2 top and 3). The units of the Tabular Jura are nearly flat lying and have experienced an extensional deformation, resulting in mainly SSW–NNE oriented horst and graben structures. The units of the Folded Jura were deformed under compressional conditions, resulting in W–E oriented folds and thrusts.

The tunnel crosses Quaternary sediments near the surface, and Mesozoic bedrock with a stratigraphic extent reaching from the Gipskeuper Formation (bottom) to the Opalinus Clay Formation (top). The Quarternary sediments consist of fluvio-glacial gravels close to the valley of the nearby river Ergolz, and colluvium at the slopes of the hill Chienberg. The Mesozoic bedrock is dominated by argillaceous marlstone with some dolomitic interbeds. Large parts of the tunnel cross the Gipskeuper Formation, containing the sulfate minerals anhydrite and gypsum. These minerals appear as thin layers, nodules and veins, as well as finely dispersed in a clay–marlstone rock matrix. Close to the surface, the sulfate minerals are often leached.

2.2. Model concept

The hierarchical nature of the topography leads to a hierarchical pattern of flow systems: Generally, regional, intermediate and local flow systems can be distinguished. Groundwater flow at a certain location can be described as a superposition of these topographically driven systems (Zijl, 1999). To understand the effects of a tunnel excavation on local groundwater flow at the tunnel scale, it is important to include also the intermediate and regional flow systems. For this reason, the investigations of the present study are conducted at a regional scale.

Another advantage of considering groundwater flow at a regional scale concerns the boundary conditions. Typically, there are no or very little measurements of the hydraulic head in the bedrock to define boundary conditions. At a regional scale, however, realistic assumptions of boundary conditions can be made:

1. Major receiving streams drain regional groundwater flow systems and therefore mark regional groundwater divides (Freeze and Witherspoon, 1967). It is therefore reasonable to assume no flow conditions perpendicular to a vertical line through stream valleys.
2. The water table can be approximated by the topographic level of the ground surface at a regional scale (Hubbert, 1940; Tóth, 1963), allowing to assign a constant head boundary to the ground surface with the hydraulic head corresponding to the elevation.

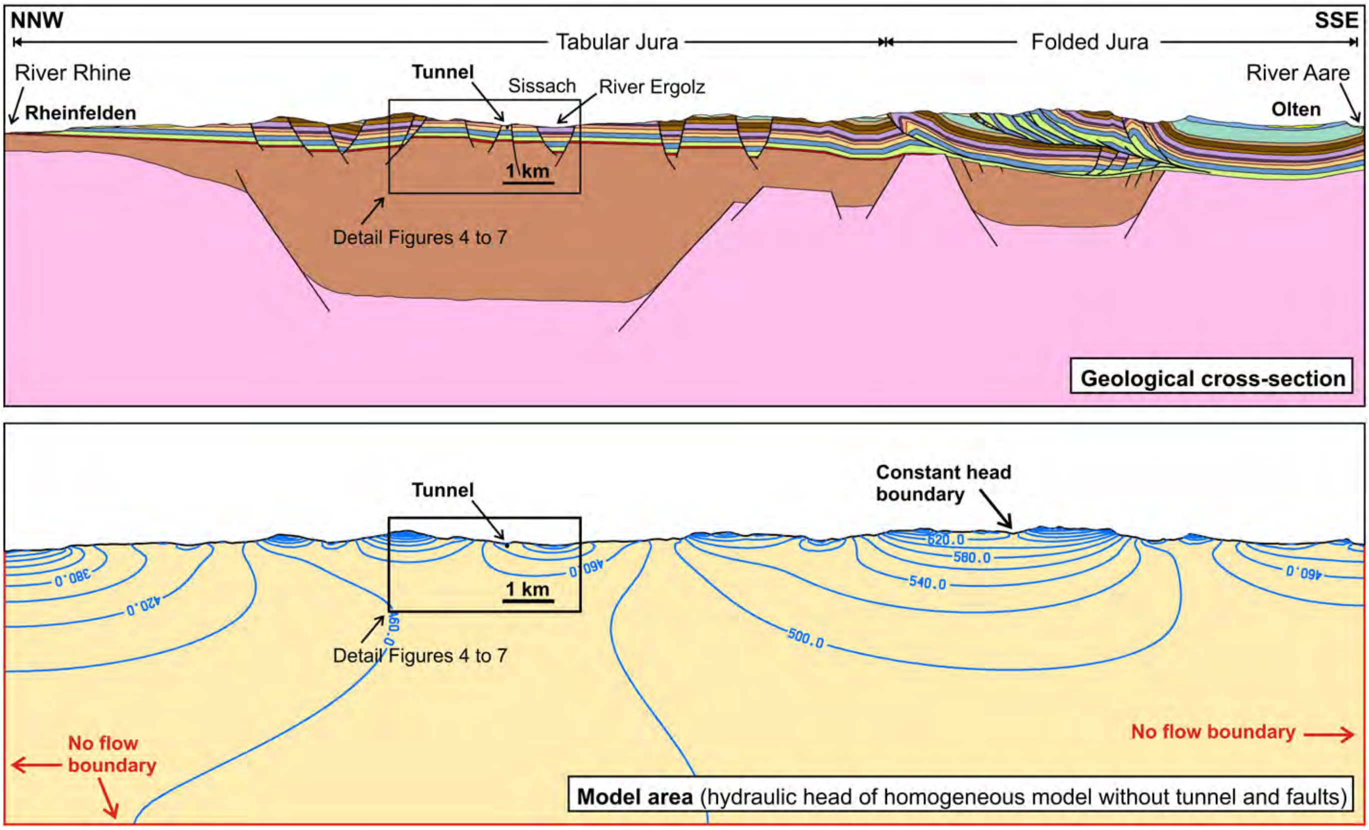

Fig. 2. Top: Geological cross-section of the study area (Figure 3 can serve as legend). The cross-section is the basis for the finite element groundwater models used in this study. Bottom: Model area, boundary conditions and solution for the hydraulic head field of the most simple model setup (homogeneously distributed hydraulic conductivity, without tunnel and faults). The rectangles mark the detail of the model area which is described in the text and illustrated in Figs. 4–7.

3. The penetration of groundwater flow systems into depth is limited and depends on the wavelength of variations in the water table (Tóth, 1963; Zijl, 1999). Taking also the low hydraulic conductivity of basement rocks into account, it is justified to assume that flow perpendicular to the horizontal level can be neglected at sufficiently great depths.

To analyze the changes induced by tunnel excavation on regional groundwater flow systems, 2D numerical finite element flow models were developed that include the test site of the present study. The model area (Figure 2 bottom) corresponds to the regional scale cross-section described in more detail at the beginning of the methodology section (Figure 2 top), which was constructed using geological data provided by NAGRA/SGK (1984) and Pfiffner et al. (1997). The boundary conditions of the models were defined based on the model concept outlined above (the numbering below corresponds to the numbering of the list in the section above):

1. The model boundaries in the NNW and SSE were defined as no flow boundaries. Here, a groundwater divide can be expected, because the rivers at the model boundaries (rivers Rhine and Aare) are major receiving streams, which are oriented perpendicular to the direction of the cross section.
2. The upper model boundary was defined as a constant head boundary, with the hydraulic head corresponding to the elevation of the ground surface. At a regional scale, it can be expected that the subsurface water table approximately follows the land surface.
3. The lower boundary of the model is at 5000 m below sea level and defined as a no flow boundary. It is expected that flow perpendicular to the horizontal level can be neglected at these depths.

The models were calibrated by fitting the simulated water flow into the model to the mean groundwater recharge at the study site (flow into the model occurs only through the upper model boundary, i.e. the ground surface). The mean annual groundwater recharge was estimated based on precipitation and actual evapotranspiration data provided by BAFU (2009) and corresponds to 550 mm/a in the study area. Model parameters included horizontal hydraulic conductivities and an anisotropy factor (vertical to horizontal conductivity). Different model setups were realized and calibrated (see next section). The estimated horizontal conductivities and the anisotropy factor of hydrostratigraphic units implemented in the individual model setups are indicated in Fig. 3. The estimated conductivities of the hydrostratigraphic units are in accordance with data from Northern Switzerland (NAGRA, 2002) and from the literature (e.g., Delleur, 1999 and references therein).

2.3. Numerical simulations

Several model setups containing different structural elements were used to perform simulations. Major goals were both to investigate the effects of tunnel excavation on regional flow patterns depending on the hydrogeological setting, and to provide a conceptual framework to define the relations between subsurface structure and rock swelling. The setups with the different combination of structural elements are summarized in Table 1. The implemented elements are as follows:

1. The tunnel: All simulations are conducted with and without tunnel. This is a basic requirement to analyze the effects of the tunnel excavation on regional groundwater flow. The tunnel is implemented by specifying the hydraulic head at the tunnel floor with

System	Hydrostratigraphic unit (not to scale)	Lithology	Thickness [m] (Tabular J. / Folded J.)	K-value [m/s] / anisotropy of homogeneous models	K-value [m/s] / anisotropy of aquifer-aquitard models	K-value [m/s] / anisotropy of hydrostratigraphic models
Quaternary	Quaternary	Gravel, sand, silt	Varying	8e-7 / 0.1	2e-6 / 0.1	1e-5 / 0.1
Tertiary	Tertiary	Conglomerate, sandstone	Varying	8e-7 / 0.1	1e-10 / 0.1	1e-10 / 0.1
Jurassic	Upper Jurassic Limestone	Limestone	100 / 100	8e-7 / 0.1	2e-6 / 0.1	2e-6 / 0.1
	Upper Jurassic Marlstone	Marlstone	300 / 250	8e-7 / 0.1	1e-10 / 0.1	1e-10 / 0.1
	"Upper" Middle Jurassic	Marlstone, limestone	80 / 70	8e-7 / 0.1	1e-10 / 0.1	1e-8 / 0.01
	Hauptrogenstein	Limestone	90 / 100	8e-7 / 0.1	2e-6 / 0.1	2e-6 / 0.1
	"Lower" Middle Jurassic	(Sandy) marlstone, limestone	80 / 70	8e-7 / 0.1	1e-10 / 0.1	1e-8 / 0.01
	Opalinus Clay	Argillaceous marlstone	95 / 100	8e-7 / 0.1	1e-10 / 0.1	1e-12 / 0.1
	Lower Jurassic	(Argill.) marlstone, limestone	30 / 30	8e-7 / 0.1	1e-10 / 0.1	1e-10 / 0.1
Triassic	Upper Keuper	Marlstone (sandstone)	55 / 50	8e-7 / 0.1	1e-10 / 0.1	1e-10 / 0.1
	Gipskeuper & Lower Keuper	(Sulfatic) marlstone	85 / 90	8e-7 / 0.1	1e-10 / 0.1	1e-10 / 0.1
	Muschelkalk aquifer	(Dolomitic) limestone	90 / 90	8e-7 / 0.1	2e-6 / 0.1	2e-6 / 0.1
	Muschelkalk aquitard	(Dolomitic, sulfatic) marlstone, salt	90 / 90	8e-7 / 0.1	1e-10 / 0.1	1e-10 / 0.1
	Buntsandstein	Sandstone, conglomerate, marlstone	30 / 0	8e-7 / 0.1	1e-10 / 0.1	1e-8 / 0.01
Permo-Carboniferous	Permo-Carboniferous trough	(Argillaceous) Sand-/siltstone, conglomerate	-	8e-7 / 0.1	1e-10 / 0.1	1e-10 / 0.1
	Crystalline basement	Granite, gneiss	-	8e-7 / 0.1	1e-10 / 0.1	1e-12 / 0.1

Fig. 3. Hydrostratigraphic units of the study area and respective hydraulic properties attributed to the finite element groundwater models. Lithostratigraphic column adapted from Bitterli-Brunner and Fischer (1988).

Table 1
Overview of considered subsurface features and corresponding model setups.

Subsurface features	Name of model setup	
	Without tunnel	With tunnel
Homogeneous model	Ho	Ho-t
Homogeneous model, with faults	Ho-f	Ho-ft
Aquifer–aquitard model	Aa	Aa-t
Hydrostratigraphic model	Hs	Hs-t

the respective elevation (here: 366 m a.s.l.). This specification is based on the assumption that the tunnel excavation leads to atmospheric pressure at the tunnel walls.

2. Faults: Faults may contain highly fractured zones that act as preferential pathways for groundwater flow (Caine et al., 1996). Faults may therefore strongly modify the hydraulic changes induced by the tunneling (Freeze and Witherspoon, 1967). In our study, scenarios are simulated where faults are considered as

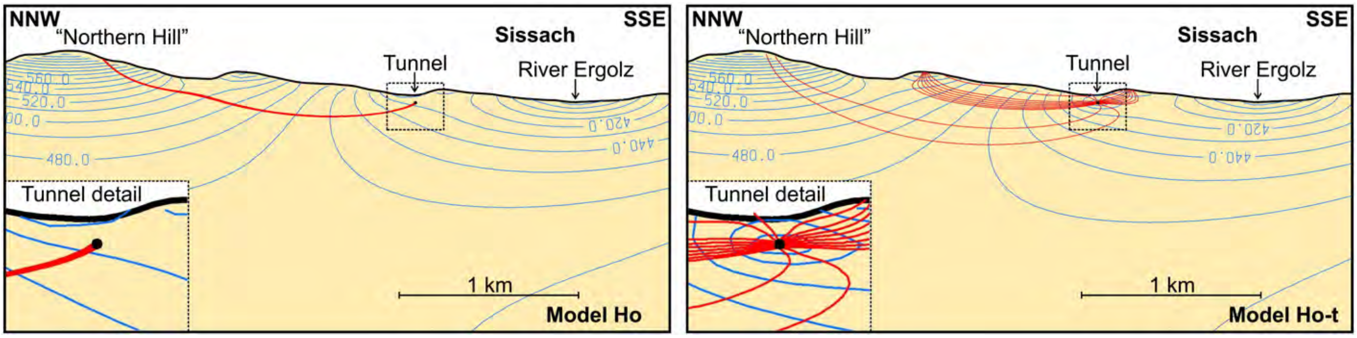

Fig. 4. Hydraulic head field and flow paths towards the tunnel perimeter calculated with the homogeneous model setup without faults. Left: without tunnel; right: with tunnel as subsurface feature.

elements with a cross-sectional area of 1 m^2 having an increased hydraulic conductivity (here: 2.5e−5 m/s) parallel to the faults' orientation.

3. Homogeneous hydraulic conductivity (homogeneous models): The hydraulic conductivity was uniformly attributed to the subsurface in order analyze the effects of the tunnel excavation on groundwater flow without superimposing effects caused by the alternation of lithological units with different hydraulic properties in the subsurface.
4. Contrasts in hydraulic conductivity (aquifer–aquitard models): The layering of lithological units with highly varying hydraulic properties leads to large contrasts in rock permeability, strongly influencing regional groundwater flow (Freeze and Witherspoon, 1967). Therefore, models were setup differentiating between aquifer layers (with high hydraulic conductivities) and aquitard layers (with low hydraulic conductivities).
5. Distributed hydraulic conductivity (hydrostratigraphic models): In some models the layering of lithological units was implemented by assigning each hydrogeological unit a specific hydraulic conductivity and anisotropy value. This setup allows analyzing the effects of small contrasts in hydraulic subsurface properties on regional groundwater flow.

Fig. 2 (bottom) shows the solution for the hydraulic head field of the most simple model setup (homogeneously distributed hydraulic conductivity, without tunnel and faults).

3. Results

This section presents the results of the numerical simulations using the different model setups indicated in Table 1. The distribution of the hydraulic head and flow paths towards the tunnel, visualized by backward tracking of 20 particles from the tunnel perimeter as starting points to the ground surface (or model boundary), are used to analyze the effects of the implemented structural elements on regional groundwater flow (Figures 4–7; these figures show the detail of the model area as indicated in the cross section Figure 2). In addition, flow rates at the tunnel (flow through the tunnel perimeter) are estimated and summarized in Table 2.

3.1. Homogeneous models (Ho, Ho-t)

The hydraulic head fields of the homogeneous models (Figure 4) show typical characteristics of topographically driven groundwater flow. The hydraulic head increases with depth at topographic highs (hills), resulting in downward directed groundwater flow. Topographic highs are therefore areas of groundwater recharge. Correspondingly, the hydraulic head decreases with depth at topographic lows (valleys), causing the groundwater to flow upward. Valleys are therefore areas of groundwater discharge. In between, groundwater flow has a horizontal flow component resulting in hydrostatic conditions (i.e., constant hydraulic head over depth). Close to the land surface, subordinate highs and lows result in small scale flow patterns. Hydraulic gradients are highest below major topographic elements. The hierarchical nature of the topography (highs and lows at different scales) results in a hierarchical structure of flow systems. The resulting flow field can be summarized as a superposition of regional, intermediate and local flow systems.

At the position of the tunnel, but without the tunnel as structural element (Figure 4 left), the groundwater flow is directed upward, with a pronounced horizontal component. The capture zone of the water passing through the (future) tunnel is a very narrow area originating from the hill in the north of the regarded model detail (in the following and in Figures 4–7, this hill is addressed as the "northern hill"). After the tunnel excavation (Figure 4 right), the capture zone is largely broadened and distributed to the northern hill and to other minor hills. The individual recharge areas on the hills are also broadened. One flow path originates from the valley above the tunnel.

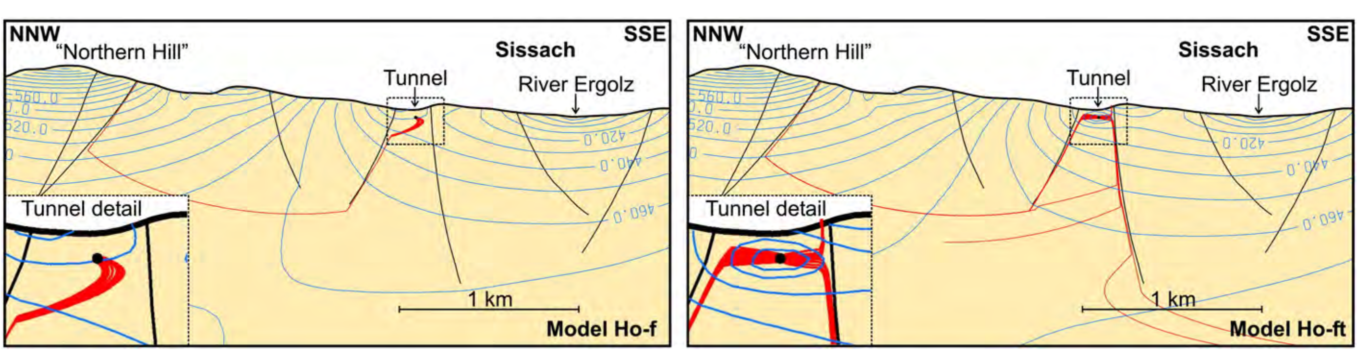

Fig. 5. Hydraulic head field and flow paths towards the tunnel perimeter calculated with the homogeneous model setup with faults. Left: without tunnel; right: with tunnel as subsurface feature.

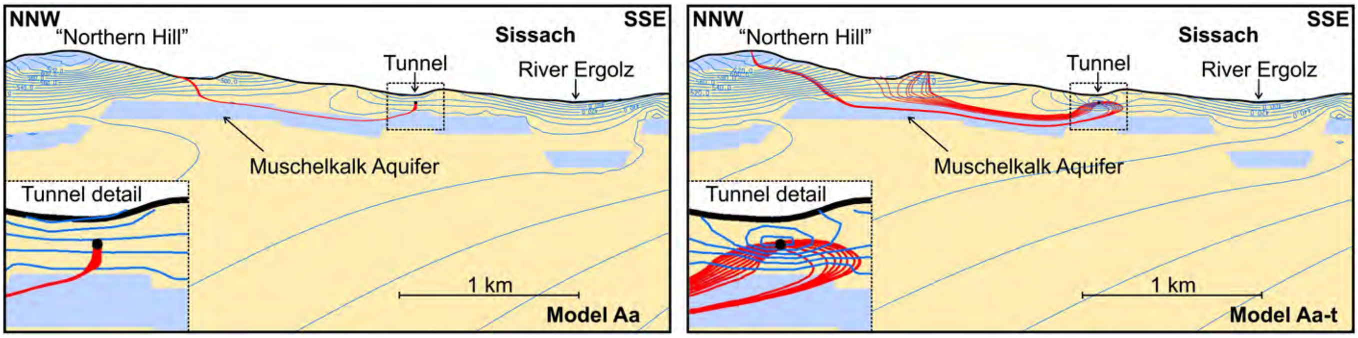

Fig. 6. Hydraulic head field and flow paths towards the tunnel perimeter calculated with the aquifer–aquitard model setup. Left: without tunnel; right: with tunnel as subsurface feature.

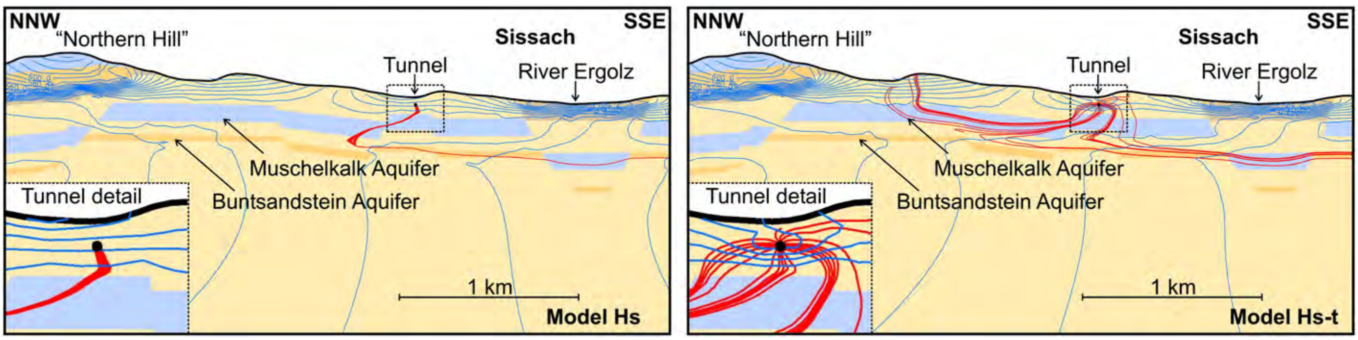

Fig. 7. Hydraulic head field and flow paths towards the tunnel perimeter calculated with the hydrostratigraphic model setup. Left: without tunnel; right: with tunnel as subsurface feature.

The average distances from the recharge areas to the tunnel strongly decrease, whereas the gradient of the hydraulic head in the immediate tunnel surroundings increases. Flow is directed towards the tunnel after the excavation. The calculated flow rates through the tunnel perimeter after the excavation increased by a factor of 31.5 compared to the rates before the tunneling (Table 2).

3.2. Homogeneous models with faults (Ho-f, Ho-ft)

The homogeneous model with faults implemented as preferential path ways show a hydraulic head field very similar to the model without faults (Figure 5). Only a slight deflection of the heads' contour lines can be observed at faults. However, the calculated flow paths are strongly influenced by the faults. There is a pronounced vertical component added to the flow paths. The resulting circulation systems reach at greater depths. In the model without tunnel as structural element (Figure 5 left), the capture zone of water passing through the (future) tunnel is narrow and originates at the outcrop of a fault on the Northern Hill. In the immediate surroundings of the (future) tunnel, groundwater flow is directed upward with a horizontal component from south to north.

After the tunnel excavation, the capture zone of the tunnel is widely distributed (Figure 5 right). In addition to flow paths via faults north of the tunnel, there are also deep flow paths via the fault south of the tunnel. The latter flow paths originate from outside the regarded model detail. In addition, there are flow paths from the near ground surface at the outcrop of the fault in the south of the tunnel. The flow paths in the immediate surroundings of the tunnel are almost horizontal, and originate from both north and south. The gradient of the hydraulic head is increased in the immediate tunnel surroundings and directed towards the tunnel after the excavation. The calculated flow rates through the tunnel perimeter after the excavation increased by a factor of 20.2 compared to the rates before the tunneling (Table 2).

3.3. Aquifer–aquitard models (Aa, Aa-t)

The implementation of aquifer layers with high hydraulic conductivity results in a hydraulic head field that is characterized by low gradients in the aquifers and high gradients in the aquitards (Figure 6). The capture zone of the tunnel perimeter before the excavation is very narrow, similar to the case without aquifer–aquitard contrasts (Figure 6

Table 2
Flow rates in liters per day per m tunnel section (l/d per m) into the tunnel perimeter calculated for the different model setups (c.f. Table 1) before and after the tunnel excavation. Note: The generally lower flow rates in the aquifer–aquitard and hydrostratigraphic models compared to those of the homogeneous models are due to the lower hydraulic conductivities at the position of the tunnel in these models.

Model setup	Homogeneous model without faults	Homogeneous model with faults	Aquifer–aquitard model	Hydrostratigraphic model
Before tunnel excavation	19.8	18.0	4.7e−3	4.8e−3
After tunnel excavation	623.0	363.0	47.4e−3	283.4e−3
Ratio (after/before tunnel excavation)	31.5	20.2	10.1	59.0

left). However, the flow paths towards the (future) tunnel follow the aquifer layer below the tunnel (the Muschelkalk Aquifer; c.f. Figure 2) over a long distance, and leave this aquifer closely below the tunnel area. In the immediate tunnel area the flow paths establish a vertical connection between the aquifer and the tunnel. The recharge area of the water flowing through the tunnel area is situated at the southern bottom of the Northern Hill in the described detail.

After the tunnel excavation, the flow paths towards the tunnel still follow the aquifer under the tunnel over a large distance (Figure 6 right). In contrast to the case before the excavation, the flow paths approach the tunnel approximately horizontally from the south and north in the immediate tunnel area. The capture zone becomes wider, the recharge area is larger. One narrow recharge area is situated on the top of the northern hill; another broad recharge area reaches from the valley south of the Northern Hill to the top of the next small hill. The gradient of the hydraulic head is increased in the immediate tunnel surroundings and directed towards the tunnel after the excavation. The calculated flow rates through the tunnel perimeter after the excavation increased by a factor of 10.1 compared to the rates before the tunneling (Table 2).

3.4. Hydrostratigraphic models (Hs, Hs-t)

The vertical increase of the hydraulic gradient in low conductivity layers becomes very pronounced in the model where every hydrostratigraphic unit is attributed an own hydraulic conductivity (Figure 7). This is especially obvious within the Opalinus Clay having the lowest conductivity (c.f., Figures 2 and 3). The flow paths towards the tunnel are strongly influenced by high conductivity layers. However, not only “high conductivity aquifers” such as the Muschelkalk Aquifer play an important role for the developing circulation systems. Also “intermediate conductivity aquifers” like the Buntsandstein (c.f. Figure 2), with hydraulic conductivities between the aquifers and the aquitards (c.f. Figure 3), provide important path ways for groundwater flow.

Before the tunnel excavation, the flow paths towards the tunnel form a narrow capture zone with a recharge area south of the tunnel and outside the regarded model detail (Figure 7 left). In the far field of the tunnel, the flow paths mainly follow the Buntsandstein layer (and a connected Muschelkalk Aquifer layer in a tectonic graben). A few hundred meters north of the tunnel, the flow paths shift to the Muschelkalk Aquifer above, accompanied by a shift in flow direction. In the vicinity of the tunnel, water flow is directed upward, and the flow paths are vertically connecting the Muschelkalk Aquifer with the (future) tunnel area.

After the tunnel excavation, the capture zone is pronouncedly broadened (Figure 7 right). Flow paths approach the tunnel from all directions in the immediate tunnel area. The flow paths in the far field are both attributed to the Muschelkalk and the Buntsandstein Aquifer. Recharge areas include the small hills north and south of the tunnel, as well as an area far outside the presented model detail. The gradient of the hydraulic head is increased in the immediate tunnel surroundings and directed towards the tunnel after the excavation. The calculated flow rates through the tunnel perimeter after the excavation increased by a factor of 59.0 compared to the rates before the tunneling (Table 2).

3.5. Synthesis: Common effects of the tunnel in the different model setups

Even though the hydraulic head fields are different for all simulated model setups, there are noticeable similarities between all models regarding the effects of the tunnel excavation on hydraulic head, flow paths and flow rates. These effects can be summarized as follows:

1. In the immediate tunnel surroundings, the direction of flow shifts from vertically upward before the tunnel excavation to horizontally from both sides (or from all sides in some cases) after the tunnel excavation.
2. The capture zone of the tunnel broadens after the tunnel excavation.
3. The recharge areas get broader (except for the setup with faults) and are widely distributed to different locations after the tunnel excavation. In some cases, they include areas very close above the tunnel after the excavation.
4. The flow rates through the tunnel perimeter increase by a factor of 10 to 60 after the tunnel excavation. The increase in flow rates is only caused by the increased hydraulic gradients in the immediate tunnel surroundings; an expected increased permeability around the tunnel in the excavation damaged zone is not implemented in the models.

4. Discussion

In this study, the effects of the Chienberg tunnel on the groundwater flow regime at the tunnel and in the adjacent areas have been investigated. In particular, the influences of the topography, the distribution of hydraulic subsurface properties and of preferential pathways provided by faults have been accounted for. The study suggests that the excavation of the tunnel has similar effects on the hydraulic head around the tunnel regardless of the hydrogeological setting. The head decreases in the immediate tunnel surroundings, and the capture zone of the tunnel broadens. The origin of the groundwater flowing through the tunnel area is more widely distributed after the excavation due to additional recharge zones. However, the actual change in flow paths before and after the tunnel excavation differs from case to case and depends on the structural elements in the subsurface, i.e., the overall hydrogeological setting.

The study provides a basis to analyze the impact of the tunnel excavation on regional flow patterns in the light of possible effects on the swelling of clay–sulfate rocks. The results show several changes in regional flow patterns caused by the tunnel excavation that may trigger rock swelling:

1. The tunnel excavation leads to an increase in flow rates around the tunnel. This effect may provide the possibility for enhanced water access to the clay rocks containing anhydrite and, by that, facilitate the transformation of anhydrite into gypsum.
2. The tunnel excavation leads to broadened, shifted and more distributed capture zones. The residence time of the groundwater circulating through the tunnel area may be shorter compared to the residence times before the excavation. A different groundwater age and origin is likely to change the chemical composition of the pore water in the tunnel surroundings, possibly favoring gypsum precipitation.
3. The tunnel acts as drainage. In the vicinity of major flow paths (preferential flow along fractures, flow in high conductivity units (aquifers), interflow close to the land surface), groundwater from these flow paths is attracted by the drainage effect of the tunnel. This groundwater originating from preferential flow paths may cause the anhydrite being transformed into gypsum.
4. The hydraulic head, i.e., pore water pressure, is decreased around the tunnel after the excavation. Lowering of pressure may disturb the thermodynamical equilibrium and reduce the solubility of gypsum (e.g., Marsal, 1952), causing gypsum precipitation.

A problem with the first two processes listed above is that water flow is very slow in clay–sulfate rocks, because the hydraulic conductivities are very low. However, rock swelling in the Chienberg tunnel started immediately after the excavation. This means that water access to the clay–sulfate rocks must occur rapidly. However, there are several possibilities that may allow fast water access. An excavation damaged zone (EDZ) is expected to occur around artificial subsurface openings (Tsang et al., 2005). This zone is characterized by enhanced fracturing, induced by the excavation itself and the stress redistribution. The induced fractures lead to a considerable increase in rock permeability and provide the possibility for preferential flow. Another possibility to provide rapid water access is given when faults directly penetrate the zone that is subject to swelling. These faults may be minor and not detectable from exploration boreholes before tunnel construction. As suggested by the simulations of the present study, changes in the hydraulic head field caused by the tunnel excavation may generate flow along faults towards the clay–sulfate rocks.

The simulation of groundwater systems before and after the excavation of the Chienberg tunnel give first indications of the processes that are involved in triggering swelling of clay–sulfate rocks in tunnel engineering as discussed above. However, there are also processes that cannot be evaluated with the used models. For example, the inclusion of the effects of longitudinal groundwater flow along the tunnel axis within the EDZ would require a model setup parallel to the tunnel axis. Nevertheless, the methodology presented here would be applicable. In contrast, temporal aspects of the simulated processes cannot be assessed by the used steady-state models. In view of the rapid appearance of swelling phenomena after the tunnel excavation in spite of the slow groundwater movement in low permeability rocks (c.f., discussion above), this is a major limitation of the methodology.

A large problem with verifying the processes that are suggested by the modeling study is that hydraulic data from test sites in low permeability rocks are typically scarce. The decrease in pore water pressure as an effect of the tunnel excavation has rarely been measured in low permeability rocks. However, there are a few experiments that document the decrease in pore water pressure and increase in hydraulic gradients around excavations in argillaceous rocks (Marschall et al., 2004). Such experiments were carried out in underground rock laboratories operated to investigate the adequacy of low permeability formations for the long term storage of radioactive waste. The problem of data scarcity not only concerns hydraulic, but also hydrogeological data. Field examples that document changes in the capture zones induced by the tunneling, as predicted in this study, do hardly exist. There is a pressing need for hydrogeological in-situ experiments in tunnels built in clay–sulfate rocks, such as tracer tests, isotopic studies and continuous records of pore water pressures.

Flow through the subsurface and the mechanical properties of the subsurface are linked through their effects on each other (Neuzil, 2003). The physical interaction between hydraulic and mechanical processes is known as hydromechanical (HM) coupling. Parameters for which HM coupling might play a role in the swelling behavior of clay–sulfate rocks are rock strength (the weaker the rock, the greater the floor heaves) and hydraulic boundary conditions. For example, Anagnostou (1992) explained the absence of significant swelling in certain tunnel sections in clay–sulfate rocks as a consequence of the inhomogeneous hydraulic head field. The consideration of HM coupled effects on the swelling of clay–sulfate rocks is still in the fledgling stages and requires more attention in future works.

A major future need is to downscale the results of the present study to the local scale of the tunnel section and its immediate surroundings. Further, different orientations or three dimensional (3D) models are required to account also for the 3D nature of groundwater flow. Because of the scarcity of hydraulic and hydrogeological data in low permeability environments, the knowledge of regional circulation patterns as determined at the scale of the present study is an important prerequisite for locale scale flow models to estimate hydraulic boundary conditions.

In the present study, the concept of topographically driven flow systems, which are modified by the structure of the subsurface, was applied to the problem of swelling clay–sulfate rocks in tunneling. The basic ideas behind this concept are not new. They have been established as early as the 1940s (Hubbert, 1940) and have been further developed until the end of the last century (e.g., Tóth, 1963; Freeze and Witherspoon, 1967; Zijl, 1999). But, in spite of its significance, regional groundwater flow attracts little attention in geotechnical engineering practice. The conceptual approach and the presented methodology are applied to a problem in tunnel engineering in this study. However, the approach and methodology would also be applicable to many other geotechnical problems, including geothermal energy usage, nuclear waste storage and CO_2 sequestration.

5. Conclusions and perspectives

The overall aim of the study is to contribute to an improved scientific basis for decisions made during project planning, cost planning and realization of tunnel projects in clay–sulfate rocks. The presented numerical simulations highlight the effects of tunnel excavation on groundwater flow patterns depending on the hydrogeological setting. The simulated changes in groundwater circulation systems in the area of the Chienberg tunnel induced by the tunneling indicate hydrogeological processes that may favor anhydrite dissolution and gypsum precipitation, and therefore are suited to trigger the swelling of clay–sulfate rocks in tunnel engineering. These processes include (1) increase of flow rates around the tunnel, (2) broadened, shifted and more distributed capture zones leading to a change in origin and age of groundwater, (3) access of groundwater from preferential flow paths (e.g. faults) due to the drainage effect of the tunnel, and (4) change in geochemical equilibrium conditions because of decreased pore water pressures in the tunnel area.

The study provides a conceptual framework that defines the relations between morphological, hydrological and geological structures and rock swelling. These relations contribute towards understanding the complex coupled hydraulic-mechanical and geochemical processes that occur during rock swelling. The modeled regional groundwater systems exhibit an indispensable basis for more detailed investigations at the local scale of the tunnel by providing adequate boundary conditions.

Acknowledgements

The presented study is part of the project ASTRA FGU 2008/5, funded by the Swiss Federal Roads Office (ASTRA).

References

Anagnostou, G., 1992. Untersuchungen zur Statik des Tunnelbaus in quellfähigem Gebirge. PhD thesis, ETH Zurich.

Anagnostou, G., 2007. Design uncertainties in tunneling through anydritic swelling rocks. Felsbau 25 (4), 48–54.

Hydrological Atlas of Switzerland. In: BAFU (Ed.), Bundesamt für Umwelt (BAFU), Bern. http://www.hydrologie.unibe.ch/hades/index.html. Available online at, accessed 16 October 2010.

Bitterli-Brunner, P., Fischer, H., 1988. Erläuterungen zum Blatt Arlesheim 1067. Geologischer Atlas der Schweiz. Federal Office of Topography swisstopo, Bern.

Caine, J.S., Evans, J.P., Forster, C.B., 1996. Fault zone architecture and permeability structure. Geology 24 (11), 1025–1028.

Delleur, J.W. (Ed.), 1999. The handbook of groundwater engineering. CRC Press, Boca Raton (FL), Springer, Heidelberg.

Einstein, H.H., 1996. Tunnelling in difficult ground — swelling behaviour and identification of swelling rocks. Rock mechanics and rock engineering 29 (3), 113–124.

Freeze, R.A., Witherspoon, P.A., 1967. Theoretical analysis of regional groundwater flow. 2. Effect of water-table configuration and subsurface permeability variation. Water Resources Research 3 (2), 623–634.

Hubbert, M.K., 1940. The theory of ground-water motion. Journal of Geology 48 (8), 785–944.

Jeschke, A.A., Vosbeck, K., Dreybrodt, W., 2001. Surface controlled dissolution rates of gypsum in aqueous solutions exhibit nonlinear dissolution kinetics. Geochimica et Cosmochimica Acta 65 (17), 27–34.

Kovári, K., Chiaverio, F., 2007. Modular yielding support for tunnels in heavily swelling rock. Preprint STUVA Conference 07, 26–29 November 2007, Köln.

Madsen, F.T., Nüesch, R., 1991. The swelling behaviour of clay–sulphate rocks. 7th Int. Congr. on Rock Mech, pp. 263–267.
Marsal, D., 1952. Der Einfluss des Druckes auf das System $CaSO_4$–H_2O. Heidelberger Beiträge zur Mineralogie und Petrographie 3, 289–296.
Marschall, P., Croisé, J., Schlickenrieder, L., Boisson, J.Y., Vogel, P., Yamamoto, S., 2004. Synthesis of hydrogeological investigations at the Mont Terri site (phases 1 to 5). In: Heitzmann, P. (Ed.), 2004. Mont Terri Project – Hydrogeological synthesis, osmotic flow. Reports of the Federal Office for Water and Geology (FOWG), Geology Series No. 6, Bern.
NAGRA, 2002. Projekt Opalinuston – Synthese der geowissenschaftlichen Untersuchungsergebnisse. NAGRA Technical Report NTB 02-03. Nationale Genossenschaft für die Lagerung radioaktiver Abfälle (NAGRA), Wettingen.
NAGRA/SGK, 1984. Geologische Karte der zentralen Nordschweiz 1:100'000 mit angrenzenden Gebieten von Baden-Württtemberg. Edited by Nationale Genossenschaft für die Lagerung radioaktiver Abfälle (NAGRA), Wettingen, and Schweizerische Geologische Kommission (SGK), Bern.
Neuzil, C.E., 2003. Hydromechanical coupling in geologic processes. Hydrogeology Journal 11, 41–83.
Nüesch, R., Steiner, W., Madsen, F.T., 1995. Long time swelling of anhydritic rocks: mineralogical and microstructural evaluation. 8th International Congress on Rock Mechanics, Sept. 25–30, Tokyo, Japan, pp. 285–288.
Pfiffner, O.A., Lehner, P., Heitzmann, P., Müller, S., Steck, A. (Eds.), 1997. Deep Structure of the Swiss Alps. Results of NRP 20. Birkhäuser Verlag, Basel.
Pierau, B., Kiehl, J.R., 1996. Widerstands- und Ausweichprinzip: Vergleich zweier Entwurfsmethoden für Tunnelbauten in quellfähigem Gebirge. Taschenbuch für den Tunnelbau 1996, Verlag Glückauf, Essen.
Pimentel, E., 2007. A laboratory testing technique and a model for the swelling behavior of anhydritic rock. 11th Congress of the International Society for Rock Mechanics, Lisbon, pp. 143–146.
Tóth, J., 1963. A theoretical analysis of groundwater flow in small drainage basins. Journal of Geophysical Research 68 (16), 4795–4812.
Tóth, J., 1999. Groundwater as a geologic agent. An overview of causes, processes and manifestations. Hydrogeology Journal 7 (1), 1–14.
Tsang, C.F., Bernier, F., Davies, C., 2005. Geohydromechanical processes in the Excavation Damaged Zone in crystalline rock, rock salt, and indurated and plastic clays — in the context of radioactive waste disposal. International Journal of Rock Mechanics & Mining Sciences 42 (1), 109–125.
Zijl, W., 1999. Scale aspects of groundwater flow and transport systems. Hydrogeology Journal 7 (1), 139–150.

Exhibit 3

CHAPTER 34

Environmental impacts of tunnels in fractured crystalline rocks of the Central Alps

Simon Loew[1], Volker Luetzenkirchen[2], Ulrich Ofterdinger[3], Christian Zangerl[4], Erik Eberhardt[5] and Keith Evans[1]

[1]Chair for Engineering Geology, Department of Earth Sciences, ETH Zuerich, Switzerland
[2]Chair for Engineering Geology, Department of Earth Sciences, ETH Zuerich, Switzerland
Now at mbn AG, 5400 Baden, Switzerland
[3] Chair for Engineering Geology, Department of Earth Sciences, ETH Zuerich, Switzerland
Now at Queen's University Belfast, Northern Ireland
[4]Chair for Engineering Geology, Department of Earth Sciences, ETH Zuerich, Switzerland
Now at alpS – GmbH, Grabenweg 3, 6020 Innsbruck, Austria
[5]Chair for Engineering Geology, Department of Earth Sciences, ETH Zuerich, Switzerland
Now at Geological Engineering, University of British Columbia, Vancouver, B.C., Canada

ABSTRACT: This paper reviews unique case histories from the Central Swiss Alps that illustrate the effects intermediate and deep tunnels in crystalline rocks can have on groundwater flow systems, surface springs and surface deformations. Serious impacts on surface waters occur in weathered and de-stressed high permeability areas close to the tunnel portals, or along tunnels running only a few hundred meters below ground surface. In these areas, water table drawdown can reach the elevation of the tunnel and significantly affect surface springs and wetlands over lateral distances of several kilometers within a few weeks. Similarly, deep tunnels located 500–1500 m below ground surface can have considerable impacts on natural flow systems, although their effects are much less visible; groundwater flow is redirected towards the draining tunnel, re-locating groundwater divides and reversing flow directions over lateral distances larger than one kilometer. In addition, strong pressure reductions created by draining tunnels at depth can result in consolidation of the rock mass and large scale deformations leading to surface settlements in excess of 10 cm.

1 INTRODUCTION

In mountainous terrain like the European Alps, many tunnels and drifts are excavated deep below ground surface, acting as hydraulic drains below the regional groundwater table. Sedimentary systems in such mountain environments often behave like a succession of confined aquifers and aquitards (e.g., Stini 1950), whereas crystalline rocks in such settings are better described as heterogeneous phreatic aquifers (e.g., Ofterdinger 2001).

Opening a deep tunnel excavation to atmospheric pressure acts to generate significant pore pressure drawdown around the excavation and influences groundwater heads and flow fields over large distances. Depending on the recharge conditions at ground surface, effective hydraulic conductivities and specific yields of the rock mass around the tunnel, a tunnel in crystalline rocks can also induce a water table drawdown with serious environmental impacts at ground surface. Such impacts include the disappearance of surface springs and wetlands (e.g., Stapff 1882; Stini 1950). Even without significant water table drawdown, the pore pressure reductions induced by deep draining tunnels can lead to considerable ground subsidence at surface (Zangerl 2003; Zangerl et al. 2003). Such hydromechanically coupled effects are well known in high porosity soils and weak rocks, but much less so for low porosity crystalline rocks.

Many of the European countries that are currently planning or building deep tunnels through the Alps are seriously confronted with these environmental issues and have started to develop codes of practice on how to handle such problems (e.g., BUWAL 1998). In support of such projects, a series of Ph.D. projects have recently been completed at the ETH Zürich, focusing on the Gotthard massif of the Swiss Alps and that study the underlying mechanisms of such processes (Ofterdinger 2001; Luetzenkirchen 2002; Zangerl 2003).

This paper reviews observations and interpretations of environmental impacts of deep tunnels from the Gotthard massif of the Central Swiss Alps. After a discussion of the key hydrogeological properties of this study area, three case studies are presented demonstrating: (1) the impacts of deep tunnel sections on regional flow systems and groundwater recharge, (2) the impacts of shallow tunnel sections on surface springs and wetlands, and (3) the impacts of draining tunnels on surface settlements. The case study results are representative of many existing underground structures excavated during the last 100 years in the crystalline massifs in the central Swiss Alps.

2 KEY HYDROGEOLOGICAL PROPERTIES OF THE STUDY AREA

2.1 *Geology and tectonics*

Figure 1 provides an overview of the tectonic units and steeply dipping geological boundaries found in the external crystalline massifs of the investigation area (Aar Massif, Tavetsch Massif, Gotthard Massif) in the Central Alps of Switzerland. The investigation area is about 1200 km^2 and has strong mountainous relief, with valley floor elevations ranging from 500 to 1500 meter above sea level (masl) and summits up to 2000 to 3000 masl.

About 95 % of the rocks in the study area (Figure 2) belong to the pre-Alpine crystalline basement which is composed of pre-Variscan gneisses, schists, migmatites and mainly late Variscan (upper Carboniferous) magmatic rocks (granites, diorites, syenites, less abundant volcanics and aplite/lamprophyre dykes). The remaining 5% are late-paleozoic and mesozoic marls, conglomerates, sandstones and dolomites in autochthonous to par-autochthonous position relative to the crystalline basement. A summary of the petrographic characteristics of this area can be found in Labhart (1999).

In the Gotthard massif, medium to upper greenschist facies conditions were reached during Tertiary metamorphism, with an increase in peak pressure and temperature from north to south. Along the southern boundary, amphibolite facies conditions were achieved (Frey et al. 1980; Labhart 1999). The main Alpine deformation phase in the Gotthard massif starts in the lower Oligocene around 35 and 30 Ma (Schmid et al. 1996), corresponding with the peak metamorphic overprint characterised through a ductile deformation regime.

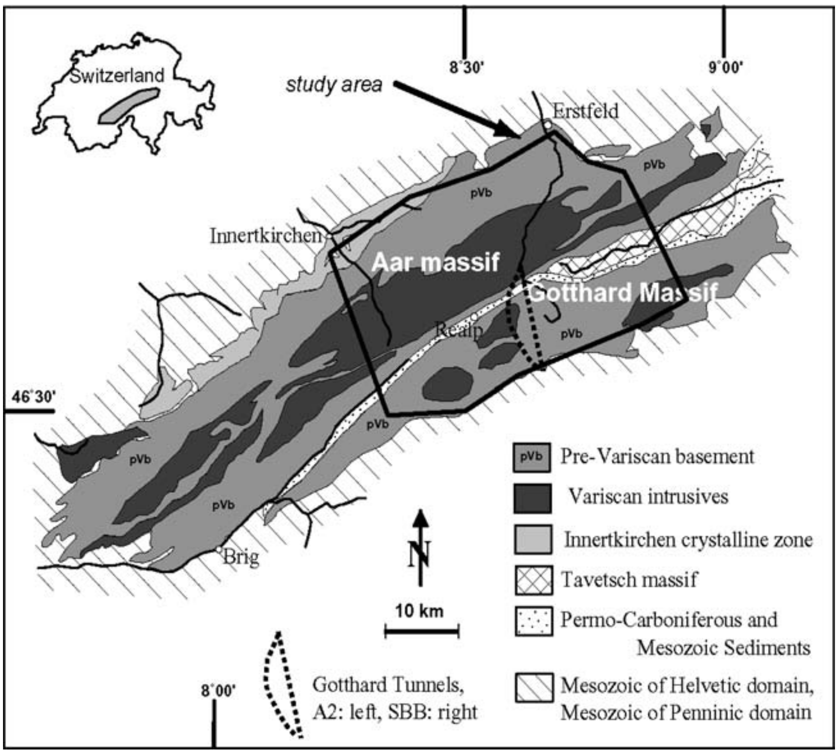

Figure 1. Tectonic map of the Aar and Gotthard Massif in the Swiss Alps, showing outline of study area (see Figure 2).

In the central Gotthard massif this deformation phase led to the formation of Alpine shear zones and a penetrative foliation that strikes NE-SW or E-W and dips southwards in the northern part and northwards in the southern part, forming a fan like structure (Labhart 1999).

During later stages, ongoing deformation changed gradually from a ductile to a brittle deformation regime characterised by brittle faulting. Recently much work was done on the formation of brittle structures within the Gotthard massif (Luetzenkirchen 2002; Zangerl 2003). Compared to the moderate brittle deformation in the Aar massif, the Gotthard massif shows a high density of brittle faults and fault zones of remarkable extension and width. Figure 3 shows the trace pattern of mapped and inferred brittle fault zones at the surface in the Gotthard pass area near Sustenegg. In this area two major sets striking NE-SW (set F1) and NNE-SSW (set F2), and one minor W-E set (set F3) can be distinguished. Across the Gotthard massif, the brittle faults follow the orientation of Alpine foliation forming the same fan-like structure, characterized North of Sustenegg by southeast dipping structures and South of Sustenegg by northwest dipping structures. The total spacing of all brittle fault sets estimated normal to their mean orientation is approximately 35 m (Zangerl et al. 2001). Both tunnel and surface derived mapping data show similar pole distribution

Figure 2. Geological map of study area (rotated), location of studied traffic tunnels and hydropower drifts. Rectangles mark approximate locations of Figures 3 (right) and 4 (left).

patterns, although it is not possible to resolve clearly the three different fault sets at depth. Based on the observations reported in Zangerl (2003), most of the mapped fault zones can be classified as pure strike-slip faults following the classification scheme by Angelier (1994). The rest can be grouped as oblique-slip faults.

All of these observations relate to the youngest faulting events. Based on zeolite parageneses identified in fractures from brittle fault rocks, Luetzenkirchen (2002) concluded that these faulting events terminated before metamorphic temperatures dropped below 190° C (Figure 6). Neotectonic activity must be very low in the study area, however, postglacial rebound superficially "reactivated" some of the fault zones along the main NE-SW striking valleys (Luetzenkirchen 2002; Frei and Löw 2001).

During this same period, the Aar massif underwent only moderate brittle deformation, which generated minor shear fractures and joint systems locally filled with hydrothermal crystallizations (Steck 1968a; Bossart & Mazurek 1991; Laws 2001). Like in the Gotthard massif, these brittle structures overprint ductile Alpine shear zones.

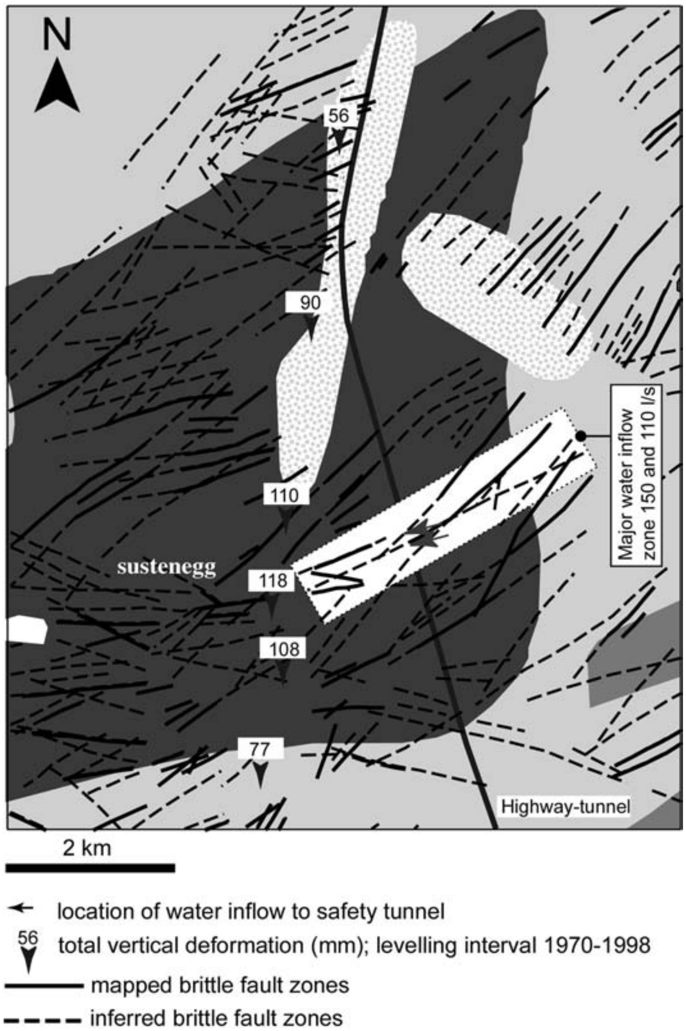

Figure 3. Brittle fault zones mapped in the Gamsboden granitic gneiss, north of Gotthard pass. Black lines represent mapped brittle fault zones, dashed lines represent inferred fault zones based on aerial photos and geomorphological mapping. Vertical arrows indicate locations of levelling points and subsidence values measured along the Gotthard pass road. Highlighted is the location of singular inflows to the Gotthard highway and safety tunnel.

2.2 *Hydrology and groundwater recharge*

The study area corresponds to the main water divide in the central Alps. Precipitation in the study area is high, but varies strongly spatially. Mainly depending on altitude, the mean annual precipitation ranges between 1600 and 3600 mm/yr (BWG 2001). In most years, relatively little precipitation falls between December and February. Snow heights at the end of winter (April–May) represent about 1000 mm of water. In general, glaciers and non-permanent permafrost occur above 2500 masl and feed creeks and rivers in summertime. Evapotranspiration ranges between 200 and 500 mm per year, again depending on altitude.

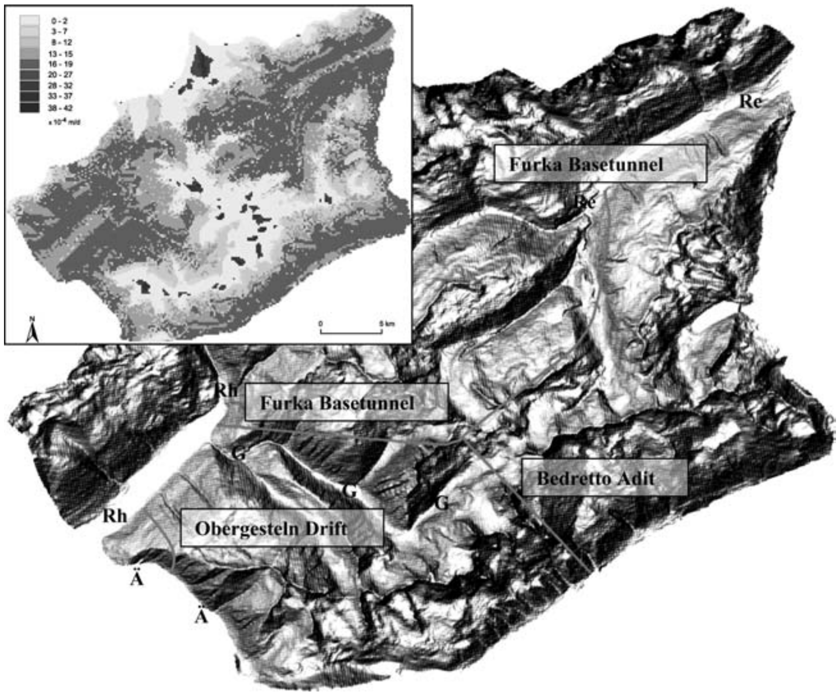

Figure 4. Topography and geography of Rotondo area with Furka basetunnel, Bedretto adit and Obergesteln drift. G: Geren valley with Gerental basin, Ä: Äginen Valley, R: Rhone Valley, Reuss Valley, GP: Gotthard Pass. Inset map showing distributed annual groundwater recharge in the same Rotondo area. Highest recharge rates occur in glaciated areas. Lowest recharge rates occur on steep bare high altitude rock slopes.

Depending on topography, land use, vegetation and slope exposure, groundwater recharge shows strong variations across the catchments (e.g., Lehner et al. 1990). Given that the study area is situated in a highly mountainous area covering a wide range of elevation zones, the spatial distribution of the groundwater recharge rates (i.e., the upper boundary condition for groundwater flow models) is a crucial factor for understanding the natural and artificially disturbed groundwater flow systems. For this reason, the recharge rates were studied in a test catchment of 40 km^2, the Gerental basin (Figure 4), with a calibrated hydrological model. The applied GIS-based model PREVAH (Precipitation-Runoff-EVapotranspiration-Hydrotope model) combines the spatial differentiation of hydrologically similar response units (HRU), or hydrotopes, and a runoff generation concept that allows the separate calculation of the water balance within each hydrotope (Gurtz et al. 1999). The hydrotopes were defined to represent hydrologically homogeneous areas according to the most important factors controlling evapotranspiration and runoff formation processes, such as the meteorological inputs, topography (catchment area, altitude, exposure and slope), landuse and soil characteristics (Gurtz et al. 1990). For the glaciated areas a conceptual model was applied which was developed for a research study in the Rhône area (Badoux 1999). This concept attributes melt-water from glaciated areas below the equilibrium line (ELA) preferentially to the fast runoff storage, while melt-water originating above the ELA preferentially contributes to the slow runoff storage, i.e. to groundwater recharge.

The hydrological model was first calibrated and validated in the Gerental catchment and then applied to the larger domain of the Rotondo area using identical model parameters as calibrated in the Gerental basin. The hydrograph simulation for the gauging station at the Gerental catchment outlet was performed for the period January 1991 to October 1999. The results of the hydrograph simulation are discussed elsewhere (Vitvar and Gurtz 1999). The temporal variations of the simulated recharge rates show maximum recharge rates in the upper Geren valley during spring and summer (April–September), commencing with the onset of the melting period. The resulting recharge distribution shows a strong spatial variability, especially in the high altitude regions where steep bare rock slopes with low recharge areas contrast to the upper regions of the glaciers, characterized by high recharge rates within small restricted areas (inset Figure 4). Another striking feature in the recharge distribution is the observation of low to moderate recharge rates along the valley floor and lower valley slopes. However, from a hydrodynamic perspective these areas are expected to constitute potential groundwater exfiltration areas, where essentially no groundwater recharge should occur. This conceptual discrepancy might lead to a small systematic error in the spatial distribution of the recharge rates, as the overall water budget in the catchment is well constrained by measurements and controlled in the model. For the purpose of numerical simulations an average recharge rate distribution was extracted from the 9-year average. The spatial average recharge rate of this distribution for the whole model domain is 12E-4 m/d, which is in agreement with studies in similar topographic and geological settings in the Central Alps (Kölla 1993), giving a range of 3 to 22E-4 m/d with a most probable value of 11E-4 m/d.

The groundwater table across the entire study area has never been directly measured with surface based boreholes (or piezometers). Most of the information about the location of the groundwater table comes from pore pressures measured in subsurface boreholes and the locations of systematically mapped surface springs (Frei und Löw 2001; Luetzenkirchen 2002). These parameters or observations indicate that the intersection of the groundwater table with the steep and bare valley slopes occurs several hundreds of meters below the local peak elevation (the spring line is often found between 2000 and 2400 m elevation). Water tables derived from subsurface water pressure measurements in the KW Vorderrhein adit are 100–200 meters higher than the local spring line elevation. This has to be expected because hydraulic heads have to increase from the valley slopes to the mountain crests.

2.3 *Distribution of groundwater flow and hydraulic conductivity from tunnel observations*

Figure 5 illustrates, with examples from the Gotthard N2 highway and Gotthard SBB railway tunnels, the characteristic patterns of early time tunnel inflows that were observed in most of the underground excavations found within the study area. Seeping inflows (dripping water) occur along most of the tunnel sections in a seemingly random ubiquitous distribution. Continuous (flowing) water inflows occur in clusters at a few specific locations, for example between tunnel meter (Tm) 8000 and 11,000 in the Gotthard N2 highway tunnel. The early time volumetric rate of these continuous inflows is typically in the order of 5 to 20 l/s per 100 m of tunnel length. In addition to these clustered inflows, there are a few locations with extremely high inflows. In the Gotthard N2 tunnel such singular structures can be found at Tm 9910 and 9935 and showed early time inflow rates of 110 and 150 liters per second, respectively.

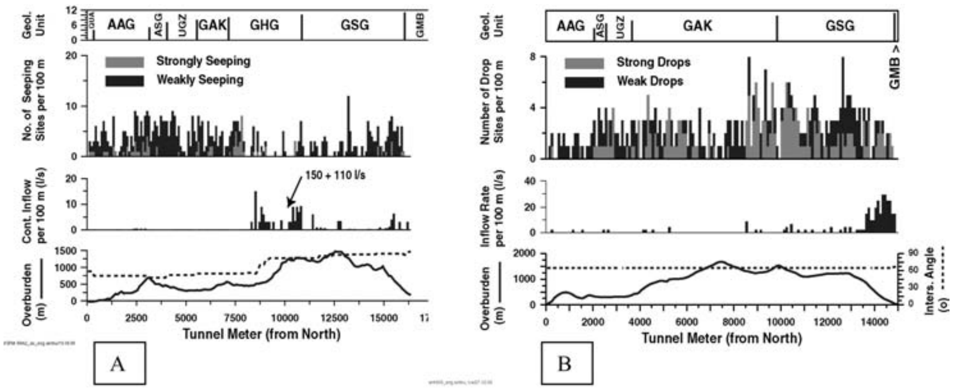

Figure 5. Geology, water inflows and topography of (A) Gotthard N2 Highway Tunnel and (B) Gotthard Railway Tunnel. Geologic Units: Aar Massif (AAG, ASG); Permo-Carboniferous and Mesozoic sediments (UGZ); Gotthard Massif (GAK, GHG, GSG); Mesozoic sediments of Penninic domain (GMB).

As many of the tunnels are lined with concrete, steel sets or shotcrete and the existing reports do not give detailed information, geologic descriptions of groundwater pathways originate from new observations in selected tunnels of the Gotthard Massif (e.g., Bedretto adit of the Furka basetunnel, Gotthard N2 highway tunnel). Here small continuous inflows (0.01 to 0.1 l/s) originate in most cases from mm-wide channels that lay in the planes of fractures intersecting the tunnel walls. Most of the fractures containing such channels are steeply inclined shear fractures (small faults) with polished and striated surfaces and, occasionally, mm-thin gouge layers. These fracture-fillings have a width of a few mm to a few cm and the fracture length exceeds in most cases the local tunnel diameter (3 m). The flowing water channels occur where these fractures intersect other minor fractures (joints). The shear fractures often occur close and parallel to existing lithological (mechanical) heterogeneities, for example older ductile shear zones and dykes, or within the damage zone of larger cataclastic faults.

Medium to large continuous inflows occur mostly in the zone of near-surface weathering, toppling and stress relief or along deeply reaching and extended brittle fault zones. The zone of near surface weathering and stress relief is characterised by a high density of open fractures, sometimes accompanied by flexural toppling, and reaches depths of up to 200 m below ground surface. Fault zones generating medium to large inflows are always dominated by brittle deformation (overprinting ductile shear zones in most cases) and sometimes contain cohesionless fault breccias or gouges of up to several meters thickness (Luetzenkirchen 2002; Zangerl 2003). As shown in Figure 5, most of the inflows occur along faults in granitic rocks (Variscan intrusions) of the Gotthard massif. These interrelationships between fault zone hydraulic conductivity and deformation type also becomes obvious when comparing the bulk tunnel inflows in the sections of the Aar massif (hardly any continuous inflows; mainly ductile shear zones) with the Gotthard massif (many clusters of continuous inflows; mainly granitic gneisses with intensive brittle faulting). Typical examples of permeable brittle fault zones of moderate size from the Bedretto adit to the Furka basetunnel are shown in Figure 6. Photomicrographs from thin sections show that open fractures in fault rocks are partially filled with low-temperature mineral paragenesis (zeolites) and that the open pore space is remarkably high.

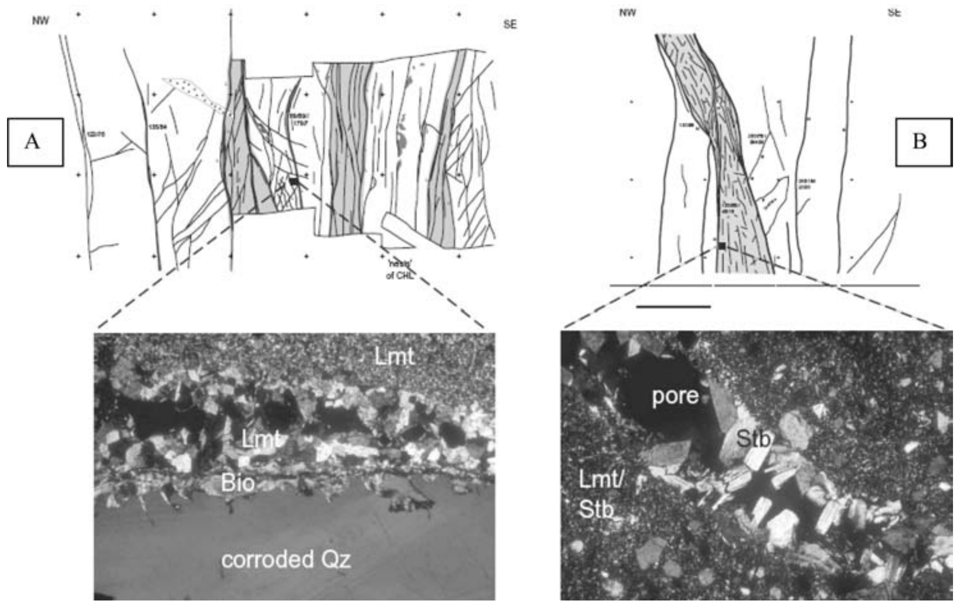

Figure 6. Schematic representation of mapped (A) brittle-ductile fault zone, and (B) brittle fault zone from the Bedretto adit of Furka basetunnel. Crosses mark the 1-m spaced mapping grid used on the tunnel wall Fault core composed of weak to soft chemically altered material (mainly gauge) is marked in grey. Shear fractures with slickenside striations shown as bold lines. Photomicrographs from fractures partially filled with zeolites (left: laumontite Lmt; right: stilbite Stb). Open pore space shown in black.

A quantitative analysis of such tunnel inflows has shown that the crystalline basement rocks in the investigated area have a strongly anisotropic hydraulic conductivity, especially in the regions with significant continuous inflows. Assuming radial flow directed towards a constant head tunnel drain, Loew (2001) derived 100–1000 meter scale hydraulic conductivities in the direction of the Alpine foliation (normal to the tunnel axes). For tunnel sections with moderate inflows (e.g., Gotthard railway tunnel without inflows close to the southern portal) typical values of 10^{-8} m/s were derived. For areas with high tunnel inflows close to the portals, mean hydraulic conductivity in the plane of the Alpine foliation typically ranges between 10^{-3} and 10^{-5} m/s (Loew 2001).

3 IMPACTS OF DEEP TUNNELS ON REGIONAL GROUNDWATER FLOW SYSTEMS

Environmental impacts of deep tunnel sections (500 m–1500 m) in crystalline rocks of the Gotthard and Aar massifs are not well constrained by direct observations. In most cases no environmental impacts can be seen directly on ground surface. However, the subsurface flow systems change considerably over large distances. These changes can be derived from theoretical considerations and numerical modeling. A detailed numerical study has been carried out by Ofterdinger (2001) for the Rotondo area covering the Furka basetunnel and Bedretto adit (Figure 4). These underground structures were constructed in the years 1975–1980.

Today the Furka basetunnel is in operation as a single-line intra-alpine rail tunnel having an elevation of about 1500 masl. The Bedretto adit is an unlined support segment, which is not in operation and has recently been adopted as an ETH Zurich research facility. The geology in the Furka and Bedretto excavations consists mainly of the Variscan Rotondo Granite (about 220 Mio years old) with orthogneiss of early Paleozoic age (about 420 Mio years). Like in the rest of the study area, both rock types show Alpine foliation and shear zones, and are composed of several Alpine fracture sets with a dense pattern of brittle faults. One major regional brittle fault zone of more than 100 m total thickness follows the upper part of the Geren valley (striking about N 60 E) intersecting the Bedretto adit in its northern part. In the Furka and Bedretto tunnels, the overburden typically ranges between 1000 and 1500 m.

3.1 *3D groundwater model of the Rotondo area*

Simulations of the regional scale groundwater flow in the Rotondo area (Figure 4) have been carried out for the natural system and that following construction of the Furka and Bedretto tunnels using a 3D continuum model (FEFLOW, Diersch 1998). The mesh consisted of 141,022 nodes and 259,156 elements distributed over 13 layers with one regional fault zone. The base of the model is at 0 masl. The total projected area of the model comprises 262 km^2. The vertical discretization was chosen to enable a good resolution of the free and moving groundwater table, to assign depth dependant values of effective hydraulic conductivity, and to achieve a dense mesh discretization around the galleries. From the results of the hydrological model described in the previous section, the spatially distributed long-term mean recharge rates were extracted as upper boundary conditions for the model. The Furka basetunnel and the Bedretto adit are represented as line sinks with fixed elevation heads. The perennial streams and rivers are also treated as fixed inner head boundary conditions.

The model was calibrated in steady-state using the inflow rates to the tunnels as measured in 1999 (i.e., 20 years after excavation), and pore pressures measured in a 100 m long subsurface research borehole. Typical inflow rates in these tunnel sections with large overburden range between 8 l/s and 10 l/s per tunnel kilometer. Figure 7 shows two recorded quasi steady-state inflows to the Bedretto adit from typical moderate sized fault zones. As is clearly visible in this Figure, there is no direct interaction with the seasonally varying precipitation at ground surface. Calibration resulted in an effective hydraulic conductivity of 6E-9 m/s for the Rotondo Granite intersecting the central parts of the tunnel (see Figure 2), 6E-8 m/s for the regional fault zone (generating an influx of 7.5 l/s), and 3E-9 m/s for the surrounding para-gneisses of the pre-variscan basement. Ofterdinger (2001) studied a series of model scenarios where the effects of fault zones, hydraulic anisotropy, and various types of recharge distributions at ground surface were investigated.

3.2 *Tunnel induced changes in water table elevation and flow fields in Rotondo area*

In each of the modelled scenarios, the simulated steady-state location of the groundwater table without tunnels was located substantially below all major mountain crests and peaks within the Rotondo area. These crests and peaks, shown in Figure 4B, have an elevation ranging between 2700 and 3200 masl. For the different scenarios simulated, the depth of the water table ranged from 100–150 m below the ridges above the Furka basetunnel to 250 m below the steepest peaks in the area. Besides topography, the spatially varying recharge rates at ground

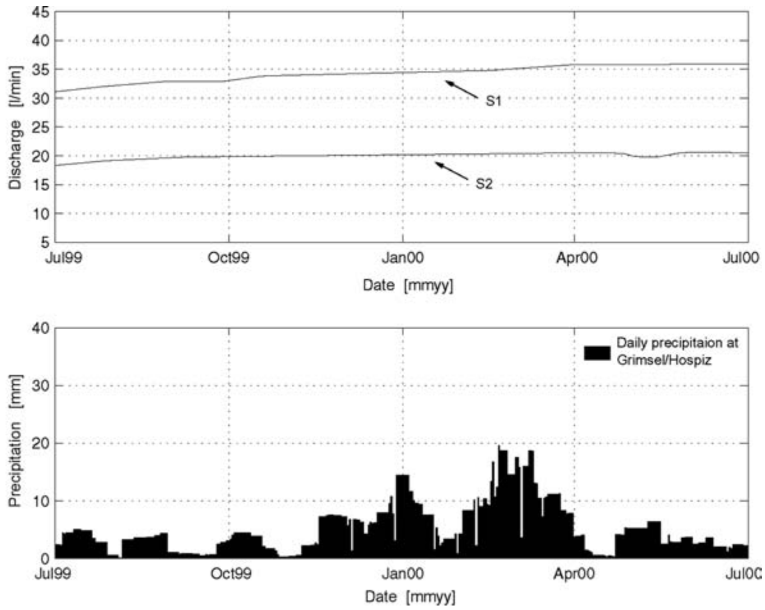

Figure 7. Late time inflows into the Bedretto adit at the location of two brittle fault zones. Comparison with daily precipitation at Grimsel Hospiz.

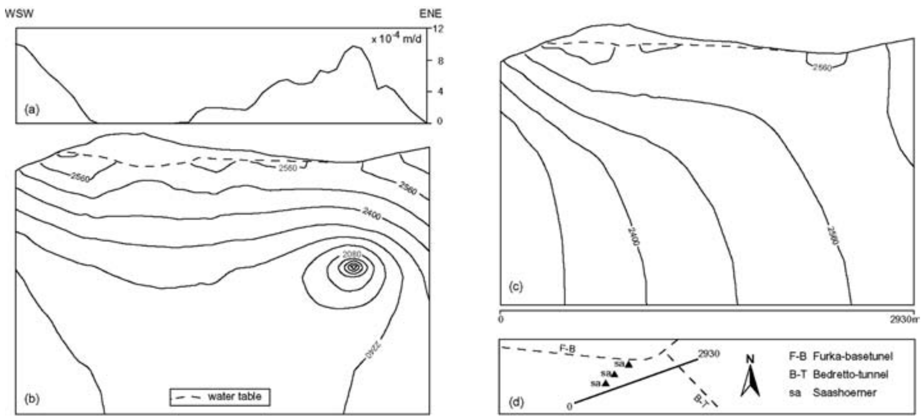

Figure 8. 2-D section through a 3-D hydrodynamic model of Rotondo area, showing: (A) Imposed groundwater recharge rate at ground surface, (B) position of free groundwater table and hydraulic head isolines with Bedretto and Furka tunnels, (C) position of free groundwater table and hydraulic head isolines without Bedretto and Furka tunnels, and (D) location of 2D section in plan view. Vertical exaggeration of (B) and (C) is 0.7.

surface were important factor influencing the location of the water table below ground surface. As expected, the valley floors and adjacent slopes act as groundwater discharge areas.

The deep tunnels create a local decrease in water table elevation compared to the natural situation (Figure 8). In the Rotondo area this tunnel induced water table drawdown occurs only locally below peaks and crests in the near vicinity of the tunnel traces, up to a lateral distance of about 1 km. In the area above the Bedretto adit water tables decrease by about 100 m, and close to the junction with the Furka basetunnel, below the steepest peaks, the drawdown amounts to 350 m. Even though the water table position below the crests differs significantly between the model scenarios, the elevations of the springs as mapped today in the Rotondo area is reproduced by all models within an accuracy of 20–100 m. Typical altitudes of springs in the test area close to the Bedretto adit (Gerental) are between 2200 and 2300 masl., i.e. 100–200 m above the valley floor. During construction of the tunnels, no impacts on surface springs were observed in these central parts of the tunnels. This could be related to the fact that significant water table reductions only occurred locally and in steep flanks at high altitudes, where springs are normally not diverted, used and/or monitored.

Compared to the small surface impacts, these tunnels create a big impact on the flow fields, leading to reversals of the natural flow directions over lateral distances of approximately 1 kilometer. This is illustrated in the cross-section shown in Figure 8. The recharge areas for the Bedretto adit are strongly influenced by the imposed recharge distribution at ground surface, in this case, the presence of glaciers above the equilibrium line. This effect is apparent when comparing these results with simulations for an equivalent uniform mean recharge rate. In the latter case, recharge areas are more regularly distributed on both sides of the draining tunnels, reaching laterally to distances of up to 1.5 kilometers. In general, the groundwater recharge areas from the hydrodynamic model compare well with the recharge areas derived from groundwater isotopic compositions (Ofterdinger et al. 2004).

4 IMPACTS OF SHALLOW TUNNELS ON SURFACE SPRINGS AND WETLANDS

The best data set showing the environmental impacts of shallow tunnels (or tunnel sections close to their portals) is derived from an analysis of the Obergesteln drift at the northern boundary of the Gotthard massif (Figures 2 and 4). Klemenz (1974) gives a detailed description of this case study and the analysis of tunnel drainage related water table drawdown in this area. The 2346 meter long Obergesteln tunnel was constructed between February 1972 and May 1973 for a transalpine gas pipeline. Driven southwards, the excavation consists of a 600 m long horizontal drift, followed by a 1280 m long and 22° inclined shaft, and then another 466 m long horizontal drift (Figure 9). The overburden reaches a maximum value of 500 m in the middle of the excavation. With the exception of 400 m in the south and 100 m in the north, the drift and shaft were excavated with a 5 m diameter tunnel boring machine.

4.1 *Hydrogeological situation in Obergesteln area*

After Schneider (1974), the Obergesteln excavation runs mostly (in the northern and central parts) at an angle of 90 to 85° to the foliation and cuts from north through a sequence of mica and feldspar rich biotite-plagioclase-gneisses (Tm 0–1745), quartzite (Tm 1745–1800), mixed ortho-para-gneisses (Tm 1800–1960), ortho-gneisses (Tm 1960–2306) and Quaternary sediments (Tm 2306–2346). The northern 800 m of the Obergesteln drift intersect a rock mass with deeply reaching flexural toppling and many open fractures running parallel to the foliation (Figure 9). Due to this toppling, the dip increases from 65° at the portal to 90° at the end of the horizontal drift.

The Obergesteln drift runs between two deeply incised tributary creeks to the Rhone valley: the Äginen creek in the southwest (1.8 km distance from the northern portal), and the Goneri creek in the northeast (2.5 km from the northern portal). Before the construction of the drift, springs mainly occurred Southwest of the Obergesteln drift, on the slopes of the Ägene creek at lateral distances of 1 to 2 kilometers. Many of these were used for drinking and irrigation water supply of Obergesteln and the surrounding alpine pastures. When projected onto the longitudinal section, the elevation of the Äginen valley is slightly lower than the Obergesteln drift; the horizontal distance decreases to the south (dotted line and distances in Figure 9). In Figure 9 all springs between the two creeks are shown as horizontal projections along the direction of the strike of foliation. From the altitude of the important and depleted springs, the original elevation of the groundwater table can be deduced.

4.2 *Transient groundwater inflows in Obergesteln area*

As reported by Klemenz (1974) during construction of the northern section of Obergesteln drift, large inflows occurred in the first 820 meters. In the vicinity of the northern portal the inflows only occurred in the first tens of meters behind the advancing tunnel face. These inflows mainly came from open foliation fractures and rarely from tectonic fractures intersecting these foliation planes. Water inflows started to occur at 150 meters from the portal with 15 l/s). The highest inflow rates of at least 210 l/s were reached at Tm 550. The inflow rates decreased between Tm 600 and 780 and increased again until Tm 820, where the rock mass became nearly dry (i.e., only a few dripping sites).

Most of the inflows ran dry very quickly (after 20–40 meters of excavation which corresponds to 1–2 weeks). However, the sum of the inflow from Tm 600–820, measured at the foot of the shaft since November 1972 remained between 50 and 60 l/s until the end of excavation (May 31, 1973). This implies that inflows at deeper tunnel sections decreased less quickly than those near the northern portal. One year later (mid-1974) the total inflow from the entire permeable section had dropped to steady state values of about 10 l/s, as measured during dry seasons. During snowmelt and after heavy rain, i.e. under conditions of strong vertical recharge, these total inflows react quickly and reach about 50 l/s.

4.3 *Depleted springs in Obergesteln area*

In response to this tunnel drainage, ten surface springs ran dry shortly after the tunnel had intersected this very permeable drift section. Figure 9 shows these depleted springs as measured on August 9, 1972 when the excavation had reached TM 620 (bold tunnel section). As reported in Klemenz (1974), depleted springs were observed by the owners "very soon" after the high tunnel inflows had occurred. The sequence of observed spring depletion is also shown in Figure 9 and clearly follows the excavation progress in the direction of the drift axes. Also, springs located at very low elevations relative of the drift elevation (e.g., No. 506 and 617) become totally depleted, implying that the groundwater table was lowered to the drift elevation within a very short time. For spring No. 609, which reacted last, the response time must have been less than 1–2 weeks. The horizontal distance between the springs and the drift, as measured along strike of the foliation, does not systematically effect the response time. Most importantly, during the southwardly progressing excavation,

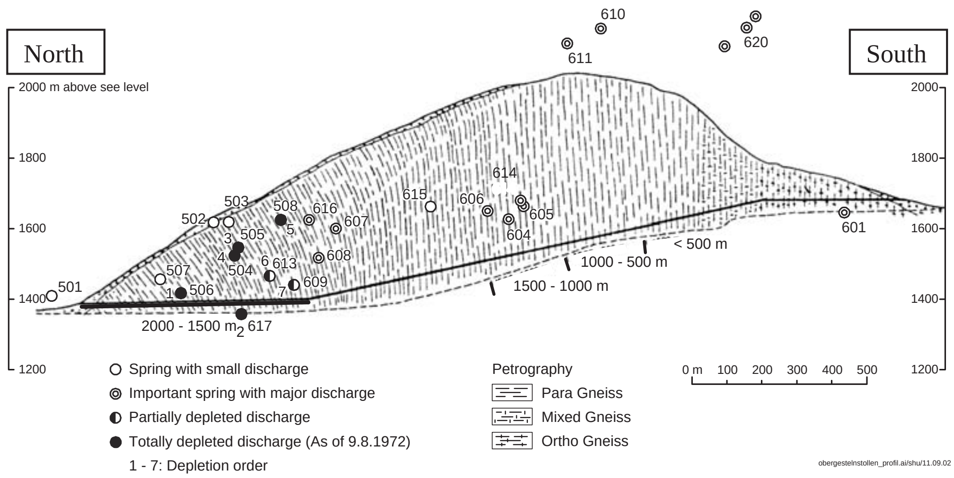

Figure 9. Longitudinal section along the Obergesteln drift. Horizontally projected springs (partially depleted; 1–7 indicate depletion order) along strike of foliation and Äginen Creek (broken line, with lateral distances indicated in the figure). Modified after Klemenz (1974).

no hydraulic interactions between the tunnel and surface springs were observed perpendicular to the strike of the toppled foliation.

These transient tunnel inflows and water table drawdowns can be explained reasonably well using a 2D analytical model that approximates the flow pattern in the planes normal to the tunnel axes by a superposition of linear horizontal flow with vertical flow to the tunnel. Inverse modeling of the observed inflows and inferred water table drawdowns yields anisotropic hydraulic conductivities in the toppled rock mass decreasing from the portal area (1E-3 m/s) to the lower bottom of the toppled rock mass (1E-5 m/s).

This situation is very typical for all underground excavations in the external crystalline massifs of the central Alps: Springs become depleted in the portal areas where stress relief, weathering or toppling can strongly increase the bulk hydraulic conductivity of the rock mass and early-time tunnel inflow rates. A very similar situation to that in the Obergesteln drift, was observed in the Bedretto adit of the Furka basetunnel at the southern margin of the Gotthard Massif. Here again, many surface springs ran dry above the tunnel portals located in toppled schists and gneisses of variable mineralogical composition. In the deeper or more distant tunnel sections, i.e. without surface related disturbances, no indications of environmental impacts on surface springs have been observed.

5 IMPACTS OF DRAINING TUNNELS ON SURFACE SETTLEMENTS

Recent high-precision levelling measurements of surface displacements along the Gotthard pass road have revealed up to 12 cm of subsidence along sections that pass several hundred meters above the Gotthard N2 highway tunnel (Figures 3 and 10). The Swiss Federal Office of Topography carried out the levelling measurements in 1993/1998 as a closed loop over the old Gotthard-pass road and through the N2 road tunnel (unpublished reports Swiss Federal Office of Topography 1997, 1998). Two earlier measurement campaigns were made along this N–S profile over the old Gotthard pass road in 1918 and 1970 before

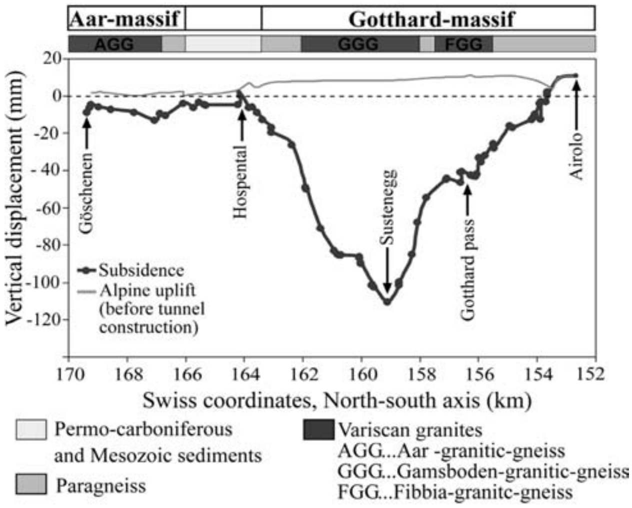

Figure 10. Levelling profile along the Gotthard pass road showing surface subsidence in the time interval 1970 to 1993/98 (after tunnel construction) and Alpine uplift (measured before tunnel construction).

tunnel construction. During the time interval, an undisturbed alpine uplift rate of 1 mm/year was detectable (Figure 9). This uplift rate concurs with estimated rates of 0.6 mm/year as determined using fission-track techniques (Kohl et al. 2000). In contrast, the time interval between 1970 and 1993/1998 (i.e., after tunnel construction) shows significant downward displacements along a 10-km region above the tunnel (Figure 10). More recently, surface triangulation measurements have confirmed the existence of a subsidence trough (Salvini 2002) over the tunnel. These results show that the extension of the trough in the EW direction is considerably smaller than in the NS direction.

5.1 *Surface settlements induced by inflows to the Gotthard N2 highway tunnel*

The close spatial proximity between the singular tunnel inflows of 110 and 150 l/s (early time inflow at Tm 9910 and 9935, respectively) and maximum settlement (Figure 3) and the temporal relationship between tunnel construction and settlement clearly shows causality between water drainage into the tunnel and surface deformation. Localized surface processes, e.g. creeping landslides or flexural toppling, could be excluded as alternative explanations given the absence of local indicators and the extent over which the settlements were measured (10 km along a N–S line, roughly parallel to the tunnel axis). Of surprise was the relatively small tunnel interval over which the high initial inflow cluster occurred (3 km, see Figure 5A) relative to the measured settlement trough (10 km). As discussed in detail in Zangerl (2003) and Zangerl et al. (2003), this subsidence is related to large-scale consolidation resulting from fluid drainage and pore-pressure changes in the rock mass (i.e., fractures and intact rock). These pore pressure changes might have also lead to reductions in the elevation of the groundwater table. However, during construction of the Gotthard N2 highway tunnel, no depleted surface springs were reported over the central and deep sections of the tunnel. Today a spring line can be mapped at an elevation of 2100 to 2500 masl in the area of Figure 3. An alternative explanation could also be that the initial spring line was higher and that water table drawdowns only occurred locally, i.e. close to the major groundwater pathways.

5.2 *Coupled hydro-mechanical deformation models of Gotthard pass area*

The collective observations and possible hydro-mechanical mechanisms described in detail in Zangerl (2003) led to the working hypothesis that the permeable fault zones provided a high-permeability conduit that permitted pore pressure drainage to penetrate deeply and relatively rapidly into the rock mass in a WSW-ENE direction, and that lateral diffusion of pore pressure drawdown into the relatively intact rock blocks (bounded by the fault zones; see Figure 9) occurred on longer timescales. Estimates for the time required for drawdown of pore pressures within the intact blocks, conditioned by field observations of block-size distribution and laboratory-derived estimates of the poro-elastic properties, suggest timescales of days to several years for block-sizes of 10 m to 100 m respectively. Thus, steady-state pore pressure conditions likely prevailed by the time the 1993/98 geodetic surveys revealed the subsidence trough, 21 years after tunnel construction.

For these reasons, the steady-state geometry of the settlement trough was modelled using a 2-D section running parallel to the tunnel axes, i.e. normal to the major permeable fault zones. Simulations with the 2D distinct element code UDEC and the continuum code VISAGE provided very useful insights into the underlying mechanisms. As most of the preferential pathways for groundwater flow and most of the discontinuities at depth are steeply inclined (the frequency of horizontal fractures strongly decreases with depths), the surface deformations could not be explained with closure of subhorizontal fractures alone. As described in detail in Zangerl (2003) and Zangerl et al. (2003), different deformation models had to be considered for the explanation of the observed surface deformations (Figure 11): normal closure of the subhorizontal fractures induced by a reduction of normal effective stress across the subhorizontal fractures; normal closure of vertical fractures or faults due to drainage, resulting in expansion of (impermeable) rock blocks in the horizontal direction and contraction in the vertical direction (i.e., Poisson ratio effect); linear poro-elastic behavior of rock blocks; and combined effects leading to shear along persistent inclined discontinuities (faults).

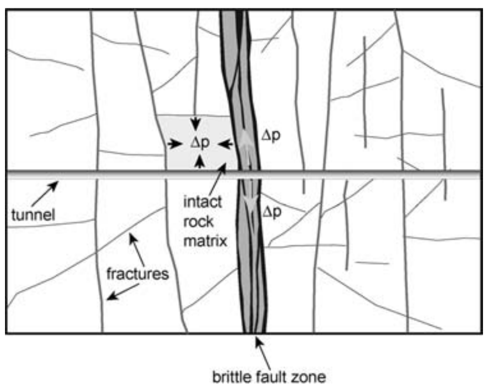

Figure 11. Conceptual model of coupled hydro-mechanical processes in crystalline rocks of Gotthard pass area.

Results from a 2D UDEC discontinuum Model that consider normal closure and shear of subhorizontal and subvertical joints and faults, as well as deformation of impermeable blocks are shown on Figure 12. The contours of vertical displacement generated by the effective stress changes that accompany drainage into the tunnel are shown in Figure 12a, and the corresponding profile of surface subsidence in Figure 12b. Vertical strain arises from closure of horizontal joints and the faults which, because they are mostly steeply inclined, allow the intact blocks to expand laterally. This generates vertical contraction strain through the Poisson's ratio effect. The maximum predicted subsidence of 0.042 m is shifted several hundred metres to south of the major inflow zone due to topographic, structural and hydraulic conductivity effects. The modeled subsidence trough extends about 9000 m in width with subsidence values greater than 0.01 m occurring over an area that is more than 4500 m wide. Shear deformations on faults and fractures, predominately of elastic type, are also indicated in Figure 12a. Within the central subsidence trough, shear displacements of up to 4 mm occurred on faults. Thus, the shape of the subsidence trough calculated in the distinct-element simulations reproduced both the general asymmetry and several key inflections observable in the measured subsidence profile. This agreement between the measured and modelled subsidence curves is directly related to the explicit inclusion of the fault zones mapped at surface and in the Gotthard N2 highway tunnel, both in terms of location and orientation.

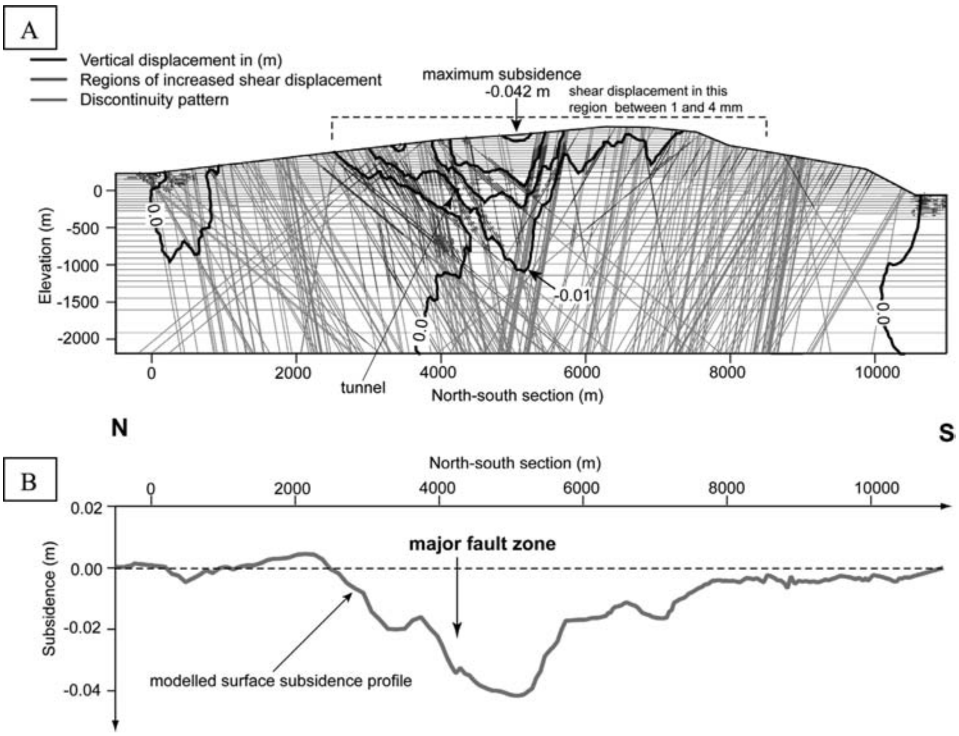

Figure 12. Discontinuum/distinct-element model results showing (A) discontinuity pattern, vertical displacements and shear displacements along steeply inclined fault zones, and (B) resulting modelled surface subsidence profile.

Results obtained from poroelastic continuum analysis produced a subsidence profile that for the most part was symmetrical about the point of tunnel drainage. However, numerical results also showed that the intact rock matrix can considerably contribute to rock mass deformation through poroelastic strains. Such poroelastic strains seem to be required in addition to the fracture related deformations, illustrated by the UDEC results of Figure 12, which yield only about 50% of the measured total subsidence above the Gotthard N2 highway tunnel.

6 CONCLUSIONS

The observations presented from the Gotthard massif in the Central Swiss Alps illustrate the effects tunnels in fractured crystalline rocks can have on groundwater flow systems, surface springs and surface deformations. Serious environmental impacts on surface waters are observed in high permeability areas close to the tunnel portals, or for tunnels running only a few hundred meters below ground surface. In these areas, water table drawdown can reach the elevation of the tunnel and significantly affect surface springs and wetlands over lateral distances of several kilometers within a few weeks. Also tunnels located deep below ground surface (500–1500 m) have considerable impacts on natural flow systems. Their effects are however much less visible: surface recharged groundwaters will flow towards the draining tunnels, re-locating groundwater divides and reversing flow directions over lateral distances larger than one kilometer. Pore pressure reductions created by draining tunnels at depth may also lead to large scale rock mass deformations leading to surface settlements exceeding 10 cm.

With all these processes, brittle deformations play a key role, either in the form of small scale fracturing or large scale shear under low temperature brittle conditions. In the investigated area, the most dominant of these structures are steep and co-planar (striking WSW-ENE), generating an important hydraulic anisotropy and preferential pathways for groundwater flow and pressure diffusion.

Towards surface (in the upper hundred meters), gravitational, unloading and weathering processes locally increase bulk rock mass hydraulic conductivity, leading to initially very high tunnel inflows and quickly propagating environmental impacts.

Most of the models used to interpret these observations have assumed equivalent continuum hydraulic properties. Nevertheless, they succeeded well in explaining most of the critical observations. This is mainly due to the fact that most of the available data sets do not refer to individual fault zones or groundwater pathways, but to larger scale observations, such as bulk tunnel inflows or large scale surface settlements. The authors hope that in future tunneling projects, transient data about inflows, temperatures and hydrogeochemical compositions (including isotopes) are collected for individual permeable fault zones.

Most of the analyses have either assumed steady state 3-D groundwater flow or transient 2-D flow. Obviously tunnels create a transient 3-D flow field during incremental excavation advancement. These effects will also have to be investigated in future studies.

Besides rock mass bulk hydraulic conductivity, groundwater recharge is an important factor for the location of a free groundwater table in mountainous systems and also for the long term inflow to a draining tunnel. Both groundwater recharge and the locations of groundwater tables are poorly constrained in Alpine terrain. In order to better predict environmental impacts of such tunnels, deep surface-based boreholes for monitoring purposes would be of very high value.

ACKNOWLEDGEMENTS

We would like to thank Werner Klemenz and Dr. Susanne Laws for many insightful discussions. Many thanks are also extended to the Furka Oberalp Bahn AG for providing access to the Bedretto adit.

REFERENCES

Angelier J (1994) Fault slip analysis and palaeostress reconstruction. In: Hancock (ed) Continental deformation. Pergamon Press , pp 53–100

Badoux A (1999) Untersuchung zur flächendifferenzierten Modellierung von Abfluss und Schmelze in teilvergletscherten Einzugsgebieten. Master's thesis, Institute of Geography, Federal Institute of Technology, Zurich, Switzerland (in German)

Bossart P, Mazurek M (1991) Structural Geology and Water Flow-Paths in the Migration Shear-Zone. Nagra NTB 91 (12):1–55

Burkhard M (1999) Strukturgeologie und Tektonik im Bereich Alptransit. In: Löw et al. Vorerkundung und Prognose der Basistunnels am Gotthard und am Lötschberg. GEAT Symposium, Zürich, Balkema Publishers, Rotterdam:45–56

BUWAL (1998) Wegleitung zur Umsetzung des Grundwasserschutzes bei Untertagebauten. Bundesamt für Umwelt Wald und Landschaft, Bern, 32 pp

BWG (2001) Hydrologischer Atlas der Schweiz, Landeshydrologie. Bundesamt für Wasser und Geologie, Bern

Challandes (2001) Behavior of Rb-Sr and Ar-Ar systems in metagranite shear zones (Roffna granite and Grimsel granodiorite, Swiss alps). PhD dissertation, University of Neuchatel

Choukroune P, Gapais D (1983) Strain pattern in the Aar granite (central alps). Orthogneiss developed by bulk inhomogenous flattening. J. Struct. Geol. 5(3/4):411–418

Frei B, Löw S (2001) Struktur und Hydraulik der Störzonen im südlichen Aar-Masssiv bei Sedrun. Eclogae geol. Helv. 94:13–28

Frey M, Mählmann RF (1999) Alpine Metamorphism of the Central Alps, Schweiz. Mineral Petrogr. Mitt. 79:135–154

Frey M, Bucher K, Frank E, Mullis J (1980) Alpine metamorphism along the geotraverse Basel-Chiasso – a review. Ecologae geologicae Helvetia 73:527–546

Gurtz J, Peschke G, Mendel O (1990) Hydrologic processes in small experimental areas influenced by vegetation cover. In: Hydrological Research Basins and Environment, Proceedings and Information No 44, International Conference Wageningen, pp 61–69

Gurtz J, Baltensweiler A, Lang H (1999) Spatially distributed hydrotope-based modelling of evapotranspiration and runoff in mountainous basins. Hydrological processes 13(17):2751–2768

Klemenz W (1974) Die Hydrogeologie des Gebirges im Obergestelnstollen. Gaz – Wasser – Abwasser 54/7:287–289

Kohl T, Signorelli S, Rybach L (2000) Constraints on palaeo-topography by revised apatite fission track uplift rates. European geophysics society, 25th General Assembly, V2, Nice

Kölla E (1993) Gotthard-Basistunnel – Regionale Hydrogeologie im Projektgebiet unter besonderer Berücksichtigung des Ritom-Gebietes. Unpublishes Report, 30.11.1993

Labhart T (1999) Aarmassiv, Gotthardmassiv und Tavetscher Zwischenmassiv: Aufbau und Entstehungsgeschichte. In: Löw S, Wyss R (eds) Vorerkundung und Prognose der Basistunnels am Gotthard und am Lötschberg. Proceedings Symposium Geologie Alptransit, pp 31–43

Laws S (2001) Structural, Geomechanical and Petrophysical Properties of Shear Zones in the Eastern Aar Massif. PhD dissertation, Federal Institute of Technology, Zurich No.14245

Lerner DN, Issar AS, Simmens I (1990) Groundwater Recharge – A Guide to Understanding and Estimating Natural Recharge. International Contributions of Hydrogeology, IAH, Hannover: 8, 345 pp

Loew S (2001) Natural Groundwater Pathways and Models for Regional Groundwater Flow in Crystalline Rocks. In: New Approaches to Characterizing Groundwater Flow, IAH International Congress, Munich, pp 1013–1018

Luetzenkirchen V (2002) Structural Geology and Hydrogeology of Brittle Fault Zones in the Central and Eastern Gotthard Massif, Switzerland. PhD dissertation, Federal Institute of Technology, Zurich, No.14749

Marquer D., Gapais D. (1985) Les massifs cristallins externes sur uns transversale Guttanen-Val Bedretto (Alpes Centrales): structures at histoire cinematique. C.R. Acad. Sc. Paris t.301, Serie II, No 8, 543–546

Ofterdinger U (2001) Groundwater flow systems in the Rotondo Granite, Central Alps, Switzerland. PhD dissertation, Federal Institute of Technology, Zurich, No.14108

Ofterdinger U, Balderer W, Loew S, Renard P (2004) Environmental isotopes as indicators for ground water recharge to fractured granite, Ground Water 42/6:868–879

Salvini D (2002) Deformationsanalyse im Gotthardgebiet. Institut für Geodäsie und Photogammetrie, ETH Zürich

Schmid SM, Pfiffner OA, Froitzheim N, Schönborn G, Kissling E (1996) Geophysical-geological transect and tectonic evolution of the Swiss-Italian Alps. Tectonics 15(5):1036–1064

Stapff FM (1882) Geologische Aufnahme des Gotthard-Bahntunnels. 60 Geologische Tunnelprofile 1:200 (Längen- und Horizontalschnitte) – Quartalsberichte zu Händen des Schweizerischen Bundesrates

Steck A, Hunziker JC (1994) The tertiary structural and thermal evolution of the Central Alps – Compressional and extensional structures in an orogenic belt. Technophysics 238:229–254

Steck A (1968) Die alpdischen Strukturen in den zentralen Aaregraniten des westlichen Aarmassivs. Ecologae geol Helv 61(1):19–48

Stini J (1950) Tunnelbaugeologie. Springer Verlag, Wien

Vitvar T, Gurtz J (1999) Spatially distributed hydrological modeling in the Rotondo area, western Gotthard-massif. Technical report 3465/16, Federal Institute of Technology, Zurich, Engineering Geology

Zangerl C (2003) Analysis of Surface Subsidence in Crystalline Rocks above the Gotthard Highway Tunnel, Switzerland. PhD dissertation, Federal Institute of Technology, Zurich, No. 15051

Zangerl C, Eberhardt E, Löw S (2001) Analysis of ground settlements above tunnels in fractured crystalline rocks. In: Särkkä P, Eloranta P (eds) Eurorock Symposium, Rock Mechanics – A Challenge for Society, Espoo, Finland pp 717–722

Zangerl C, Eberhardt E, Loew S (2003) Ground settlements above tunnels in fractured crystalline rock: numerical analysis of coupled hydromechanical mechanisms. Hydrogeology Journal 11:162–173

Exhibit 4

Wildlife Behavior in Response to Traffic Disturbance

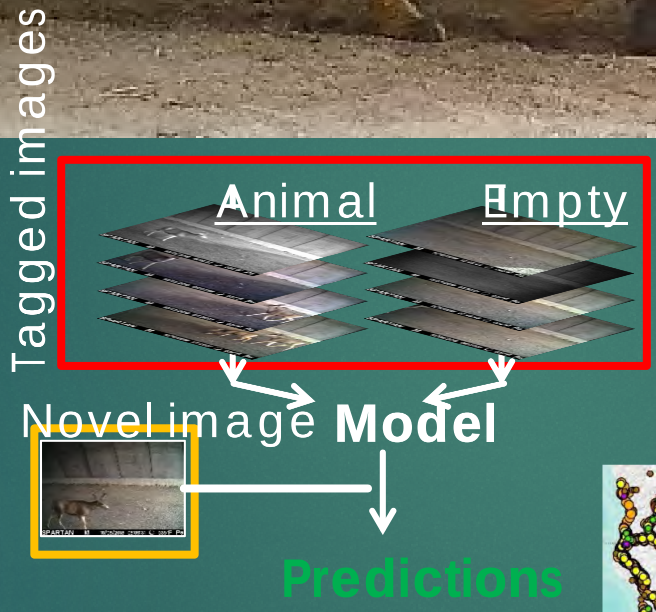

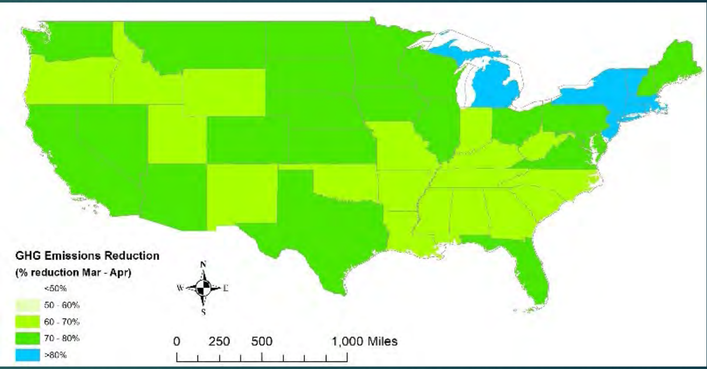

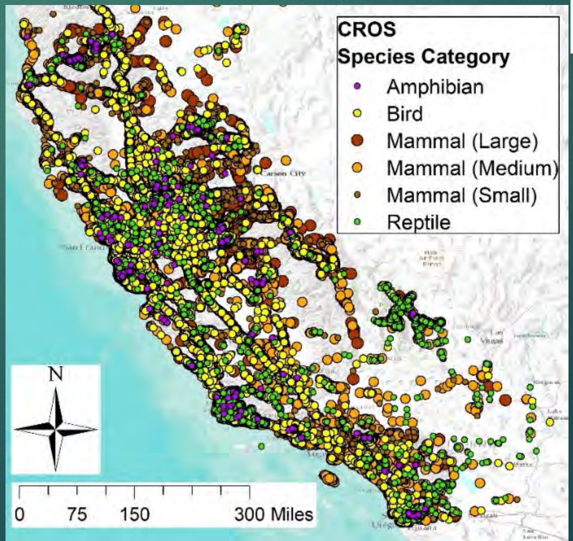

FRASER SHILLING

ROAD ECOLOGY CENTER

HTTPS://ROADECOLOGY.UCDAVIS.EDU

FMSHILLING@UCDAVIS.EDU

Wildlife Behavior in Response to Traffic Disturbance

FRASER SHILLING

AMY COLLINS

TRAVIS LONGCORE (UCLA)
WINSTON VICKERS (UCD)

Acknowledgements

This research was sponsored by the National Center for Sustainable Transportation (NCST), supported by the U.S. Department of Transportation (USDOT, including FHWA) and the California Department of Transportation (Caltrans) through the University Transportation Centers program.

I would like to thank the NCST, the USDOT, and Caltrans for their support of university-based research in transportation, and especially for the funding provided in support of this project. I would also like to thank Clark Stephens, Dr. David Waetjen, Rich Codington, Jamie Bourdon, Ben Banet, Colin Raff, Catherine Le, and 16 undergraduate researchers for their invaluable help

Main Messages and Findings

1) Wildlife are variably sensitive to traffic disturbance, including noise and light from vehicles

2) This sensitivity will cause different impacts on their distribution and use of crossing structures, which will have environmental impacts (e.g., on predator-prey interactions, juvenile dispersal, resilience to climate change, forage diversity, competitive species interactions, population genetics and recovery, etc.)

3) The mechanism for distribution/visits could be wildlife behavior in response to traffic

4) It is possible that designing the approaches to crossing structures could reduce impacts and improve wildlife use

Background

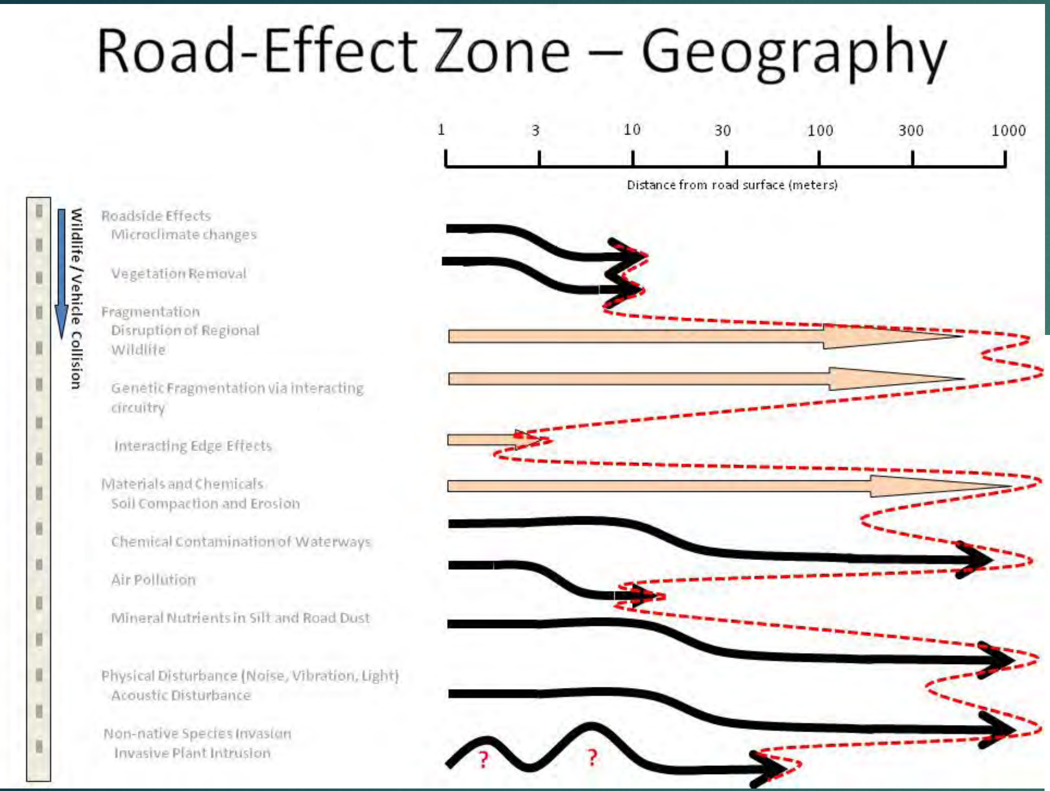

Road-Effect Zone – Geography
1
3
10
30
100
300
1000
Distance from road surface (meters)
Wildlife / Vehicle Collision
Roadside Effects
Microclimate changes
Vegetation Removal
Fragmentation
Disruption of Regional Wildlife
Genetic Fragmentation via interacting circuitry
Interacting Edge Effects
Materials and Chemicals
Soil Compaction and Erosion
Chemical Contamination of Waterways
Air Pollution
Mineral Nutrients in Silt and Road Dust
Physical Disturbance (Noise, Vibration, Light)
Acoustic Disturbance
Non-native Species Invasion
Invasive Plant Intrusion
?
?

Policy and Management Nexus for Road Effect Zone
Highway Project Development
Planning (DOT, MPO)
Advance avoidance
Programming (DOT, MPO)
Funding tied to REZ performance
Assessment (DOT, Resource Agencies)
Environmental protection laws
Final Project Design ROW (DOT)
Determination of REZ-mitigation
Construction Monitoring (DOT, Resource Agencies)
Environmental protection laws
Maintenance, Mitigation Effectiveness (DOT, Resource Agencies)

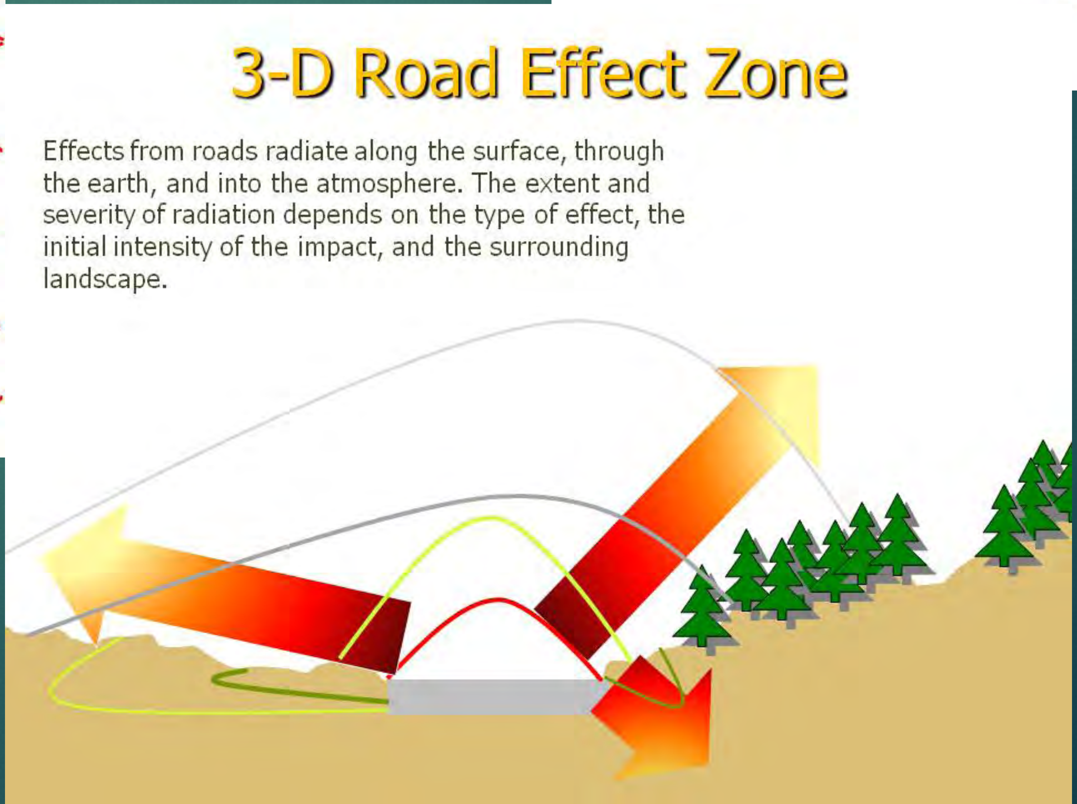

3-D Road Effect Zone
Effects from roads radiate along the surface, through the earth, and into the atmosphere. The extent and severity of radiation depends on the type of effect, the initial intensity of the impact, and the surrounding landscape.

Background

- Traffic is loud and variable
- Noise can extend hundreds of meters beyond the road

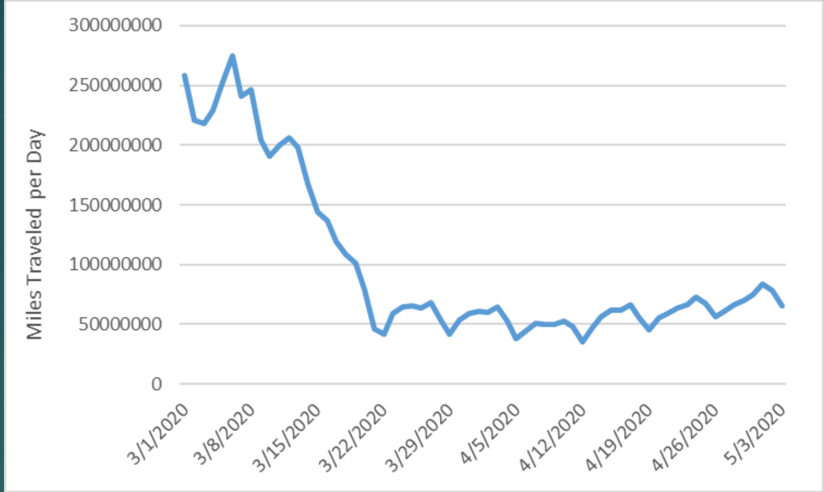

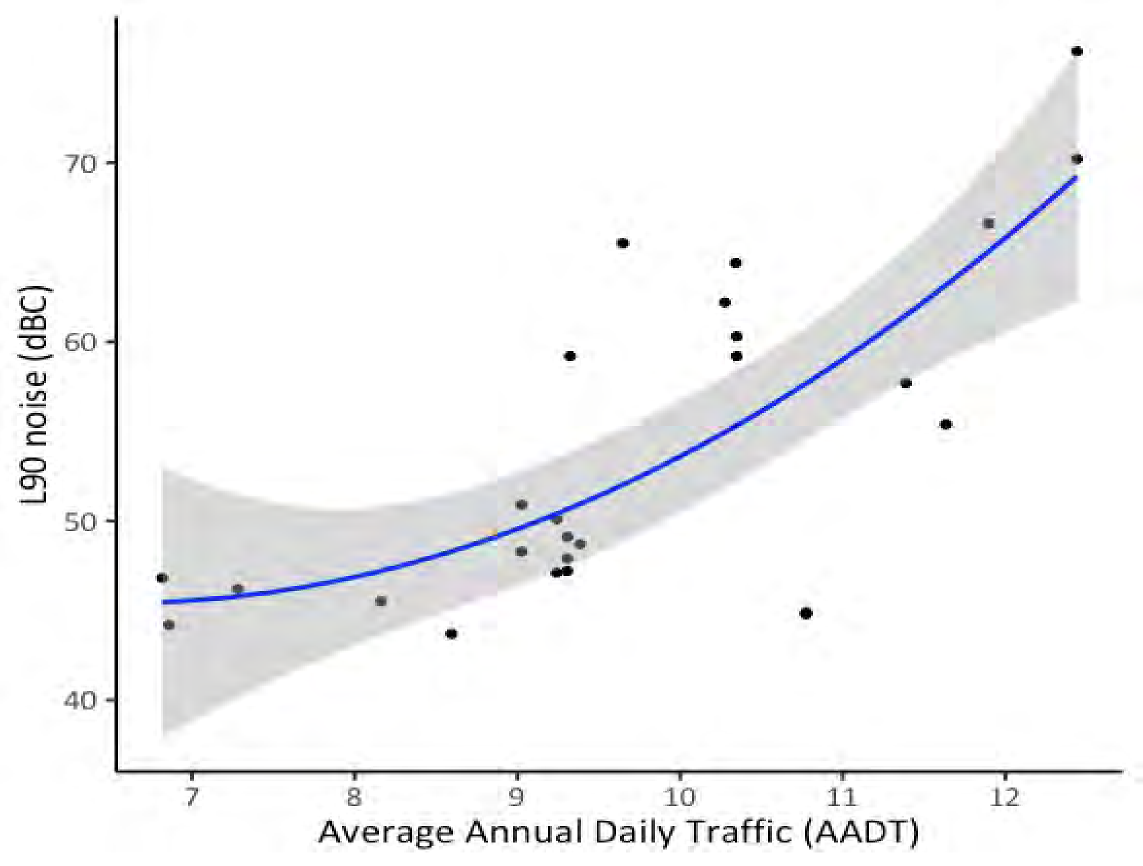

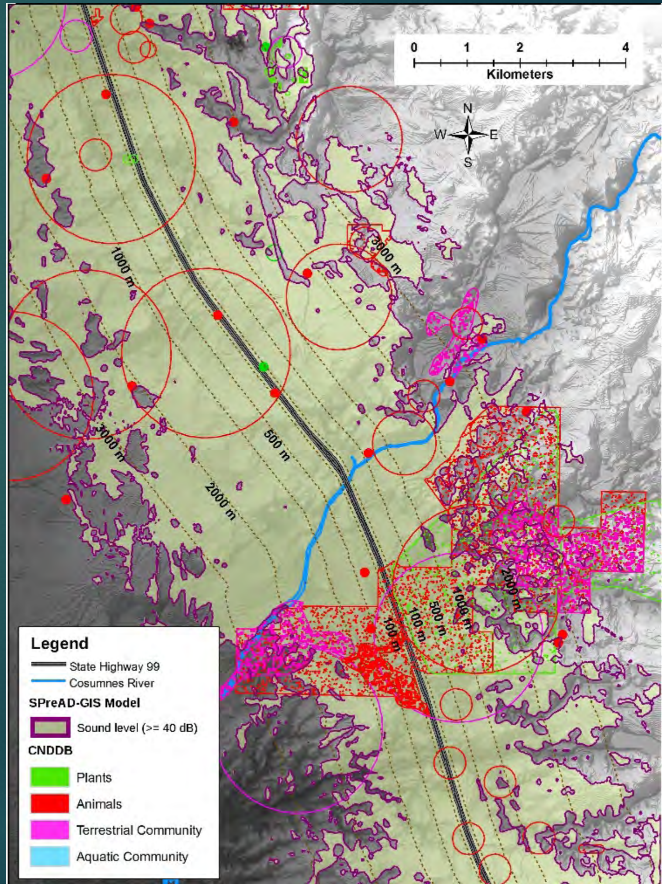

Traffic is loud (and bright)

Noise and light propagation across real landscapes is complex

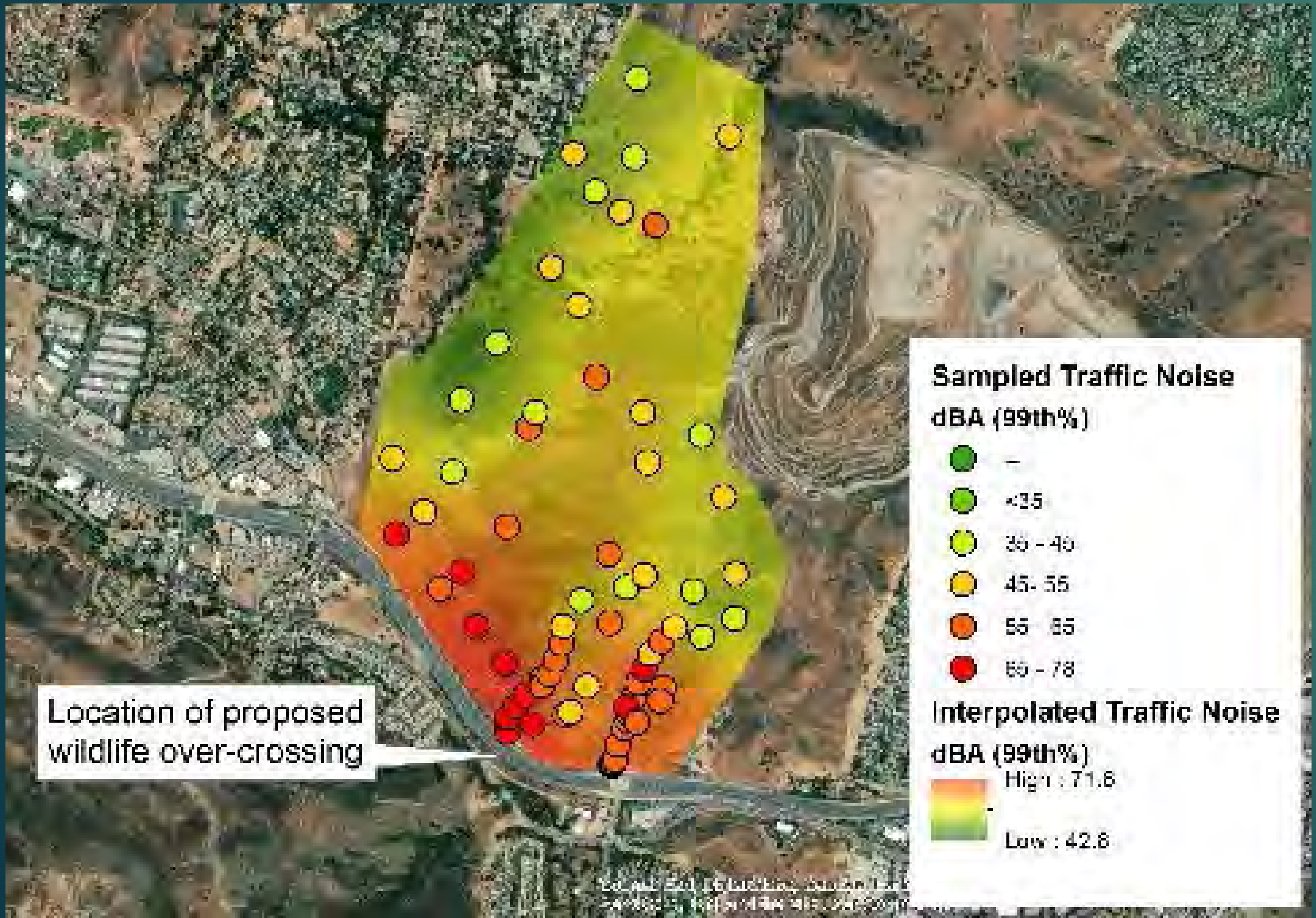

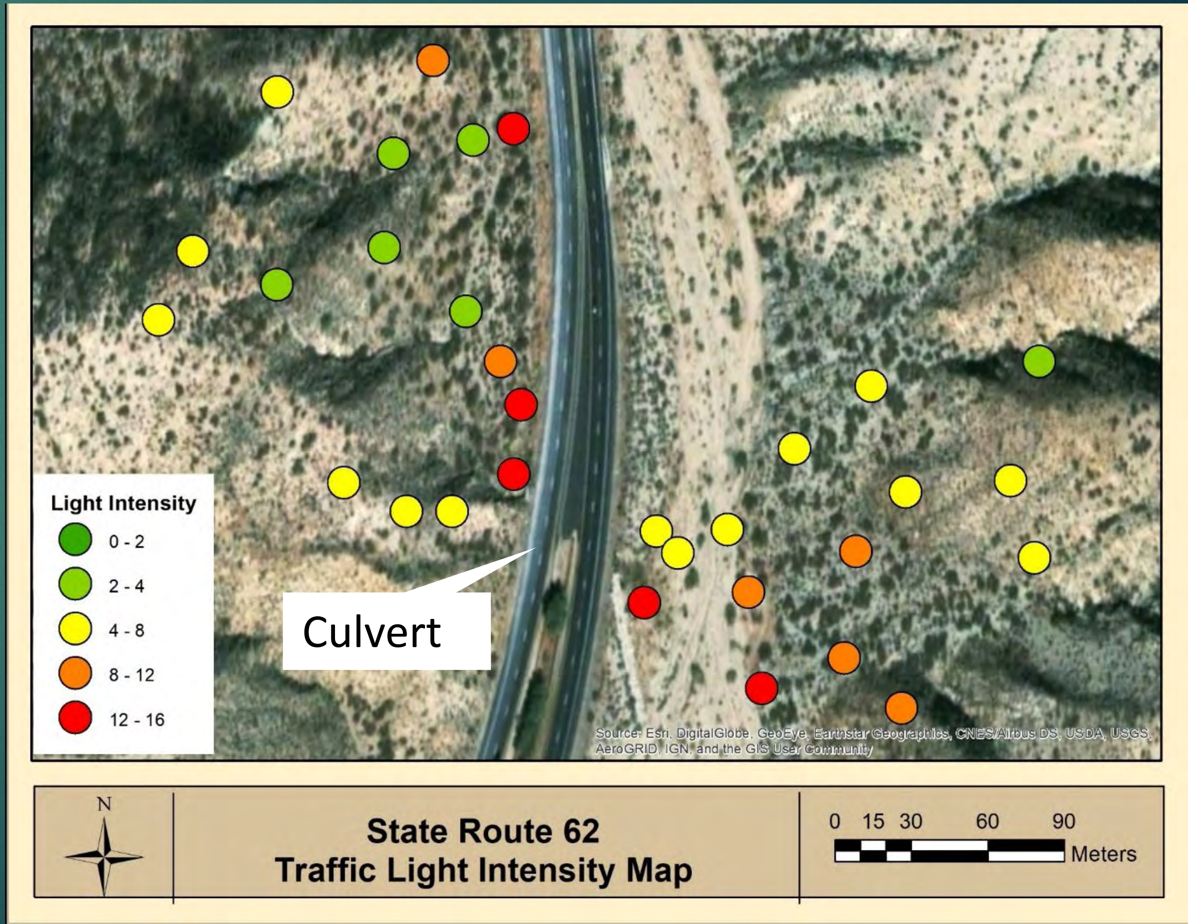

Are underpasses effective with noise and light disturbance?

Approach Zone

- Crossing structure
- Human and other activity
- Approach zone

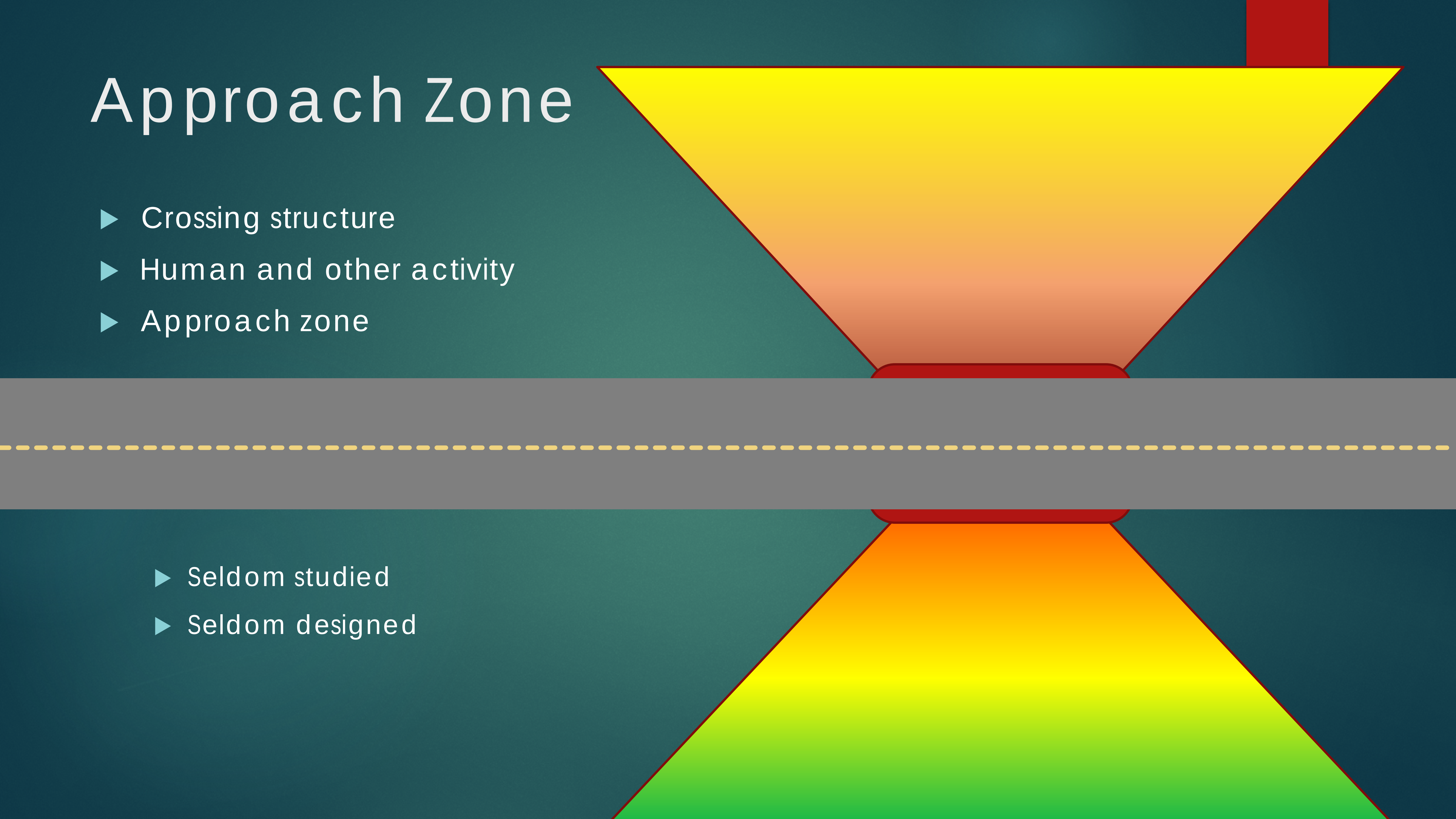

- Seldom studied
- Seldom designed

Workflow

- Field work
- Data processing and management through CamWON (https://wildlifeobserver.net), including removing false positives, counting humans/vehicles, summarizing events/species, events/data etc.
- Wildlife behavior analysis with BORIS (http://www.boris.unito.it/)
- Statistical modeling to find best explanation for data
- Develop "wildlife-responsive design" elements and structures to increase likelihood of structure use

Field work

Camera trap, noise (dBA, dBC) & light measurements

- 26 sites in California
- Structures across 1 – 5 lane highways
- 3 years of field study (2016-2019)

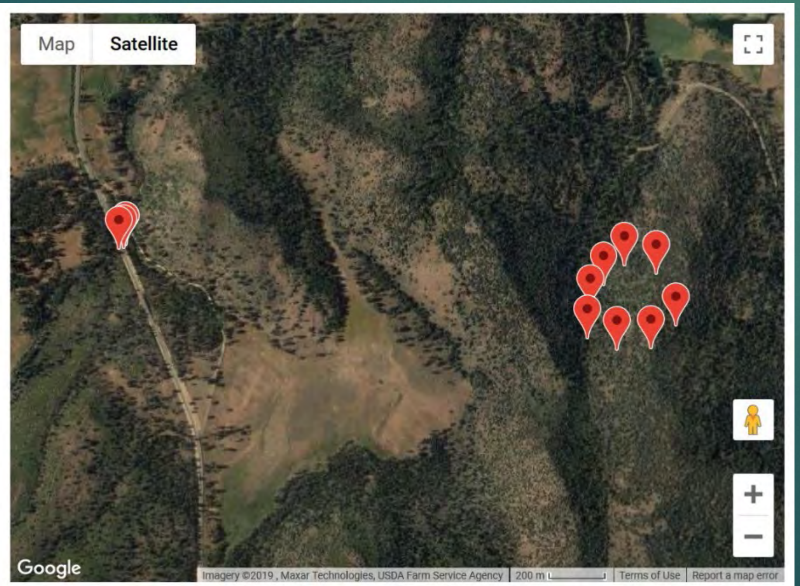

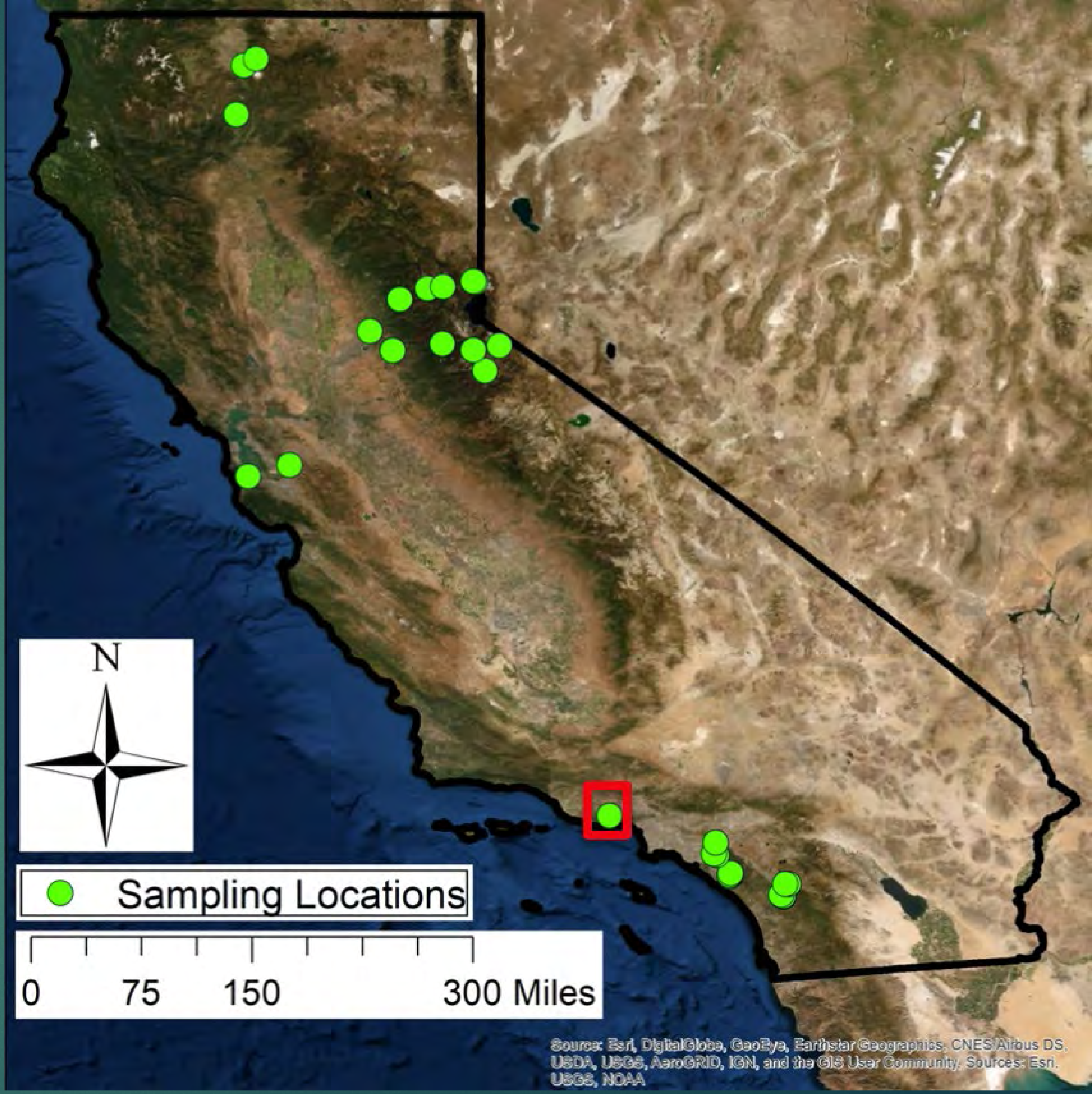

Light and noise

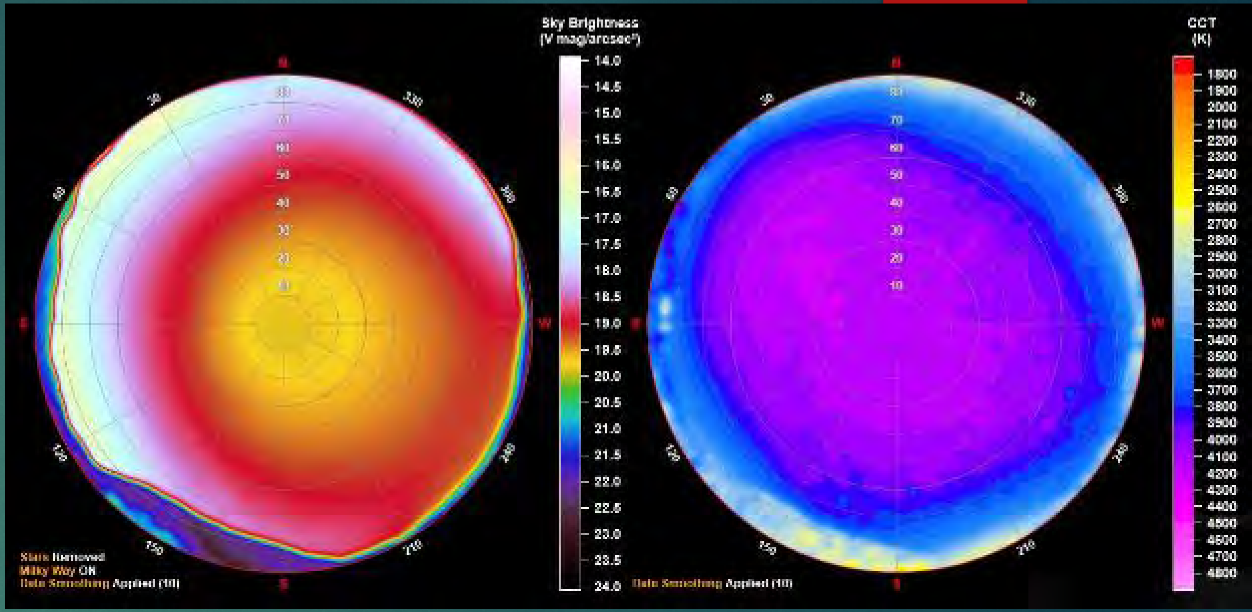

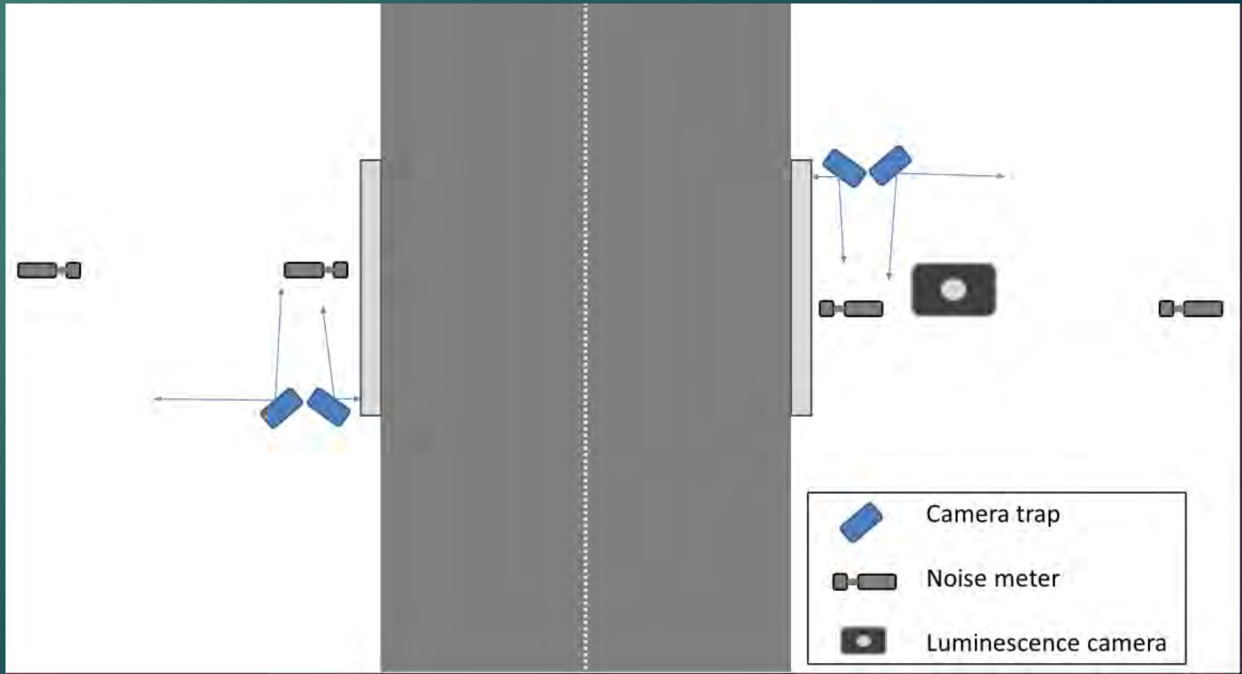

Analysis

Comparison of wildlife distribution in background areas and crossing structures

Analysis of animal activity relative to traffic disturbance, structural and approach zone attributes, human activity, time of day/night

9,360 trap nights

> 28,300 observations!

32 mammal species captured!


Western spotted skunk
Spilogale gracilis


American badger
Taxidea taxus


Black bear
Ursus americanus


Mountain lion
Puma concolor


Gray fox
Urocyon cinereoargenteus


Coyote
Canis latrans

Species richness: underpass vs background

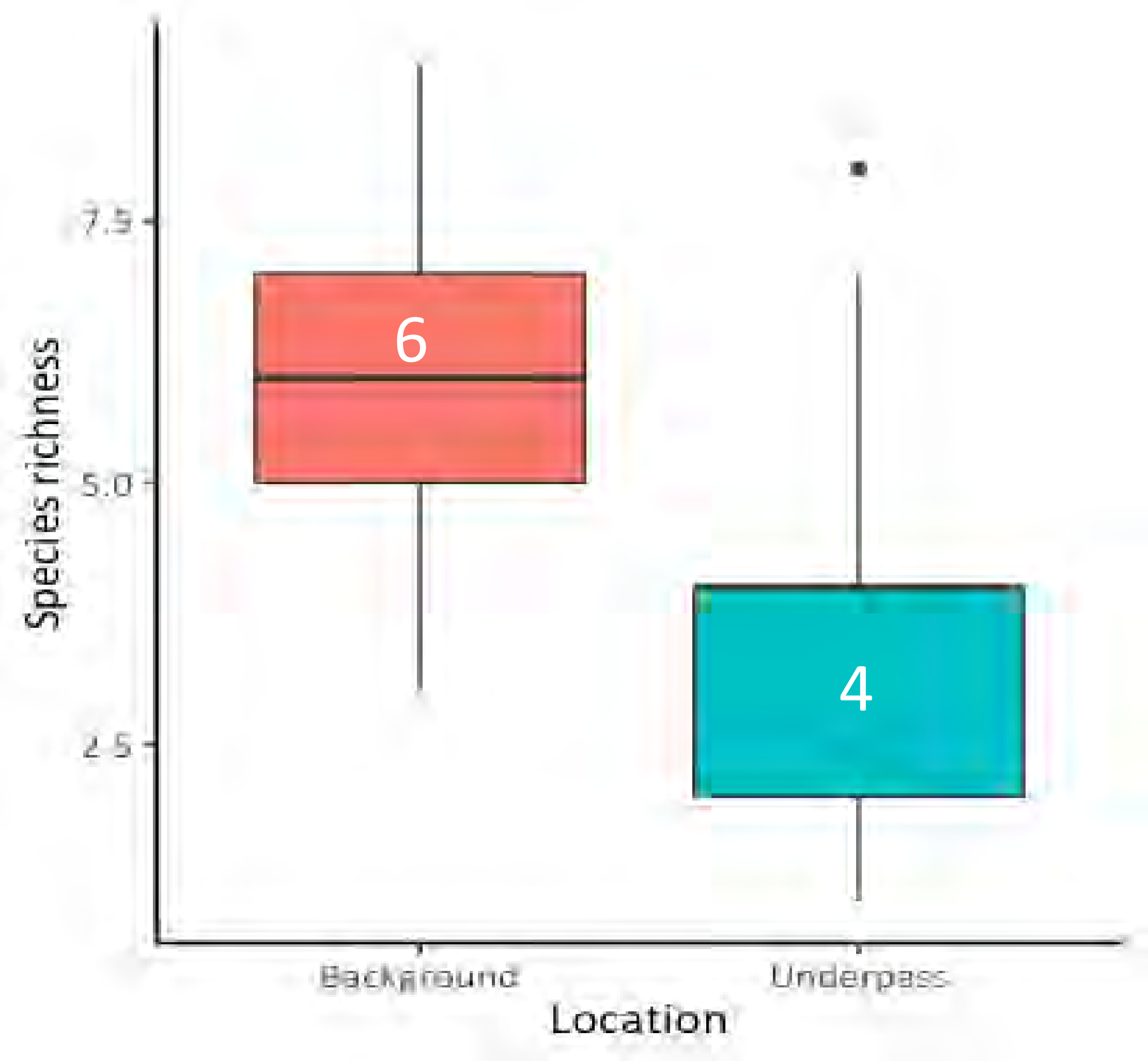

Complete avoidance?

Response variable: Species richness at underpass

- Generalized linear model (environmental characteristics, underpass characteristics, humans, location in CA)
- Best model:

variable	P - value	Relationship to species richness
CA location (south)	0.009 **	-
Elevation	0.02 *	-
1-week minimum noise (dbC)	0.04 *	-
Underpass width	0.09	
Human presence	0.2	

Decreased frequency of visits?

- Response: visits/day
- GLM
- Light had no relationship
- Vehicular noise (1-week) - inverse U

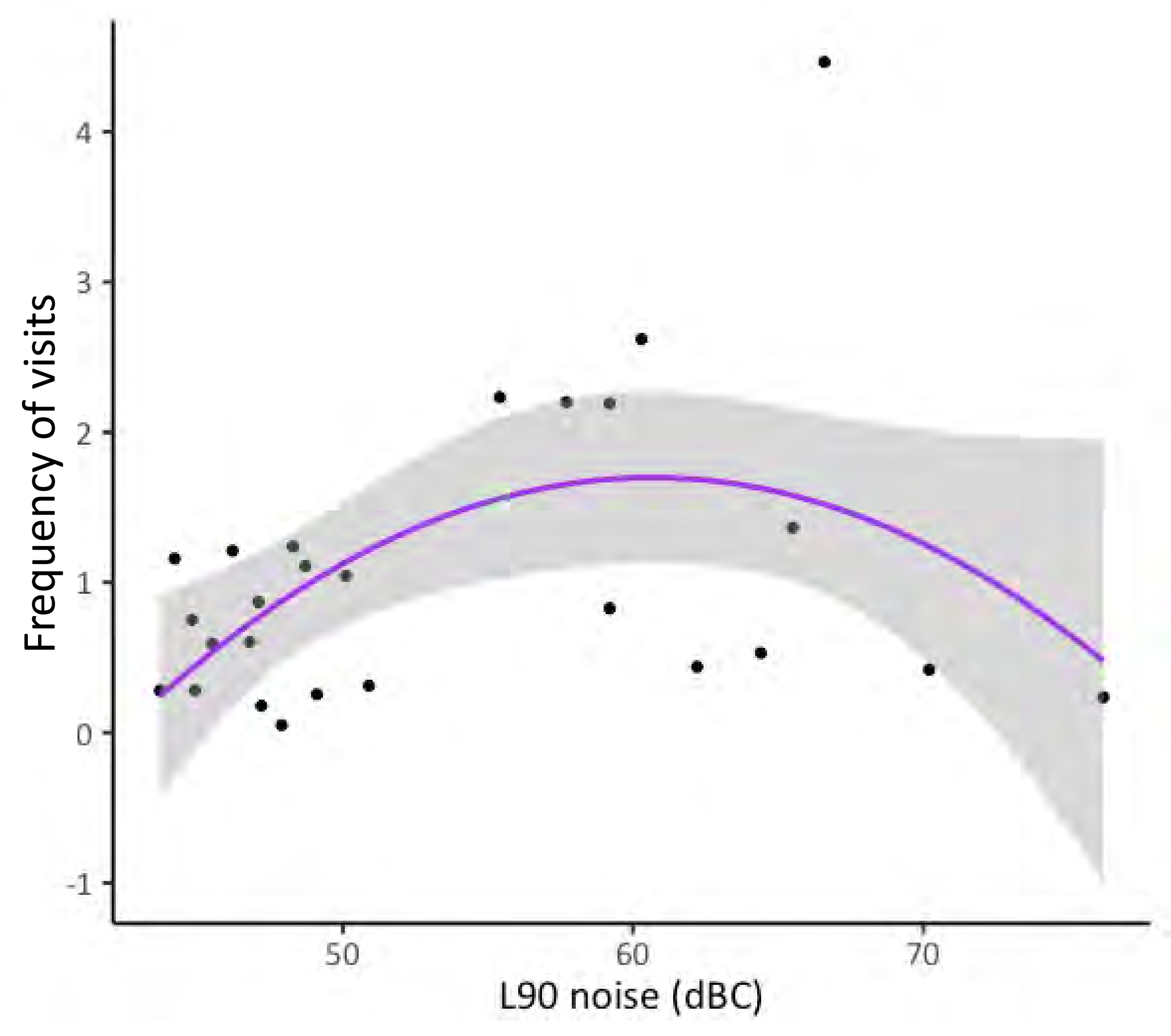

Decreased frequency of visits?

- GLM
- Light had no relationship
- Vehicular noise (1-week) - inverse U
- Similar response roadkill vs AADT

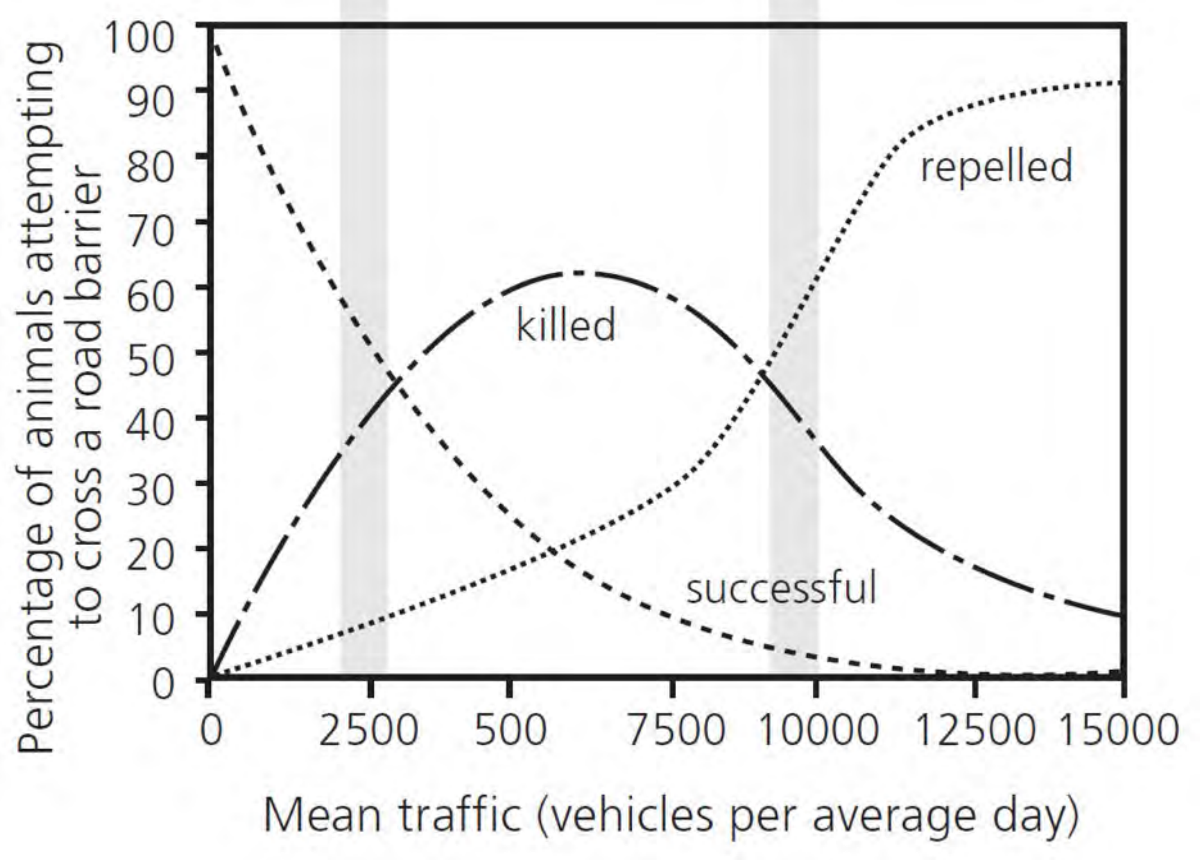

Andreas Seiler, 2003. Effects of infrastructure on Nature

Most wildlife avoid traffic noise

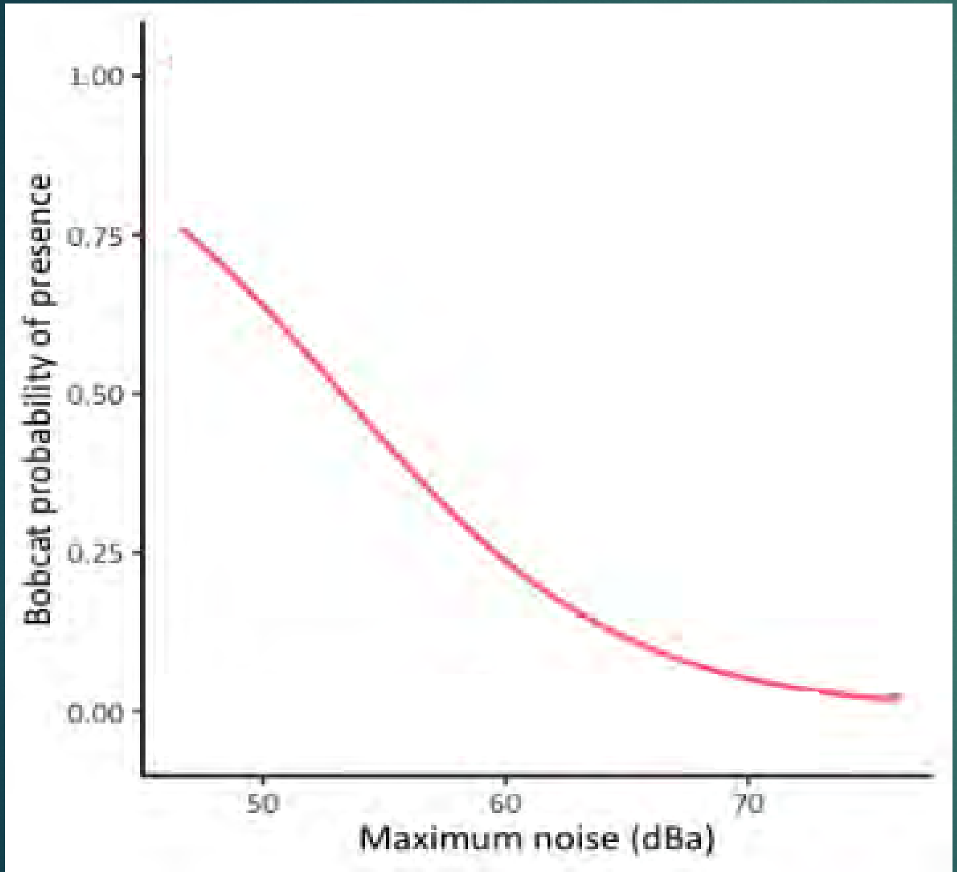

Los Angeles to build world's largest wildlife bridge across 10-lane freeway

An $87m corridor will extend over Highway 101 to reconnect the ecosystem and possibly save mountain lions from extinction

▲ A wildlife corridor, the biggest in the world, is planned to extend over Highway 101 north-west of Lost Angeles. Photograph: RCD of the Santa Monica Mountains, Clark Stevens (architect), Raymond Garcia (illustrator)

Wildlife behavior with traffic

- Behavioral Observation Research Interactive Software
  - User annotates video
  - Indicates time spent on different behaviors

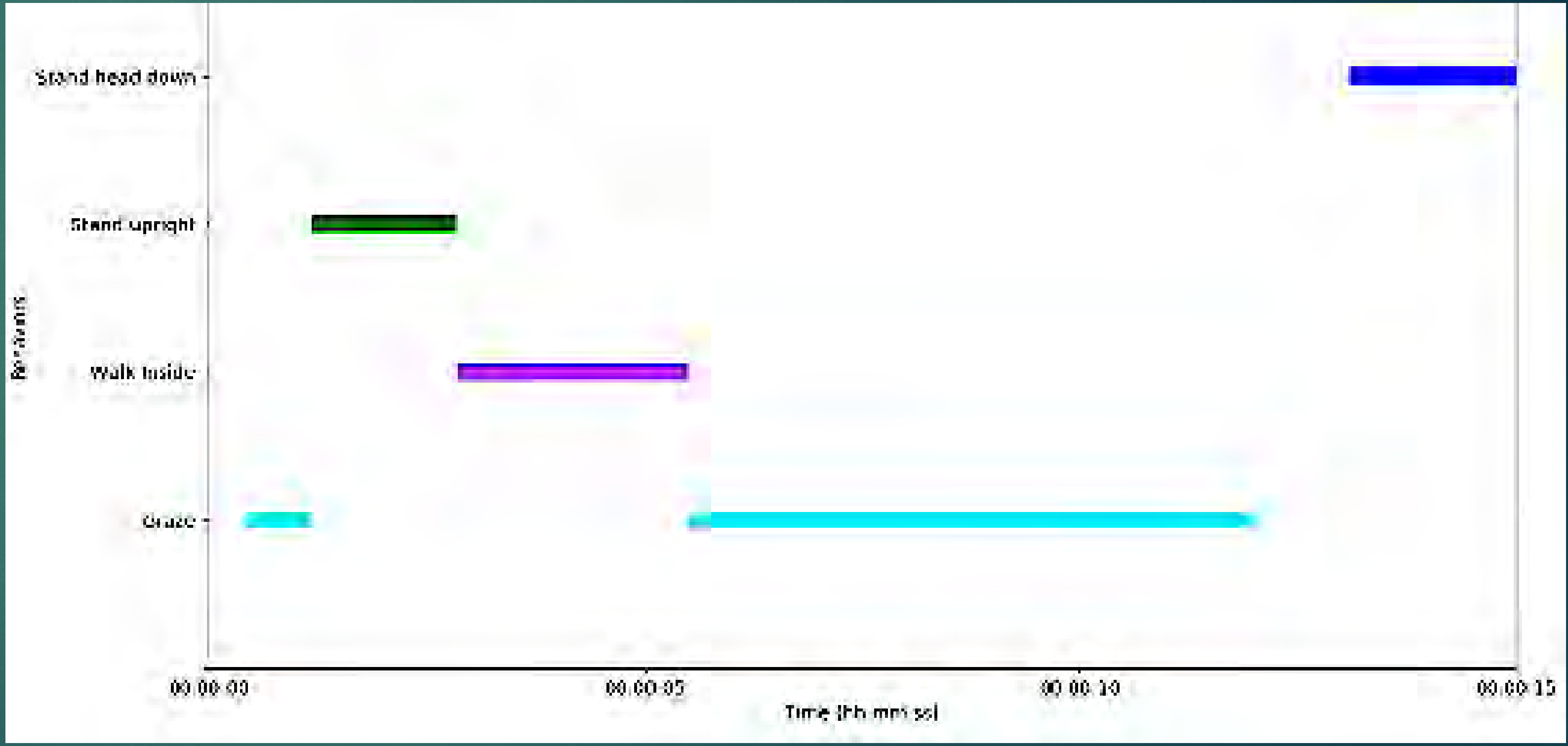

https://wildlifeobserver.net/behaviorid/

Wildlife behavior with traffic

- Mule deer

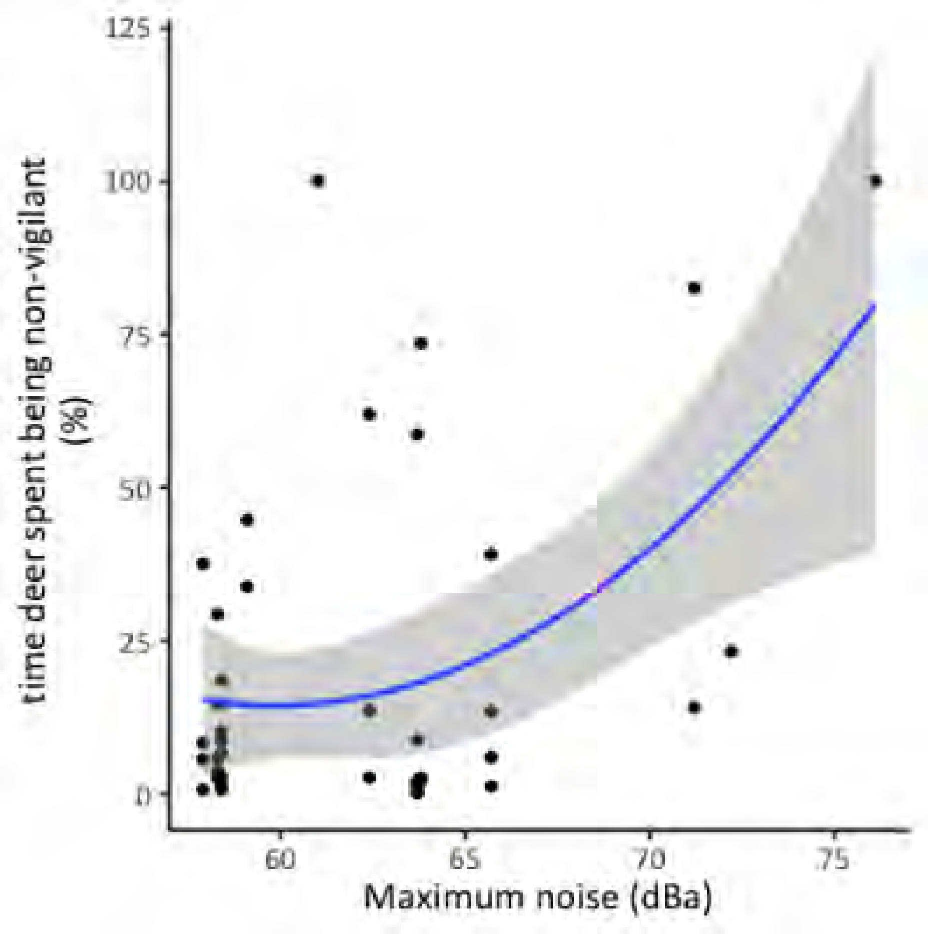

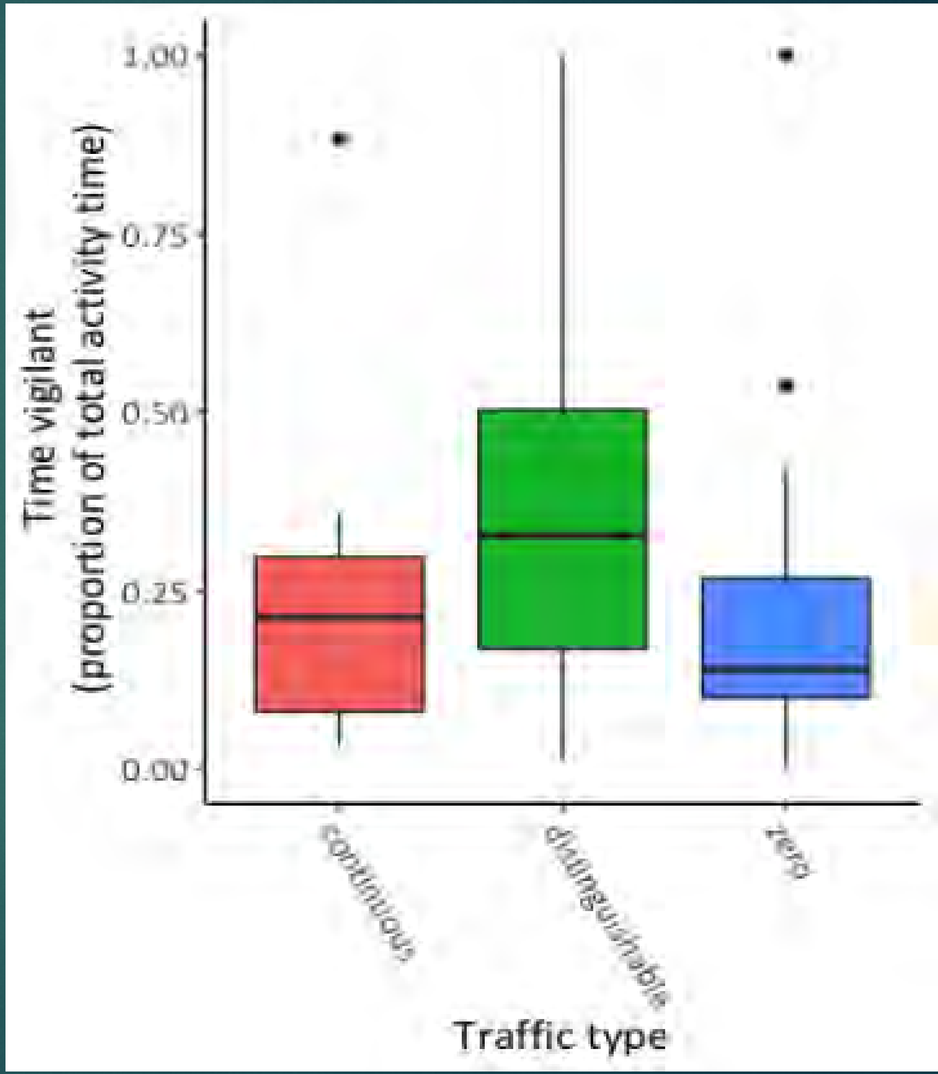

Most wildlife avoid traffic noise

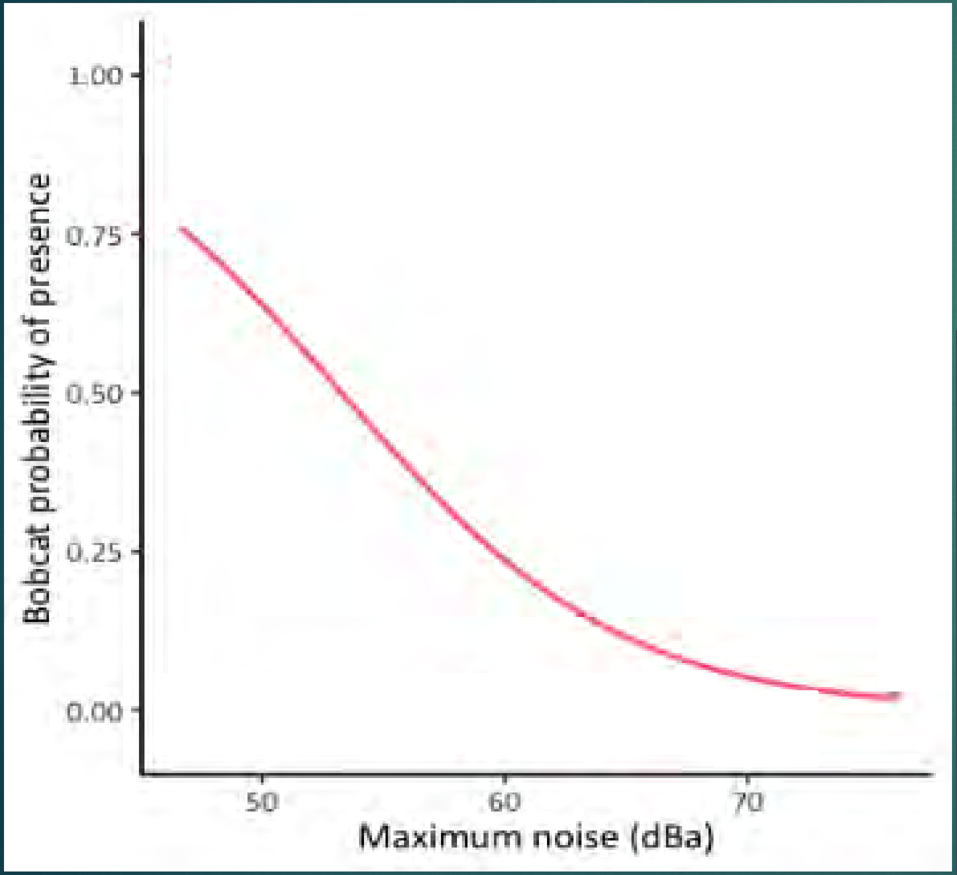

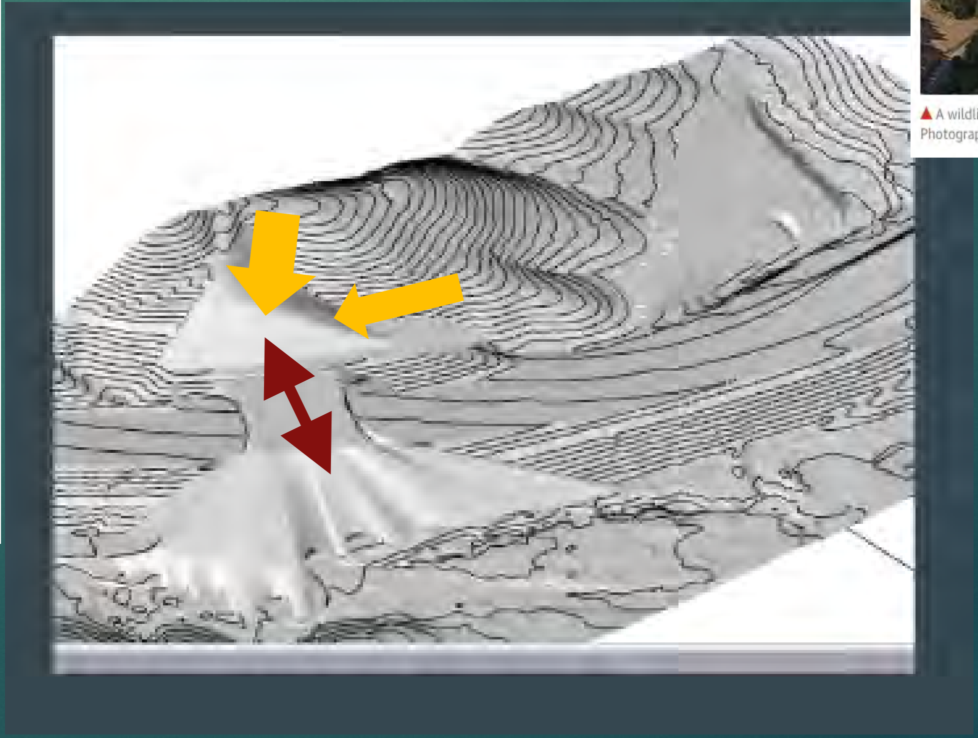

Los Angeles to build world's largest wildlife bridge across 10-lane freeway

An $87m corridor will extend over Highway 101 to reconnect the ecosystem and possibly save mountain lions from extinction

A wildlife corridor, the biggest in the world, is planned to extend over Highway 101 north-west of Lost Angeles. Photograph: RCD of the Santa Monica Mountains, Clark Stevens (architect), Raymond Garcia (illustrator)

Designing for wildlife

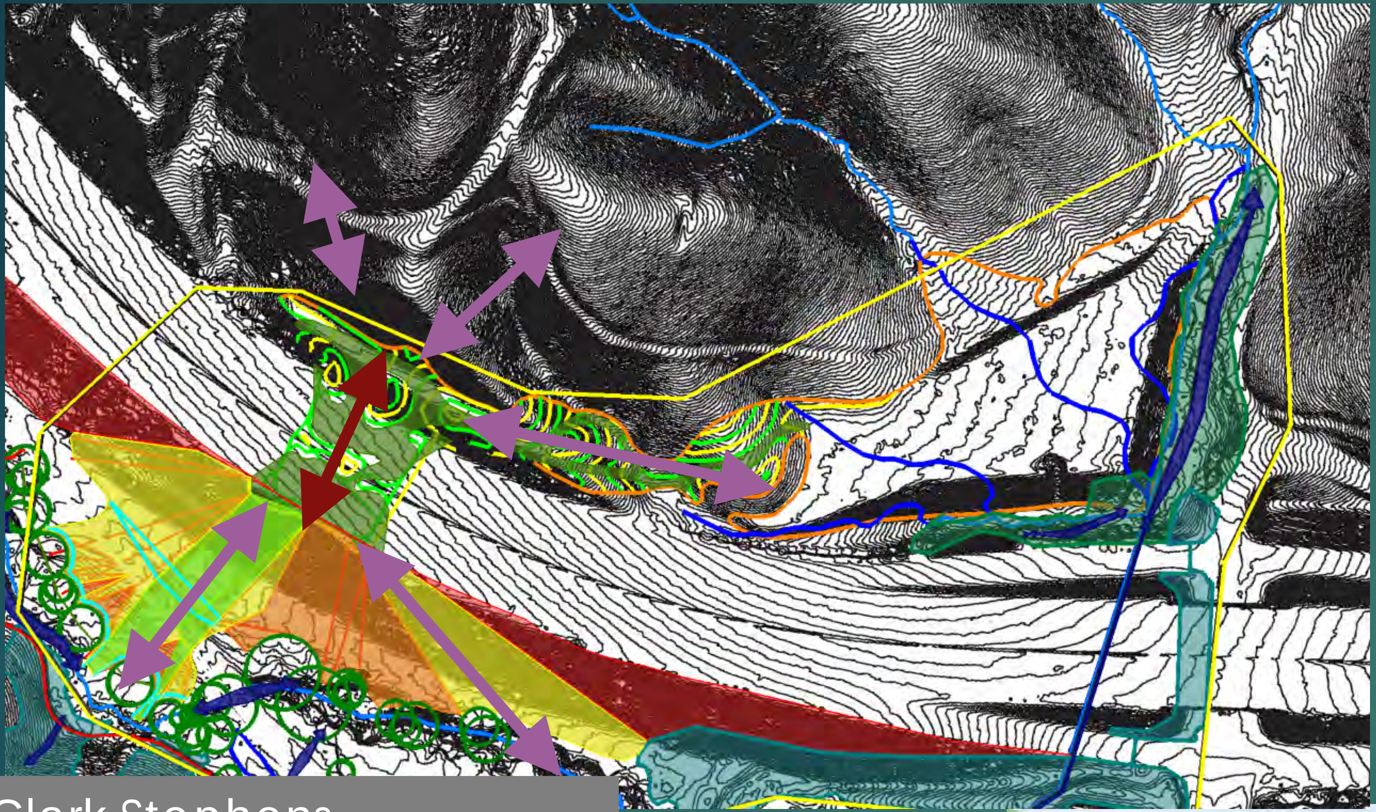

Clark Stephens

Los Angeles to build world's largest wildlife bridge across 10-lane freeway

An $87m corridor will extend over Highway 101 to reconnect the ecosystem and possibly save mountain lions from extinction

▲ A wildlife corridor, the biggest in the world, is planned to extend over Highway 101 north-west of Lost Angeles. Photograph: RCD of the Santa Monica Mountains, Clark Stevens (architect), Raymond Garcia (illustrator)

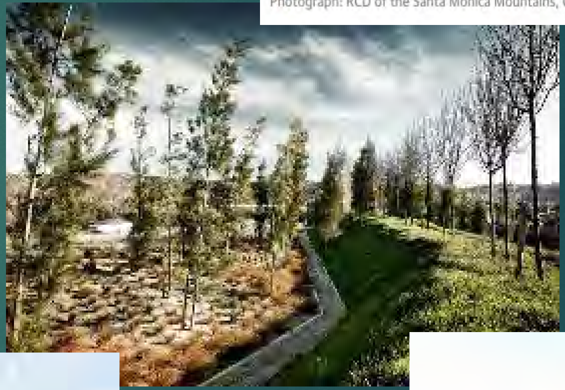

Annabelle Louderback-Valenzuela, Jeff Scott, Mia McNeill, Mia Guarnieri, Parisa Farman, Rachel Alsheikh, Pao Perez, Tricia Nguyen, Vivian lei, Harrison Knapp, Sean McDowell, Adetayo Oke, Jamie Bourdon, Rich Codington, Ben Banet, Collin Raff, Dirk Van Vuren lab, Rahel Sollmann, Catherine Le

IRVINE RANCH CONSERVANCY

OC parks

REGIONAL PARK AND OPEN-SPACE DISTRICT RIVERSIDE COUNTY

Completed Project

Exhibit 5

ECOLOGY LETTERS

Ecology Letters, (2019) doi: 10.1111/ele.13344

LETTER

Fear of humans as apex predators has landscape-scale impacts from mountain lions to mice

Justin P. Suraci,[1]* Michael Clinchy,[2] Liana Y. Zanette[2] and Christopher C. Wilmers[1]

[1]Center for Integrated Spatial Research, Environmental Studies Department University of California Santa Cruz, CA 95064, USA

[2]Department of Biology Western University London, ON N6A 5B7, Canada

*Correspondence: E-mail: justin.suraci@gmail.com

Abstract

Apex predators such as large carnivores can have cascading, landscape-scale impacts across wildlife communities, which could result largely from the fear they inspire, although this has yet to be experimentally demonstrated. Humans have supplanted large carnivores as apex predators in many systems, and similarly pervasive impacts may now result from fear of the human 'super predator'. We conducted a landscape-scale playback experiment demonstrating that the sound of humans speaking generates a landscape of fear with pervasive effects across wildlife communities. Large carnivores avoided human voices and moved more cautiously when hearing humans, while medium-sized carnivores became more elusive and reduced foraging. Small mammals evidently benefited, increasing habitat use and foraging. Thus, just the sound of a predator can have landscape-scale effects at multiple trophic levels. Our results indicate that many of the globally observed impacts on wildlife attributed to anthropogenic activity may be explained by fear of humans.

Keywords

Ecology of fear, human impacts, landscape of fear, large-scale field manipulation, playback experiment.

Ecology Letters (2019)

INTRODUCTION

The fear of predators can itself be powerful enough to drive demographic and community-level changes in wildlife systems, as demonstrated in a growing number of recent experiments (Zanette *et al.* 2011; LaManna & Martin 2016; Suraci *et al.* 2016). The impacts of fear are typically mediated by changes in prey behaviour (Schmitz *et al.* 1997; Brown & Kotler 2004), which may vary spatially with changes in the prey's perception of predation risk across the landscape (Gaynor *et al.* 2019). Anthropogenic activity is reshaping wildlife behaviour across human-dominated landscapes, disrupting movement (Tucker *et al.* 2018), forcing shifts to nocturnality (Gaynor *et al.* 2018) and changing the way predators interact with their prey (Smith *et al.* 2015). Humans are themselves major predators (Darimont *et al.* 2009), killing some species, particularly large and medium-sized carnivores, at many times the rate at which they are killed by non-human predators (Darimont *et al.* 2015), and fear of the human 'super predator' (Darimont *et al.* 2015) may therefore be a significant driver of observed changes in wildlife behaviour (Oriol-Cotterill *et al.* 2015; Suraci *et al.* 2019). Given that humans have evidently superseded large carnivores as apex predators in many ecosystems (Ordiz *et al.* 2013a; Oriol-Cotterill *et al.* 2015; Kuijper *et al.* 2016), our mere presence may be expected to generate landscapes of fear (Gaynor *et al.* 2019) with spatial extents and breadth of trophic impacts equal to or greater than those presently attributed to large carnivores (Laundré *et al.* 2001; Palmer *et al.* 2017). Yet, whether fear of the human 'super predator', or indeed any large apex predator, generates landscapes of fear with impacts across wildlife communities remains to be tested experimentally.

A large number of correlative studies suggest that some wildlife species respond fearfully to human activity (Fernandez-Juricic *et al.* 2005; Stankowich & Blumstein 2005; Bateman & Fleming 2017), but whether such responses are driven by perceived risk from humans as predators or by a generalised response to 'disturbance' (e.g. sudden noises, looming objects) is often unclear (Frid & Dill 2002; Stankowich 2008). Experimentally testing predator-specific responses requires manipulating something the prey is likely to perceive as being specific to that predator (e.g. vocalisations, odours) in conjunction with a non-predator-specific control for the generalised disturbance potentially caused by manipulations. Recently, small-scale (≤ 50 m), short-term (≤ 2 h) controlled experiments on single prey species have demonstrated that wildlife regularly killed by humans exhibit strong fear responses to human vocalisations, just as prey respond fearfully to the vocalisations of any other predator (Hettena *et al.* 2014; McComb *et al.* 2014; Clinchy *et al.* 2016; Smith *et al.* 2017). By isolating human predator-specific responses, such experiments differentiate the impacts of fear of humans as predators from the myriad other aspects of the anthropogenic environment likely to affect wildlife behaviour [e.g. enhanced food resources, habitat fragmentation (Bateman & Fleming 2012; Newsome *et al.* 2015; Tucker *et al.* 2018)]. By scaling up such experiments, we can thus quantify how the fear of humans as predators impacts wildlife at the landscape and community levels.

To experimentally test whether the magnitude of effects caused by fear of an apex predator (in this case humans) can extend to having landscape-scale impacts across wildlife communities, we conducted spatially replicated, landscape-scale manipulations of perceived human presence. We sequentially broadcast playbacks of people talking or control sounds for 5 weeks (followed by the opposite treatment for a subsequent 5 weeks) over spatial scales (1 km^2) comparable to those of the largest mammalian predator exclusion experiments (Salo *et al*. 2010), and simultaneously quantified the responses of multiple mammal species across three trophic levels. The study was conducted in the Santa Cruz Mountains of central California. Like an increasingly large proportion of the planet (Venter *et al*. 2016), this region consists of wildlife habitat in close proximity to urban and suburban development, and is thus heavily used by people (Wang *et al*. 2015). The Santa Cruz Mountains support a single native large carnivore, the mountain lion (*Puma concolor*), and several smaller predators (for brevity, referred to as 'medium-sized carnivores') including bobcats (*Lynx rufus*), striped skunks (*Mephitis mephitis*) and Virginia opossums (*Didelphis virginiana*), all of which have been shown to alter their behaviour in response to the gradient of human development that exists across the region (Wilmers *et al*. 2013; Wang *et al*. 2015). Small-scale experiments replicated across this region previously demonstrated that mountain lions here exhibit strong fear responses to hearing human voices, fleeing food caches and feeding less as a consequence (Smith *et al*. 2017). Medium-sized carnivores similarly exhibited fear-induced reductions in feeding and shifts in temporal activity in response to the small-scale experimental presentation of human voices (Clinchy *et al*. 2016). As is true for large and medium-sized carnivores globally (Ordiz *et al*. 2013a; Darimont *et al*. 2015), humans are a major source of mortality for mountain lions in our study area, with legal and illegal shooting accounting for 59.1% of known-cause mortalities of collared animals since 2008 (C. Wilmers, *unpublished data*). Bobcats, skunks and opossums are all common targets of predator control (Conner & Morris 2015), and are all legally hunted in California, with no legal limits on killing skunks and opossums (California Department of Fish & Wildlife 2018). Correlational results from our study area indicate that bobcats are sensitive to risk from humans, decreasing diurnal activity in areas of high human development, but suggest that skunks and opossums may prefer more developed areas (Wang *et al*. 2015). Medium-sized carnivores such as skunks and opossums often rely heavily on human subsidies, including food waste (Bateman & Fleming 2012), and thus could be forced to balance the risk of anthropogenic mortality against the benefits of living near humans.

Given the evidence that carnivores fear humans as predators, both in our study area and in general, our objective was to experimentally test whether such fear leads to landscape-scale impacts across wildlife communities. We quantified the large-scale effects of fear of humans as predators on carnivore movement, activity and foraging behaviour using GPS collars (mountain lions) and camera traps (bobcats, skunks and opossums). Correlational studies suggest that fear-induced suppression of carnivore behaviour by apex predators may cascade to benefit small mammal prey (Brook *et al*. 2012; Gordon *et al*. 2015), although this has yet to be shown experimentally. We therefore additionally tested whether the fear that humans induce in carnivores can have cascading effects on the behaviour of lower trophic level animals, using live trapping and provisioned food patches to document effects on habitat use and foraging by small mammals (deer mice *Peromyscus* spp. and woodrats *Neotoma fuscipes*) known to be preyed upon by several of the carnivores in our study (Azevedo *et al*. 2006; Smith *et al*. 2018).

In a major reclarification of the landscape of fear concept, Gaynor *et al*. (2019) define it as spatial variation in the prey's perception of predation risk, influenced by, but distinct from, both the physical landscape and actual risk of mortality from predators. Here, we use the sequential presentation of human and control vocalisations at each of our 1-km^2 sites to manipulate the perception of predation risk across the same physical landscapes, thus keeping physical characteristics and actual mortality risk constant. We thereby experimentally demonstrate that a landscape of fear, resulting solely from variation in the perception of risk from an apex predator, can have pervasive effects across wildlife communities. That such effects can result from the fear of humans as predators indicates that this may be an important factor underlying many of the globally observed changes in wildlife behaviour associated with anthropogenic activity (Gaynor *et al*. 2018; Tucker *et al*. 2018).

METHODS

Study area

The study was conducted at two 1-km^2 experimental sites (SA and SVR), separated by 26 km (Fig. S1). Both sites were closed to public access, and human presence was therefore low relative to elsewhere in the Santa Cruz Mountains. The presence of humans (including researchers) and vehicles did not differ between experimental sites during the study (Mann–Whitney *U*-test comparing occurrences per camera night on $n = 12$ cameras per site; humans: $P = 0.643$; vehicles: $P = 0.655$). Work was conducted between 29 May and 31 August 2017.

For additional details on the study area and species, see Appendix S1. All procedures described below were approved by the Institutional Animal Care and Use Committee of the University of California, Santa Cruz (Protocol WilmC1612) and the California Department of Fish and Wildlife (Permits SC-11968 and SC-12383).

Playbacks and study design

We manipulated the perceived presence of humans on the landscape using playbacks of human and control vocalisations broadcast sequentially for 5 weeks each at both 1-km^2 experimental sites. Following established protocols (Suraci *et al*. 2016; Smith *et al*. 2017), we compared wildlife responses to human vocalisations with responses to Pacific treefrog (*Pseudacris regilla*) vocalisations. Tree frogs, like humans, can be heard both day and night in our study area, but unlike humans, their perceived presence should be completely benign given that treefrogs are unlikely to be predators, competitors or prey of any study species. As discussed in detail in Appendix S1 (Supplementary Methods – Playback Treatments), there is ample evidence to suggest that wildlife in the

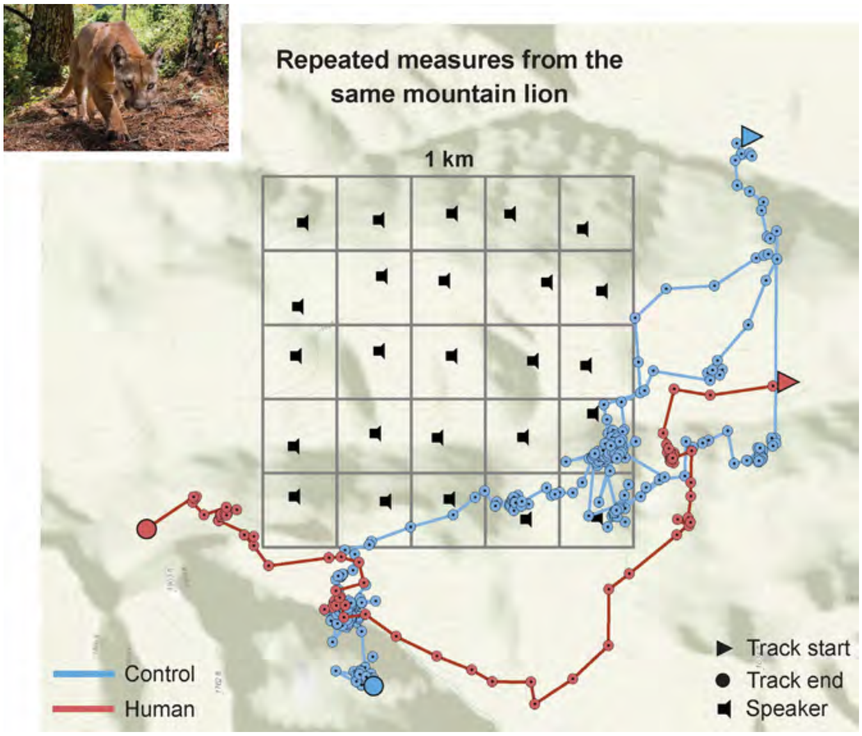

Figure 1 Example of the landscape-scale impacts of fear of humans on mountain lion behaviour, illustrated by repeated-measures movement tracks from a single mountain lion during the control (blue) and human (red) treatments. Points are 5-min GPS fixes, and connecting lines illustrate the approximate movement path. Black speaker icons denote playback speaker locations and the grey grid illustrates the 1-km^2 experimental site. Photo © Sebastian Kennerknecht.

Santa Cruz Mountains will be familiar with both human and tree frog vocalisations.

Playbacks were broadcast from 25 speakers arranged in a 5 × 5 grid at each experimental site (Fig. S1). Each speaker played a randomised playlist of human or frog recordings (n = 10 exemplars of each) interspersed by silence such that each individual speaker was broadcasting 40% of the time and silent 60% of the time. Speakers were thus continuously active, but presentation of cues was random and sporadic across the playback grid. The human treatment thereby mimicked a wildland–urban interface in that human vocalisations were relatively infrequent, but from any location within the playback grid, a human could occasionally be heard at any time. All playbacks were broadcast at a standardised volume of ~ 80 dB at 1 m (human = 78.7 dB ± 1.9 SD; frog = 79.2 dB ± 2.4). Additional details of the playback treatments are provided in Appendix S1.

We employed a repeated-measures design with each experimental site receiving either the human or control treatment for 5 weeks (treatment period 1), followed by the opposite treatment for a subsequent 5 weeks (treatment period 2) with 8 days of silence between the two treatment periods. Thus, both experimental sites received each treatment in opposite order, and as such, detecting consistent responses to playback treatments across sites is critical to concluding that treatments had a significant effect. We therefore included a test for treatment × site interaction in all analyses presented below and only concluded that treatments drove observed changes when no significant interaction was detected (see Tables S1–S8). We also present visualisations of site-level data for all analyses (Figs S2–S7) to illustrate the consistency of treatment effects across sites.

Monitoring mountain lion responses to playbacks

We monitored the responses of seven mountain lions (four females and three males) whose home ranges overlapped one of our two experimental sites. Five individuals (four females and one male) used SVR, while two males used SA. Mountain lions were captured using trailing hounds or cage traps and fitted with GPS collars (GPS Plus, Vectronics Aerospace, Berlin, Germany) with a 5-min fix interval.

We focused mountain lion movement analyses on only those periods when an individual was within audible range of a playback grid (termed an 'encounter' with the playbacks) and used a repeated-measures design to compare responses of individual mountain lions to both playback treatments (Fig. 1). We considered the audible range of the speakers to extend 200 m out from the speaker grid itself (see Appendix S1), and also ran all analyses using a smaller buffer size (150 m), which yielded similar results. Five mountain lions encountered the playbacks on multiple occasions, with subsequent encounters separated by 19.1 days on average (range = 4.6–38.6 days). The median number of encounters per individual was 2 (range = 1–5; total encounters across all individuals = 17).

For all mountain lion GPS locations taken within the 200 m audible range, we determined the distance to the nearest playback speaker and the animal's movement speed. For each encounter, we then calculated average distance to the nearest speaker (an estimate of speaker avoidance) and average movement speed across all locations for that encounter. We took the inverse of movement speed as an estimate of 'cautiousness', moving more slowly being considered greater cautiousness. We tested for effects of playback treatment, experimental site and a treatment × site interaction on avoidance and cautiousness using linear mixed-effects models (LMM), with mountain lion ID as a random effect. Cautiousness (movement speed^{-1}) was log-transformed to meet normality assumptions. Unless otherwise noted, we confirmed adequate fit of these and all other frequentist models through visual inspection of residuals and assessed significance of model terms using Type II Wald's chi-squared tests (Table S1). Finally, we confirmed that observed changes in medium-sized carnivore behaviour between treatments (see below) were not due to changes in mountain lion presence by testing for differences in time spent by mountain lions near experimental sites (see Appendix S1 and Table S1 for details).

Medium-sized carnivore responses to playbacks

At each experimental site, we deployed a grid of 12 camera traps, which ran continuously throughout the experiment (camera deployment details in Appendix S1). We scored camera trap images for the presence of three medium-sized carnivore species that occurred at both experimental sites, which prior correlational research in the region indicates are affected by human development (Wang *et al*. 2015): bobcats, striped skunks and Virginia opossums. We considered images of the same species on the same camera to be separate detections if they were separated by > 30 min (Wang *et al*. 2015; Suraci *et al*. 2017). Two other medium-sized carnivore species (raccoons *Procyon lotor* and gray foxes *Urocyon cinereoargenteus*) occasionally occurred on camera traps, but were detected too infrequently to permit statistical analyses, raccoons only occurring on three cameras at one site and foxes only during a subset of treatment periods.

Bobcat temporal activity

Prior research (Wang *et al*. 2015) shows that, whereas bobcats are diurnally active 29.6% of the time, skunks and opossums are almost exclusively nocturnal (94 and 96.6% nocturnality respectively). We therefore tested whether playback treatments affected temporal activity for bobcats, the only species with sufficient diurnal activity to expect an effect. We calculated the overlap between temporal activity during control and human treatments using the kernel density estimation procedure described by Ridout and Linkie (Ridout & Linkie 2009; Linkie & Ridout 2011). We estimated probability density distributions for bobcat occurrences on camera across the 24-h day separately for the control and human treatment periods. We then calculated the coefficient of overlap ($\hat{\Delta}$, range 0–1) between these two activity distributions (Ridout & Linkie 2009), along with 95% CIs (via 10 000 bootstrap replicates (Linkie & Ridout 2011)) using the overlap package in R (Meredith & Ridout 2014). We calculated overlap separately for each experimental site and then with data from both sites pooled. We considered there to be evidence of a change in temporal activity if overlap in activity distributions during control and human treatment was < 0.90.

Bobcats exhibited a consistent shift in temporal overlap between human and control treatments across both experimental sites (Table S2). We therefore quantified the degree to which this temporal shift constituted a reduction in diurnal activity in favour of nocturnality during the human treatment. For each bobcat detection on camera (n = 44 on 12 cameras), we calculated the absolute value of the difference (in hours) between the timestamp of the detection and the middle of the night (the midpoint between sunset and sunrise, averaged across the study period; 01:15) such that detections near midday received the highest values of this diurnal activity metric. We tested for the effects of playback treatment, experimental site and a treatment × site interaction on diurnal activity using LMM with camera site as a random effect.

Modelling medium-sized carnivore occupancy and detection frequency at camera sites

To test whether fear of humans affected medium-sized carnivore behaviour at the landscape scale, we developed a hierarchical model describing (1) use by a given species of individual camera sites within each experimental site and (2) frequency of detections of that species at used camera sites, a proxy for activity level. We based our model on multispecies occupancy models (Burton *et al*. 2012; Broms *et al*. 2016), but with two distinctions: (1) we consider camera site use (rather than occupancy *per se*), as individual carnivores could use more than one camera site, and (2) we modelled the frequency of detections of a given species at a camera site (a Poisson process), rather than the binary estimate of detected/not detected typically used in occupancy models. We treated each week of the experiment as a survey period (Wang *et al*. 2015; Moll *et al*. 2018), yielding five replicate surveys per treatment at each camera site. Three data points were excluded from the analysis when cameras failed to record data for the full week. We formulated our analysis as a zero-inflated negative binomial model (Moll *et al*. 2018), allowing occupancy at a camera site (binomial submodel) to vary between playback treatments, and explicitly modelling detection frequency (negative binomial submodel) as a function of experimental site, playback treatment and their interaction. We analysed the hierarchical detection frequency model in a Bayesian framework using the JAGS language (Plummer 2003) via the R2jags package (Su & Yajima 2015) in R. For a full model description and details on the Bayesian analysis (including JAGS code and model fit), see Appendices S1 and S2. Model results are present in Tables S3 and S4.

The above model indicated a substantial reduction in skunk detection frequency during the human treatment at both sites. To confirm the robustness of this result, we performed a simplified version of the analysis, using a Wilcoxon matched-pairs test to compare total skunk detections during the human and control treatments on each camera.

Medium-sized carnivore foraging trials

We created feeding patches (consisting of a single boiled chicken egg) at each of the 12 camera locations within each experimental site. We estimated patch discovery rate (i.e. days required for a medium-sized carnivore to find and consume the egg, determined from camera trap images) as an index of carnivore foraging efficiency. Eggs were set out twice during each treatment period (during weeks 2 and 4), yielding a total of 96 trials. To standardise availability, we consider only those trials in which a medium-sized carnivore ultimately discovered the patch (n = 36), as some eggs were taken by other species (e.g. corvids) before being discovered by carnivores. Discovery rate data were log-transformed to satisfy normality assumptions and fit by LMM, using camera site as a random effect. We tested for effects of treatment, experimental site, species, session (first or second deployment during each treatment), and treatment × site interaction. Opossums made the majority of foraging patch discoveries (n = 20) and skunks made the remainder (n = 16), with no discoveries made by bobcats. We first analysed data from opossums and skunks combined, and then fit species-specific models, using the model terms just mentioned with the exception of species (Table S5).

Deer mouse spatial capture–recapture

We conducted a spatial capture–recapture study using four grids of live traps at each experimental site. Grids were trapped immediately prior to the start of any playbacks, and immediately following each playback treatment period. All captured mice were marked with unique ear tags. See Appendix S1 and Fig. S1 for live trapping details. We analysed live trapping data using spatial capture–recapture (SCR) models (Royle *et al.* 2013), which permit quantification of the amount of space used by individual animals (σ in SCR models; Appendix S1 and (Royle *et al.* 2013)). We modelled spatially explicit capture histories using a zero-inflated binomial model with data augmentation (Royle & Dorazio 2008; Royle *et al.* 2013). Detection probability and/or space use could be affected by playback treatment if mice alter their movements in response to treatment-induced changes in carnivore behaviour. We estimated the effect of playback treatment on detection probability and space use by calculating averages of these parameters (across all trapping grids) for trapping sessions following the control and human treatments. Treatment-level averages were then subtracted to estimate the average difference in parameter values between control and human treatments. If the 95% credible intervals (CrI) of the difference between treatments did not cross zero, we considered there to be evidence of a treatment effect on the parameter of interest (Table S6). Average values (± 95% CrI) of the space use parameter (σ) during each treatment were used to calculate the average area of habitat used during each treatment, following the procedure outlined by Royle *et al.* (2013, pg. 136). For a full description of the deer mouse SCR model and the Bayesian analysis of this model, see Appendices S1 and S2. Model results are presented in Tables S6 and S7.

Small mammal foraging trials

Two small mammal foraging patches, separated by < 3 m, were deployed at each of the 12 camera locations within each experimental site, one under protective cover (shrubs) and one in the open. Each patch consisted of an aluminium tray filled with 10 g of millet seed mixed into 1 l of sifted sand. Patches thus required time to exploit, allowing time for the accumulation of camera trap images and/or small mammal droppings in trays. Patches were deployed twice during each 5-week treatment period (during weeks 2 and 4) and were left in place for two consecutive nights, with millet and sand refreshed after the first night. We focus our analyses on the proportion of available patches visited on a given night and include only those trials in which visitation or lack thereof by small mammals (deer mice or woodrats) could be determined with high confidence based on the presence or absence of camera trap images and/or droppings (n = 256). Preliminary analysis indicated that open patches were largely avoided overall (Appendix S1, Table S8). We therefore restricted our analysis to patches under cover.

We coded whether a particular patch was visited (1) or not (0), and analysed these data using a generalised LMM with binomial error distribution, including camera site as a random effect. We tested for effects of treatment, experimental site, night (first or second night of patch deployment), moon illuminance and a treatment × experimental site interaction. Adequate model fit was assessed through inspection of scaled residuals using the DHARMa R package (Harting 2018).

RESULTS

Fear of humans drove significant changes in how mountain lions moved through the same physical landscape (Fig. 1). Mountain lions avoided areas of perceived human presence, encountering the playback grids 30% less often when human sounds were broadcast, and maintaining a 29% greater distance to the nearest speaker during human playbacks relative to controls (Figs. 2a and S2; LMM: Wald's $\chi^2_1 = 6.33$, P = 0.012). Mountain lions also moved more cautiously when hearing human playbacks, reducing average movement speed by 34% (Figs 2a and S2; LMM: Wald's $\chi^2_1 = 4.66$, P = 0.031).

Fear of humans had an overall suppressive effect on medium-sized carnivore behaviour (Fig. 2b). Bobcats reduced diurnal activity by 31% when hearing humans (Figs. 2b and S3; Table S2; LMM: Wald's $\chi^2_1 = 4.71$, P = 0.030), shifting their diel activity patterns towards increased nocturnality [overlap ($\hat{\Delta}$) in activity between treatment and control = 0.68 (95% CI: 0.48–0.86); Fig. S8]. Skunks were the only species to exhibit a reduction in overall activity (Table S4), reducing activity levels by 40% during the human treatment [Figs. 2b and S4; detection frequency model: treatment coefficient = −1.12 (95% CrI: −2.37 to −0.04)], and were therefore detected less frequently on camera traps (Wilcoxon test, P = 0.007; n = 24). When considering all trials in which a medium-sized carnivore discovered a provisioned food patch, fear of humans had a significant negative effect on food patch discovery rate (Table S5; LMM: Wald's $\chi^2_1 = 5.88$, P = 0.015). Species-specific models indicated that this effect was largely driven by opossums. The sound of humans led to a 66% reduction in opossum foraging efficiency (Figs. 2b and S5;

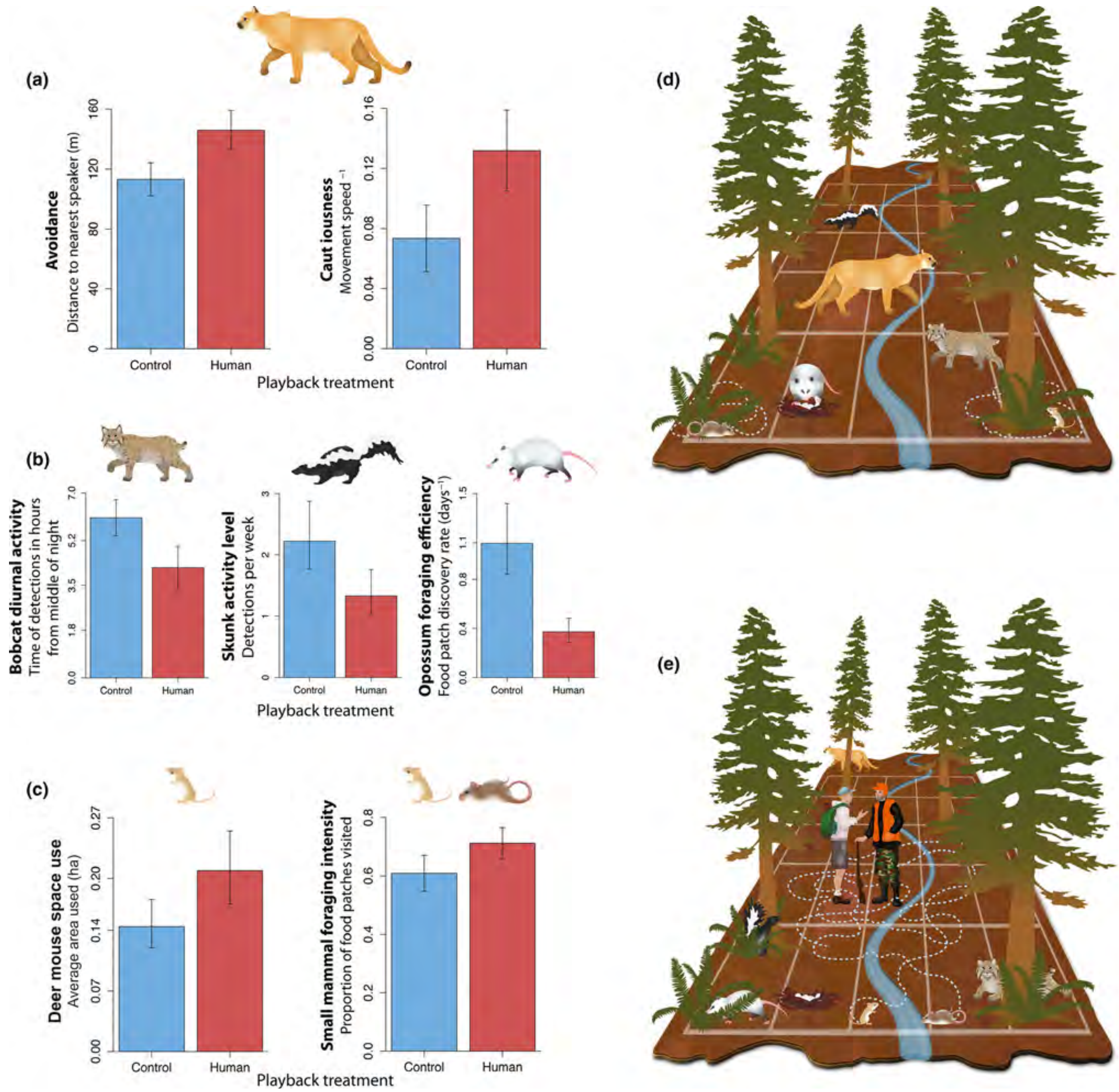

Figure 2 Fear of humans has landscape-scale impacts on wildlife across multiple trophic levels. (a) Fear of humans affects mountain movement behaviour. Mountain lion avoidance behaviour (left panel) is shown as average distance (m) to the nearest playback speaker and cautiousness (right panel) is shown as the inverse of average movement speed (mins/m). Bar plots illustrate means ± SEM. N = 10 control and 7 human. (b) Fear of humans suppresses medium-sized carnivore behaviour. Bobcat diurnal activity from camera trap detections (left panel; means ± SEM; n = 26 control and 18 human) is shown as time (h) from the middle of the night. Skunk overall activity level (middle panel) is shown as posterior mean and 95% credible intervals for number of detections per week on camera traps. Opossum foraging efficiency (right panel; means ± SEM; n = 10 control and 10 human) is shown as rate of discovery (days^{-1}) of provisioned food patches. (c) Suppression of larger predators induced by fear of humans benefits small mammals. Deer mouse space use (left panel) is shown as posterior mean and 95% credible intervals of average area (ha) used. Small mammal (deer mouse and woodrat) foraging intensity (right panel; mean ± SEM; n = 64 control and 73 human) is shown as proportion of provisioned food patches visited on a given night. All bar plots illustrate behaviours during control (blue) and human (red) playback treatments. (d) and (e) conceptual illustrations of the landscape-scale effects of fear of humans on wildlife communities. Where the human apex predator is absent or rare (d), large and medium-sized carnivores exhibit greater movement (mountain lion on grid), activity (bobcats and skunks active) and foraging (opossum eating a bird nest), while small mammals exhibit reduced space use (constricted movement paths, shown as dashed lines). Where humans are present (e), fear of humans suppresses the activity, foraging and/or habitat use of large and medium-sized carnivores, while small mammals increase their total space use and foraging intensity. Original artwork by Corlis Schneider.

Table S5; LMM: Wald's $\chi^2_1 = 8.77$, $P = 0.003$) such that opossums took on average 1.8 days longer to discover food patches during the human treatment.

Small mammals benefitted from the apparent presence of humans, increasing both the amount of habitat and number of foraging opportunities exploited. During the human treatment, deer mice expanded their space use by 45% relative to controls (Figs. 2c and S6), increasing average area used by 649 m^2 (95% CrI = 116–1209 m^2) while maintaining an overall consistent detection probability across treatments (Tables S6 and S7). Mice and woodrats increased foraging intensity by 17% during the human treatment (Fig. 2c, Table S8; GLMM: Wald's $\chi^2_1 = 4.71$, $P = 0.030$), visiting a significantly higher proportion of provisioned food patches (Figs. S7 and S9).

DISCUSSION

Our results experimentally demonstrate that fear of humans as predators can have pervasive impacts across wildlife communities, suppressing movement and activity of large and medium-sized carnivores, with cascading benefits for small mammals (Fig. 2d and e). Thus, spatial variation in the perception of risk from an apex predator can itself create a landscape of fear (Gaynor *et al.* 2019), manifesting in widespread changes in wildlife behaviour.

Mountain lions significantly altered their movement through the same physical landscape in response to hearing humans (Fig. 1), exhibiting antipredator behaviours comparable to those previously documented in small-scale experiments (Smith *et al.* 2017), but at a substantially larger scale (Fig. 2a). Observational and manipulative studies have similarly found that risk from humans affects large carnivore behaviour across the landscape (Valeix *et al.* 2012; Ordiz *et al.* 2013b, 2019; Oriol-Cotterill *et al.* 2015; Suraci *et al.* 2019), including in our study area, where increased human development is correlated with impacts on mountain lion movement and habitat use (Wilmers *et al.* 2013; Wang *et al.* 2017). Our results confirm that, even in the absence of changes in human infrastructure (e.g. buildings, roads) or habitat fragmentation, increased human presence can impact large carnivore movement by inducing antipredator responses, which, if sustained for long periods, could lead to effective habitat loss for carnivores by limiting hunting and feeding behaviour (Smith *et al.* 2015) or forcing individuals to abandon high risk areas of their home range (Schuette *et al.* 2013).

Fear of humans had suppressive effects on medium-sized carnivore activity across all three study species (Fig. 2b), yet as expected from the diversity of carnivore behaviours, their exact responses differed. Our experimental results confirm previous correlational findings (Wang *et al.* 2015) that bobcats become more nocturnal in response to human presence, demonstrating that fear of humans may contribute to the documented global pattern of increased wildlife nocturnality in disturbed habitats (Gaynor *et al.* 2018). Fear of humans also impacts skunks and opossums, causing reductions in overall activity or foraging behaviour by these often human-associated species. These results highlight the trade-off such species face between the potential benefits of living in an anthropogenic environment [e.g. abundant food subsidies (Bateman & Fleming 2012; Newsome *et al.* 2015)] and the fear-induced costs of sharing habitat with humans (Fig. 2b). Interestingly, none of the three medium-sized carnivores exhibited changes in overall habitat use between treatments (number of camera sites used; Tables S3), potentially reflecting a limited capacity to do so, at least for species (i.e. skunks and opossums) whose relatively small home ranges likely overlapped substantially with our experimental sites (Appendix S1).

Finally, significant increases in small mammal space use and foraging documented during the human playback treatment (Fig. 2c) experimentally demonstrate that the suppression of carnivore behaviour induced by fear of an apex predator (in this case, humans) can have cascading effects on small mammal prey (Brook *et al.* 2012; Gordon *et al.* 2015). These cascading behavioural changes suggest that the presence of people may in some cases act as a 'human shield' (Berger 2007) for small mammals, reducing their perceived risk of predation from carnivores. Human shield effects have been suggested to occur in some large carnivore-ungulate systems, with ungulates preferring areas of high human activity because these areas are avoided by carnivores (Hebblewhite *et al.* 2005; Berger 2007; Muhly *et al.* 2011). If similar human shield effects for small mammals are common where human activity is high, this could ultimately lead to increased small mammal abundance in wildlife areas frequented by people, a potentially undesirable consequence of ecotourism (Geffroy *et al.* 2015).

Our work provides strong evidence that many of the globally observed changes in wildlife behaviour stemming from anthropogenic activity, including changes in large carnivore habitat use (Valeix *et al.* 2012), broader disruptions of animal movement (Tucker *et al.* 2018), and increased nocturnality (Gaynor *et al.* 2018), can be explained in part by the fear of humans as predators. Moreover, if fear of humans triggers substantial sublethal effects comparable to those fear itself has been demonstrated to cause in other predator–prey systems [e.g. increased physiological stress (Zanette *et al.* 2014), reduced reproductive success (Zanette *et al.* 2011; Cherry *et al.* 2016)], this may translate to additional widespread but largely unmeasured impacts of humans on wildlife populations. Given the potential for sublethal effects, apparently 'human-tolerant' species (e.g. medium-sized carnivores using developed areas) could nonetheless experience substantial costs from chronic exposure to perceived risk from humans (Clinchy *et al.* 2016). Pervasive fear of humans may also precipitate widespread community-level changes by disrupting natural predator–prey interactions. Human-induced antipredator behaviour could compromise top-down ecosystem regulation by large carnivores (Kuijper *et al.* 2016) and limit medium-sized carnivore suppression of small mammals (Levi *et al.* 2012). Given continued human encroachment into most wildlife habitats (Venter *et al.* 2016), we suggest that the fear we human 'super predators' inspire, independently of our numerous other impacts on the natural world, may contribute to widespread restructuring of wildlife communities.

ACKNOWLEDGEMENTS

We thank A. Crabb, L. Vu, R. King, K. Briner and P. Houghtaling for help in the field, and several volunteers for field assistance and camera trap image scoring. J. Estes, A. Ordiz, C. Packer, V. Penteriani, M. Power, E. Preisser, T. Williams and two anonymous reviewers provided valuable feedback on earlier versions of the manuscript. The funding was provided by the Gordon and Betty Moore Foundation, National Science Foundation grant #1255913 to CCW, and a Natural Sciences and Engineering Research Council of Canada Discovery Grant to LYZ.

AUTHORSHIP

All authors conceived and designed the study. JPS led the fieldwork and analysis with support from CCW. JPS drafted the manuscript and all authors provided valuable feedback on the paper.

DATA AVAILABILITY STATEMENT

Data available from the Figshare Repository: https://doi.org/10.6084/m9.figshare.8315417

REFERENCES

Azevedo, F.C.C., Lester, V., Gorsuch, W., Larivière, S., Wirsing, A.J. & Murray, D.L. (2006). Dietary breadth and overlap among five sympatric prairie carnivores. *J. Zool.*, 269, 127–135.

Bateman, P.W. & Fleming, P.A. (2012). Big city life: carnivores in urban environments. *J. Zool.*, 287, 1–23.

Bateman, P.W. & Fleming, P.A. (2017). Are negative effects of tourist activities on wildlife over-reported? A review of assessment methods and empirical results. *Biol. Conserv.*, 211, 10–19.

Berger, J. (2007). Fear, human shields and the redistribution of prey and predators in protected areas. *Biol. Lett.*, 3, 620–623.

Broms, K.M., Hooten, M.B. & Fitzpatrick, R.M. (2016). Model selection and assessment for multi-species occupancy models. *Ecology*, 97, 1759–1770.

Brook, L.A., Johnson, C.N. & Ritchie, E.G. (2012). Effects of predator control on behaviour of an apex predator and indirect consequences for mesopredator suppression. *J. Appl. Ecol.*, 49, 1278–1286.

Brown, J.S. & Kotler, B.P. (2004). Hazardous duty pay and the foraging cost of predation. *Ecol. Lett.*, 7, 999–1014.

Burton, A.C., Sam, M.K., Balangtaa, C. & Brashares, J.S. (2012). Hierarchical multi-species modeling of carnivore responses to hunting, habitat and prey in a West African protected area. *PLoS ONE*, 7, e38007.

California Department of Fish and Wildlife (2018). California fish and wildlife commission mammal hunting. *Regulations*, 2018–2019, 472.

Cherry, M.J., Morgan, K.E., Rutledge, B.T., Conner, L.M. & Warren, R.J. (2016). Can coyote predation risk induce reproduction suppression in white-tailed deer? *Ecosphere*, 7, e01481.

Clinchy, M., Zanette, L.Y., Roberts, D., Suraci, J.P., Buesching, C.D., Newman, C., et al. (2016). Fear of the human "super predator" far exceeds the fear of large carnivores in a model mesocarnivore. *Behav. Ecol.*, 27, 1826–1832.

Conner, L.M. & Morris, G. (2015). Impacts of mesopredator control on conservation of mesopredators and their prey. *PLoS ONE*, 10, e0137169.

Darimont, C.T., Carlson, S.M., Kinnison, M.T., Paquet, P.C., Reimchen, T.E. & Wilmers, C.C. (2009). Human predators outpace other agents of trait change in the wild. *PNAS*, 106, 952–954.

Darimont, C.T., Fox, C.H., Bryan, H.M. & Reimchen, T.E. (2015). The unique ecology of human predators. *Science*, 349, 858–860.

Fernandez-Juricic, E., Venier, M.P., Renison, D. & Blumstein, D.T. (2005). Sensitivity of wildlife to spatial patterns of recreationist behavior: a critical assessment of minimum approaching distances and buffer areas for grassland birds. *Biol. Conserv.*, 125, 225–235.

Frid, A. & Dill, L.M. (2002). Human-caused disturbance stimuli as a form of predation risk. *Conserv. Ecol.*, 6, 11.

Gaynor, K.M., Hojnowski, C.E., Carter, N.H. & Brashares, J.S. (2018). The influence of human disturbance on wildlife nocturnality. *Science*, 360, 1232–1235.

Gaynor, K.M., Brown, J.S., Middleton, A.D., Power, M.E. & Brashares, J.S. (2019). Landscapes of fear: spatial patterns of risk perception and response. *Trends Ecol. Evol.*, 34, 355–368.

Geffroy, B., Samia, D.S.M., Bessa, E. & Blumstein, D.T. (2015). How Nature-based tourism might increase prey vulnerability to predators. *Trends Ecol. & Evol.*, 30, 755–765.

Gordon, C.E., Feit, A., Grüber, J. & Letnic, M. (2015). Mesopredator suppression by an apex predator alleviates the risk of predation perceived by small prey. *Proc. R. Soc. B.*, 282, 20142870.

Harting, F. (2018). DHARMa: Residual diagnostics for hierarchical (multi-level/mixed) regression models. R package version, (2).

Hebblewhite, M., White, C.A., Nietvelt, C.G., McKenzie, J.A., Hurd, T.E., Fryxell, J.M., et al. (2005). Human activity mediates a trophic cascade caused by wolves. *Ecology*, 86, 2135–2144.

Hettena, A.M., Munoz, N. & Blumstein, D.T. (2014). Prey responses to Predator's sounds: a review and empirical study. *Ethology*, 120, 427–452.

Kuijper, D.P.J., Sahlén, E., Elmhagen, B., Chamaillé-Jammes, S., Sand, H., Lone, K., et al. (2016). Paws without claws? Ecological effects of large carnivores in anthropogenic landscapes. *Proc. R. Soc. B.*, 283, 20161625.

LaManna, J.A. & Martin, T.E. (2016). Costs of fear: behavioural and life-history responses to risk and their demographic consequences vary across species. *Ecol. Lett.*, 19, 403–413.

Laundré, J.W., Hernández, L. & Altendorf, K.B. (2001). Wolves, elk, and bison: reestablishing the "landscape of fear" in Yellowstone National Park, USA. *Can. J. Zool.*, 79, 1401–1409.

Levi, T., Kilpatrick, A.M., Mangel, M. & Wilmers, C.C. (2012). Deer, predators, and the emergence of Lyme disease. *PNAS*, 109, 10942–10947.

Linkie, M. & Ridout, M.S. (2011). Assessing tiger–prey interactions in Sumatran rainforests. *J. Zool.*, 284, 224–229.

McComb, K., Shannon, G., Sayialel, K.N. & Moss, C. (2014). Elephants can determine ethnicity, gender, and age from acoustic cues in human voices. *PNAS*, 111, 5433–5438.

Meredith, M. & Ridout, M. (2014). Overlap: estimates of coefficient of overlapping for animal activity patterns. R package version, (3), 2.

Moll, R.J., Cepek, J.D., Lorch, P.D., Dennis, P.M., Robison, T., Millspaugh, J.J., et al. (2018). Humans and urban development mediate the sympatry of competing carnivores. *Urban Ecosyst*, 21, 765–778.

Muhly, T.B., Semeniuk, C., Massolo, A., Hickman, L. & Musiani, M. (2011). Human activity helps prey win the predator-prey space race. *PLoS ONE*, 6, e17050.

Newsome, T.M., Dellinger, J.A., Pavey, C.R., Ripple, W.J., Shores, C.R., Wirsing, A.J., et al. (2015). The ecological effects of providing resource subsidies to predators. *Global Ecol. Biogeogr.*, 24, 1–11.

Ordiz, A., Bischof, R. & Swenson, J.E. (2013a). Saving large carnivores, but losing the apex predator? *Biol. Conserv.*, 168, 128–133.

Ordiz, A., Støen, O.-G., Sæbø, S., Sahlén, V., Pedersen, B.E., Kindberg, J., et al. (2013b). Lasting behavioural responses of brown bears to experimental encounters with humans. *J. Appl. Ecol.*, 50, 306–314.

Ordiz, A., Moen, G.K., Sæbø, S., Stenset, N., Swenson, J.E. & Støen, O.-G. (2019). Habituation, sensitization, or consistent behavioral responses? Brown bear responses after repeated approaches by humans on foot. *Biol. Conserv.*, 232, 228–237.

Oriol-Cotterill, A., Valeix, M., Frank, L.G., Riginos, C. & Macdonald, D.W. (2015). Landscapes of Coexistence for terrestrial carnivores: the ecological consequences of being downgraded from ultimate to penultimate predator by humans. *Oikos*, 124, 1263–1273.

Palmer, M.S., Fieberg, J., Swanson, A., Kosmala, M. & Packer, C. (2017). A 'dynamic' landscape of fear: prey responses to spatiotemporal variations in predation risk across the lunar cycle. *Ecol. Lett.*, 20, 1364–1373.

Plummer, M. (2003). JAGS: A program for analysis of Bayesian graphical models using Gibbs sampling. In: *Proceedings of the 3rd international workshop on distributed statistical computing* (eds Hornik, K., Leisch, F. & Zeileis, A.). DSC,Vienna, Austria, pp. 1–8.
Ridout, M.S. & Linkie, M. (2009). Estimating overlap of daily activity patterns from camera trap data. *JABES*, 14, 322–337.
Royle, J.A. & Dorazio, R.M. (2008). *Hierarchical Modeling and Inference in Ecology: The Analysis of Data from Populations*, Metapopulations and Communities. Academic Press, London, UK.
Royle, J.A., Chandler, R.B., Sollmann, R. & Gardner, B. (2013). *Spatial capture-recapture*. Academic Press, Waltham.
Salo, P., Banks, P.B., Dickman, C.R. & Korpimäki, E. (2010). Predator manipulation experiments: impacts on populations of terrestrial vertebrate prey. *Ecol. Monogr.*, 80, 531–546.
Schmitz, O.J., Beckerman, A.P. & O'Brien, K.M. (1997). Behaviorally mediated trophic cascades: effects of predation risk on food web interactions. *Ecology*, 78, 1388–1399.
Schuette, P., Creel, S. & Christianson, D. (2013). Coexistence of African lions, livestock, and people in a landscape with variable human land use and seasonal movements. *Biol. Conserv.*, 157, 148–154.
Smith, J.A., Wang, Y. & Wilmers, C.C. (2015). Top carnivores increase their kill rates on prey as a response to human-induced fear. *Proc. R Soc. B*, 282, 20142711.
Smith, J.A., Suraci, J.P., Clinchy, M., Crawford, A., Roberts, D., Zanette, L.Y., et al. (2017). Fear of the human 'super predator' reduces feeding time in large carnivores. *Proc. R Soc. B*, 284, 20170433.
Smith, J.A., Thomas, A.C., Levi, T., Wang, Y. & Wilmers, C.C. (2018). Human activity reduces niche partitioning among three widespread mesocarnivores. *Oikos*, 127, 890–901.
Stankowich, T. (2008). Ungulate flight responses to human disturbance: a review and meta-analysis. *Biol. Conserv.*, 141, 2159–2173.
Stankowich, T. & Blumstein, D.T. (2005). Fear in animals: a meta-analysis and review of risk assessment. *Proc. R Soc. B*, 272, 2627–2634.
Su, Y.-S. & Yajima, M. (2015). R2jags: A Package for Running jags from. R. R package, version, 0.5-7.
Suraci, J.P., Clinchy, M., Dill, L.M., Roberts, D. & Zanette, L.Y. (2016). Fear of large carnivores causes a trophic cascade. *Nat. Commun.*, 7, 10698.
Suraci, J.P., Clinchy, M. & Zanette, L.Y. (2017). Do large carnivores and mesocarnivores have redundant impacts on intertidal prey? *PLoS ONE*, 12, e0170255.
Suraci, J.P., Frank, L.G., Oriol-Cotterill, A., Ekwanga, S., Williams, T.M. & Wilmers, C.C. (2019). Behavior-specific habitat selection by African lions may promote their persistence in a human-dominated landscape. *Ecology*, 100, e02644.
Tucker, M.A., Böhning-Gaese, K., Fagan, W.F., Fryxell, J.M., Moorter, B.V., Alberts, S.C., et al. (2018). Moving in the Anthropocene: Global reductions in terrestrial mammalian movements. *Science*, 359, 466–469.
Valeix, M., Hemson, G., Loveridge, A.J., Mills, G. & Macdonald, D.W. (2012). Behavioural adjustments of a large carnivore to access secondary prey in a human-dominated landscape. *J. Appl. Ecol.*, 49, 73–81.
Venter, O., Sanderson, E.W., Magrach, A., Allan, J.R., Beher, J., Jones, K.R., et al. (2016). Sixteen years of change in the global terrestrial human footprint and implications for biodiversity conservation. *Nat. Commun.*, 7, 12558.
Wang, Y., Allen, M.L. & Wilmers, C.C. (2015). Mesopredator spatial and temporal responses to large predators and human development in the Santa Cruz Mountains of California. *Biol. Conserv.*, 190, 23–33.
Wang, Y., Smith, J.A. & Wilmers, C.C. (2017). Residential development alters behavior, movement, and energetics in an apex predator, the puma. *PLoS ONE*, 12, e0184687.
Wilmers, C.C., Wang, Y., Nickel, B., Houghtaling, P., Shakeri, Y., Allen, M.L., et al. (2013). Scale dependent behavioral responses to human development by a large predator, the puma. *PLoS ONE*, 8, e60590.
Zanette, L.Y., White, A.F., Allen, M.C. & Clinchy, M. (2011). Perceived predation risk reduces the number of offspring songbirds produce per year. *Science*, 334, 1398–1401.
Zanette, L.Y., Clinchy, M. & Suraci, J.P. (2014). Diagnosing predation risk effects on demography: can measuring physiology provide the means? *Oecologia*, 176, 637–651.

SUPPORTING INFORMATION

Additional supporting information may be found online in the Supporting Information section at the end of the article.

Editor, Greg Grether
Manuscript received 27 April 2019
First decision made 28 May 2019
Manuscript accepted 23 June 2019

Exhibit 6

WHY ARE SO MANY STRUCTURES BURNING IN CALIFORNIA?

Alexandra D. Syphard[1] and Jon E. Keeley[2,3]

California has earned a reputation for wildfires that inflict serious damage on human infrastructure, dating back to images of Richard Nixon hosing down the roof of his house in the 1961 Bel-Air fire, and of the famous "fireproof" home of grocery store entrepreneur Fred Roberts burning to the ground in 1982. In recent years, this notoriety has been transformed into public alarm, reflected in the apocalyptic headlines of recent newspaper articles suggesting the "end of California" (*New York Times*, 30 October 2019) and that "California is becoming unlivable" (*The Atlantic*, 30 October 2019). Now the phrase "the new normal" has worked its way into the lexicon, sustained by record-breaking structure loss numbers in 2017 and 2018 despite significantly lower structure losses in 2019.

It remains to be seen whether or not those two recent years were back-to-back one-in-a-hundred-year events, or if the trend has crossed some kind of tipping point, but data do show a long-term trend of significant increase in structures lost to wildfires since the beginning of the 20th century (Fig. 1). What was an average of ~500 homes lost per year in Southern California from about 1950–2000 (CalFire 2000) has recently climbed to ~2700 structures per year statewide from 2000–2018 (Syphard and Keeley 2019). California is not alone in the U.S., or in the world, in suffering increasing impacts from wildfires (e.g., Blanchi et al. 2012, Haynes 2015, Viegas 2018). Impacts so far in the current Australian bushfire season have been record-breaking, with several thousand structures lost, more than 25 fatalities, and unthinkable losses to wildlife. The question that follows, then, is why?

Although trends vary from region to region, one clear reason for increasing wildfire-related losses is the overall

Above: **Aerial retardant drop on a chaparral wildfire in coastal southern California, taken July 5, 2008, in the foothills of the Los Padres National Forest.** *[Dan Lindsay]*

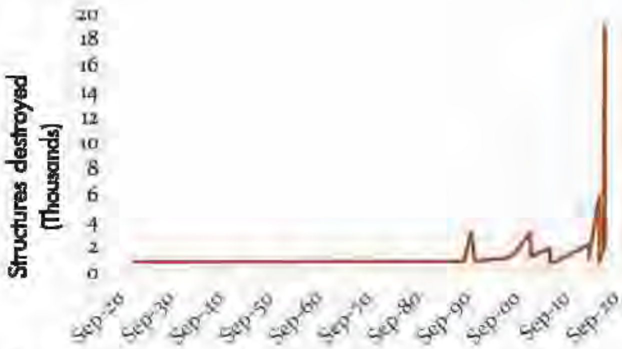

Figure 1. Annual number of structures destroyed in wildfires in California from 1920 to 2018. Source: California Department of Forestry & Fire Protection

increase in wildfire activity. Although, counter to intuition, the number of wildfires has declined in the last several decades, area burned has either remained constant or increased, with substantially higher frequency of large wildfires (Keeley and Syphard 2018), and as discussed further in Keeley and Syphard (this issue). Perhaps an even stronger explanation for increased wildfire-related structure loss is the rapid development of the wildland-urban interface (WUI), which not only exposes more structures to wildland fire, but also increases the likelihood for more human-ignited fires (Radeloff et al. 2018). Despite these trends, however, not all fires result in structure loss, and not all structures are impacted by wildfires they are exposed to. Thus, it is essential to study the factors that are most strongly related to structure exposure and resilience to wildfire, which could then lead to better adaptation and coexistence with wildfire in this era of the "new normal."

In response to this need, a growing number of scientists are conducting empirical research studies to answer the question of why some structures are lost in wildfires and others aren't. Results so far show that the answer to that question is complicated. That is, structure loss results from the confluence of multiple interacting factors across different temporal and spatial scales, which all vary by ecosystem. Given this complexity, misunderstandings and disagreements have arisen over the cause and direction of trends in wildfire activity (Doerr and Santín 2016), fire risk and structure loss (Mccaffrey et al. 2019), and thus, the most effective approach for prioritizing fire management decisions (Moritz et al. 2014). In fact, management techniques appropriate for one region are commonly applied inappropriately to other regions (Noss et al. 2006).

One way that this conflict over priorities can be reduced is through better information and understanding of the similarities and differences that contribute to structure loss among wildfire ecoregions. As data accumulate about the range of conditions under which losses occur, it will be increasingly possible to sort out which risk management techniques are most appropriate for different regions. Wildfire structure losses in the last several decades have already provided a wealth of data for studies comparing factors associated with structures that survived or were destroyed. Most of this work has been done in California (Maranghides and Mell 2009, Syphard et al. 2012a, 2014, 2017, 2019c, Miner 2014, Alexandre et al. 2015, Kramer et al. 2019, Syphard and Keeley 2019) and Australia (Leonard 2009, Blanchi et al. 2010, 2012, Gibbons et al. 2012, 2018, Price and Bradstock 2013, Penman et al. 2019); but some work has also been done in other parts of the continental United States (Alexandre et al. 2016, Kramer et al. 2019).

Combined, the results of this research show clear roles for both local, house-level factors (e.g., structural characteristics of a particular house and property-level landscaping) and broader, landscape-level factors (e.g., housing pattern and location, topography, fuel, and fire characteristics) in explaining why some structures survive wildfires and others don't. This is consistent with the natural hazards literature that theoretically places vulnerability within the intersection of "exposure," that is, potential contact with a hazard; and "sensitivity," or the degree to which the hazard can cause harm (Birkmann 2006). Vulnerability to wildfire is a combination of exposure and sensitivity such that vulnerability results in loss when sensitive characteristics of structures are exposed to hazard events (e.g., the wildfire) (Cutter 1996, Schumann et al. 2019). Thus, exposure is the part of vulnerability related to characteristics of a location, and sensitivity is the risk of loss due to intrinsic physical or social characteristics.

EXPOSURE

Coincidence of fires and houses

A structure's wildfire hazard exposure ultimately lies at the spatial intersection of a wildfire event and the location of the property. The probability of structure

1. Sage Insurance Holdings, LLC, 600 California Street, San Francisco, CA, 94108, USA, email: asyphard@sageunderwriters.com

2. U.S. Geological Survey, Western Ecological Research Center, Sequoia-Kings Canyon Field Station, 47050 General's Highway, Three Rivers, California 93271, USA,

3. Department of Ecology and Evolutionary Biology, University of California, 612 Charles E. Young Drive, South Los Angeles, California 90095-7246, USA email: jon_keeley@usgs.gov

1. Corresponding author

Caption here. *[Rick Halsey]*

loss thus depends on the relative likelihood that a fire ignition results in a fire within the geographical range of structures in the wildland-urban interface (WUI). In turn, this depends on the location and timing of a fire ignition, which varies depending on cause and biophysical characteristics (Syphard and Keeley 2015) relative to other determinants of fire size, including topographic conditions; fuel amount, moisture, and spatial continuity; and weather (Faivre et al. 2016). Large fires tend to be either primarily fuel-dominated or wind-dominated (Keeley and Syphard 2019), with most damage and economic loss occurring from wind-driven fire events (Jin et al. 2015, Keeley and Syphard this issue).

Large fire probability increases with the co-occurrence of human-caused ignitions and severe wind conditions (Abatzoglou et al. 2018). This means that, as population increases and development further encroaches into wildland vegetation, there is an increased risk that a human-caused ignition will coincide in place and time with hot, dry weather; flammable vegetation; and severe wind conditions. Data show that fires tend to be most frequent at low to intermediate housing and population densities (Syphard et al. 2009, Bistinas et al. 2013). Thus, the rapid increase in the spread of exurban development like that occurring now in California (Radeloff et al. 2018), has the potential to both increase the number of ignitions and decrease the overall distance between wildlands and housing.

As the distance between wildland vegetation and housing development decreases across a landscape, the overall exposure of houses to wildfire increases. This helps to explain research that shows the arrangement and location of housing development to be a top-ranked predictor of whether a structure survives or is destroyed by wildfire (e.g., Syphard et al. 2012b, Alexandre et al. 2016, Kramer et al. 2019). In terms of arrangement, data consistently show that loss to wildfire is highest at relatively low housing density (Kramer et al. 2018, Syphard et al. 2019c) and at the interface between wildlands and development (Kramer et al. 2019), regardless of the geographic region in which a structure is located,.

Other housing patterns, such as the way housing is dispersed, or the size of housing clusters, are also influential, although their relative importance in explaining structure loss varies from region to region (Alexandre et al. 2015, 2016). Topography is an additional exposure-related factor significantly related to structure loss, as fire tends to spread quickly upslope, meaning that houses on ridgetops are particularly vulnerable. An important caveat to the relationship between low structure density and structure loss is that, once a fire reaches a development, structure-to-structure spread is possible if adjacent houses are highly flammable and spaced within at least 50 meters of one another (Price and Bradstock (2013). In these circumstances, high housing density can be a significant risk factor (Maranghides and Mell 2009).

Fire patterns, altered fire regimes, and vegetation management

In addition to housing arrangement, housing location affects the potential exposure of a structure to wildfire because some areas are inherently more fire-prone than others (Syphard et al. 2012b). Certain parts of the landscape tend to burn repeatedly while others do not, and this reflects the wide variation in fire regimes across California (Syphard and Keeley in press). During the last century, fire regimes in California have been altered due to a range of factors including climate change, land use change, and legacies of fire management. However, the cause of fire regime changes, and their relative effects, have been nearly opposite in the northern and southern-coastal parts of the state (Safford and Water 2014). As described in Keeley and Syphard (this issue), a history of successful fire exclusion in dry, mixed-conifer forests contributed to an alteration of what had been a low-intensity surface fire regime that typically burned back the understory plants without reaching into the canopy and burning the large trees. The subsequent increase in the density of surface litter and the unchecked ingrowth of young trees that serve as ladder fuels now facilitate uncharacteristically severe crown fires. In contrast, in the native shrublands of southern and central coastal California, increased human-caused ignitions have resulted in unnaturally high fire frequency, with increases in wildfire further promoted by ongoing conversion of shrublands to more flammable invasive grasses (Fusco et al. 2019, Syphard et al. 2019b, 2019a).

These differences in the two fire regimes, and how they have been altered, have led to substantial controversy regarding wildfire exposure and the effects and effectiveness of vegetation management (Keeley et al. 2009, Halsey and Syphard 2015). In both northern and southern California, changes in fire regimes could lead to more dangerous or frequent wildfires, thereby increasing structure exposure to hazard. Mechanical treatments and prescribed fire in dry, mixed-conifer forests that reduce the understory and decrease small diameter tree density may help return these forests to a more resilient condition, and thereby potentially reduce exposure of structures to high fire hazard (Knapp et al. 2017).

On the other hand, in the non-forested landscapes that dominate the coastal central and southern parts of the state, vegetation management is primarily focused on reducing the extent of woody vegetation. That is, mechanical treatments are typically designed to remove and reduce the cover of native shrublands and increase the cover of herbaceous vegetation. Prescribed fire in this region *increases* the amount of uncharacteristically frequent fire, putting additional stress on native chaparral and shrublands. Therefore, in non-forested ecosystems vegetation management is inconsistent with ecological integrity and, in addition, has minimal efficacy in the wind-driven fires that result in the most structure loss (Keeley and Syphard this issue).

Access as a risk factor

While vegetation management may control fire behavior by slowing wildfire spread, wildfires during extreme wind conditions typically generate embers and burning debris that can fly kilometers ahead of the fire front. Therefore, fuels management in remote landscapes, even if it does alter fire behavior, has little possibility of preventing wind-driven fires from spreading and expanding if there are no firefighters present to control the fire. This is the likely explanation for why Penman et al. (2014) found that fire size and exposure of property to wildfire in Southern California are primarily controlled by fire weather and characteristics of the built environment, with fuel treatments or fuel load management having minimal influence. Fuel load is less likely to be limiting during wind-driven wildfires and reduction of fuel load in remote areas is unlikely to affect fire outcomes (Keeley et al. 2004, Schoennagel et al. 2004).

On the other hand, strategic placement of fuel breaks near communities may be more effective at reducing exposure because firefighters can use these for safe access to perform suppression activities (Syphard et al. 2011). In addition to strategically placed fuel breaks near communities, the road network surrounding a structure is also important for minimizing exposure from an access perspective. Wide roads and multiple access points can facilitate the transport of firefighting resources to properties within a community; in addition, a good road network provides faster and more efficient evacuation alternatives (Mangan 2000).

SENSITIVITY

Community sensitivity to wildfire, and the capacity to recover from wildfire losses, is related to the social and demographic characteristics of a region (Schumann et al. 2019). In terms of the physical nature of structure loss, however, the primary determinants of sensitivity include defensible space and home structure characteristics as well as firefighter accessibility.

Defensible space

There is certainly a degree of confusion regarding defensible space. A common sentiment is that the larger the defensible space, the better protected the home.

Figure 3. Local (a) and landscape-scale (b) examples of defensible space being performed beyond legal requirements or scientific evidence for protection

Thus, clearance far in excess of legal requirements is increasingly being carried out (Fig. 3a), sometimes at a broad scale (Fig 3b). This is not necessarily helpful or effective. At the same time, many homeowners fail to create sufficient defensible space to improve structure survival.

What does the evidence show about the effectiveness of defensible space? The state of California requires homeowners in state-defined hazardous areas to provide 30 meters (100 feet) of defensible space around their home, which involves the maintenance of specific horizontal and vertical distances of spacing between patches of woody vegetation. Empirical studies in two Southern California areas found that defensible space of approximately 5-20 meters (16-66 feet) provided significant protection, with additional distance providing little or no significant benefit, even on steep slopes (Miner 2014, Syphard et al. 2014). Empirical research looking at structure loss in Australia also found that vegetation reduction and defensible space were most effective at close proximity to the structure (Gibbons et al. 2012, Penman et al. 2019), and that regular irrigation and proper spacing could be as just as effective as clearing woody vegetation (Gibbons et al. 2018).

The largest empirical study of home survival published to date, which included more than 40,000 structures subjected to wildfires over a five year period (Syphard and Keeley 2019), showed that defensible space distance explained little or none of the variance in structure survival. Instead, characteristics of the structure itself were far more significant (Fig. 4). These results should not be interpreted to mean defensible space is not important. But they do suggest that the

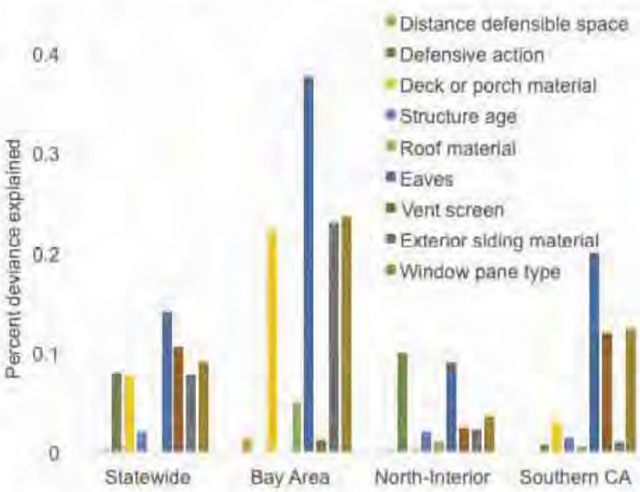

Figure 4. Relative importance (percent deviance explained) of defensible space distance and structural characteristics explaining structure loss to California wildfires from 2013–2018 for the entire state and broken into three broad regions. *Figure modified from Syphard and Keeley (2019).*

Figure 5. Image of flammable debris on a roof that could ignite from wind-blown embers, reflecting how vegetation near or overhanging structures could increase the likelihood of structure loss.

most important component of defensible space may be the characteristics of vegetation closest to the house. For example, vegetation touching the structure and trees overhanging the roof were highly significant in the two empirical examples from Southern California.

Ember cast

It needs to be appreciated that, particularly during extreme wind-driven fires, most homes do not burn from direct flame contact or from the radiant heat of the fire front, but rather from embers blown from the fire front, even from a kilometer or more away. Thus, the material that embers land on, be it vegetation or the structure itself, is key to whether the structure ignites or not. In some cases, the effect of overhanging trees or nearby vegetation is mostly related to the dead plant material or debris that is close to the structure (Fig.5). Likewise, the structural characteristics found to be most important in this recent study (Syphard and Keeley 2019) were related to the prevention of ember penetration, such as vent screens and eaves. Open eaves (Fig. 6a) are much more vulnerable to fires than closed eves (Fig. 6b). Open eaves have vents that are arranged perpendicular to the ground and thus in direct line of oncoming wind-driven ember cast. Closed eaves have vents facing down towards the ground and perhaps less prone to embers entering the vents.

Figure 6. Images of a) open eave design that may allow ember penetration into the structure more readily than b) closed eave design that has been significantly associated with structure survival in California wildfires.

CONCLUSION

The studies described above illustrate that some structures are destroyed in wildfires and others are not because of multiple, often interacting, factors that variably influence the exposure and sensitivity of a property to wildfire. In an ideal world, strategies to increase community resistance to wildfire would be ranked and prioritized according to their relative potential for success in preventing structure loss in any given ecosystem. Of course, an ideal world would also not have to account for factors such as cost, effort, and feasibility, which add to the complexity of decision-making in the real world.

While most empirical research on structure loss has so far focused on either exposure or sensitivity factors independently, an integrated analysis in Southern California provided a comparison of the relative importance of different exposure-related and sensitivity-related variables (Syphard et al. 2017, Fig. 7) in distinguishing destroyed from surviving structures. Study results suggested that exposure (when measured by structure density) was the most important factor overall that distinguished destroyed from surviving structures. The relative importance of different sensitivity variables (e.g., structure age or landscaping characteristics) varied depending upon whether the structure was highly exposed (i.e., at low housing density) or less exposed (i.e., at high housing density) (Fig. 7).

These results suggest that, in an ideal world, the most effective strategy at reducing future structure loss would focus on reducing the extent of low-density housing via careful land planning decisions. This conclusion is rather obvious given that reducing exposure reduces the chance that a wildfire could reach a structure in the first place. In the real world, regardless of land use planning decisions for future development, there is extensive existing development that may be exposed to future wildfires. Therefore, strategies like ignition prevention and strategic vegetation management could potentially reduce the exposure of these houses by focusing on the initiation or spread of the wildfire.

Once a fire reaches a property, structure sensitivity then becomes the key determinant for survival. In many areas, effective efforts to minimize sensitivity to wildfire include education and increased awareness of appropriate defensible space practices, development of Firewise Communities (Jakes et al. 2007), and improvement in building codes. Nonetheless, some communities underinvest in defensible space (Taylor et al. 2019), while in others, homeowners create excessive clearance (Fig. 3) that may increase the extent of invasive grass on the property. Conversion of native woody vegetation into grass in the non-forested landscapes of Southern California, for example, could increase the flammability of the property (Fusco et al. 2019), particularly if the grass is not irrigated regularly (Gibbons et al. 2018).

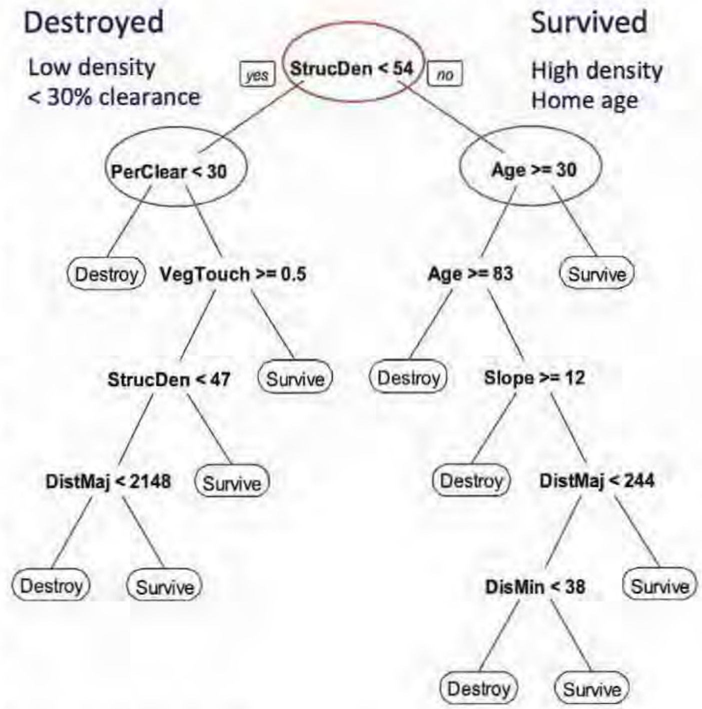

Figure 7. Classification tree showing the hierarchy of factors that best distinguished destroyed from survived structures in Southern California wildfires. Abbreviations are: StrucDen = structure density; PerClear = percentage woody vegetation clearance on property; Age = age of structure; VegTouch = number of sides of structure with vegetation touching; Slope = percentage slope on property; DistMaj = distance in meters to a major road; DisMin = distance in meters to a minor road. *Modified from Syphard et al. 2017.*

Given the importance of structural characteristics in home survival in recent California wildfires (Syphard and Keeley 2019), the improvement of building codes has been a positive development overall. However, there is already extensive existing residential development in fire-prone areas that was built prior to the adoption of new building codes. Reducing the fire sensitivity of these homes generally entails retrofits and modifications, which can be expensive (Quarles and Pohl 2018). However, some of the most effective actions, such as eave coverings and vent screens, are generally less expensive than replacing roofing or exterior siding, although window replacement can also be expensive (Quarles and Pohl 2018).

The 2017 Thomas Fire. *[Stuart Palley, U.S. Forest Service]*

one, from the individual homeowner, to local planning and permitting officials, to state and federal government authorities, will need to be involved in instituting preventive measures. Management appropriately informed by science and data analysis can reduce future structure losses and minimize ecological impacts to assure a more sustainable future. While these efforts may seem expensive in the present, it is much less expensive than paying for losses in the future.

It would appear, given recent improvements in adapting structures to withstand fire, that the increase in the numbers of houses burned in wildfire is not a matter of increased sensitivity. Instead, the answer lies somewhere in the combination of factors that govern exposure, including changes to wildfire behavior and activity, as well as exurban development that places structures in the path of these wildfires. Climate and vegetation change may increase the probability of large wildfires in some regions, such as the northern parts of California (Syphard et al. 2019c); but in other regions, like Southern California, climate change is likely to manifest differently, most likely indirectly, via factors such as long-term drought and vegetation change.

While the effects of climate change on wildfire vary from region to region, housing pattern variables have consistently been the most important factors explaining structure loss across California and elsewhere. This suggests that much of the increase in structure loss in California may be attributable to increases in this type of exposure—and that planning decisions could have broad-scale benefits in the future. Also consistent across regions is the potential for homeowner mitigation measures to provide significant improvement in structure survival probability. Those measures that focus on reduction of ember impact and penetration are most important.

Despite these overall consistencies, there is variation in the nature and strength of relationships in all of these factors. Wildfire frequency and behavior, and fuel characteristics, vary widely by ecosystem; thus, vegetation management efforts differ greatly in effects and effectiveness and should be implemented appropriately. Regardless of regional variations, every-

REFERENCES

Abatzoglou, J. T., J. K. Balch, B. A. Bradley, and C. A. Kolden. 2018. Human-related ignitions concurrent with high winds promote large wildfires across the USA. *International Journal of Wildland Fire* 27:377–386.

Alexandre, P. M., S. I. Stewart, N. S. Keuler, M. K. Clayton, M. H. Mockrin, A. Bar-Massada, A. D. Syphard, and V. C. Radeloff. 2016. Factors related to building loss due to wildfires in the conterminous United States. *Ecological Applications* 26.

Alexandre, P. M., S. I. Stewart, M. H. Mockrin, N. S. Keuler, A. D. Syphard, A. Bar-Massada, M. K. Clayton, and V. C. Radeloff. 2015. The relative impacts of vegetation, topography and spatial arrangement on building loss to wildfires in case studies of California and Colorado. *Landscape Ecology* 31:415–430.

Birkmann, J. 2006. Measuring vulnerability to natural hazards: towards disaster resilient societies. United Nations University Press, Tokyo.

Bistinas, I., D. Oom, A. C. L. Sá, S. P. Harrison, I. C. Prentice, and J. M. C. Pereira. 2013. Relationships between human population density and burned area at continental and global scales. *PLOS ONE* 8:e81188.

Blanchi, R., J. Leonard, K. Haynes, K. Opie, M. James, M. Kilinc, F. D. De Oliveira, and R. Van den Honert. 2012. Life and house loss database description and analysis. CSIRO.

Blanchi, R., C. Lucas, J. Leonard, and K. Finkele. 2010. Meteorological conditions and wildfire-related houseloss in Australia. *International Journal of Wildland Fire* 19:914–926.

CalFire. 2000. Wildland Fire Hazard Assessment. California Division of Forestry and Fire Protection, Sacramento, CA.

Cutter, S. L. 1996. Vulnerability to environmental hazards. *Progress in Human Geography* 20:529–539.

Doerr, S. H., and C. Santín. 2016. Global trends in wildfire and its impacts: Perceptions versus realities in a changing world. Philosophical Transactions of the Royal Society B: *Biological Sciences* 371.

Faivre, N. R., Y. Jin, M. L. Goulden, and J. T. Randerson. 2016. Spatial patterns and controls on burned area for two contrasting fire regimes in Southern California. *Ecosphere* 7:e01210.

Fusco, E. J., J. T. Finn, J. K. Balch, R. C. Nagy, and B. A. Bradley. 2019. Invasive grasses increase fire occurrence and frequency across US ecoregions. *Proceedings of the National Academy of Sciences*: 1–6.

Gibbons, P., L. van Bommel, A. Gill, G. J. Cary, D. A. Driscoll, R. A. Bradstock, E. Knight, M. A. Moritz, S. L. Stephens, and D. B. Lindenmayer. 2012. Land management practices associated with house loss in wildfires. *PLOS ONE* 7:e29212.

Gibbons, P., A. M. Gill, N. Shore, M. A. Moritz, S. Dovers, and G. J. Cary. 2018. Options for reducing house-losses during wildfires without clearing trees and shrubs. *Landscape and urban planning* 174:10–17.

Halsey, R. W., and A. D. Syphard. 2015. High-Severity Fire in Chaparral: Cognitive Dissonance in the Shrublands. The Ecological Importance of Mixed-Severity Fires: Nature's Phoenix.

Haynes, H. J. G. 2015. *Fire loss in the United States during 2014.* National Fire Protection Association, Fire Analysis and Research Division.

Jakes, P., L. Kruger, M. Monroe, K. Nelson, and V. Sturtevant. 2007. Improving wildfire preparedness: lessons from communities across the US. *Human Ecology Review:*188–197.

Jin, Y., M. Goulden, S. Faivre, V. Veraverbeke, A. Hall, M. Hand, S. Hook, and J. Randerson. 2015. Identification of two distinct fire regimes in southern California: implications for economic impact and future change. *Environmental Research Letters* 10:094005.

Keeley, J. E., C. J. Fotheringham, and M. A. Moritz. 2004. Lessons from the October 2003 Wildfires in Southern California. *Journal of Forestry.* 102: 26-31.

Keeley, J. E., H. D. Safford, C. J. Fotheringham, J. Franklin, and M. A. Moritz. 2009. The 2007 southern California wildfires: Lessons in complexity. *Journal of Forestry* 107:287–296.

Keeley, J. E., and A. D. Syphard. 2018. Historical patterns of wildfire ignition sources in California ecosystems. *International Journal of Wildland Fire* 27:781–799.

Keeley, J. E., and A. D. Syphard. 2019. Twenty-first century California, USA, wildfires: fuel-dominated vs. wind-dominated fires. *Fire Ecology* 15:24.

Knapp, E. E., J. M. Lydersen, M. P. North, and B. M. Collins. 2017. Efficacy of variable density thinning and prescribed fire for restoring forest heterogeneity to mixed-conifer forest in the central Sierra Nevada, CA. *Forest Ecology and Management* 406:228–241.

Kramer, H. A., M. H. Mockrin, P. M. Alexandre, and V. C. Radeloff. 2019. High wildfire damage in interface communities in California. *International Journal of Wildland Fire* 28:641.

Kramer, H. A., M. H. Mockrin, P. M. Alexandre, S. I. Stewart, and V. C. Radeloff. 2018. Where wildfires destroy buildings in the US relative to the wildland–urban interface and national fire outreach programs. *International Journal of Wildland Fire* 27:329–341.

Leonard, J. 2009. Report to the 2009 Victorian Bushfires Royal Commission. Building performance in bushfires. Highett, Victoria, Australia: CSIRO Sustainable Ecosystems.

Mangan, R. J. 2000. Improving firefighter safety in the wildland-urban intermix. USDA Forest Service, Technology and Development Program.

Maranghides, A., and W. Mell. 2009. A Case Study of a Community Affected by the Witch and Guejito Fires.

Mccaffrey, S. M., G. L. Duffner, and L. M. Decker. 2019. Chapter Twenty-Seven. Social Dynamics of Wildland Fire in California. *Fire in California's Ecosystems:* 507–516.

Miner, A. 2014. Defensible space optimization for preventing wildfire Structure loss in the Santa Monica Mountains. Johns Hopkins University.

Moritz, M. A., E. Batllori, R. A. Bradstock, A. M. Gill, J. Handmer, P. F. Hessburg, J. Leonard, S. McCaffrey, D. C. Odion, T. Schoennagel, and *Nature.* 515 (6):58-66.

Noss, R. F., J. F. Franklin, W. L. Baker, T. Schoennagel, and P. B. Moyle. 2006. Managing fire-prone forests in the western United States. *Frontiers In Ecology And The Environment* 4:481–487.

Penman, S. H., O. F. Price, T. D. Penman, and R. A. Bradstock. 2019. The role of defensible space on the likelihood of house impact from wildfires in forested landscapes of south eastern Australia. *International Journal of Wildland Fire* 28:4–14.

Penman, T. D., L. Collins, A. D. Syphard, J. E. Keeley, and R. A. Bradstock. 2014. Influence of fuels, weather and the built environment on the exposure of property to wildfire. *PLOS ONE* 9(10): e111414.

Price, O., and R. Bradstock. 2013. Landscape scale influences of forest area and housing density on house loss in the 2009 Victorian bushfires. *PLOS ONE* 8:e73421.

Quarles, S., and K. Pohl. 2018. Building a Wildfire-Resistant Home: Codes and Costs. Bozeman, MT.

Radeloff, V. C., D. P. Helmers, H. Anu Kramer, M. H. Mockrin, P. M. Alexandre, A. Bar-Massada, V. Butsic, T. J. Hawbaker, S. Martinuzzi, A. D. Syphard, and S. I. Stewart. 2018. Rapid growth of the US wildland-urban interface raises wildfire risk. *Proceedings of the National Academy of Sciences* 115:3314–3319.

Safford, H., and K. Van de Water. 2014. Using fire return interval departure (FRID) analysis to map spatial and temporal changes in fire frequency on national forest lands in California.

Schoennagel, T., T. T. Veblen, and W. H. Romme. 2004. The interaction of fire, fuels, and climate across rocky mountain forests. *Bioscience* 54:661–676.

Schumann, R. L., M. Mockrin, A. D. Syphard, J. Whittaker, O. Price, C. Johnson, C. T. Emrich, and V. Butsic. 2019. International Journal of Disaster Risk Reduction Wildfire recovery as a " hot moment " for creating fire-adapted communities. *International Journal of Disaster Risk Reduction:* 101354.

Syphard, A. D., T. J. Brennan, and J. E. Keeley. 2014. The role of defensible space for residential structure protection during wildfires. *International Journal of Wildland Fire* 23:1165–1175.

Syphard, A. D., T. J. Brennan, and J. E. Keeley. 2017. The importance of building construction materials relative to other factors affecting structure survival during wildfire. *International Journal of Disaster Risk Reduction* 21:140-147.

Syphard, A. D., T. J. Brennan, and J. E. Keeley. 2019a. Extent and drivers of vegetation type conversion in Southern California chaparral. *Ecosphere* 10:e02808.

Syphard, A. D., T. J. Brennan, J. E. Keeley, and T. Vaclavik. 2019b. Drivers of chaparral type conversion to herbaceous vegetation in coastal Southern California. *Diversity and Distributions* 10: 90-101.

Syphard, A. D., and J. E. Keeley. 2015. Location, timing, and extent of wildfire varies by cause of ignition. *International Journal of Wildland Fire* 24:37–47.

Syphard, A. D., and J. E. Keeley. 2019. Factors associated with structure loss in the 2013 - 2018 California wildfires. *Fire* 2:49.

Syphard, A. D., J. E. Keeley, and T. J. Brennan. 2011. Comparing the role of fuel breaks across southern California national forests. *Forest Ecology and Management* 261:2038–2048.

Syphard, A. D., J. E. Keeley, A. B. Massada, T. J. Brennan, and V. C. Radeloff. 2012a. Housing arrangement and location determine the likelihood of housing loss due to wildfire. *PLOS ONE* 14(2): e0211454.

Syphard, A. D., J. E. Keeley, A. B. Massada, T. J. Brennan, and V. C. Radeloff. 2012b. Housing arrangement and location determine the likelihood of housing loss due to wildfire. *PLOS ONE* 7:1–13.

Syphard, A. D., V. C. Radeloff, T. J. Hawbaker, and S. I. Stewart. 2009. Conservation Threats Due to Human-Caused Increases in Fire Frequency in Mediterranean-Climate Ecosystems. *Conservation Biology* 23:758–769.

Syphard, A. D., H. Rustigian-Romsos, M. Mann, E. Conlisk, M. A. Moritz, and D. Ackerly. 2019c. The relative influence of climate and housing development on current and projected future fire patterns and structure loss across three California landscapes. *Global Environmental Change* 56:41–55.

Taylor, M. H., L. Christman, and K. Rollins. 2019. Targeting policy to promote defensible space in the wildland-urban interface: evidence from homeowners in Nevada. *Land Economics* 95:531–556.

Viegas, D. X. 2018. Wildfires in Portugal. *Fire Research.*

Exhibit 7

Project Title: Santa Ana Mountains to eastern Peninsular Range Conservation Connectivity Infrastructure Planning Project for Interstate 15 and Closely Associated Roadways

Collaborators

- **Winston Vickers, UC Davis Karen C. Drayer Wildlife Health Center**
- **Trish Smith, The Nature Conservancy**
- **Brian Cohen, The Nature Conservancy**
-
- **California Polytechnic University, Pomona**
- **Senior Students led by team leaders Elena Pierce and Ali Moetazed Monajjemi**
- **Civil Engineering Faculty leading and advising student teams were:**
- **Wen Cheng, Xudong Jia, and Lourdes Abellara**

- **Amy Collins and Fraser Shilling - UC Davis Road Ecology Center**
- **Travis Longcore – USC**

- **Kathy Zeller – U. Mass**
- **Justin Dellinger – CDFW**
- **Jessica Sanchez - UCD**

- **UCD Field Crew – Jamie Bourdon and Rich Codington**

From CESA 2019 petition to list 6 southern and coastal populations as threatened or endangered. Map adapted from Gustafson et al. 2018

Santa Ana Mountains circled

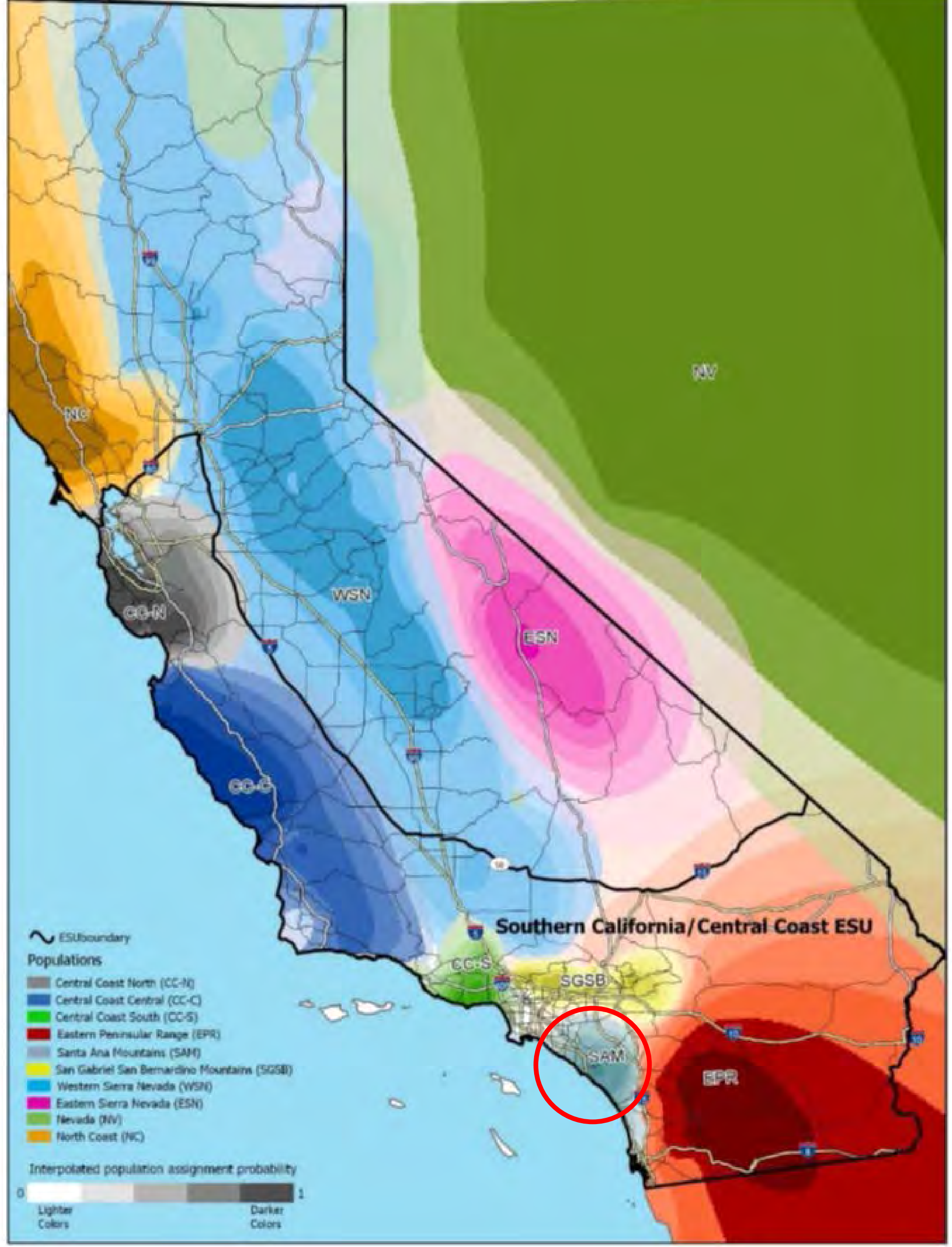

Project study area with 5 mile buffers around the highways that are focus of the study.

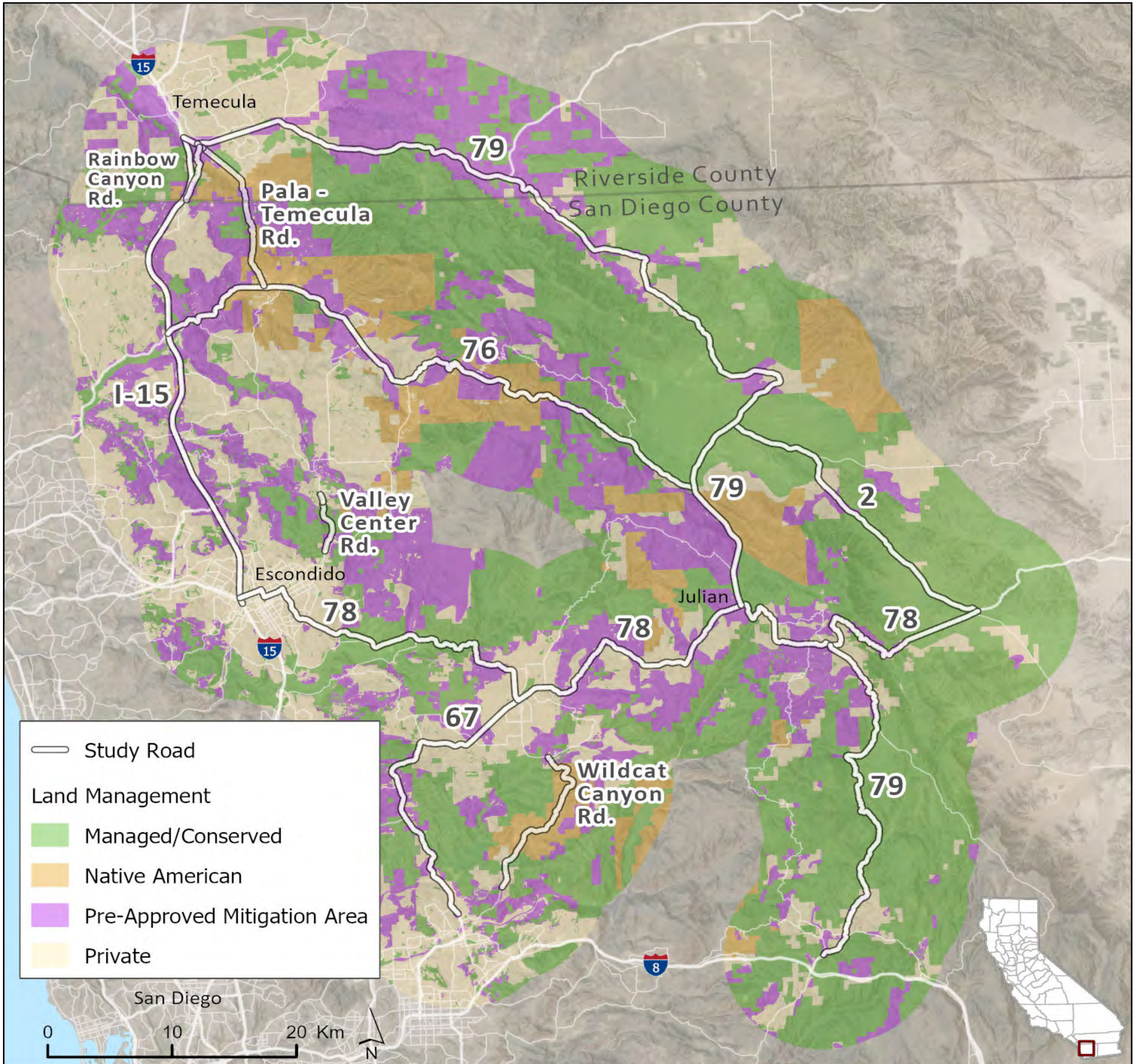

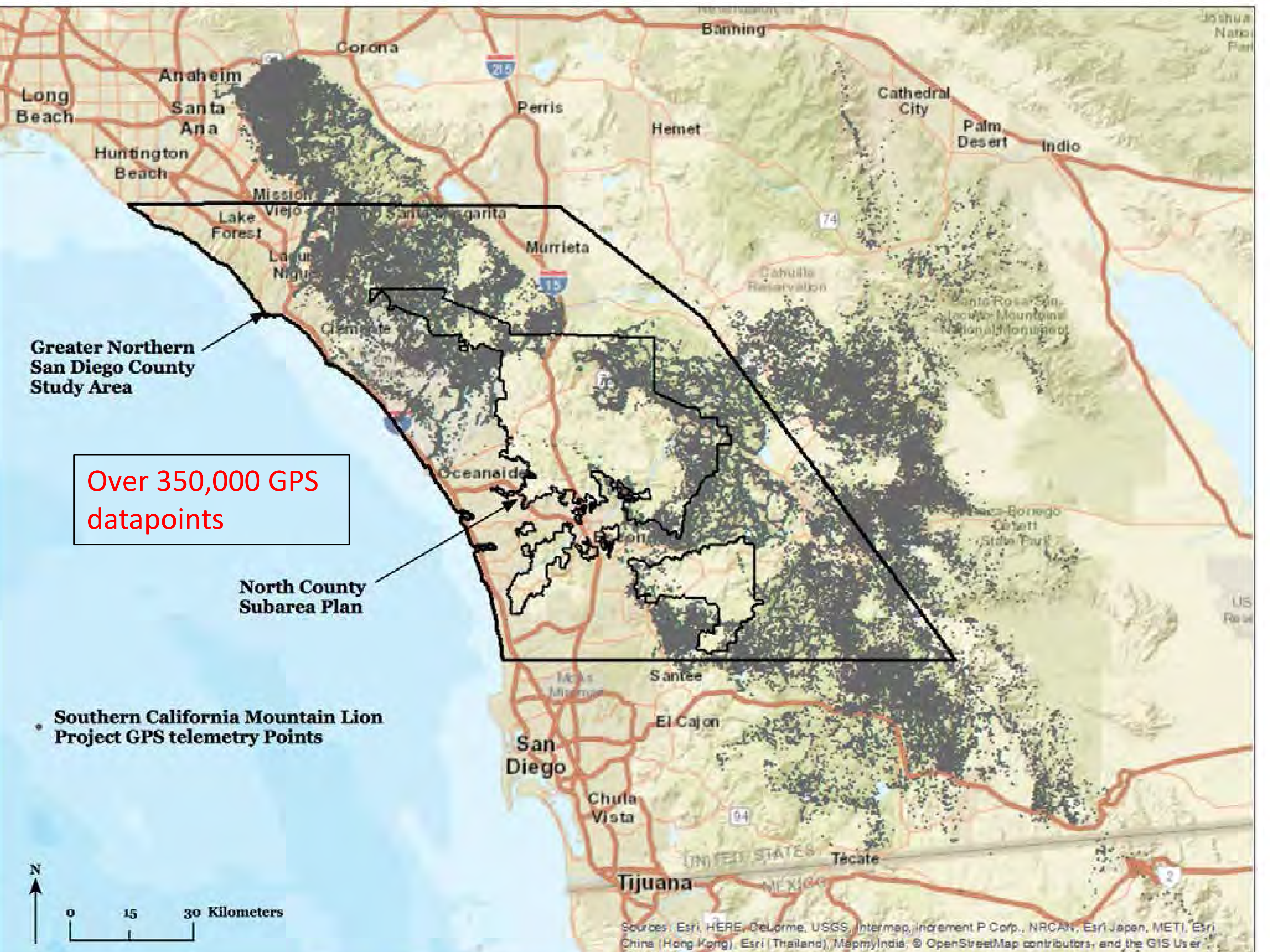

Greater Northern San Diego County Study Area
Over 350,000 GPS datapoints
North County Subarea Plan
Southern California Mountain Lion Project GPS telemetry Points
N
0 15 30 Kilometers
Long Beach
Anaheim
Santa Ana
Huntington Beach
Corona
Banning
Perris
Hemet
Cathedral City
Palm Desert
Indio
Mission Viejo
Lake Forest
Murrieta
Oceanside
Santee
El Cajon
San Diego
Chula Vista
Tijuana
Tecate

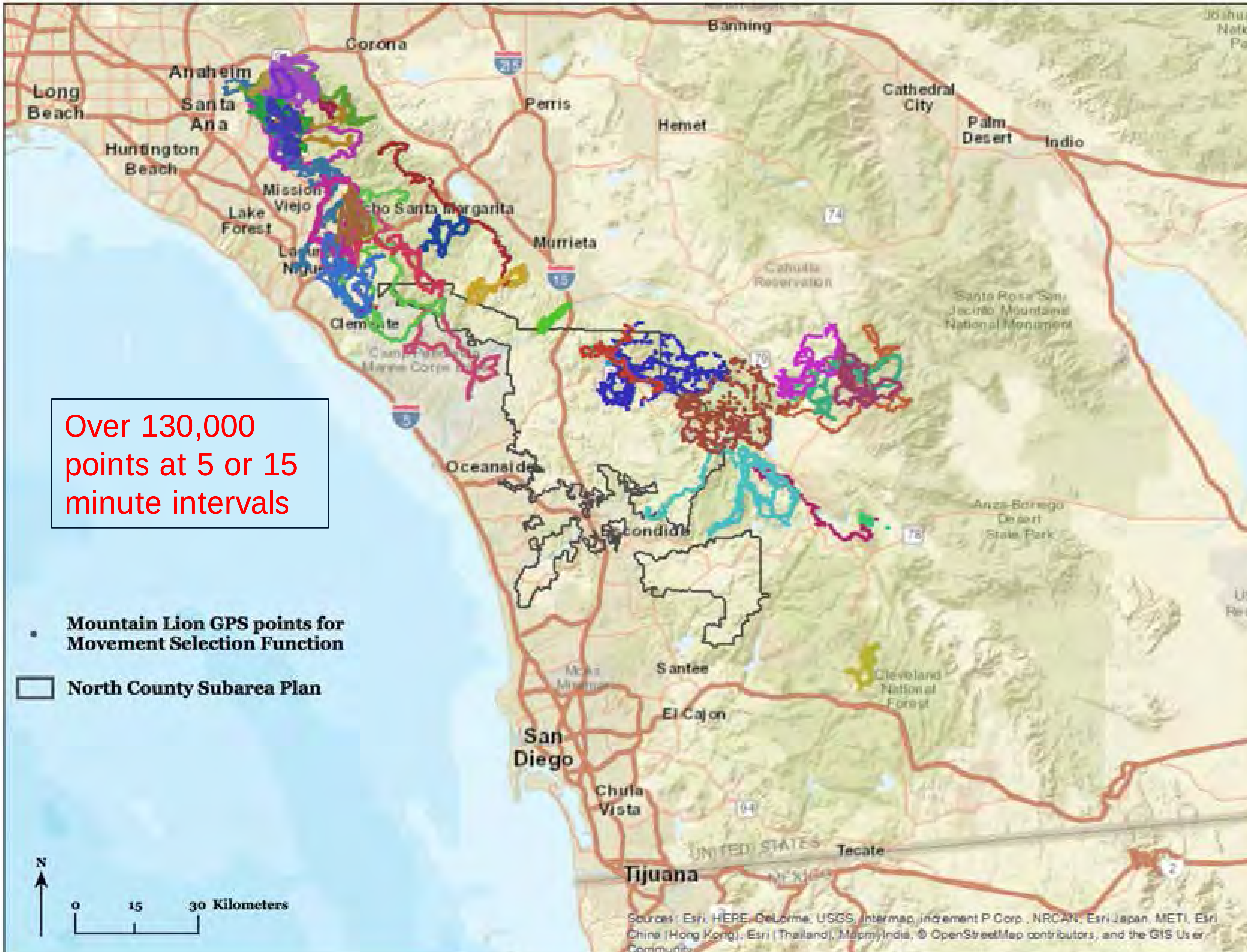
Over 130,000 points at 5 or 15 minute intervals
Mountain Lion GPS points for Movement Selection Function
North County Subarea Plan
N
0
15
30 Kilometers
Banning
Corona
Anaheim
Long Beach
Santa Ana
Huntington Beach
Mission Viejo
Lake Forest
Perris
Hemet
Cathedral City
Palm Desert
Indio
Murrieta
Oceanside
Escondido
Santee
El Cajon
San Diego
Chula Vista
Tijuana
Tecate
Cahuilla Reservation
Santa Rosa San Jacinto Mountains National Monument
Anza-Borrego Desert State Park
Cleveland National Forest
UNITED STATES
Sources: Esri, HERE, DeLorme, USGS, Intermap, increment P Corp., NRCAN, Esri Japan, METI, Esri China (Hong Kong), Esri (Thailand), MapmyIndia, © OpenStreetMap contributors, and the GIS User Community

In San Diego Co. 51 collared pumas
1,540 crossings of major highways
16% were struck (Vickers et al. 2015,201

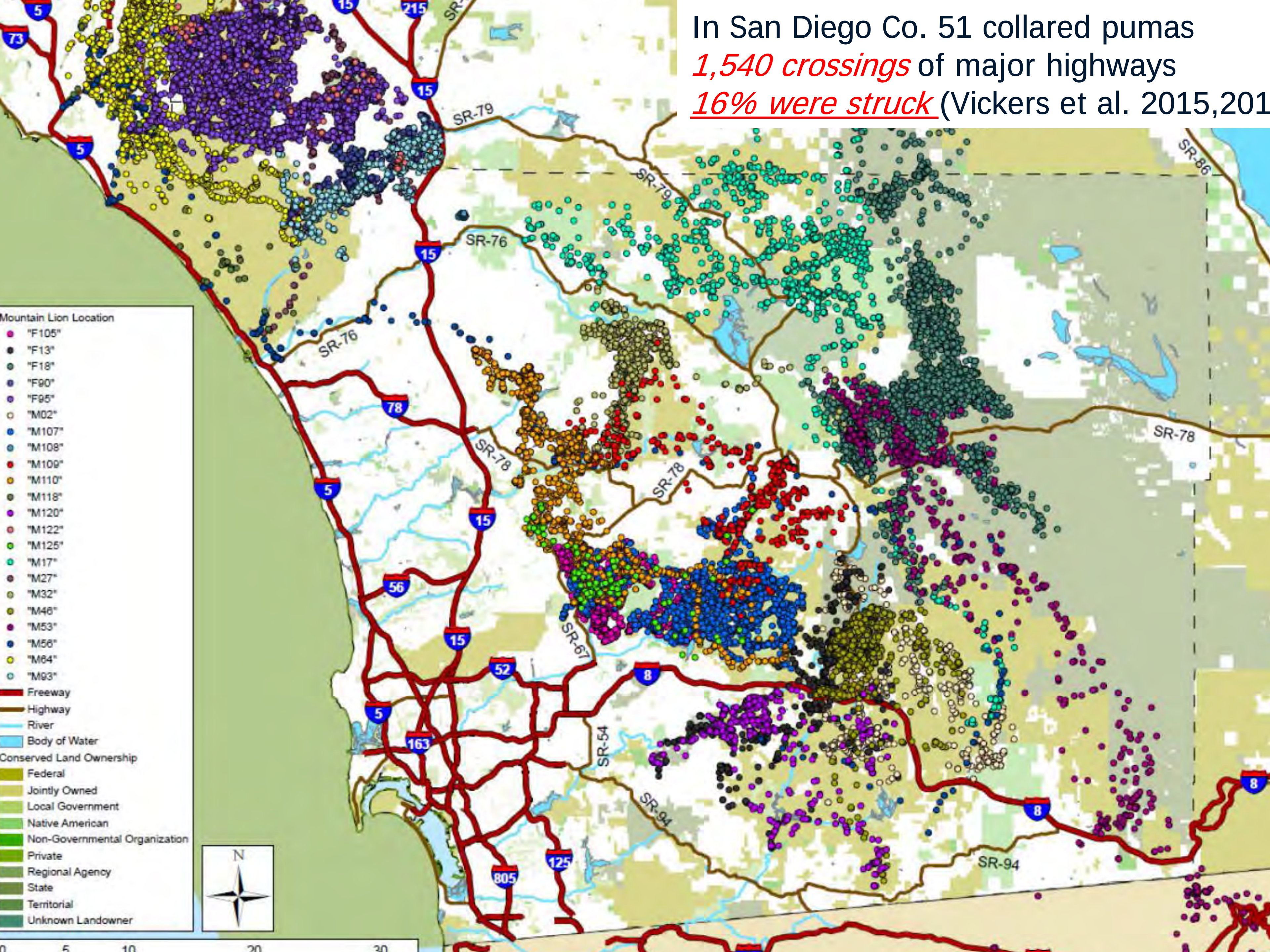

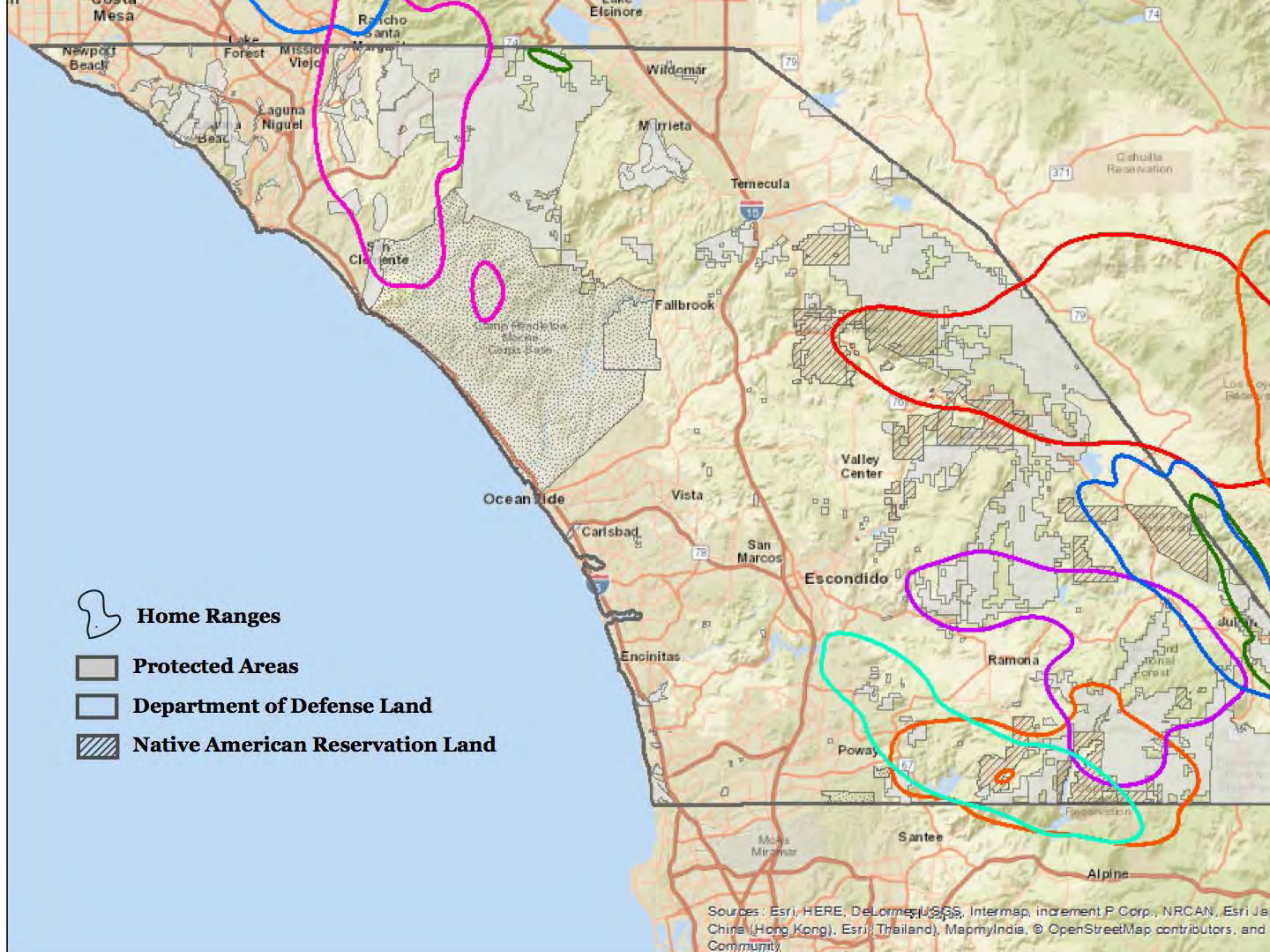
Home Ranges
Protected Areas
Department of Defense Land
Native American Reservation Land
Costa Mesa
Newport Beach
Lake Forest
Mission Viejo
Laguna Niguel
Elsinore
Wildomar
Temecula
Fallbrook
Valley Center
Oceanside
Vista
Carlsbad
San Marcos
Escondido
Encinitas
Ramona
Poway
Santee
Alpine
Sources: Esri, HERE, DeLorme, USGS, Intermap, increment P Corp., NRCAN, Esri Ja
China (Hong Kong), Esri (Thailand), MapmyIndia, © OpenStreetMap contributors, and
Community

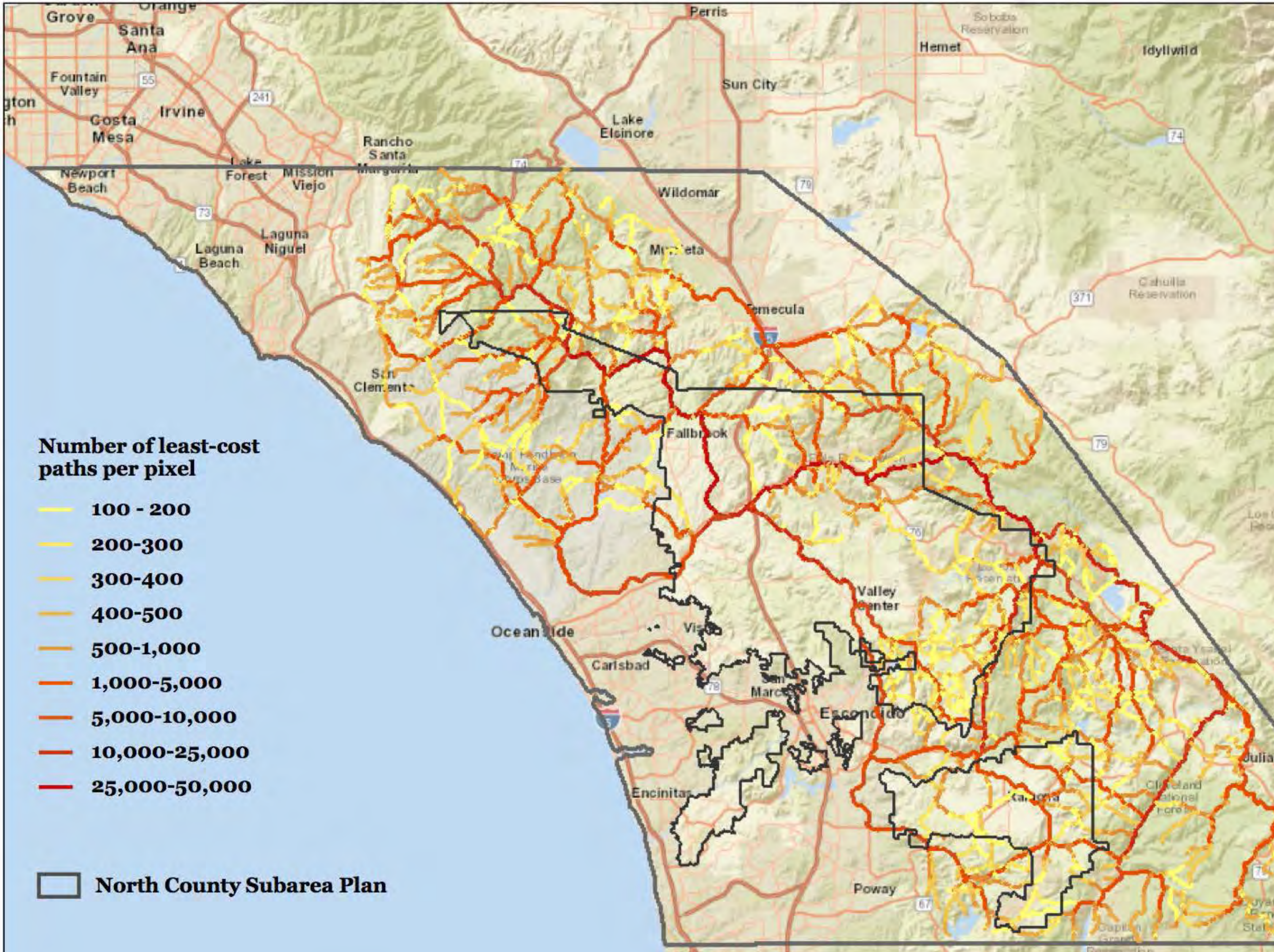
Number of least-cost paths per pixel
100 - 200
200-300
300-400
400-500
500-1,000
1,000-5,000
5,000-10,000
10,000-25,000
25,000-50,000
North County Subarea Plan
Grove
Santa Ana
Fountain Valley
Irvine
Costa Mesa
Newport Beach
Forest
Mission Viejo
Rancho Santa
Laguna Beach
Laguna Niguel
Perris
Hemet
Idyllwild
Sun City
Lake Elsinore
Wildomar
Temecula
Cahuilla Reservation
Fallbrook
Valley Center
Oceanside
Carlsbad
Escondido
Encinitas
Poway

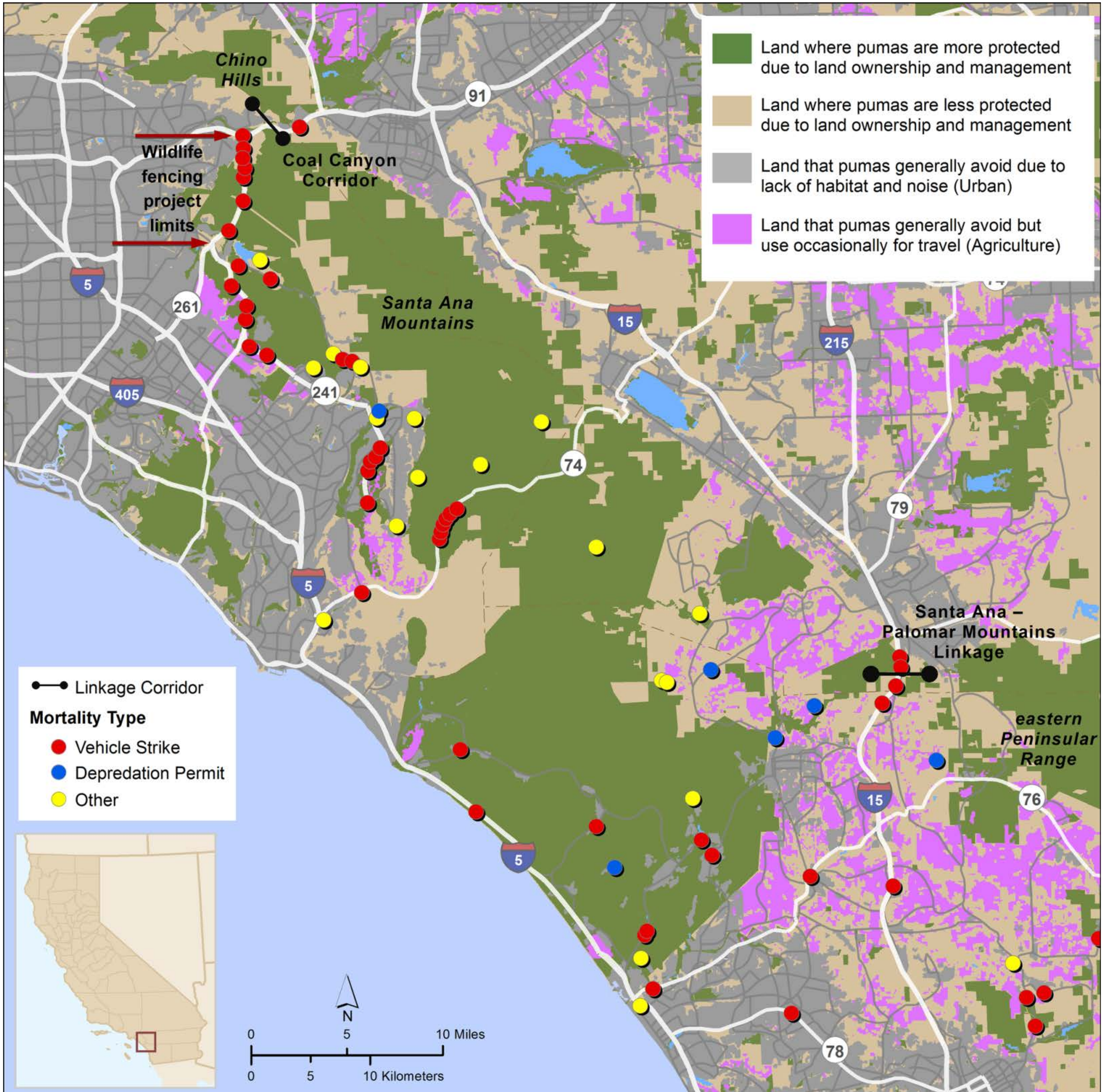

Land where pumas are more protected due to land ownership and management
Land where pumas are less protected due to land ownership and management
Land that pumas generally avoid due to lack of habitat and noise (Urban)
Land that pumas generally avoid but use occasionally for travel (Agriculture)
Chino Hills
Wildlife fencing project limits
Coal Canyon Corridor
Santa Ana Mountains
Santa Ana – Palomar Mountains Linkage
eastern Peninsular Range
91
5
261
15
215
405
241
74
79
76
78
Linkage Corridor
Mortality Type
Vehicle Strike
Depredation Permit
Other
N
0
5
10 Miles
0
5
10 Kilometers

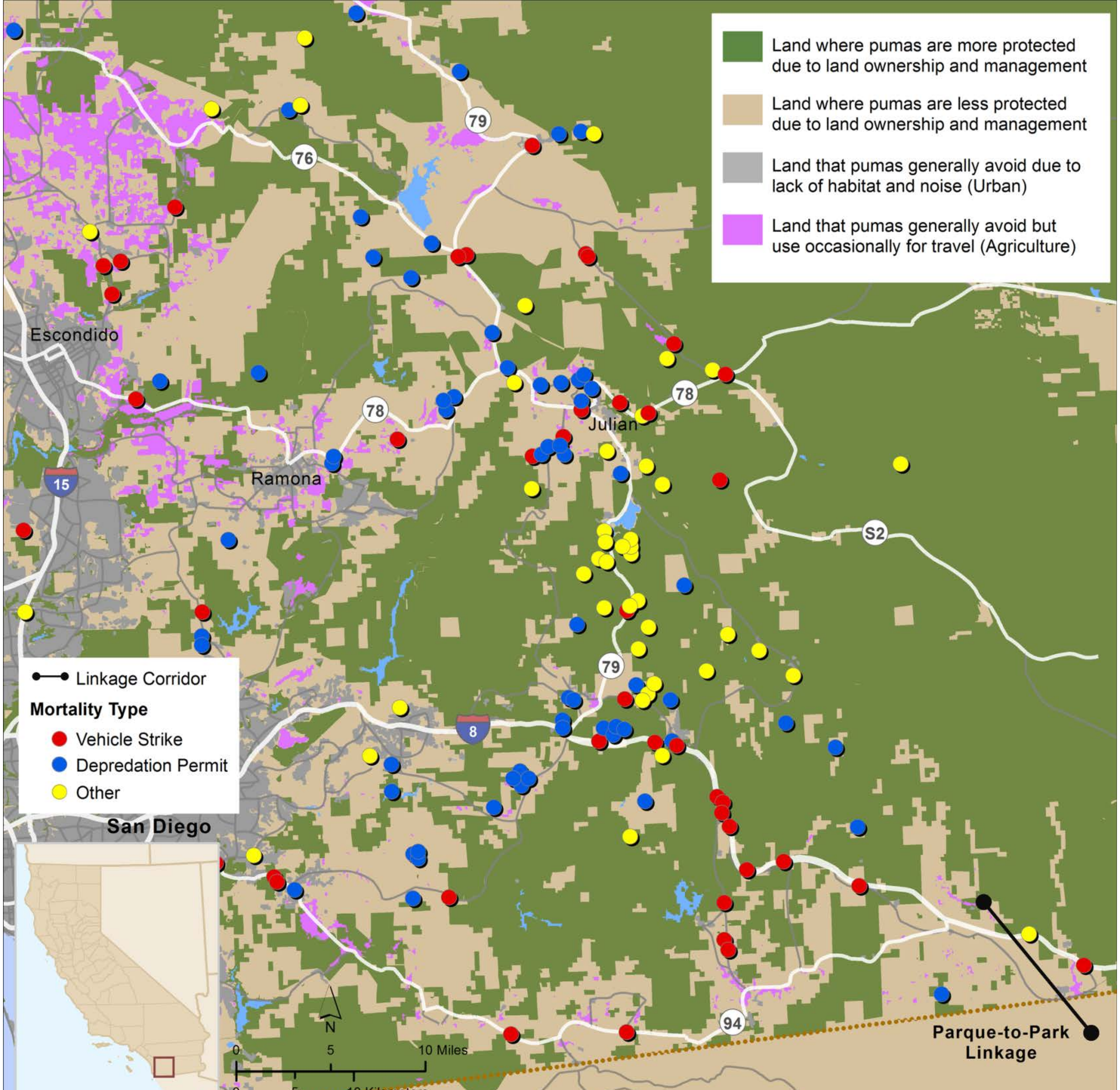

Land where pumas are more protected due to land ownership and management
Land where pumas are less protected due to land ownership and management
Land that pumas generally avoid due to lack of habitat and noise (Urban)
Land that pumas generally avoid but use occasionally for travel (Agriculture)
Linkage Corridor
Mortality Type
Vehicle Strike
Depredation Permit
Other
Escondido
Ramona
Julian
San Diego
79
76
78
15
8
S2
94
Parque-to-Park Linkage
N
0
5
10 Miles

Project Tasks as defined in the funding grants were:

- Task 1 (NCCP-LAG): Conduct wildlife crossing infrastructure assessments for the approximately 7-mile portion of I-15 in the SA-ePR linkage region

- Task 1 (SANDAG):
- Conduct Highway Crossing Assessments and create Wildlife Crossing Improvement Plans for portions of I-15, SR's 76, 78, and 79, as well as other major highways

- Task 2 (NCCP- LAG): Collaborate with Cal Poly Pomona engineering faculty and students, and other highway engineers, to assess feasibility of infrastructure changes

- Task 3 (NCCP-LAG): Coordinate and consult with stakeholders on findings and create maps and other tools to illustrate findings.

- **Potential crossing sites:**
- 190 sites examined – full data from 183 sites, 2 others with structure grades
- **Identified via:**
- Known successful crossings from cameras, or 5 to 15 minute frequency collar data (over 130,000 datapoints) – (n=53 – over half on SR76)
- Unsuccessful crossing attempts (Roadkill – n=11 [13 lions])
- Zeller least cost path modeling, previous modeling – (n=108)
- Sites named in Missing Linkages Report/expert opinion/other – (n=13)
- A few sites were too dangerous to access due to traffic and landscape factors

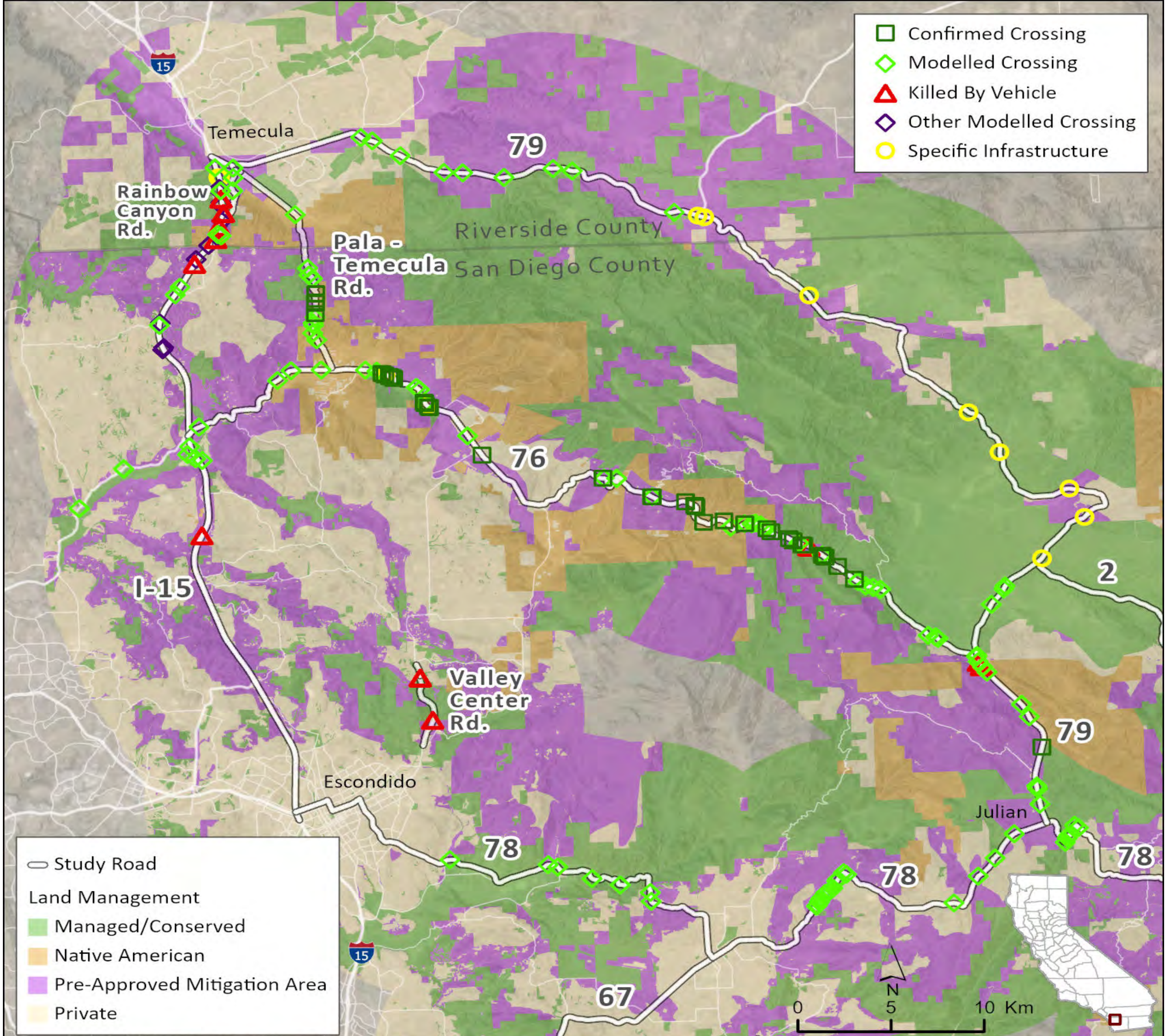

Confirmed Crossing
Modelled Crossing
Killed By Vehicle
Other Modelled Crossing
Specific Infrastructure
Temecula
15
79
Rainbow Canyon Rd.
Pala - Temecula Rd.
Riverside County
San Diego County
76
2
I-15
Valley Center Rd.
79
Escondido
Julian
78
78
78
67
15
Study Road
Land Management
Managed/Conserved
Native American
Pre-Approved Mitigation Area
Private
N
0
5
10 Km

- Grading of sites re infrastructure present

Structure Grade - 0= no structure, 1=culvert <3 ft, 2 = culvert 3 ft or more, 3 = bridge
Constraint/Plus Factor Score: 3 if can see through and trails, tracks, other evidence of use of structure by wildlife (ideal); 2 if can see through but no evidence of use, or if evidence of use but can't see through; 1 if can't see through and no evidence of use; 0 if full time water, accessibility compromised, or likely human presence at night.
Landscape score: 2 if suggests likely crossing point; 1 if minor contraints of landscape; 0 if significant landscape negatives
Confirmed crossing this location: 2 if yes; 0 if no

- Of the 185 sites examined and characterized:
- Culverts >3 ft dia: n=43 sites; 23%
- Bridges: n=36 sites; 19%
- Smaller culverts: n=49 sites; 26%
- No culvert or bridge: n=56 sites; 30%

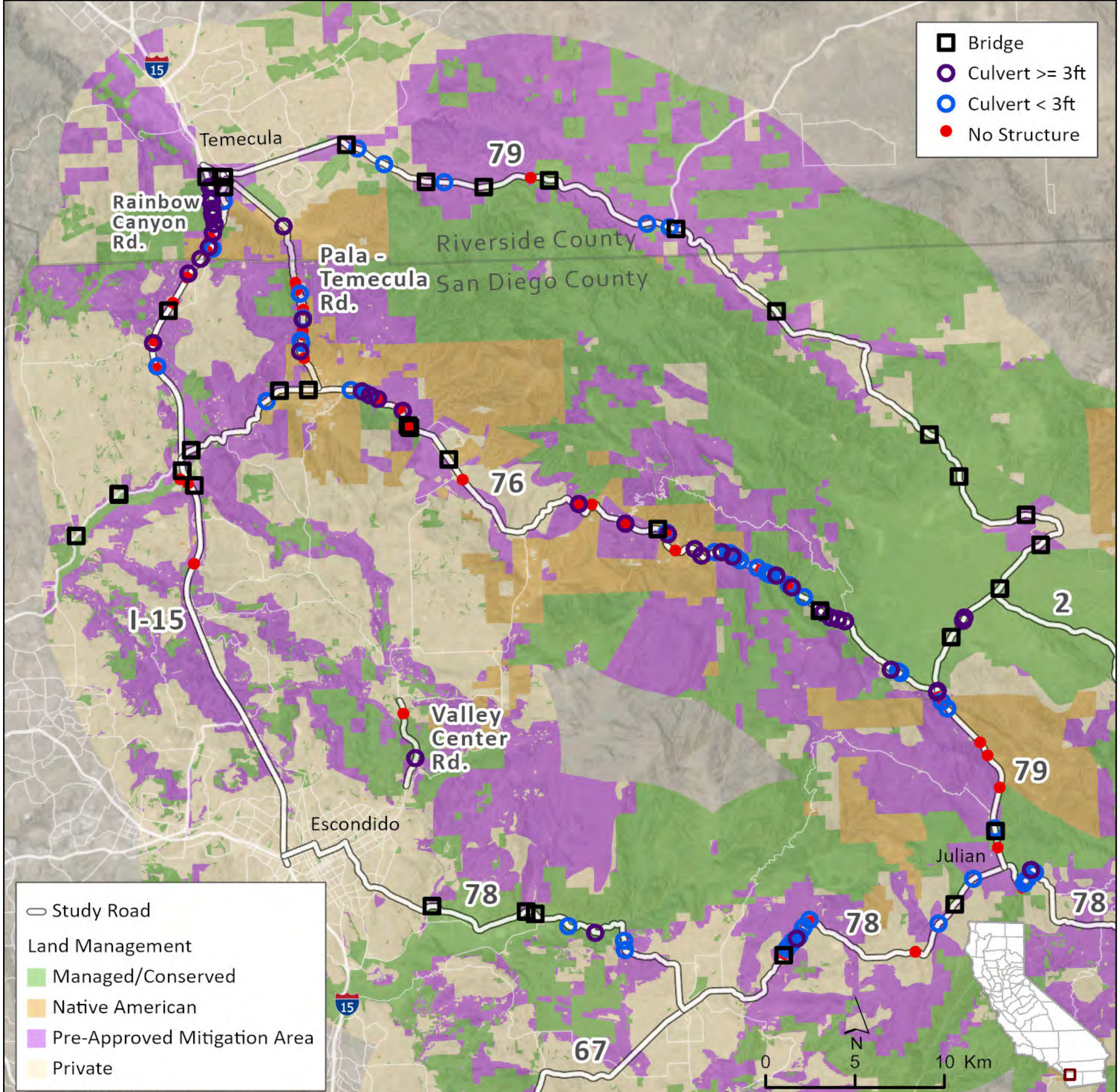

Bridge
Culvert >= 3ft
Culvert < 3ft
No Structure
Temecula
79
Rainbow Canyon Rd.
Pala - Temecula Rd.
Riverside County
San Diego County
76
2
I-15
15
Valley Center Rd.
79
Escondido
Julian
78
78
78
67
Study Road
Land Management
Managed/Conserved
Native American
Pre-Approved Mitigation Area
Private
N
0
5
10 Km

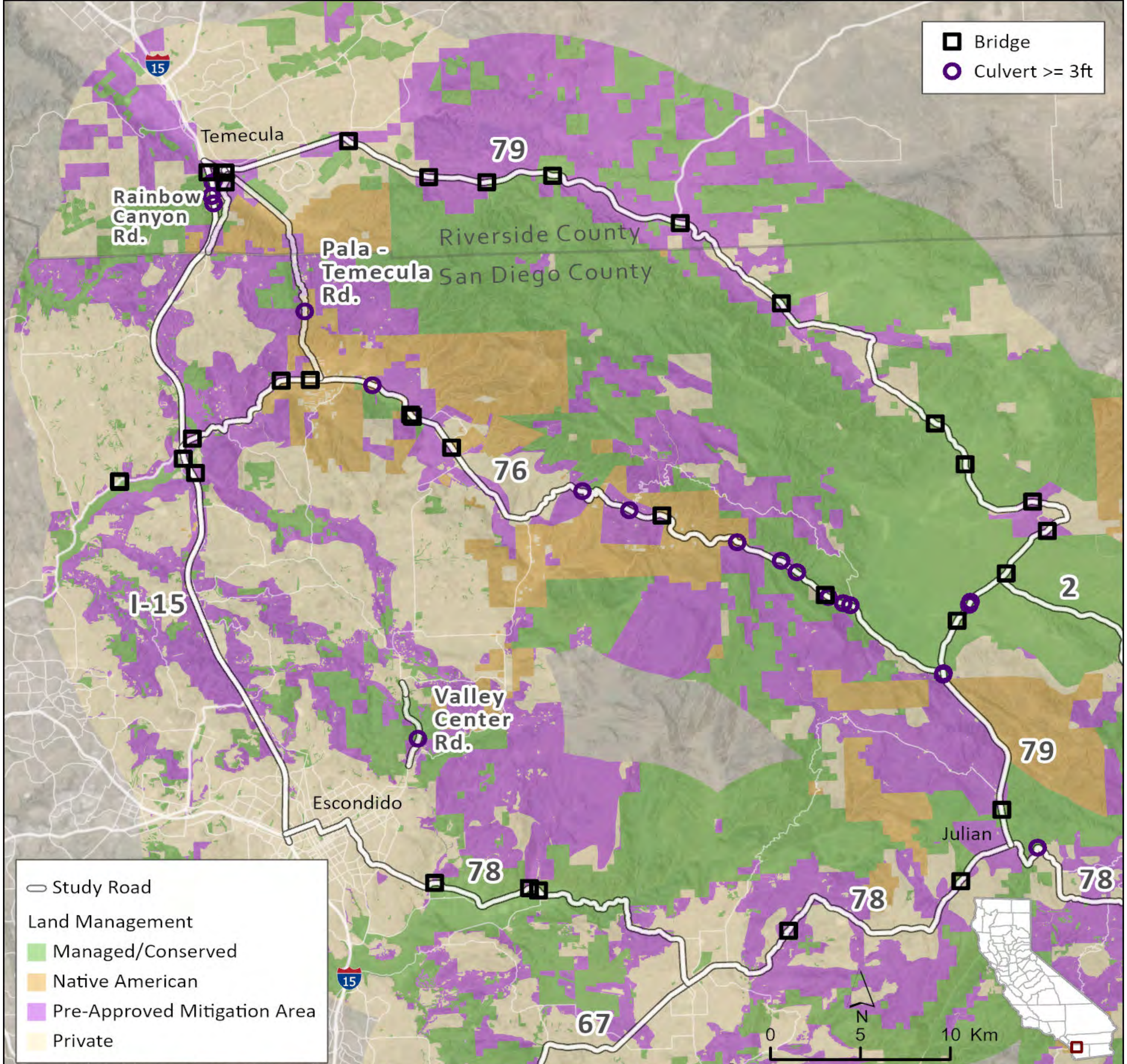

Bridge
Culvert >= 3ft
Temecula
Rainbow Canyon Rd.
Pala - Temecula Rd.
Riverside County
San Diego County
79
76
I-15
15
2
Valley Center Rd.
Escondido
Julian
78
67
Study Road
Land Management
Managed/Conserved
Native American
Pre-Approved Mitigation Area
Private
N
0
5
10 Km

Table 4. Number of sites examined on each highway, with structure types and number present. For bridges and larger culverts, the number of structures with no or only partial constraints is in parenthesis.

Highway name	Bridges	Culverts 3 ft or more	Culverts less than 3 ft	No Culvert or Bridge	Total sites examined
I-15	3 (2)	14 (5)	0	8	25 (7)
I-15/Old Hwy 395 jct	0	0	0	1	1 (0)
Rainbow Canyon Rd.	1 (1)	0	1	1	3 (1)
Old Hwy 395	2 (1)	0	2	1	5 (1)
Pechanga Parkway	1 (1)	1 (0)	0	0	2 (1)
Pala-Temecula Rd	0	2 (1)	4	8	14 (1)
SR-79	13 (13)	3 (3)	8	8	32 (16)
SR-76	11 (10)	19 (9)	16	23	69 (19)
SR-78	5 (5)	3 (1)	18	6	32 (6)
Valley Center Rd	0	1 (1)	0	1	2 (1)
Total Sites Examined	**36 (33)**	**43 (20)**	**49**	**57**	**185 (53)**

Information recorded at surveyed sites	
Survey ID	Structure type
Survey Date	Culvert distance below road
Highway name	Height
Highway number if not listed	Width
Location	Length
NEW Location?	Structure floor material
Drop Point (Lat/Long) (latitude)	Able to see through culvert
Drop Point (Lat/Long) (longitude)	Water?
Drop Point (Lat/Long) (speed)	Human presence likely at night?
Drop Point (Lat/Long) (direction)	Describe human presence potential
Drop Point (Lat/Long) (altitude)	Constraints
Drop Point (Lat/Long) (accuracy)	Describe constraint
Surveyor	Evidence of other animals?
Road type	Describe evidence of other animals present
Estimated width of road from one pavement edge to the other	Fencing present?
Landscape character suggestive of likely crossing point	Describe fencing type and height
Describe reason landscape character not conducive to crossing	Consider for camera?
Landscape and veg structure suggest corridor	Camera suggestions
Describe limitation of landscape and veg and which side of road	Comments
Other species observed	Management recommendations

Software by Wildnote © - very useful

- **Brian Cohen scoring of the roadways:**
- Graded and scored points along the region highways at 100 meter intervals
- 4,378 points – 272 miles of roadway
- Scoring was scaled at 100, 500, and 1,500 meters

Title	Criteria	Scoring
Conservation score	Percentage of land within 100, 500, and 1,500 meters of a road point or examined site that is conserved	0 - 10
Habitat score	Quality of habitat for mountain lions within 100, 500 and 1,500 meters of a road point or examined site per K. Zeller habitat modeling	0 - 10
Resource score	Quality of resources for mountain lions within 100, 500 and 1,500 meters of a road point or examined site based on J. Dellinger resource modeling	0 - 10
Activity score	Numbers of mountain lion pathway 10 meter segments (based on GPS-Collar data) that lie within 100, 500, and 1,500 meters of a road point or examined site	0 - 10
Movement score	Likelihood of mountain lion movement within 100, 500, and 1,500 meters of a road point or examined site based on K. Zeller movement modeling	0 - 10
Observational score	Total of scores for crossing structure type (0-3); Lack of constraints on structures (0-3); Landscape structure / wildlife evidence (0-2), and confirmed crossing this location (0-2) based on on-the-ground road crossing site surveys	0 - 10
	Summary value for all scores	0 - 60

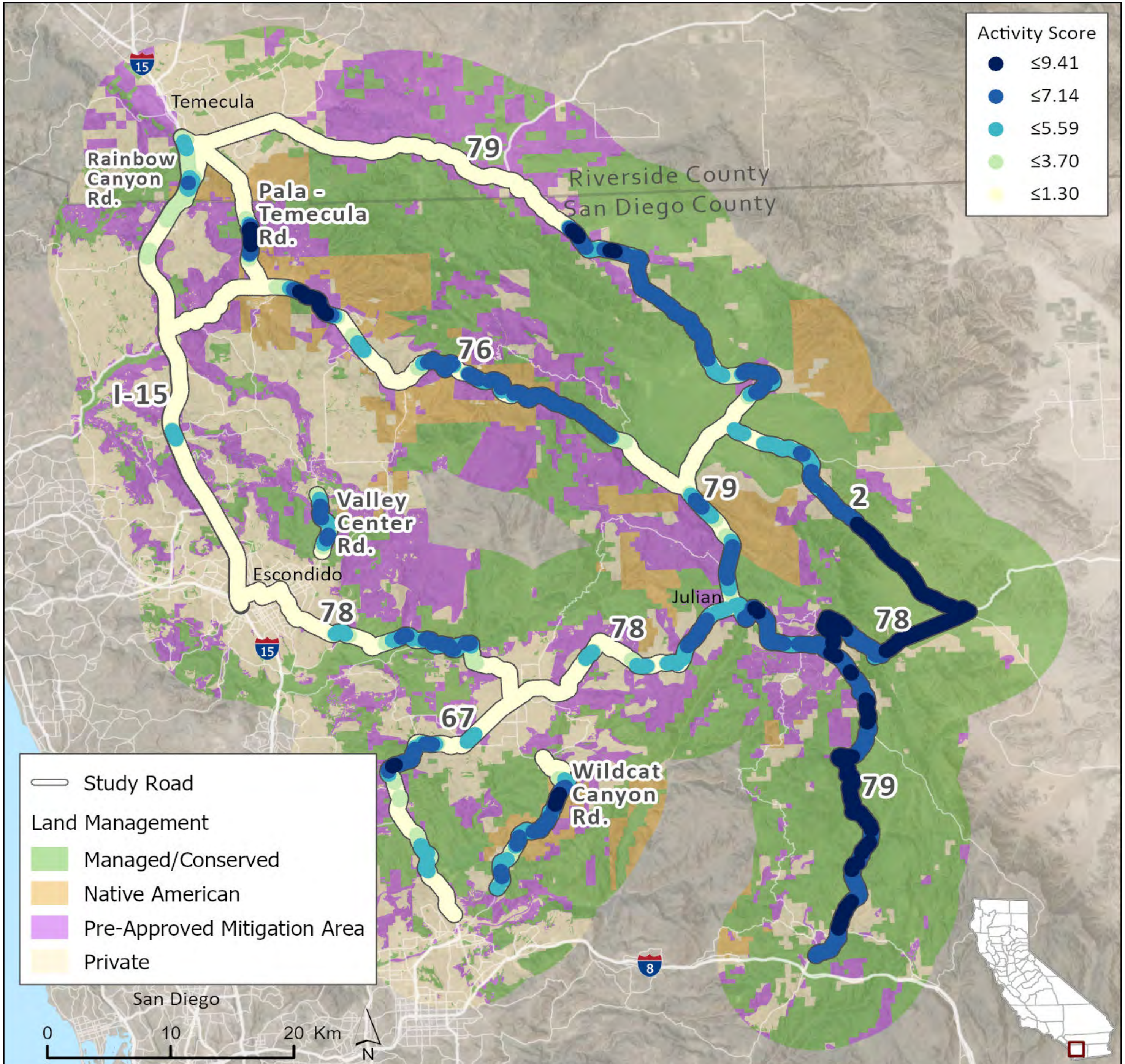
Activity Score
≤9.41
≤7.14
≤5.59
≤3.70
≤1.30
Temecula
Rainbow Canyon Rd.
Pala - Temecula Rd.
79
Riverside County
San Diego County
76
I-15
79
2
Valley Center Rd.
Escondido
Julian
78
78
78
67
Wildcat Canyon Rd.
79
Study Road
Land Management
Managed/Conserved
Native American
Pre-Approved Mitigation Area
Private
San Diego
0
10
20 Km
N

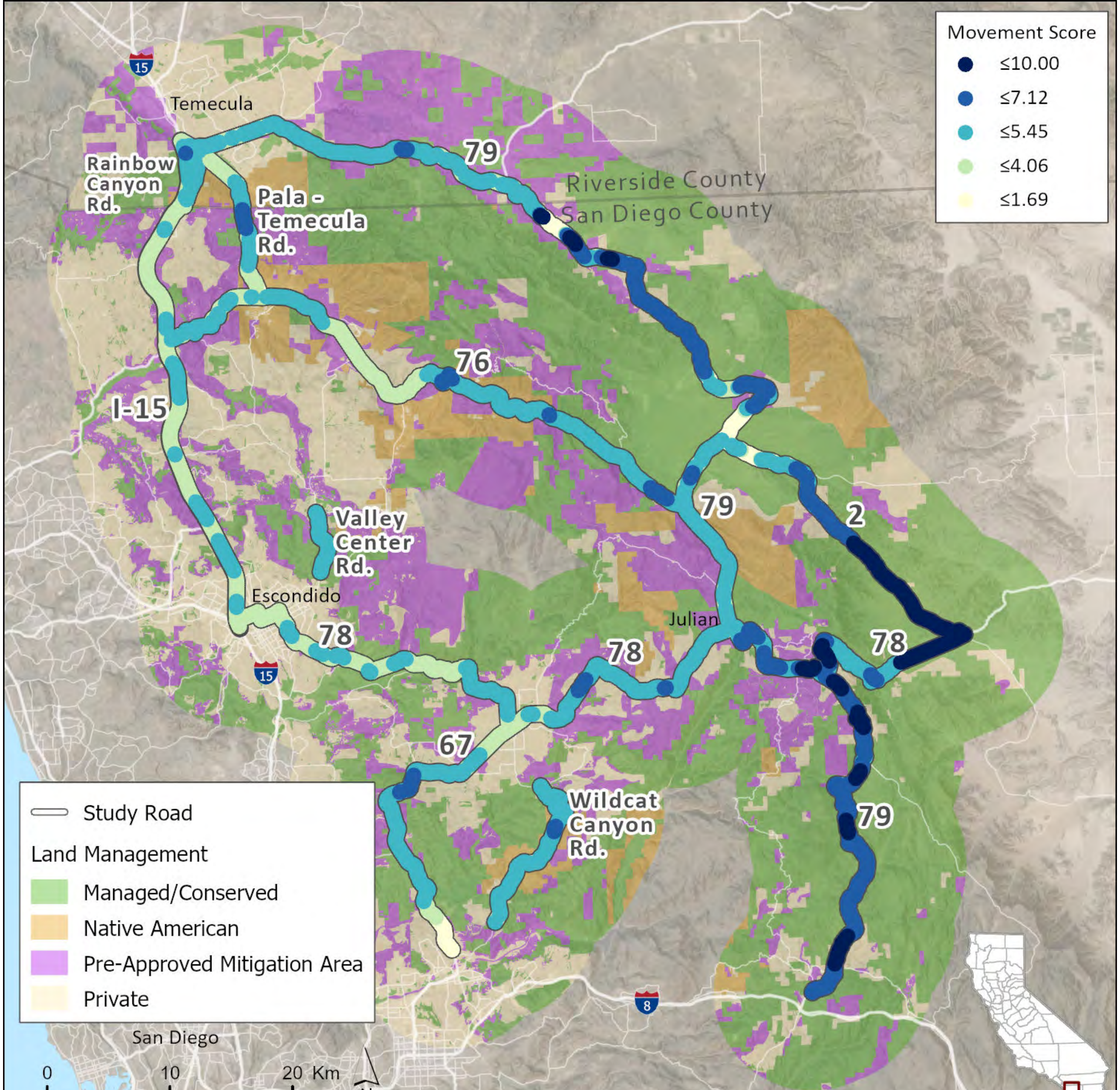

Movement Score
≤10.00
≤7.12
≤5.45
≤4.06
≤1.69
Temecula
Rainbow Canyon Rd.
Pala - Temecula Rd.
79
Riverside County
San Diego County
76
I-15
Valley Center Rd.
Escondido
78
Julian
2
67
Wildcat Canyon Rd.
Study Road
Land Management
Managed/Conserved
Native American
Pre-Approved Mitigation Area
Private
San Diego
0
10
20 Km
15
8

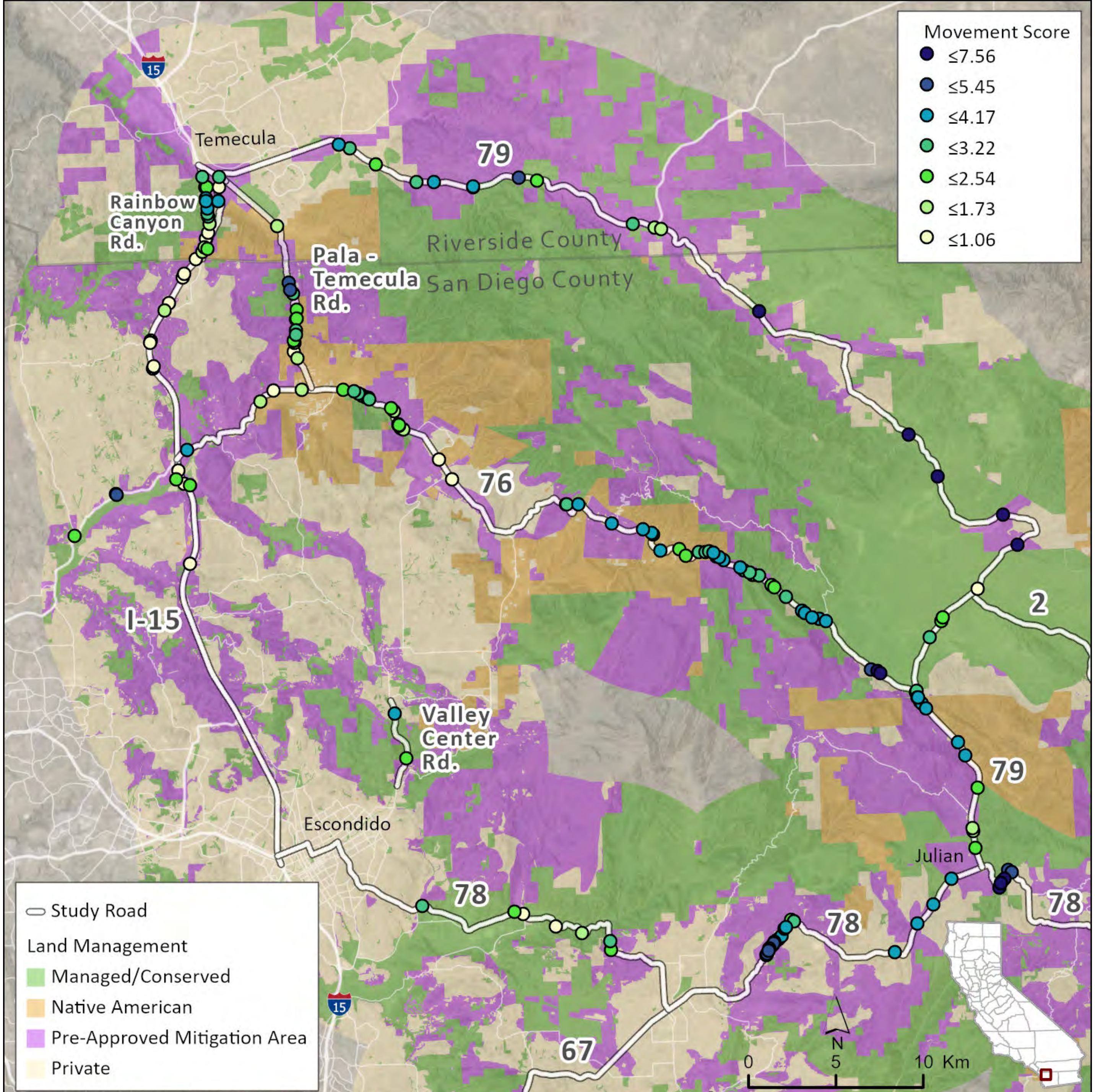

Movement Score
≤7.56
≤5.45
≤4.17
≤3.22
≤2.54
≤1.73
≤1.06
Temecula
79
Rainbow Canyon Rd.
Pala - Temecula Rd.
Riverside County
San Diego County
76
I-15
2
Valley Center Rd.
79
Escondido
Julian
78
78
78
67
Study Road
Land Management
Managed/Conserved
Native American
Pre-Approved Mitigation Area
Private
N
0
5
10 Km

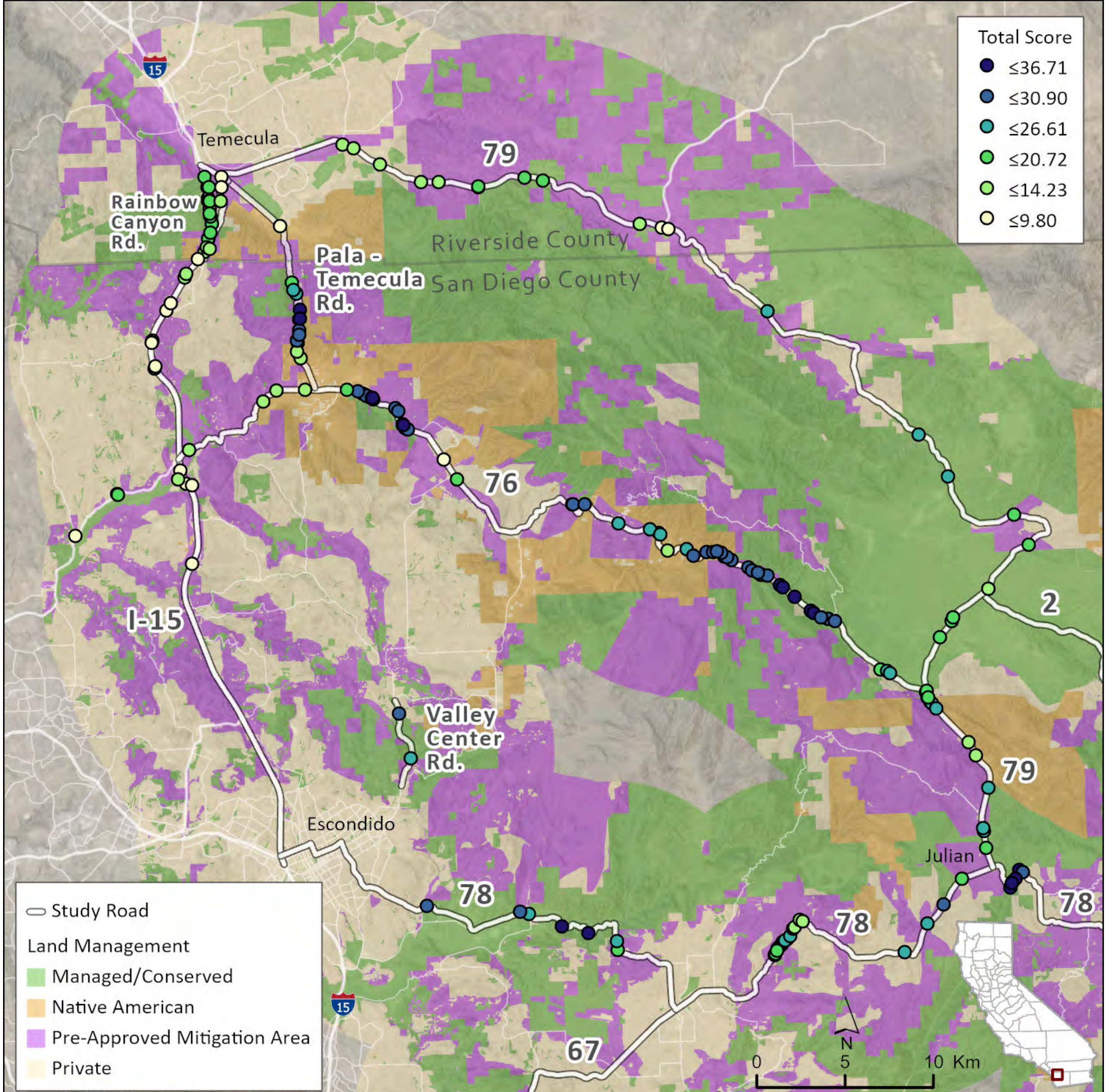
Total Score
≤36.71
≤30.90
≤26.61
≤20.72
≤14.23
≤9.80
Temecula
79
Rainbow Canyon Rd.
Pala - Temecula Rd.
Riverside County
San Diego County
76
2
I-15
Valley Center Rd.
79
Escondido
Julian
78
78
78
67
15
15
Study Road
Land Management
Managed/Conserved
Native American
Pre-Approved Mitigation Area
Private
N
0
5
10 Km

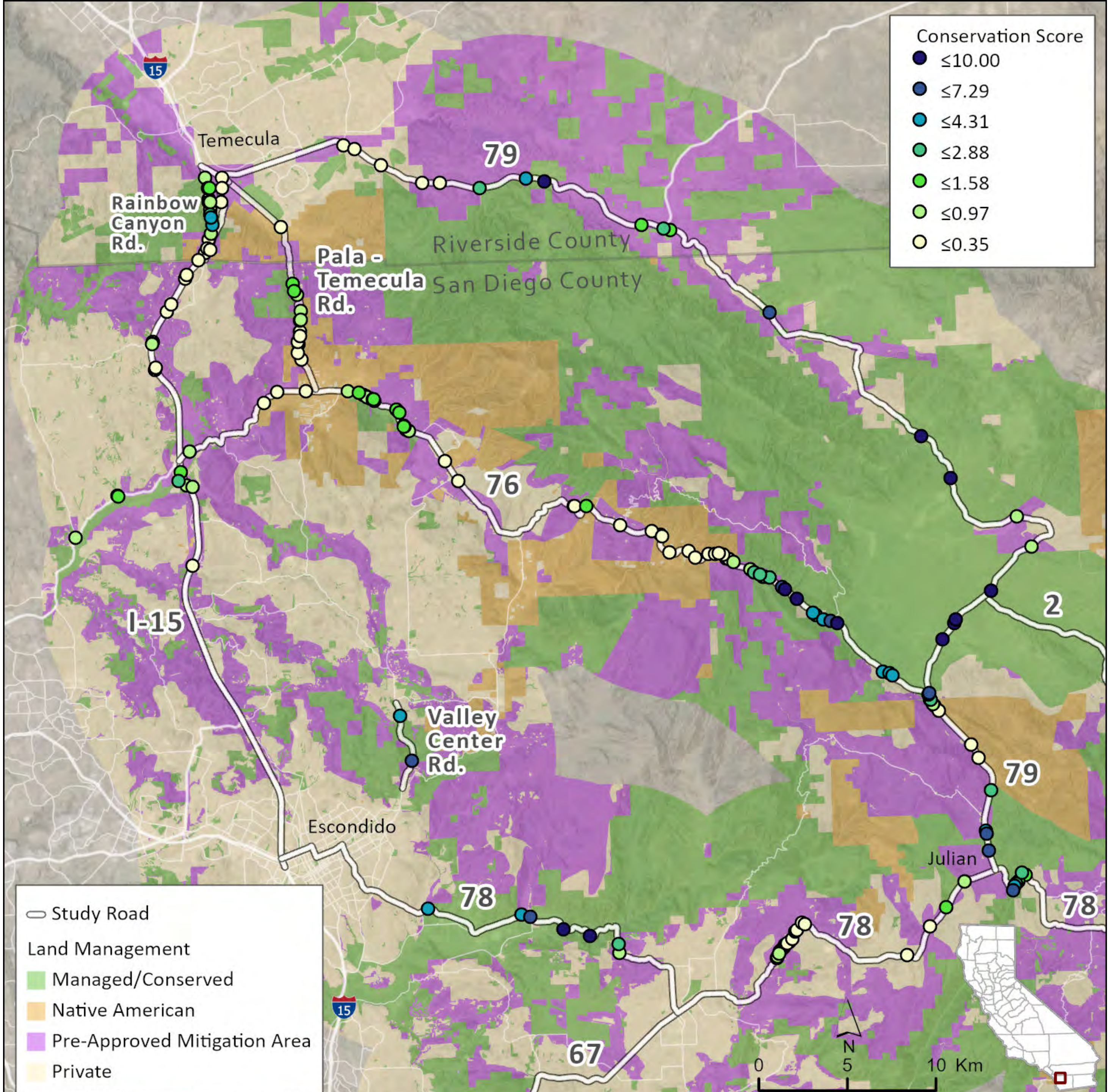
Conservation Score
≤10.00
≤7.29
≤4.31
≤2.88
≤1.58
≤0.97
≤0.35
Temecula
79
Rainbow Canyon Rd.
Pala - Temecula Rd.
Riverside County
San Diego County
76
I-15
2
Valley Center Rd.
Escondido
79
Julian
78
78
78
67
15
N
0 5 10 Km
Study Road
Land Management
Managed/Conserved
Native American
Pre-Approved Mitigation Area
Private

- Based on infrastructure present, known crossings, and higher than average Activity and Movement scores only 39 of the 185 sites have both adequate infrastructure to support long term connectivity and a high potential for mountain lion use of the sites as those areas now exist
- Based on conservation scores only 8 of the top 39 sites have over 50% of the land conserved within a 500 meter radius

Survey Locations 2020

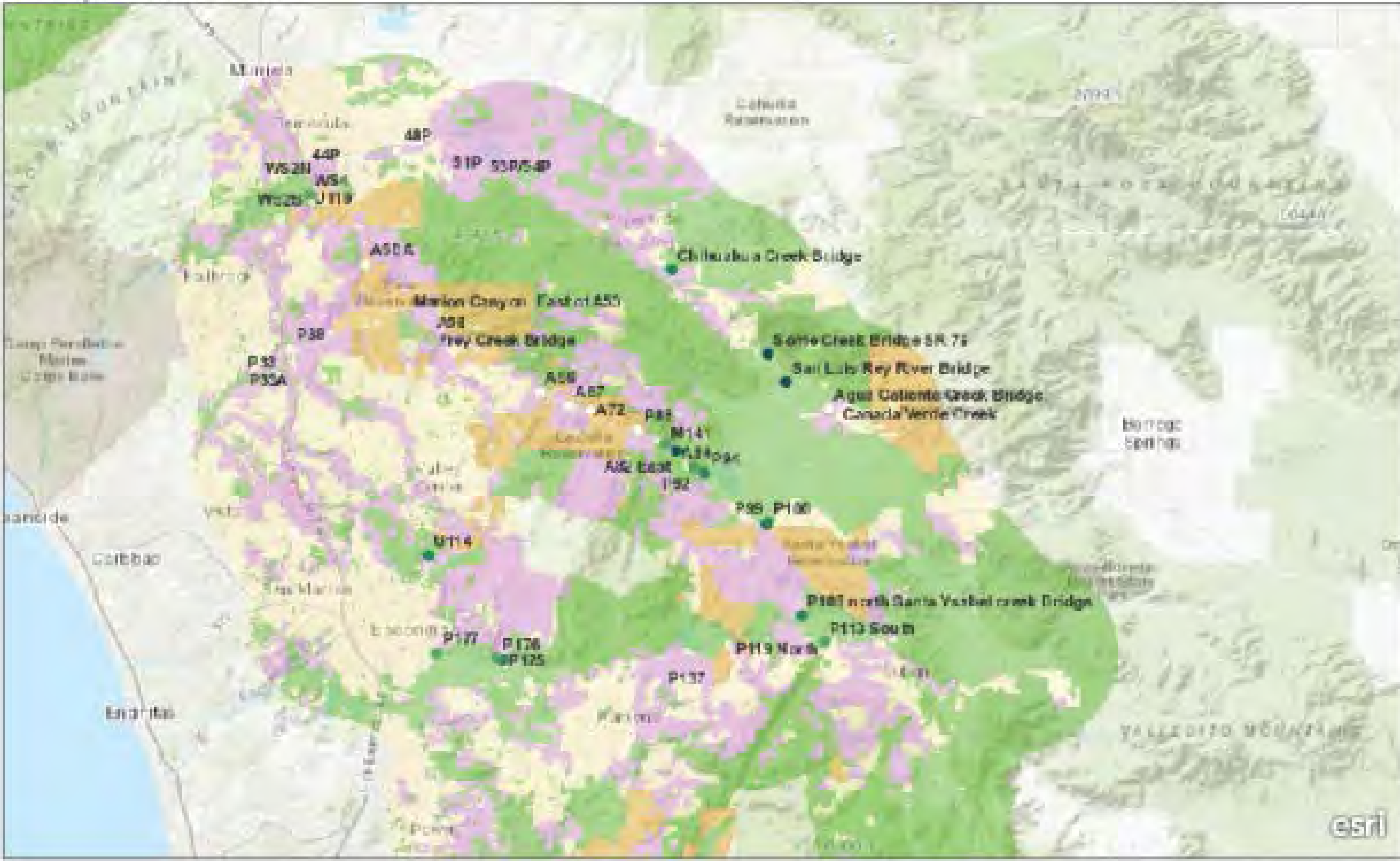

Esri, HERE, Garmin, USGS, NGA, EPA, USDA, NPS

Camera study at I-15 sites evaluated. All sites in the study had cameras present, as well as some sites on the TNC Rainbow Property adjacent to the freeway in area of proposed new crossing structure.

11 photos of lions since late 2018 and one mortality.

Site Name	General area	Latitude	Longitude	Number of mountain lion events	East or West Side of Highway
44P West C	SMER Gate	33.47428	-117.14068	1	West
44P West D	South trail closest to bridge	33.47427	-117.13932	1	West
WS4 West	I-15 West culvert	33.45466	-117.13611	1	West
U148 East D	Creek bed	33.45624	-117.13495	1	East
U119 East	East Creek bed/Culvert	33.45833	-117.135	1	East
Apple 3	TNC Rainbow Property along road	33.45256	-117.13515	4	East
Apple 4	TNC Rainbow Property along road	33.45284	-117.13204	1	East
M233 mortality site Dec 2018	I-15 near WS4	33.45141	-117.13520	1	
Apple 5	TNC Rainbow Property in Ravine	33.45172	-117.13281	1	East

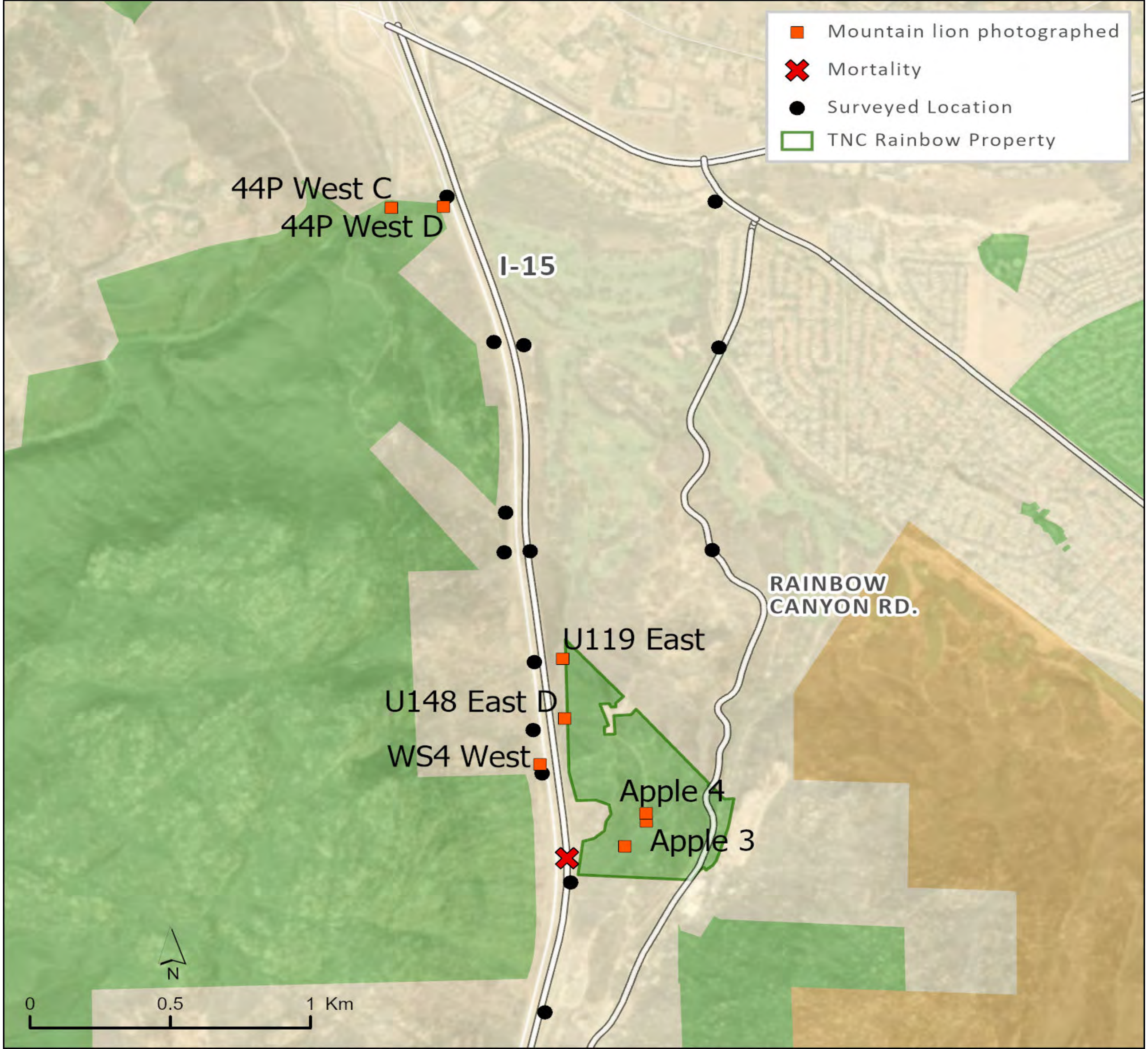
Mountain lion photographed
Mortality
Surveyed Location
TNC Rainbow Property
44P West C
44P West D
I-15
RAINBOW
CANYON RD.
U119 East
U148 East D
WS4 West
Apple 4
Apple 3
N
0
0.5
1 Km

Cal Poly Civil Engineering Assessment

Most feasible overcrossing site

Undercrossing site just to the north at head of draw on east side

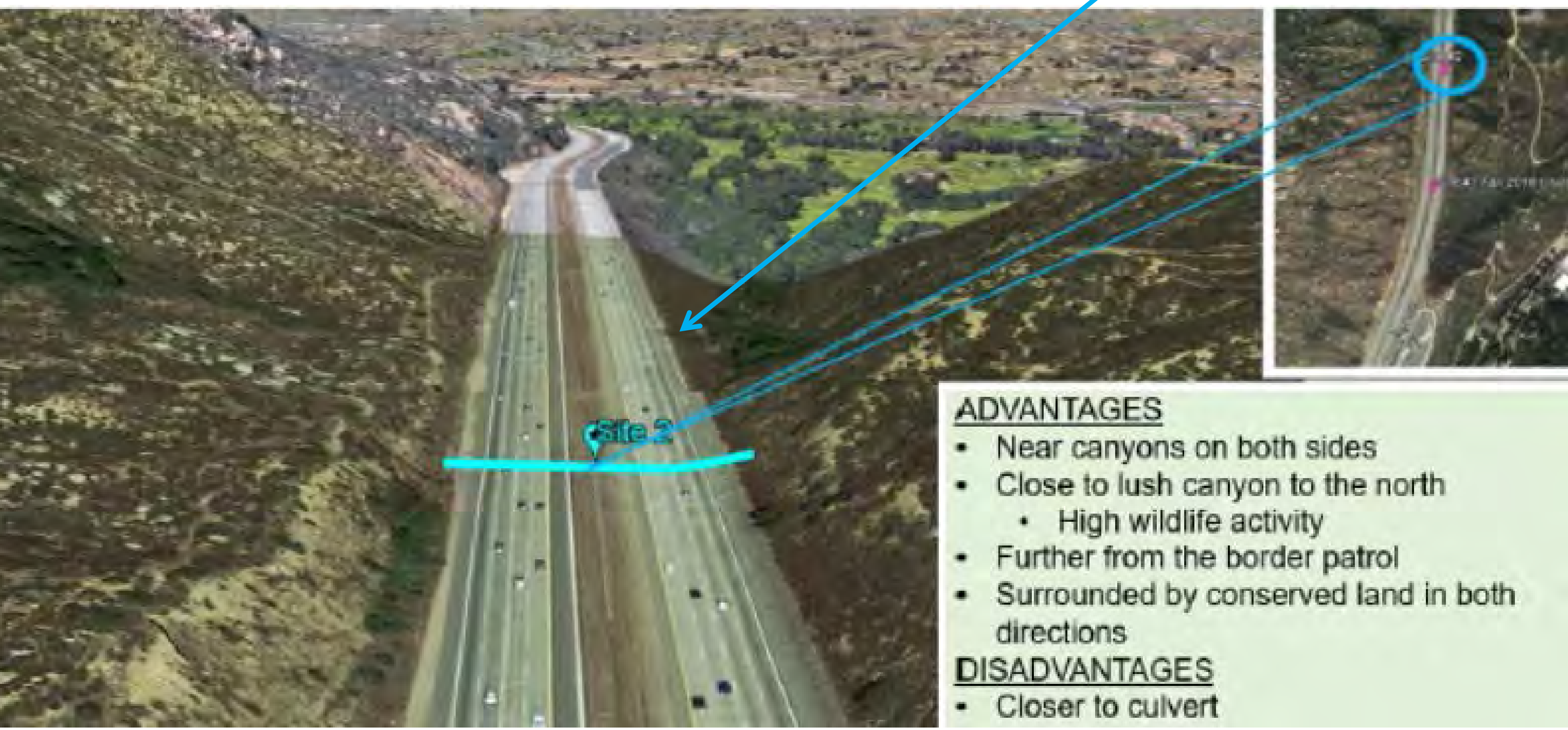

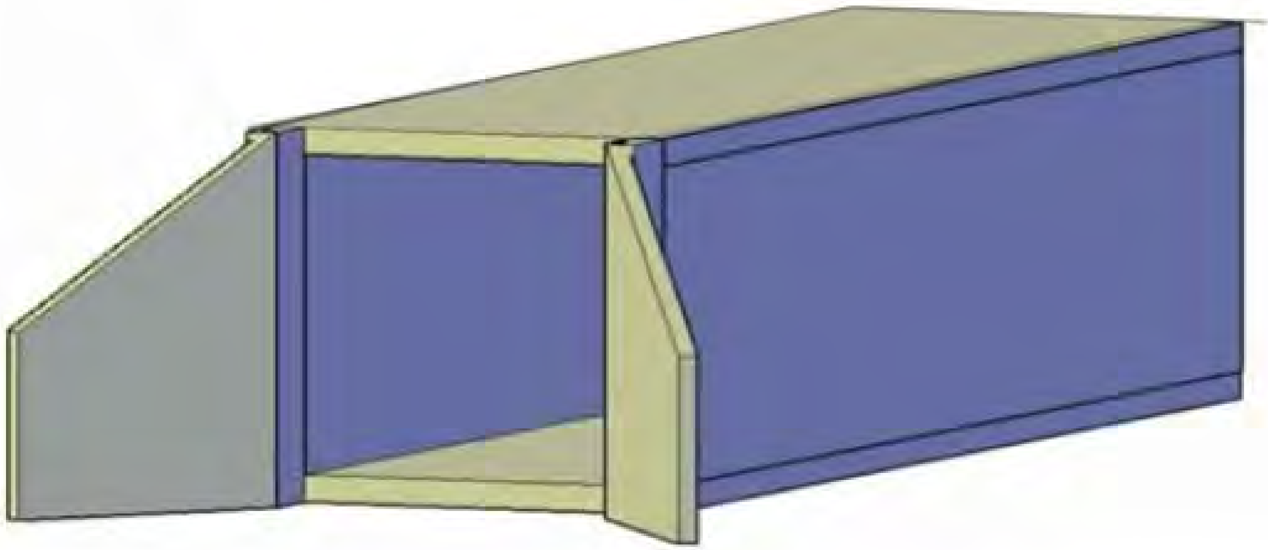

Figure 6.2. *Concrete Box Culvert Design.*

Light measurements from space. Darker areas on image are darkest on the surface. Darkest area is in the general location being considered for a new crossing.

Currently measuring light at ground level and on slopes leading down to a potential crossing site.

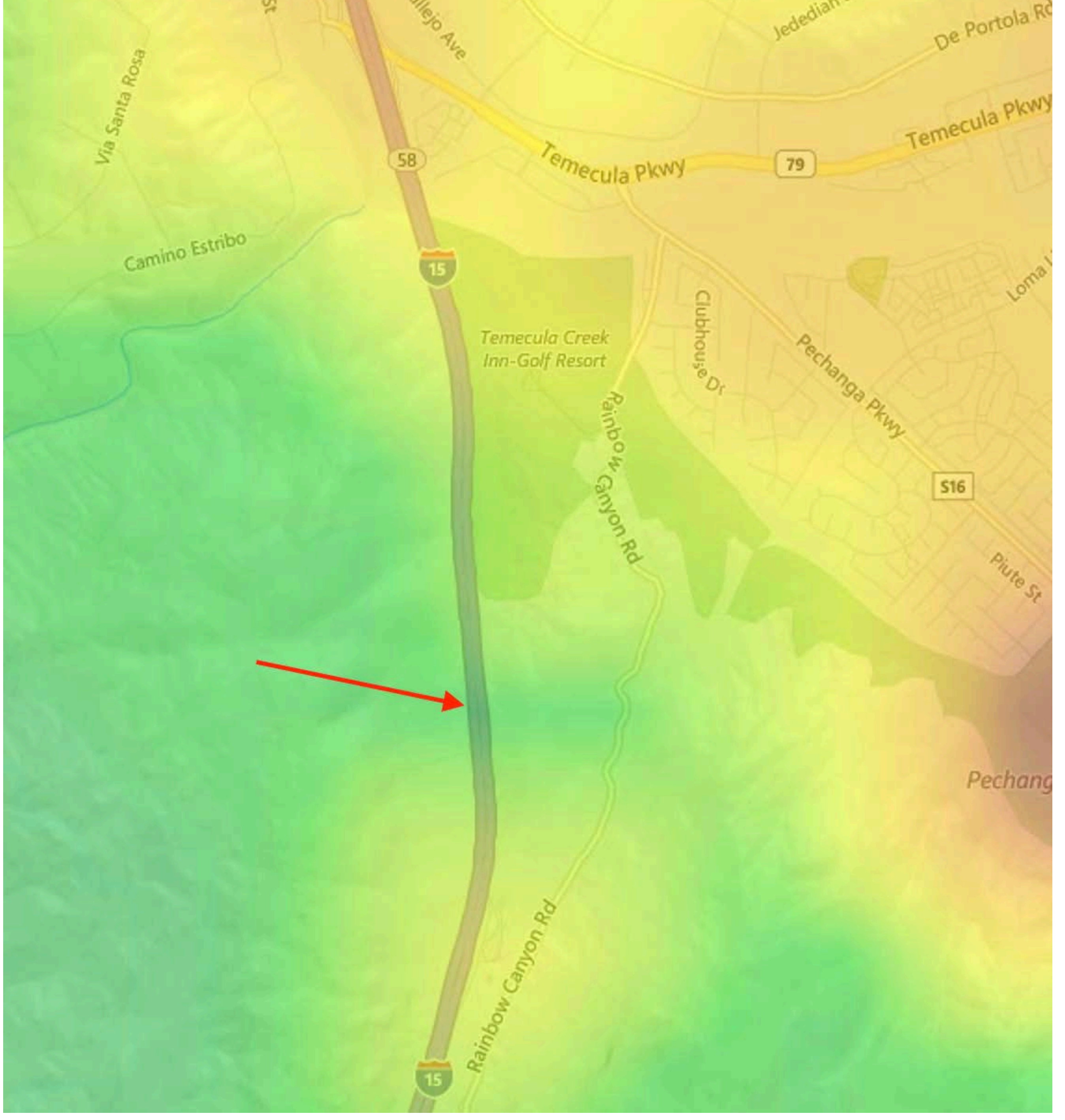

- Amy Collins sound measurements and paper pending
- Sound levels under the Temecula Creek Bridge were the same as levels right beside the freeway on the shoulder, suggesting sound dampening measures as suggested by CPP study are indicated

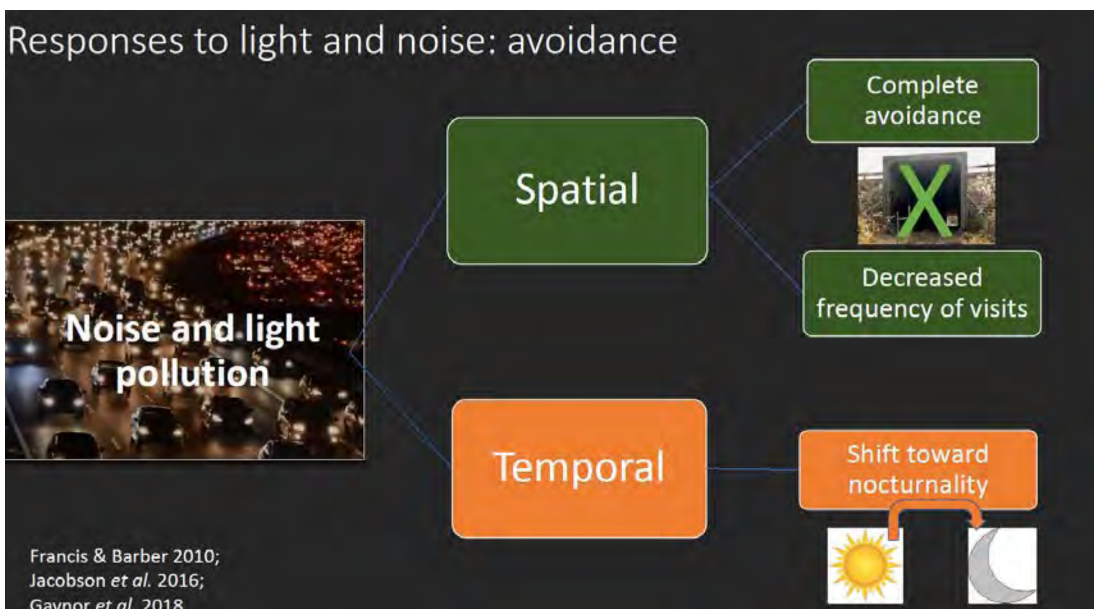

- Bottom line:
- Still adequate potential for safe crossing of regional highways – I-15 needs modifications at Bridge
- New structure north of Border check station would be HIGHLY likely to be successful
- New structure is feasible from an engineering perspective
- Light and sound studies support both Bridge mods and overcrossing so far

- Adequate infrastructure exists across the region’s highways for mountain lion safe crossings

- However, of the 39 sites with adequate infrastructure and known crossings or high use levels by mountain lions, only 8 had over 50% or more conserved land in the vicinity

- Many of the adequate sites are in vicinity of less suitable sites and funneling fencing could make crossings safer for lions and people

On line resources and recent outreach:

CPP Student team presentation for the engineering students and faculty (their project won a top award) https://streaming.cpp.edu/media/0_nxln5xps, and a website detailing the findings of their portion of the overall project https://i15wildlifecrossing.wixsite.com/calpolypomona.

Additionally a webpage and podcast was developed by TNC highlighting the connectivity issues https://www.nature.org/en-us/what-we-do/our-priorities/protect-water-and-land/land-and-water-stories/a-path-for-mountain-lions/?src=e.dfg.eg.x.pod.F

A 9-episode series of short documentaries was developed by the UCD team that has been viewed online over 50,000 times at www.camountainlions.com.

On Facebook our new one hour documentary blending portions of our 9 part series with new footage aired April 14 on P22's Facebook page, as well as a Q and A session after the showing is here https://www.facebook.com/p22mountainlionofhollywood/videos/

We will forward links to the ARC GIS tools and databases that our team developed once the report is accepted as final by the agencies and the tools are streamlined a bit for easier use.